NTNU
Norwegian University of
Science and Technology

# Synthesis of pyrrolopyrimidines for CSF-1R inhibition

Trygve Leithaug

Master of Science
Submission date: May 2017
Supervisor: Bård Helge Hoff, IKJ
Co-supervisor: Jin Han, IKJ
Thomas Aarhus, IKJ

Norwegian University of Science and Technology
Department of Chemistry

The illustration on the cover shows the computed interactions of compound **7e** with the ATP binding pocket of CSF-1R.

I hereby declare that this master's thesis is an independent work according to the exam regulations of the Norwegian University of Science and Technology

Trondheim May 2017

Trygve Leithaug

# Preface

This master thesis is based on work executed at the Department of Chemistry at NTNU during the spring of 2017. Supervisors have been Professor Bård Helge Hoff and PhD candidate Thomas Ihle Aarhus.

I would like to thank Bård Helge Hoff for accepting me as a master student in the Hoff/Sundby family. The research I have had the opportunity to participate in has been intriguing and has triggered my curiosity of both chemical and biological aspects. The weekly meetings have been much appreciated, and I am thankful for your continuous involvement in my lab work. Your advice in the writing process has also been highly valuable.

Thomas, you have been one of the key factors for what I have achieved this semester. Your knowledge and helpful attitude have been crucial for the optimization of several syntheses and the development of my competence as a chemist. I also would like to give credit to the rest of the Hoff/Sundby group for the group meetings where questions could be presented and solutions discussed.

Susanna Villa Gonzales has run the analyses of all the MS-samples for this project and your efforts are much appreciated. These results have often made the difference when it came to confirmation of the compounds synthesised. All of the chemicals applied for the lab work have been ordered through, or provided by Roger Aarvik. Your contribution has made the lab work much more convenient!

Lastly, a special dedication is given to my wife Ann-Elèn who has been a source of encouragement and motivation throughout the five-year span of the study program and even more this last semester. Without you, the finish line would have been much harder to reach.

# Abstract

Overexpression of the colony stimulating factor receptor 1 kinase (CSF-1R) has been linked to several pathological conditions. Thus, developing potent inhibitors towards the target can lead to new therapeutic agents. The aim for this master thesis was to synthesise new pyrrolopyrimidine structures as potential CSF-1R inhibitors.

The pyrrolopyrimidine base structure was prepared through a three-step synthesis. A SEM-protecting group was installed on N-7 before the substrate was further iodinated. The iodinated structure was fused with an amine at C-4 by thermal amination. Different aryl groups were then coupled to C-6 by Suzuki reactions with different arylboronic acids and esters. Additionally, one of the coupling products that contained an alcohol functionality in the *meta* position was used to perform a Williamson ether synthesis. All of the coupled products and the product from the Williamson ether synthesis were deprotected by the same procedure to give eight target compounds.

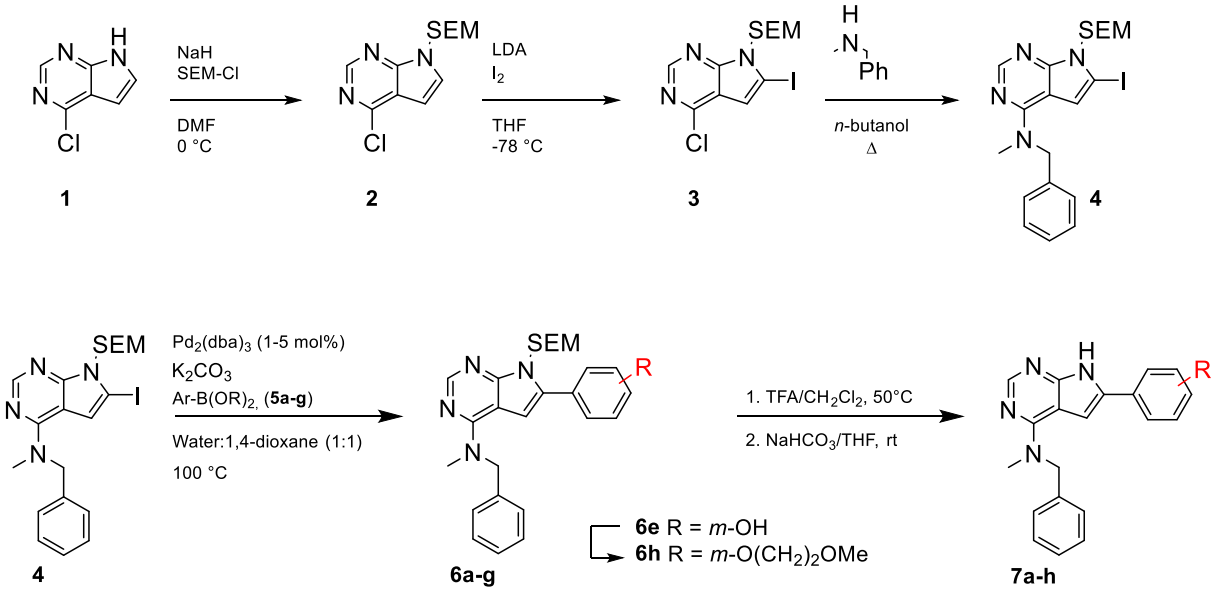


Six of the synthesised compounds were tested as inhibitors of CSF-1R and the epidermal growth factor receptor tyrosine kinase (EGFR-TK). Whereas all compounds had low nano molar activity towards CSF-1R, four of the target compounds had $IC_{50}$-values lower than 2.8 nM and the most potent inhibitor had an $IC_{50}$-value of 1.3 nM. The results show that these structures

are potent CSF-1R inhibitors that could be subjects for further testing *in vitro* and potentially *in vivo*. The structures are also valuable leads for developing new kinase inhibitors.

# Sammendrag

Overuttrykk av den kolonistimulerende faktorreseptor 1-kinasen (eng. colony stimulating factor receptor 1 kinase (CSF-1R)) har blitt knyttet opp mot flere patologiske tilstander. Som en konsekvens av dette er det av interesse å utvikle effektive hemmere av dette proteinet, som kan føre til utviklingen av nye terapeutiske virkestoffer. Målet for denne masteroppgaven var å syntetisere nye pyrrolopyrimidiner som potensielle hemmere av CSF-1R.

Et avansert pyrrolopyrimidin-mellomprodukt ble først fremstilt gjennom en trestegs syntese. Pyrrolopyrimidin-skjelettet ble beskyttet med en SEM-beskyttelsesgruppe før den ble jodert i posisjon 6. Den joderte strukturen ble videre reagert med et amin på C-4 ved en termisk prosess. Ulike arylgrupper ble så koblet til C-6 ved Suzukireaksjoner med bruk av ulike arylborsyrer og estere. Et av koblingsproduktene som inneholdt en fenolisk funksjonalitet i *meta*-posisjonen ble brukt til å utføre en Williamson etersyntese. Alle de koblede produktene og produktet fra Williamson etersyntesen ble avbeskyttet, og de åtte målstoffene ble isolert.

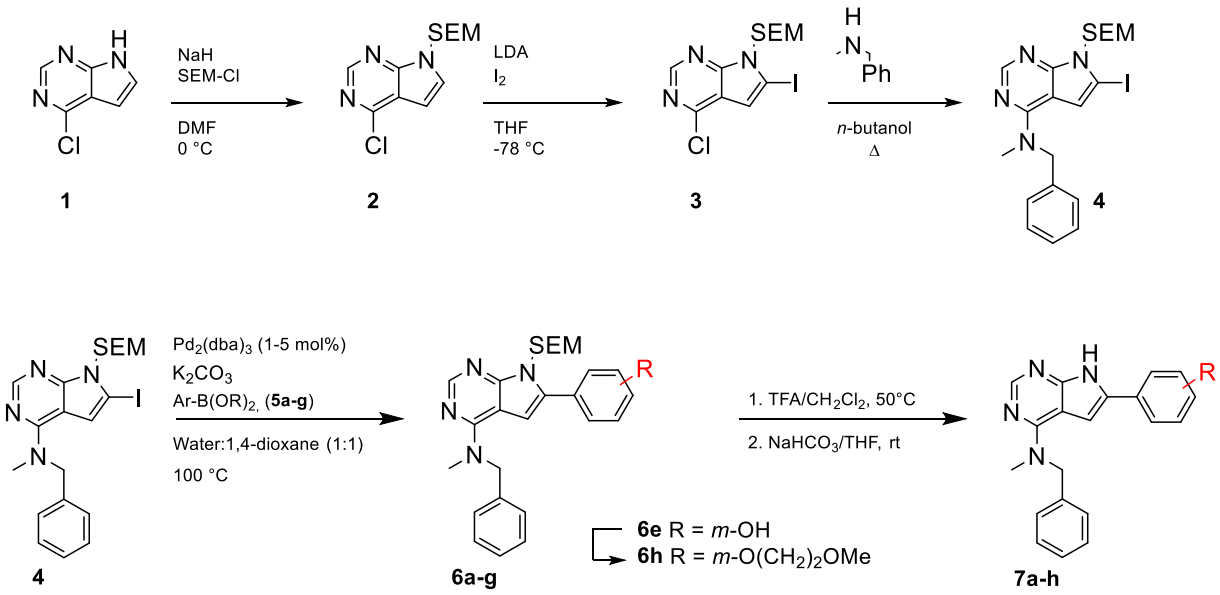


Seks av de syntetiserte målstoffene ble testet som hemmere av CSF-1R-kinasen og den epidermale vekstfaktorreseptor tyrosinkinasen (EGFR-TK). Mens alle stoffene hadde en lav nanomolar aktivitet mot CSF-1R hadde fire stoffer $IC_{50}$-verdier som var lavere enn 2.8 nM. Den mest potente hemmeren hadde en $IC_{50}$-verdi på 1.3 nM. Resultatene viser at disse

strukturene er potente CSF-1R-inhibitorer som kan være kandidater for videre testing *in vitro* og muligens for testing *in vivo*. Strukturene er også verdifulle ressurser for utvikling av nye kinaseinhibitorer.

# Table of contents

# Symbols and abbreviations.

| | |
|---|---|
| ASAP | Atmospheric Solid Analysis Probe |
| ATP | Adenosine Triphosphate |
| ADP | Adenosine Diphosphate |
| BOC | Tert-Butyloxycarbonyl |
| Bs | Benzensulfonyl |
| COSY | Correlation Spectroscopy |
| CSF-1 | Colony Stimulating Factor |
| CSF-1R | Colony Stimulating Factor Receptor |
| d | Doublet |
| decomp. | Decompose |
| DMF | Dimethylformamide |
| DMSO | Dimethyl Sulfoxide |
| EGFR | Epidermal Growth Factor Receptor |
| EtOAc | Ethyl Acetate |
| FMS | Feline McDonough Sacroma |
| g | grams |
| HMBC | Heteronuclear Multiple Bond Correlation |
| HPLC | High Performance Liquid Chromatography |
| HRMS | High Resolution Mass Spectroscopy |
| HSQC | Heteronuclear Single Bond Correlation |
| $IC_{50}$ | Half Maximum Inhibitory Concentration. |
| IL-34 | Interleukin 34 |
| IR | Infrared |
| LDA | Lithium Diisopropylamide |
| m | Multiplet |
| mg | Milligrams |
| min | Minutes |
| mp | Melting Point |
| Ms | Methanesulfonyl |
| MS | Mass Spectroscopy |

| | |
|---|---|
| NRTK | Non Receptor Tyrosine Kinase |
| Nu | Nucleophile |
| Pd(dppf)$Cl_2$ | [1,1′Bis(diphenylphosphino)ferrocene]dichloropalladium(II) |
| $Pd_2(dba)_3$ | Tris(dibenzylideneacetone)dipalladium(0) |
| $pK_a$ | Acid Dissociation Constant |
| ppm | Parts Per Million |
| PTK | Protein Tyrosine Kinase |
| $R_f$ | Retention Factor |
| rt | Room Temperature (22°C) |
| RTK | Receptor Tyrosine Kinase |
| s | Singlet |
| $S_NAr$ | Nucleophilic Aromatic Substitution |
| SEM | 2-(trimethylsilyl)ethoxymethyl |
| SES | 2-Trimethylsilylethanesulfonyl |
| t | Triplet |
| TAM | Tumour Associated Macrophages |
| TFA | Trifluoroacetic Acid |
| THF | Tetrahydrofuran |
| TKI | Tyrosine Kinase Inhibitor |
| TLC | Thin Layer Chromatography |
| Ts | Toluensulfonyl |
| XPhos | 2-Dicyclohexylphosphino-2′,4′,6′-triisopropylbiphenyl |

# Numbered compounds

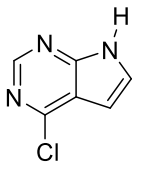

**1**

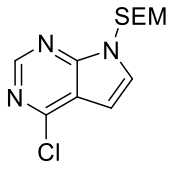

**2**

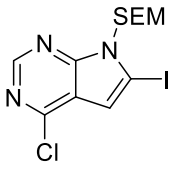

**3**

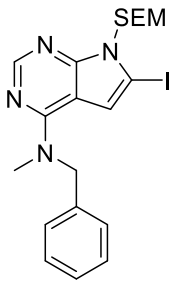

**4**

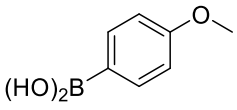

**5a**

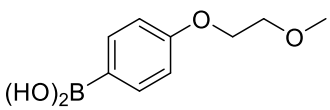

**5b**

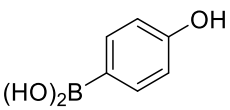

**5c**

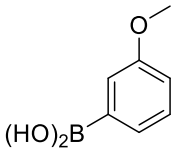

**5d**

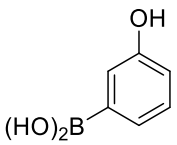

**5e**

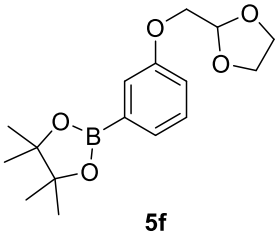

**5f**

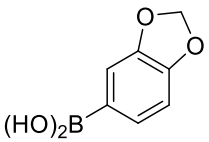

**5g**

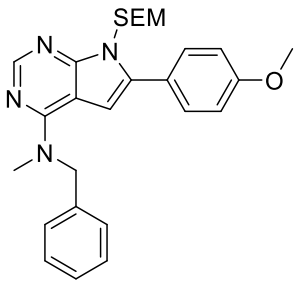

**6a**

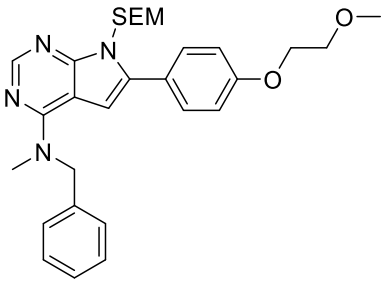

**6b**

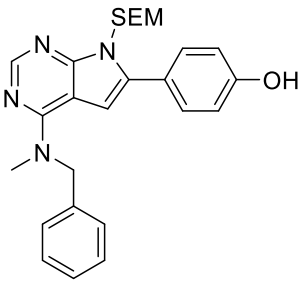

**6c**

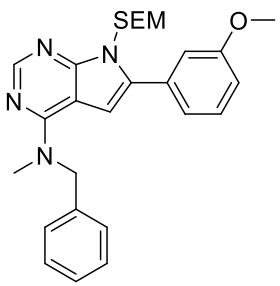

**6d**

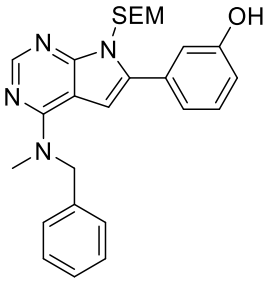

**6e**

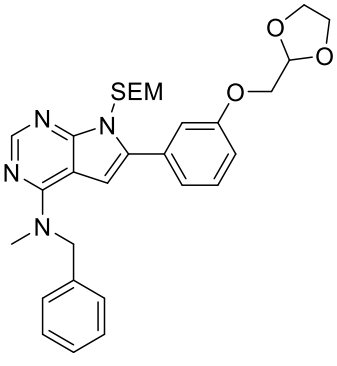

**6f**

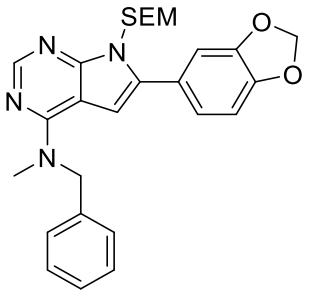

**6g**

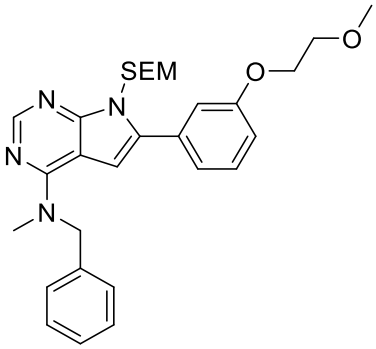

**6h**

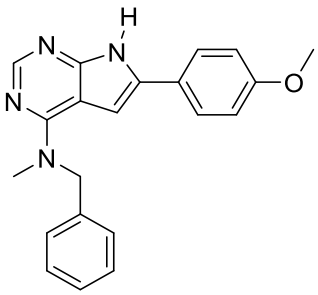

**7a**

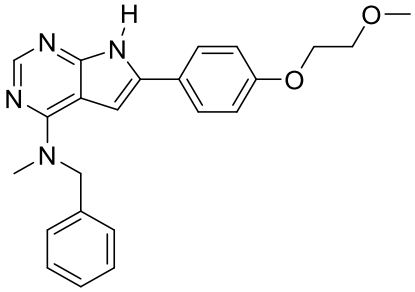

**7b**

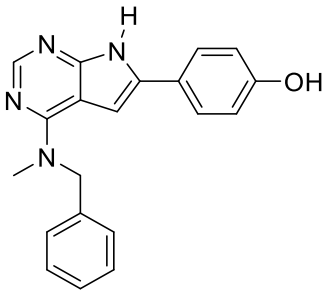

**7c**

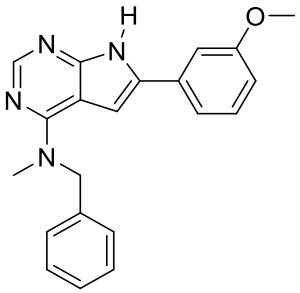

**7d**

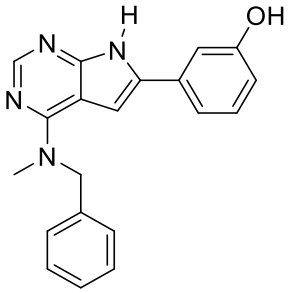

**7e**

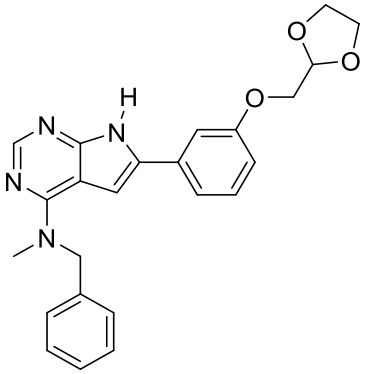

**7f**

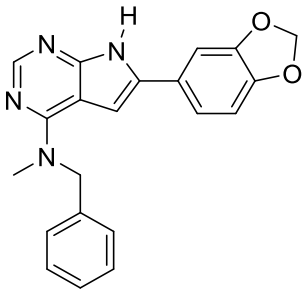

**7g**

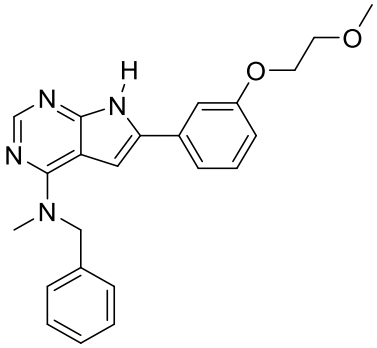

**7h**

# 1 Introduction and theory

Small-molecule drug design is a research field that have received both funding and interest the recent years [1]. One of the reasons for this interest is the fact that these kinds of drugs can regulate abnormal activity that may occur in mutated kinases [2]. Tyrosine kinases are especially important for the regulation of vital functions in the body [3]. Mutations in such kinases can lead to faulty signals in the cells signalling pathways. Diseases such as inflammation, diabetes, cancer and arteriosclerosis have been linked to such faulty signals [4]. Development of new small-molecule drugs can lead to new potent compounds, which can be used in future treatments for these diseases. The goal of this master thesis is to contribute in this important research. Several new structures were developed and synthesised to investigate their activity as colony stimulating factor receptor, CSF-1R, inhibitors. There are no CSF-1R inhibitor drugs implemented in medical treatments today, which makes this research even more exciting. A general structure of the pyrrolopyrimidine scaffold with numbered positions is presented in Figure 1, while the target compounds for this thesis are presented in Figure 2.

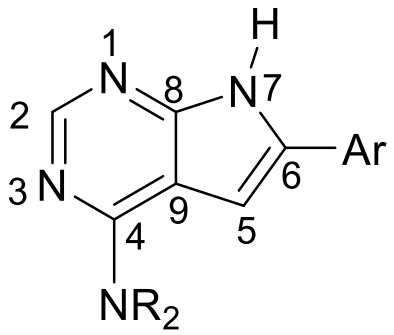


**Figure 1**: A presentation of the pyrrolopyrimidine scaffold with numbered positions.

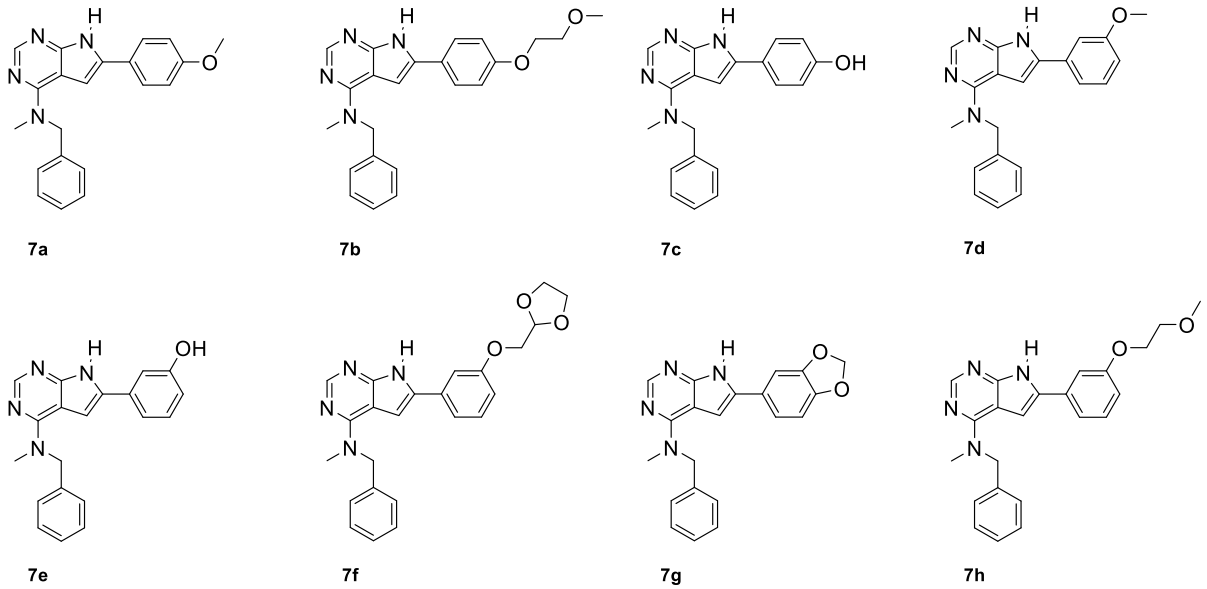


**Figure 2**: The target molecules for CSF-1R inhibition evaluation.

The structures presented above have in part been chosen by following leads from previous results published by the research group [5-7]. Long solubilising tails and polar substituents on the C-6 aryl group have been shown to increase inhibition activity and permeability for both the epidermal growth factor tyrosine kinase (EGFR) and CSF-1R inhibition. Other structures have been synthesised by curiosity and by the interest of investigating the effect of various substituents on the pyrrolopyrimidine C-6 aryl group.

## 1.1 Kinases and their physiological effects

In human cell membranes there are several different receptor containing enzymes that can react with signalling molecules in the extracellular fluid to initiate cellular response [8]. A sub-category in the range of receptor enzymes are the receptor kinases. These specific receptor-containing enzymes control several biochemical processes in the human body by catalysing phosphorylation. Phosphorylation can further activate signalling cascades that initiate vital processes like cell growth and metabolism [9]. The potential problem is overexpression of a specific kinase. Overexpression can be caused by mutations in the gene regulating the expression of the first the first catalytic kinase in a signalling pathway, or by some of the following proteins in the signalling chain [10]. Overexpression of specific kinds of kinases can lead to pathological states like cancer and inflammations [11]. Due to this fact, kinase activity and inhibition of faulty signals have become an important focus within cancer and inflammatory treatment research [12-13].

### 1.1.1 Tyrosine kinases

A type of kinases that are vital for the human body's functionality are the tyrosine kinases. The name of this kinase is based on its ability to phosphorylate tyrosine residues. Tyrosine is an amino acid that can be found in proteins, among others in trans-cellular proteins. Phosphorylation of tyrosine residues by the use of ATP results in activation of several important processes. Some examples of these processes are cell signalling, cell migration and metabolism [4, 14]. When the tyrosine residues in proteins are phosphorylated, it changes the activity of the enzyme. In this energised state, the enzyme can initiate or alter signalling cascades within the cell's cytoplasm and nucleus. How a tyrosine kinase can catalyse the phosphorylation of a tyrosine residue is illustrated in Scheme 1.

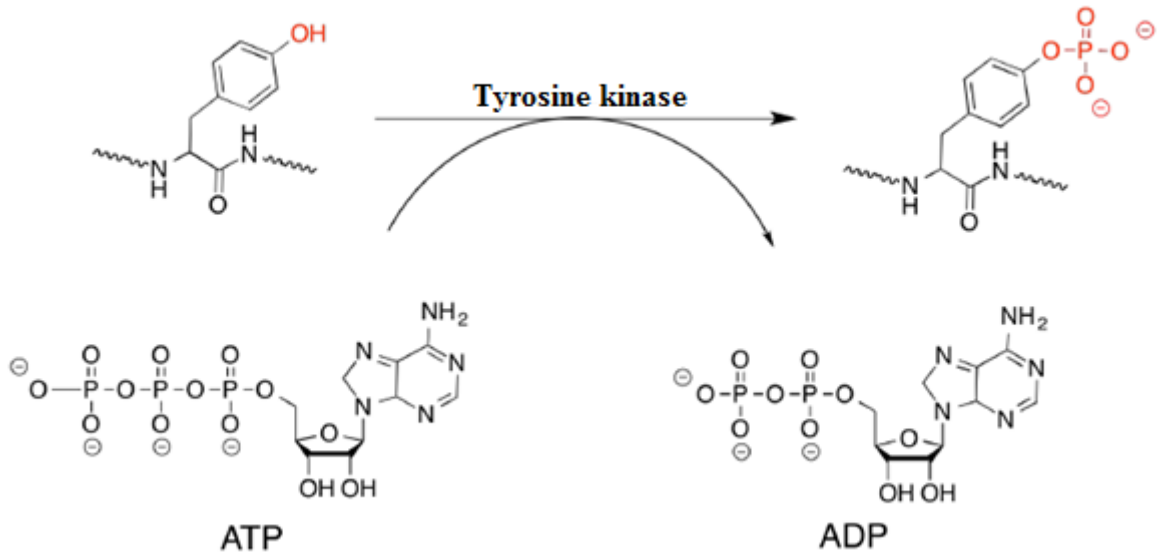


**Scheme 1**: A presentation of how the tyrosine kinase catalyses the phosphorylation of a tyrosine residue. The phosphate group is donated from ATP [7].

The tyrosine kinases can be divided into two sub-categories. The receptor tyrosine kinase (RTK) and the non-receptor tyrosine kinase (NRTK). The RTK's structure consists of three main elements. There is a receptor domain, which is found extracellularly. This part can interact with signalling molecules (for example growth factors) found in the extracellular fluid. In addition there is an intracellular section that is responsible for the catalytic phosphorylation activity, and a transmembrane section that connects these two parts together [3-4]. A signalling molecule that binds to the extracellular receptor domain can induce dimerization of the RTK-complex. This leads to phosphorylation of the intracellular domain that further can phosphorylate proteins in the following cellular signalling pathway. The process from initiation by a signalling molecule, to dimerization and phosphorylation is illustrated in Figure 3. This process can further activate a signalling cascade which may give a "message" to the cell to divide, grow or enter apoptosis [4].

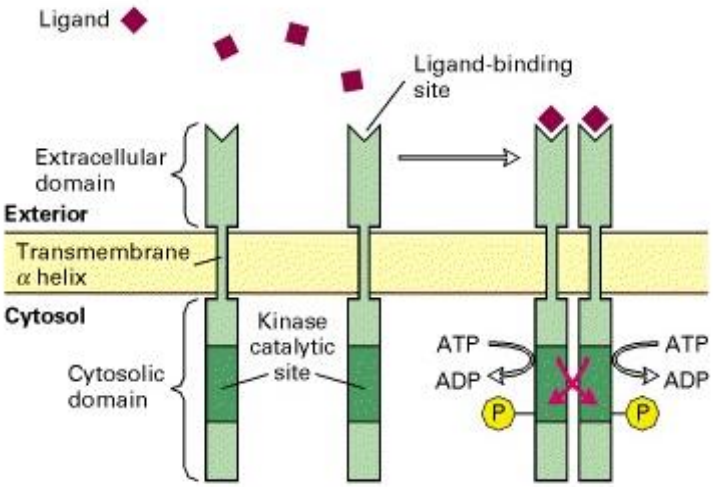


**Figure 3**: A presentation of the process of dimerization and phosphorylation following binding of a signalling molecule/ ligand [3].

Mutations in different tyrosine kinases have been linked to several pathological states [2, 4]. Such mutations can cause imbalance in what was originally healthy regulations, which may lead to harmful effects. Some of the linked diseases are leukaemia, lung cancer, pancreatic cancer and some myeloproliferative diseases [15-16]. This fact has made tyrosine kinases and tyrosine kinase inhibiting medicines a relevant field within medicinal chemistry research.

### 1.1.2 Colony stimulating factor 1 receptor

The colony stimulating factor receptor (CSF-1R) was first discovered when it was found to contain the oncogene responsible for the Feline McDonough Sarcoma which led to the acronym FMS [17]. Since this discovery, several other diseases have been linked to CSF-1R, such as the inflammatory disease rheumatoid arthritis, and different kinds of cancer [18-19].

CSF-1R is an example of a receptor tyrosine kinase. This RTK can be activated by specific signalling molecules called macrophage-colony stimulating factors (CSF) and the signalling molecule known as interleukin-34 (IL-34). These two signalling molecules bind to different sections of the extracellular receptor [18]. The CSF-1R is involved in the formation of macrophages that are essential to the human immune system [20]. One of the functions of these immune system macrophages is to neutralise bacteria that enter the blood stream by engulfing

and digesting them [21]. Macrophages can also have a pathological effect if they are associated with tumours, so called tumour-associated macrophages (TAMs). These macrophages have been shown to promote all aspects of tumour development such as initiation, growth and angiogenesis [22-23]. These discoveries have generated a motivation to develop and test different CSF-1R inhibitors so that they can be applied in medical treatment of people suffering from these and other illnesses.

Two strategies are common when it comes to CSF-1R inhibition. The first strategy is based on the use of antibodies, and blocking of the extracellular receptor domain. This blockade can deny the signalling molecule access to the receptor, see Figure 4. The second strategy is inhibition of the intracellular part of the RTK using small molecule inhibitors. ATP must interact with the intracellular domain of the RTK if phosphorylation and the following signalling cascade is to occur. Small molecule inhibitors blocks the ATP binding site in the intracellular domain hindering the phosphorylation process to occur [19].

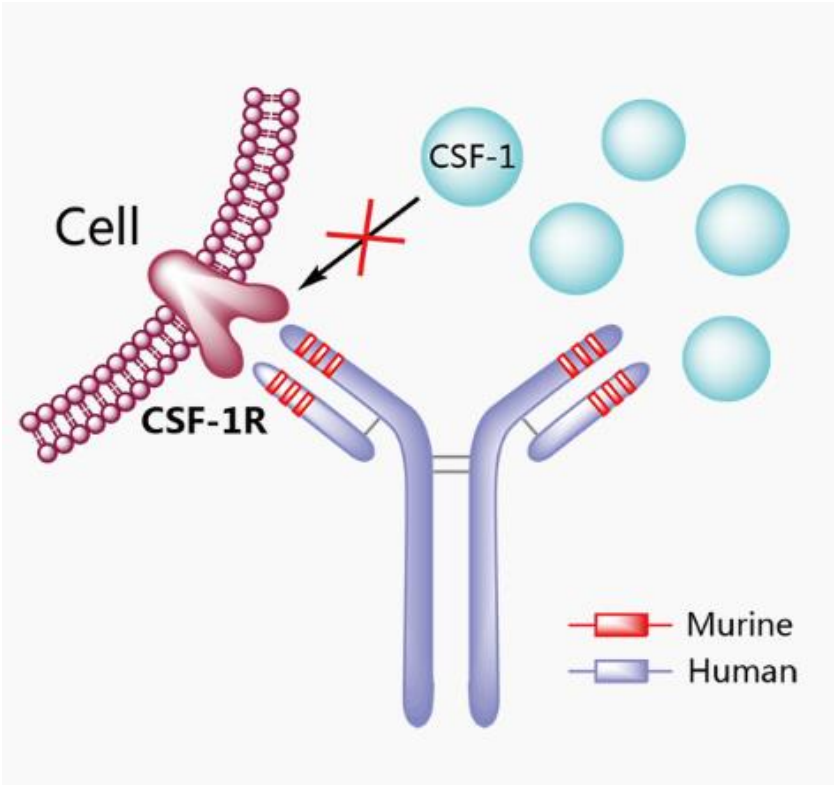


**Figure 4**: The mechanism of an anti-body inhibition of CSF-1R kinase [24]. The antibody blocks the CSF-1R, thus preventing the signalling molecule to activate the kinase.

Some potent CSF-1R inhibitors have been identified [25]. Emactuzumab (RG7155) is an antibody type inhibitor that has reached phase I trials [25]. Significant reduction of CSF-1R macrophages in tumour tissues was achieved after 4 weeks of intravenous injections of this anti-body [26]. For this phase 1 trial, there were also observations of tumour tissue reduction. Tap and associates executed a more thorough and comprehensive phase 1 trial with a small-molecule inhibitor known as PLX-3397 [27]. The phase 1 trial was divided into two parts. The first part involved 41 patients who got a base dose, while the second part involved fewer patients (23 patients) who got a higher dose. The results from the study showed that most patients had a reduced tumour volume after the treatment was completed [27]. GW2580 was one of the first orally administrated inhibitors to be reported [28]. This small-molecule inhibitor occupies the kinase binding site for ATP on the intracellular domain, and has been found to reduce tumour growth [18]. There are also studies indicating that it can be used as a therapeutic drug for arthritis patients. *In vivo* testing on mice showed that the drug could inhibit bone degradation in mouse suffering from arthritis [29]. The two small-molecule CSF-1R inhibitors mentioned in this chapter are presented in Figure 5.

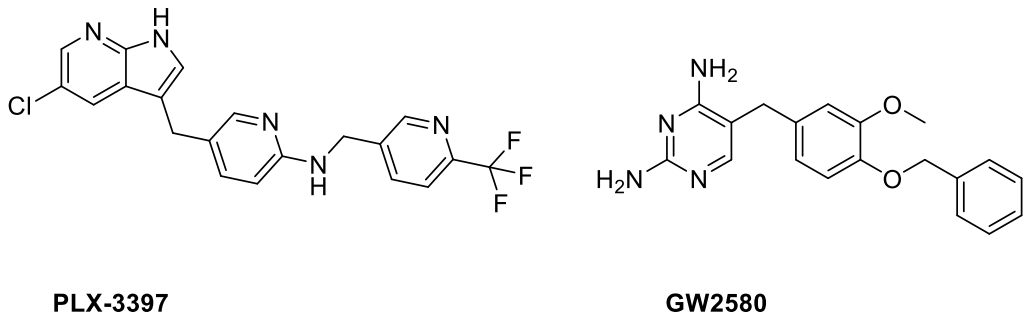


**PLX-3397** **GW2580**

**Figure 5**: The chemical structure of two potent small-molecule CSF-1R inhibitors.

## 1.1 Previous work in the research group

The research group's previous work has focused on pyrrolopyrimidines with amine substituents on C-4 [7, 30]. Thienopyrimidines with amine substituents in the same position have also been examined at a large extent [31]. The published research has focused on the EGFR-kinase. Overexpression of the EGFR-kinase has been linked with pathological states like non-small lung cancer and the formation of solid tumours [32]. There is documentation that inhibition of this kinase can prevent further tumour growth and spreading in cancer patients [33]. The general structure of the thienopyrimidine- and pyrrolopyrimidine kinase inhibitors that have been synthesised by the research group is shown in Figure 6.

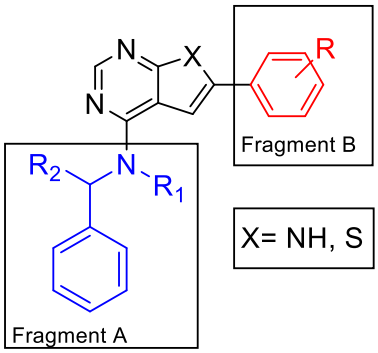


**Figure 6**: The general structure of the research group's previous work with EGFR and CSF-1R inhibitors.

This activity has also identified some decently potent CSF-1R kinase inhibitors, see Figure 7.

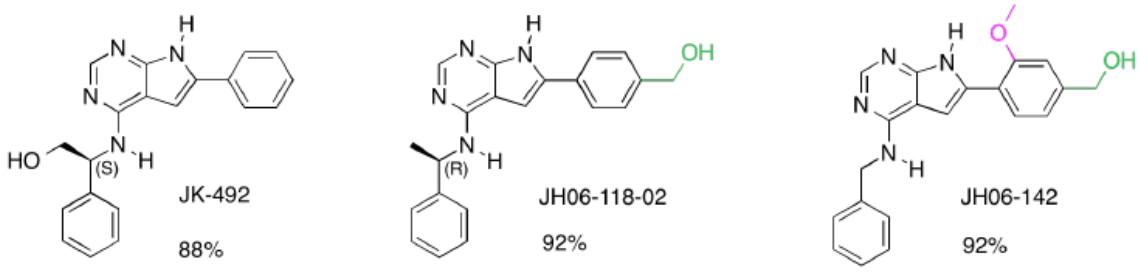


**Figure 7**: The chemical structure of some highly potent CSF-1R inhibitors synthesised by the research group. The activity is measured in percent inhibition of CSF-1R at 500 nM [5, 30].

## 1.2 Amination procedures

### 1.2.1 Nucleophilic aromatic substitution

The nucleophile substitution on an aromatic ring-system follow a mechanism called nucleophilic aromatic substitution, or $S_NAr$ [34]. The requirements for an efficient $S_NAr$ -reaction is an electron deficient aromatic ring, a good leaving group, and a strong nucleophile. The most commonly used nucleophiles are oxygen, nitrogen or cyanide nucleophiles [34-35].

In the pyrrolopyrimidine ring-system, there are two nitrogen present. These nitrogens withdraw electrons density from C-4, which makes it susceptible to a nucleophilic attack. A proposed addition-elimination mechanism for an $S_NAr$-reaction with an amine nucleophile onto C-4 is given in Scheme 2. The proposed mechanism is based on the general mechanism for an $S_NAr$-reaction.

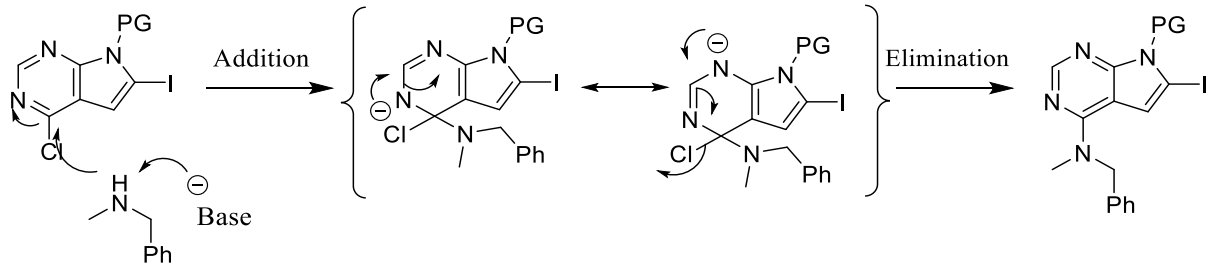


**Scheme 2**: A proposed addition-elimination mechanism for nucleophilic aromatic substitutions with an amine nucleophile [34, 36]. PG= Protective group.

The rate-determining step of the $S_NAr$-reaction depends on a combination of different factors. Some of these factors are the nucleophilicity of the reagent, the reactivity of the leaving group and which solvent is used [37]. Protic and aprotic solvents affect the system in different ways [38]. Protic solvents have a stabilizing effect on the leaving group's negative charge, which makes formation of the intermediate the rate-determining step. Aprotic solvents makes the nucleophile more reactive and therefore the addition of the nucleophile is fast, and the elimination of the leaving group might be the rate-determining step [38]. In $S_NAr$-reactions the halogen reactivity is reported to be F> Cl> Br> I [39].

### 1.2.2 Catalysed $S_NAr$ reactions

If one or more of the substrates in an $S_NAr$-reaction is non-reactive, it can be difficult to achieve an efficient reaction. This can be due to electron donating groups in the electrophile or electron withdrawing groups in the nucleophile. In these cases, metal catalysis can solve the issue. The general fact is that the presence of the right catalyst for a specific system gives faster reaction rates at lower temperatures. The general accepted mechanism for these reactions includes an oxidative addition- followed by a reductive elimination. Cu-catalysis was one of the first reported examples of these kinds of reactions, and a generalised example is presented in Scheme 3 [39-40]. Amine nucleophiles are one of the reported substrates that are reactive under these conditions and efficient procedures enabling copper-catalysed substitution with amine substrates have been reported [41-42].

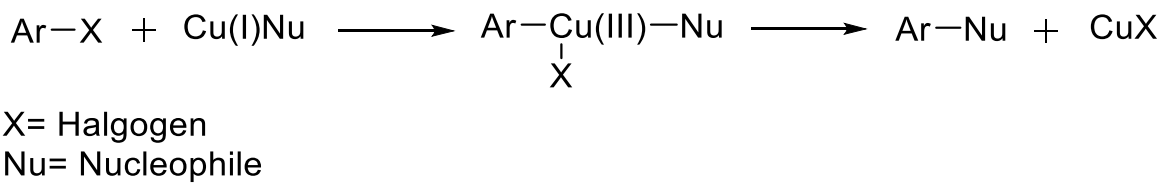


**Scheme 3**: A generalised proposal of the mechanism for a copper catalysed $S_NAr$-reaction [39-40].

### 1.2.3 Buchwald-Hartwig amination

In modern catalytic chemistry, palladium has achieved a predominant role [43]. The first reported article on palladium catalysed C-N coupling was published in 1983 by Kosugi, Masayuki and Migita [44]. They reported coupling of different aryl bromides with *N*,*N*-diethylamino-tributyltin. Unfortunately, the reaction was only successful with a few electronically neutral substrates, which reduced the versatility of the reaction. Ten years later Hartwig and Buchwald began publishing their work on catalysed C-N cross-coupling. First Hartwig published an article reviewing the reactions executed in the Migita article. This article was also the first published proposal of the fact that the aryl-halide was inserted through an oxidative addition [45]. Following this, a series of articles from Buchwald and Hartwig have been published and several new catalyst systems have reached the commercial market. Their contribution has enabled chemist all around the world to perform highly effective C-N cross-coupling reactions. Today Buchwald and Hartwig are renowned chemists within the field of catalytic cross-coupling and their work

on catalysed aminations are used in material- and pharmaceutical science among others [46-47]. In many cases, the catalyst present enables an amination reaction to occur under milder conditions and lower temperatures which can be useful when working with thermolabile structures [48]. An illustration of a current understanding of the Buchwald-Hartwig cross-coupling ,mechanism is presented in Scheme 4.

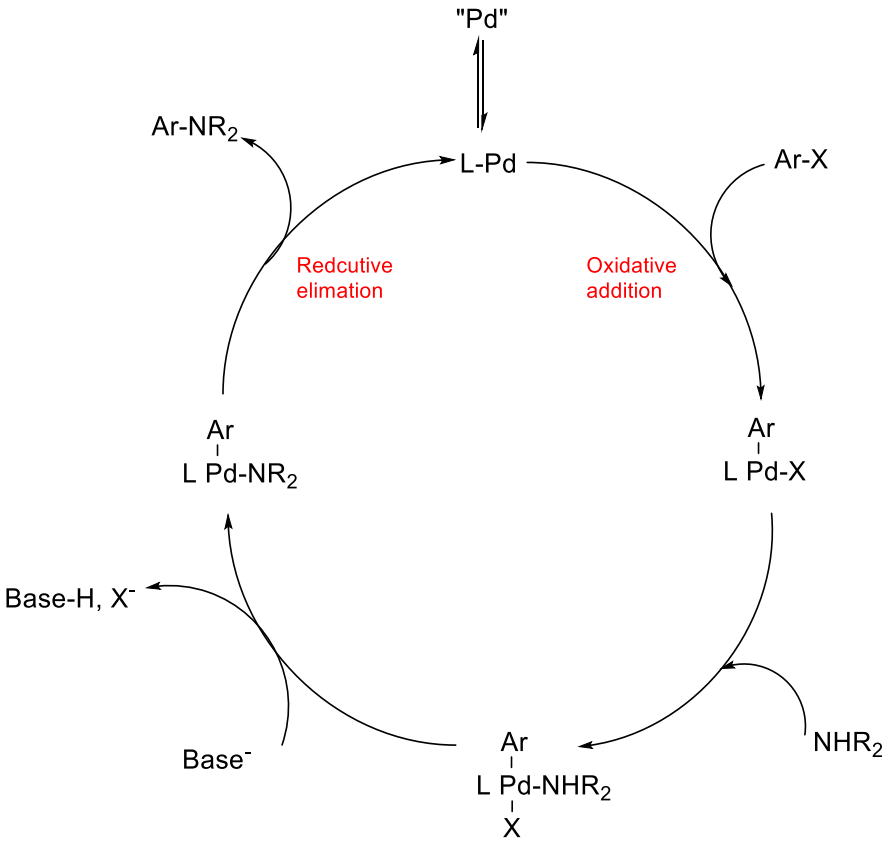


**Scheme 4**: A presentation of the Buchwald-Hartwig amination cycle, adapted from Driver et al.[49] and Sunesson et al. [50].

There are two potential challenges with the Buchwald-Hartwig cross-coupling reaction. The first potential issue is a beta hydride elimination that can compete with the reductive elimination [51-52]. This unwanted side reaction yields an imine that is detached from the Ar-Pd-complex. Racemization of the amine functionality is another issue that has been observed [53-54]. A reported solution to the potential problem of racemization is the use of appropriate catalyst systems with the ligands BINAP and Xantphos [54-55].

## 1.3 Suzuki coupling

The Suzuki coupling reaction is a reaction where new C-C bonds are formed. This is a much applied reaction, and is an important method for the formation of biarylic compounds [56]. A palladium-based catalyst system is added to couple an organic halide with an organoborane compound [57]. Akira Suzuki and his associates published the first article on these reactions in 1979 where tetrakis(triphenylphosphine)palladium(0) catalysed the coupling of alkenyldisiamylboranes with 1-alkenyl halides [58]. In 2010 Suzuki, Heck and Negishi were awarded the Nobel Prize in chemistry for their contribution to "*Palladium-catalyzed cross-couplings in organic synthesis*" [59-60]. Today the Suzuki coupling reaction is considered as one of the most important procedures for biaryl synthesis. Biarylic structures can be found in pharmaceuticals, natural products and agrochemical products, making the Suzuki reaction highly useful for industrial use [59, 61].

### 1.3.1 Suzuki coupling mechanism

The complete mechanism of the Suzuki reaction was not known when the first article was published, but Suzuki early suggested that there was a transmetallation step involved [62]. A modern proposal for the reaction mechanism visualised with the base scaffold for this thesis (**4**) is presented in Scheme 5. Through this section, the different steps of the reaction will be presented in detail based on the presentation in Scheme 5.

**Oxidative addition** is a reaction between the catalytically active $L_nPd^0$ and the aryl halide. This step is the initiator of the catalytic cycle. An oxidation of the palladium occurs, which changes the oxidation state from $Pd^0$ to $Pd^{II}$, and there is a reduction of the aryl halide. This reaction decreases the electron density of the metal, while increasing it for the aryl halide. The product of this reaction is the organopalladium complex **III** [63]. There are still disputes on the Suzuki coupling mechanism, but the oxidative addition is often regarded as the rate determining step [64-65].

**Metathesis** is the process where the iodine in the **III** species is exchanged with an OH-group. This exchange gives the more active intermediate **IV** which will accelerate the following transmetallation step [66].

**Transmetallation** features the insertion of an aryl functionality coupled to a boron species, Ar-$B(OR)_2$ onto the palladium of **IV**. The exact mechanism of this step is still under discussion. What is known is that base is required, and by this fact it is hypothesised that base is needed to activate the organoboron compound [65]. It has also been discovered that the choice of base and the base counter ion is crucial for the reaction rate of this step [67]. One proposal of different bases/ counter ions and their relative efficiency is as follows:

$$OH^- > CO_3^{2-},\ Ag^+ > nBu_4N^+ > K^+ > Cs^+ > Na^+$$ [68].

**Reductive elimination** is the final step of the catalytic cycle. It is in this step that the new C-C bond is formed in the biarylic product **VI**. The palladium catalyst is reduced so that the active $Pd^0$ catalyst (**I**) can regenerate and enter a new catalytic cycle.

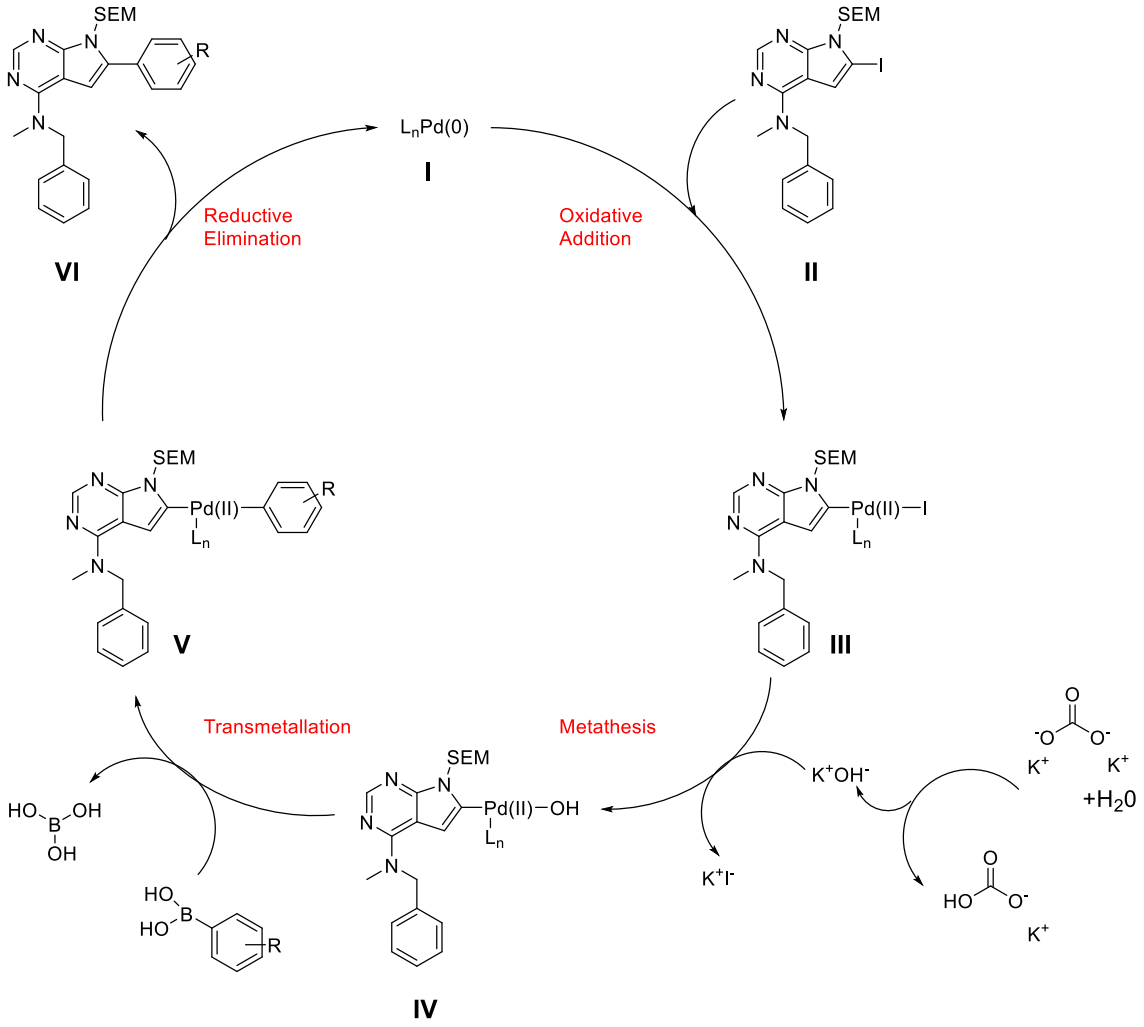


**Scheme 5**: A mechanistic overview of the Suzuki cross-coupling reaction.

### 1.3.2 Catalyst systems and ligands

In the Suzuki coupling reaction, a palladium source with ligands is used. These two components combined make up a catalyst system. The efficiency of the catalyst system can be improved by altering the size, shape and electronic properties of the ligands [69]. The palladium with associated ligands influence the reaction rate both in the oxidative addition step and the transmetallation (see Scheme 5). Tetrakis (triphenylphosphine)palladium(0), was the first reported catalyst system to be used in a Suzuki coupling reaction, and it is still a useful catalyst system today [58, 62].

For a long time triarylphosphines were the most used ligands, but into the 21th century, several new ligands have reached the market. The development of ligands that can enhance palladium activity have been one of the most important innovations to increase the efficiency of palladium

catalysed cross-coupling reactions. Especially phosphine based ligands that are bulky, and electron donating have become widely used. These ligands can enhance both selectivity and efficiency of the Suzuki reaction [70]. The development of new catalyst and ligands have made previously impossible coupling reactions possible. New catalysts has also made it possible to execute known reactions at lower temperatures and with lower catalyst loading [71]. Some of the palladium catalysts and ligands that are commercially available are presented in Figure 8.

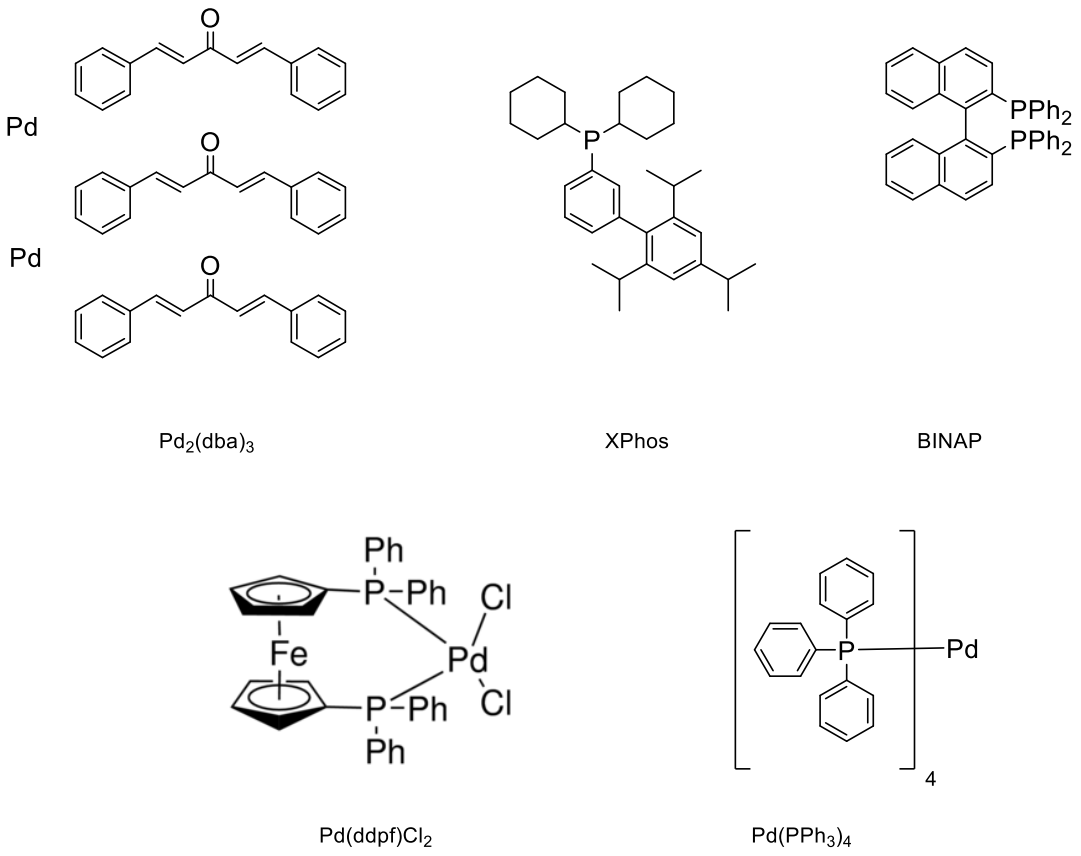


**Figure 8**: The chemical structure of different palladium catalysts and ligands used for Suzuki cross-coupling reactions.

## 1.4 Protective groups for pyrroles

Pyrrole derivatives are found in many natural products and pharmaceuticals and is a constituent of important compounds such as chlorophyll [72]. When performing synthesis on the pyrrolopyrimidine scaffolds it is often useful to insert protecting groups to hinder side reactions. The pyrrolopyrimidine has a proton at N-7 that can be removed under basic conditions. The effect of the N-7 deprotonation is an increased electron density on C-4 due to resonance effects as is shown in Scheme 6 [73]. The increased electron density will decrease the electrophilicity at C-4, thus making nucleophilic attack on this position less favourable. Because of this potential issue, it is wise to introduce a protecting group to N-7.

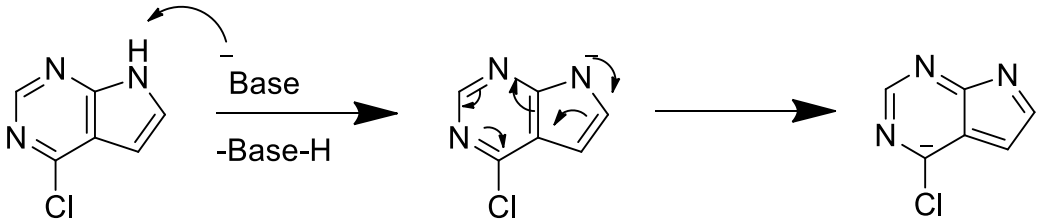


**Scheme 6**: The mechanism explaining increased electron density at C-4 due to deprotonation of N-7.

Several protecting groups with different properties can be applied for pyrrole protection. Some of the alternatives are presented in Figure 9. A widely applied class of protecting groups are the *N*-sulfonyl protecting groups. Some examples are benzenesulfonyl (Bs), methanesulfonyl (Ms) and toluensulfonyl (Ts). Benzenesulfonyl is a protecting group that has an electron withdrawing-effect on the aromatic system making the α-position more electrophilic and therefore more susceptible to an $S_NAr$-reaction with a nucleophile [74]. The Bs protecting group is typically removed using an alkaline hydrolysis procedure with for example NaOH or KOH [75].

2-(Trimethylsilyl)ethoxymethyl (SEM) is a protective group that has been applied in previous work of the research group when pyrrole chemistry has been performed [5]. One of the advantages with this group is its resistance towards oxidation and stability under basic and slightly acidic conditions [76-77]. When reacting the pyrrole with a base, a nitrogen anion is formed. This nitrogen

is highly nucleophilic and can react with 2-(trimethylsilyl)ethoxymethyl chloride through an $S_N2$-type reaction [78-79]. An $S_N1$-type reaction is also possible, but is much less favoured. Another advantage with the SEM-group is that it can have a directive effect in addition to being a protective group [74].

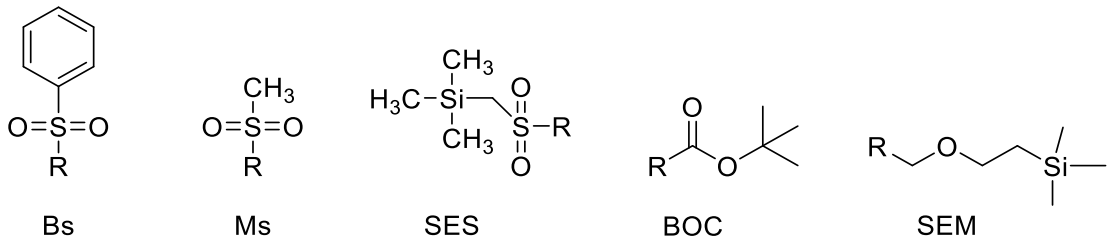


**Figure 9**: Potential protecting groups for pyrrole protection.

Different methods can be used when removing the SEM-group. One common procedure is to use TFA in an appropriate solvent [5, 79]. Milder protocols are also reported. Deprotection by lithium tetrafluoroborate is one example [80]. The two approaches mentioned utilise temperatures of 50 °C or more. There are also reports of SEM-removal executed at low temperatures. SEM-removal by tin tetrachloride have been reported to give good yields at 0 °C [81]. The exact mechanism for the SEM-deprotection is still under discussion. Two proposed mechanisms are given in Scheme 7. Both of these mechanisms are based on the presence of fluorine. TFA is a potential fluorine source. Which deprotection protocol that should be applied is dependent on the sturdiness of the compound and which functional groups are present.

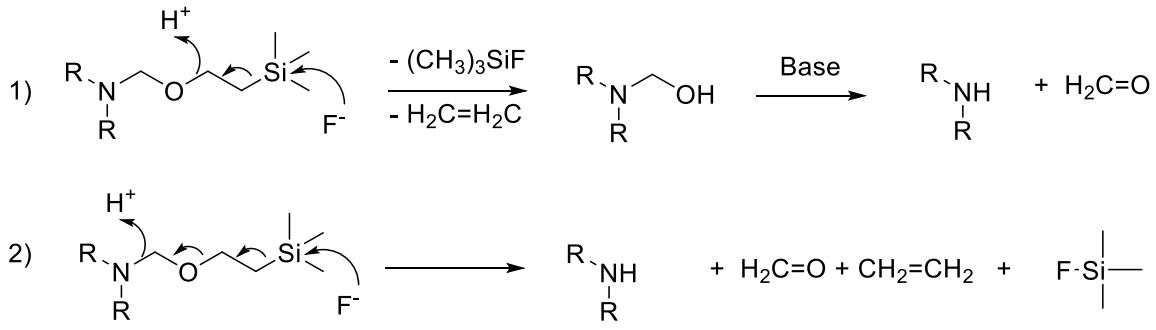


**Scheme 7**: Two proposed mechanisms for deprotection of SEM-protected pyrroles [77, 82].

# 2 Results and discussion

The goal for this master thesis was to synthesise several previously unknown pyrrolopyrimidines as potential CSF-1R inhibitors. All of the new compounds would be based on a pyrrolopyrimidine scaffold with an amine substituent on C-4. Further, different arylboronic acids and one arylboronic ester would be used to couple different aryl groups on C-6. These compounds could either be subjects to post modifications or direct SEM-deprotection. Previous results from the research group had shown that long solubilising tails on the C-6 substituent could enhance the compounds binding properties into the ATP pocket of CSF-1R [5, 7]. Such tails can also increase the aqueous solubility of the compound. Solubility is important for an effective distribution *in vivo*, which is one of the key features of a well-functioning drug. Therefore, an effort was made to synthesise different compounds with ether tails in the *para* and *meta* position of the aryl moiety on C-6. Compounds with methoxy groups in the same positions were also included in the target compound library. Aryl groups with hydroxyl substituents have also shown promising results and were therefore included in the syntheses plans. A general structure for the target compounds is presented in Figure ***10***.

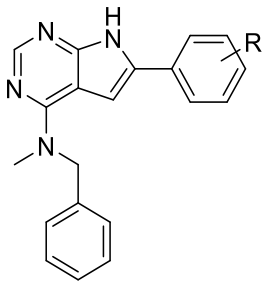


**Figure 10**: The general structure of the target compounds.

The results and discussion section is divided into six sub sections. Sub section 2.1 presents synthesis of the starting material. Sub section 2.2 covers all of the executed Suzuki coupling reactions. The third sub section concerns a Williamson ether synthesis. Following this is a section describing the deprotection experiments (2.4). Sub section 2.5 presents a proposal of assigned chemical shifts ($^{1}$H and $^{13}$C) for the synthesised compounds and the final sub section covers the results obtained from the biological assays (2.6).

## 2.1 Preparation of starting materials

Compound **4** has been the starting material for all the potential inhibitors synthesised in this thesis. This compound was not commercially available and therefore had to be synthesised. This was done through a three-step procedure where the first step was to alkylate the pyrrole nitrogen of **1** with a SEM-protecting group. The second step was to iodinate C-6 before the final step was a thermal amination to introduce an amine functionality at C-4.

In the first step, NaH was used as a base to deprotonate N-7 before SEM-Cl was added as an electrophile to initiate an alkylation of the nitrogen. This yielded the protected intermediate **2**. The reaction was performed under inert conditions at 0 °C. Procedures executed by Han *et al.* [6] and Liang *et al.* [83] were used as reference and the reaction conditions for the synthesis are presented in Scheme 8.

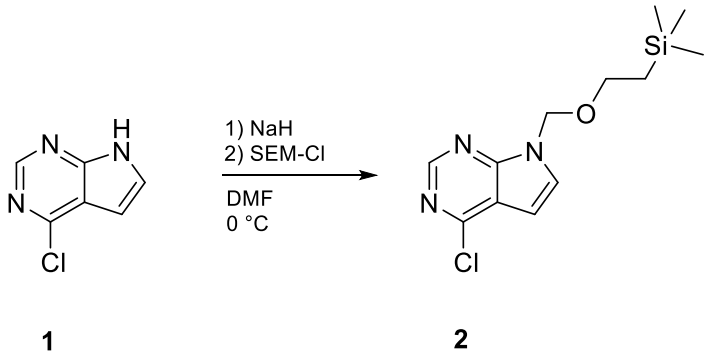


**1** **2**

**Scheme 8**: Reaction conditions for the synthesis of compound **2**.

The synthesis of compound **2** was performed on a 0.2 g scale and a 3.75 g scale. Dry solvents were used to prevent unwanted reactions between water and NaH. After the solvent had been added, the reaction was stirred and cooled for 30 min to ensure complete deprotonation. The SEM-Cl was then added by syringe over 30 min. During the addition, the colour changed from brown to a clear yellow colour. After additional 1.5 h, $^{1}$H NMR and TLC indicated full conversion. The extraction process was quite effective in removing impurities, and the $^{1}$H NMR of the crude material seemed almost as pure as the purified material after silica-gel column chromatography. Compound **2** appeared as a brown oil after silica-gel purification and the yield was 85%.

For the second step, a procedure by Larsen was used as a starting point [7]. First, the substrate was dissolved in THF and cooled to -78 °C using acetone in dry ice. LDA was used as base and elementary iodine dissolved in THF was used to iodinate C-6. The reaction conditions are presented in Scheme 9.

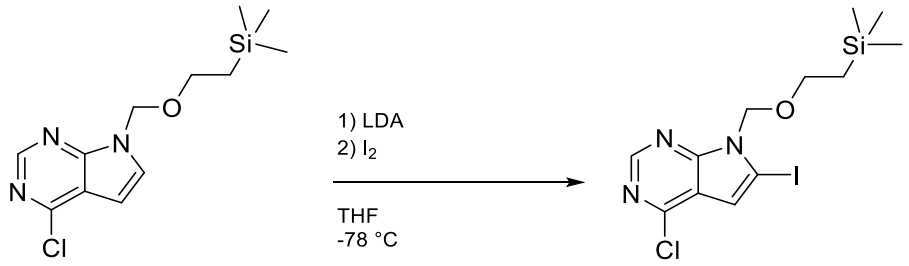


**2** **3**

**Scheme 9**: Reaction conditions for the synthesis of compound **3**.

Since compound **3** was needed for the synthesis of **4**, which was the starting material for all of the Suzuki coupling reactions it was synthesised three times. Results from all the experiments can be found in Table 1. All of the three reactions utilised a syringe pump to ensure a slow, but continuous addition of both LDA and iodine. Due to the presence of the SEM-group and its *ortho* directing effect, there was both a selective deprotonation and iodination of C-6 [7]. During the course of the reaction, there was a colour change from blank to caramel brown to dark after completed $I_2$ addition. Only the 4 g scale reaction (entry 1) gave a satisfying conversion and yield.

It was experimented with the use of recrystallization with $CH_3CN$ as a purification method on half of the crude product from the 4 g scaled reaction. The crystals that were isolated were pure, but analyses of the mother liquor showed a significant amount of product. Therefore, the mother liquor was concentrated and purified with a silica-gel column. This gave the same purity as the recrystallization and no significant loss of product during the process. Combining the pure product gave a total yield of 81%. The second reaction was a less successful experiment. After completed iodine addition and 1.5 h of stirring, the conversion was estimated to be 64% (estimated by $^1$H NMR). When the mixture had stirred for two more hours, there was no significant change in the conversion and it was decided to initiate the work up. It was quite easy

to separate the product and the starting material with silica-gel column chromatography. The recovered starting material was used for the third experiment, which gave a bit better conversion and yield, but still quite worse than the first experiment.

One potential explanation for the low conversion can be the presence of water in the solvent. In the most high yielding reaction (entry 1), the solvent was retrieved from a solvent drying machine while the next reaction (entry 2) did not apply solvents from this machine. THF from an open bottle was put on molecular sieves for 30 min, but this might not have been enough. In addition, only 1.3 eq. of LDA was added compared to 1.5 eq. in first reaction. These two factors in combination could explain the low conversion. Water has a low molar mass and therefore small amounts of water can interact with a relatively large amount of LDA. In the last reaction (entry 3), the amount of LDA was once more increased to 1.5 eq. and solvents were retrieved from a drying machine. Still, both the conversion and the yield was not satisfying. An effort was made to increase the conversion by adding more LDA followed by more iodine but the wanted effect was not achieved. A poor LDA solution with a low molarity might be an explanation to the problems experienced in the two last reactions (entry 2 and 3) which both applied LDA from the same bottle. A summary of the results is given in Table 1.

**Table 1**: Results from the synthesis of compound **3**.

| Entry | Scale (g) | Reaction time (h)[a] | State and colour | Conversion (%)[b] | Yield (%) | Melting point (°C) |
|---|---|---|---|---|---|---|
| 1[c] | 4 | 1.5 | White solid | >99 | 81 | 68-70 |
| 2 | 5.25 | 3.5 | White solid | 66 | 52 | 68-70 |
| 3 | 1.47 | 3.5 | Brown solid | 77 | 60 | 67-69 |

[a] Reaction time after finished $I_2$-additon.
[b] Conversion estimated by $^1$H NMR.
[c] Experiment executed fall 2016 [84].

As presented in Section 1.2, the most common approach in the group has been to insert an amine functionality at C-4. This was also done for this thesis. The same amine was utilised for all of the target compounds. The last step of the three-step procedure was a thermal amination

where *N*-benzylmethylamine was inserted at C-4 of the pyrrolopyrimidine scaffold. This reaction was only tested with the SEM-protected pyrrolopyrimidine **3**. Previous results have shown that this amination with an unprotected scaffold can be unfortunate [7]. The three experiments were executed with *n*-butanol as solvent and was heated on an oil bath at 125 °C or 135 °C. The reaction conditions for the reaction are presented in Scheme 10.

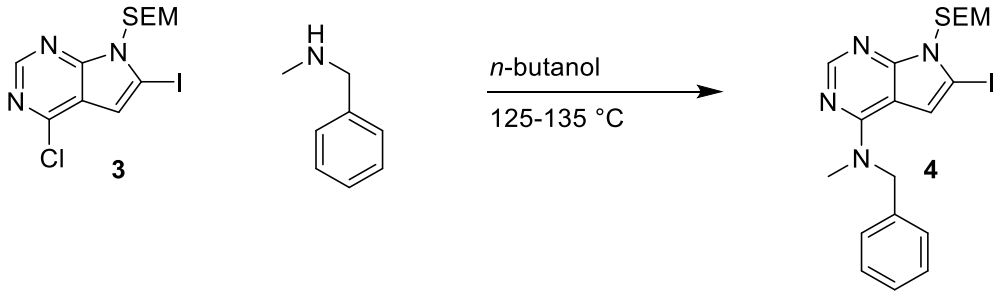


**Scheme 10**: Reaction conditions for the synthesis of compound **4**.

The amination was executed in three different scales (100 mg, 1 g and 2.7 g scale). All reactions were clean and relatively fast. After 5, 4 and 3.5 h respectively, there was a full conversion and only one product was formed as seen by TLC analysis and $^{1}$H NMR. For the 1 g scale reaction, the temperature was reduced to 125 °C. This alteration did not seem to affect the reaction time. Still, it must be said that the first analysis of all these three reactions were made quite late and there could be differences in reaction time. It might have been possible to lower the temperature even more. Still, the quality of the product was equally good at both temperatures, so there was no need to lower the temperature further. Purification by silica-gel column chromatography was quite simple for both batches. In the 100 mg scale reaction, the product was a slightly yellowish oil while the 1 and 2.7 g scale reaction gave an off-white solid when it was dried, and the melting point was 66-68 °C. This difference in physical state is probably due to differences in the impurity profile. Still, additional impurities in the 100 mg scaled reaction was not traceable in the $^{1}$H NMR spectrum. Good yields were attained in all three reactions. A summary of the results is presented in Table 2.

**Table 2**: Results from the synthesis of compound **4**.

| Scale (g) | Reaction time (h) | State and colour | Yield (%) | Melting point (℃) |
|---|---|---|---|---|
| 0.1 | 5 | Yellow oil | 88 | - |
| 1 | 4 | Off white solid | 91 | 66-68 |
| 2.7 | 3.5 | Off white solid | 97 | 66-68 |

## 2.2 Suzuki coupling reactions

### 2.2.1 Suzuki coupling of (4-methoxyphenyl)boronic acid.

This compound had not previously been synthesised and could be a potential inhibitor after SEM-deprotection. The procedure for this experiment and all the following Suzuki coupling reactions were based on previous work by Han *et al.* [5] and Bugge *et al.* [85]. This reaction was used to evaluate different catalyst systems to decide which one should be used for all of the following coupling reactions. The 4-methoxyphenylboronic acid (**5a**) is an electron rich boronic acids. This makes it a good model substrate since such boronic acids give high reaction rates when combined with electron deficient heteroaryl halide [71]. Three different catalyst systems were tested, and the results are presented and discussed in this section. A general scheme for the coupling reaction is presented in Scheme 11.

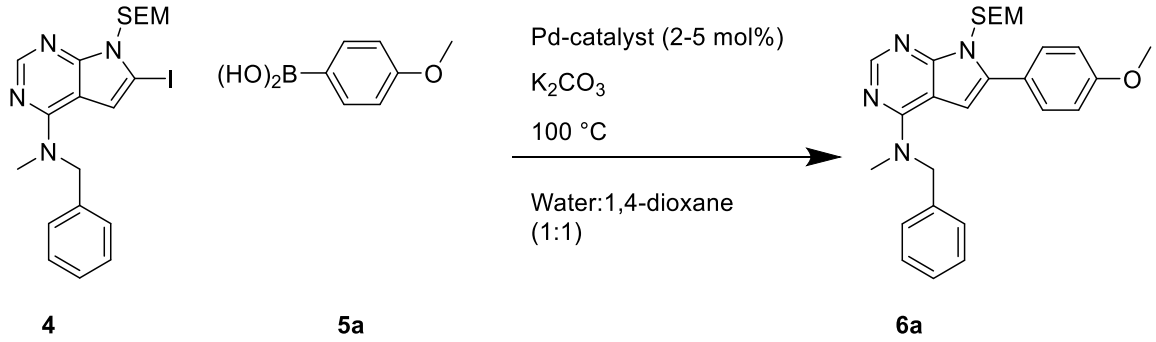


**Scheme 11**: A general overview of the conditions tested for the synthesis of compound **6a**.

The first catalyst to be tested was the Xphos system, which has been one of the frequently used catalysts in publications by our research group [5,7,53]. Analysis after 15 min indicated full conversion and formation of one product. Due to the use of 1.2 eq. of boronic acid, some additional signals were seen in the $^1$H NMR spectrum of the crude product, but the residue of boronic acid was easily removed by silica-gel column chromatography. Possibly, the reaction would be just as effective with 1.1 or 1.05 eq. of arylboronic acid. The XPhos/ XPhos Pd G2 system is a relatively expensive compared to other options. Even though it gave good results, it was reasonable to investigate if other catalysts could give similar results for a lower cost. $Pd_2(dba)_3$ and $Pd(dppf)Cl_2$ are two other catalyst that have been successfully applied for Suzuki coupling reactions by members of the research group [5, 85].

Experiments with $Pd(dppf)Cl_2$ and $Pd_2(dba)_3$ were performed to evaluate their efficiency compared to XPhos. Both these reactions proved themselves highly efficient and full conversion was reached after 15 min (as seen by $^1H$ NMR). For the $Pd(dppf)Cl_2$ reaction, a bumping in the rotary evaporator occurred, leading to a substantial loss of product and thereby a low yield. The reaction with $Pd_2(dba)_3$ had a crude weight of 95 mg (99%), but the crude product had a strong black colour, so it was clear that some palladium was present. After silica-gel column chromatography, the black colour disappeared and the isolated yield was 71%. Comparing these two procedures considering conversion of the starting material, they seemed equally efficient. Still there were more by-product signals in the crude $^1H$ NMR spectra of the reaction using $Pd(dppf)Cl_2$. These by-products could not be observed by TLC analysis. Since the reaction with $Pd_2(dba)_3$ was highly effective, an experiment with a reduced catalyst loading (2 mol%) was performed. This reaction also had full conversion after 15 min.

After executing four experiments with three different catalysts, it was decided to terminate the optimization process. The cheapest of the three catalyst systems ($Pd_2(dba)_3$) proved itself highly efficient for the Suzuki coupling onto substrate **4**. Since the same substrate would be used for all the Suzuki couplings, it was hypothesised that the following Suzuki couplings could also be efficient using $Pd_2(dba)_3$. A summary of the obtained results for the catalyst optimization is presented in Table 3.

**Table 3**: Results of the catalyst system optimization and synthesis of compound **6a**.

| Entry | Catalyst | Time (min) | Conversion (%)[a] | Yield (%) | State |
|---|---|---|---|---|---|
| 1 | Xphos/Xphos Pd G2[b] | 15 | >99 | 77 | Transparent oil |
| 2 | $Pd(dppf)Cl_2$[b] | 15 | >99 | 31[d] | Transparent oil |
| 3 | $Pd_2(dba)_3$[b] | 15 | >99 | 71 | Transparent oil |
| 4 | $Pd_2(dba)_3$[c] | 15 | >99 | 70 | Transparent oil |

[a] Conversion estimated by $^1H$ NMR.
[b] Catalyst loading 5 mol%.
[c] Catalyst loading 2 mol%.
[d] Low yield due to "lab accident".

### 2.2.2 Suzuki coupling of [4-(2-methoxyethoxy)phenyl]boronic acid

Results obtained by our research group have shown that solubilising tails on the C-6 substituent can give high inhibition activity and increased solubility. In the work published so far, amine solubilising tails have been most researched. To expand the library of compounds containing solubilising tails, efforts were made to synthesise new molecules with ether-tails as an alternative to the amine tails. [4-(2-Methoxyethoxy)phenyl]boronic acid (**5b**) with an ether tail in the *para* position was commercially available. The reaction conditions for the coupling reaction are presented in Scheme 12.

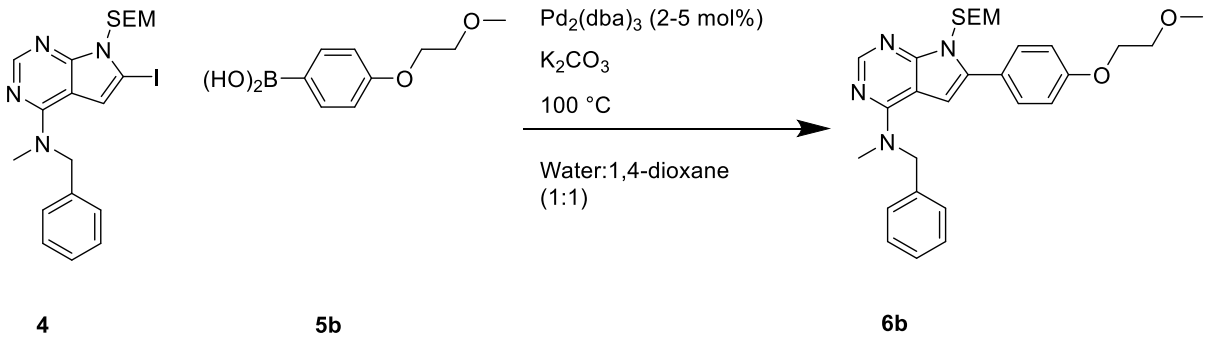


**Scheme 12**: Reaction conditions for the synthesis of compound **6b**.

The first experiment was performed with a catalyst loading of 5 mol% on a 50 mg scale. After 15 min, the colour of the mixture shifted from black/ dark green to a clear yellow colour. This colour change is most likely an indicator of full conversion. A TLC analysis at this point indicated full conversion, and this was confirmed by $^{1}$H NMR. The purification process was also straightforward and gave 78% yield. Since the reaction with 5 mol% catalyst loading was highly effective, a follow-up reaction (150 mg scale) was run with 2 mol% catalyst loading. Reducing the catalyst loading did increase the reaction time from 15 min to 3 h. After 1.5 h, the ratio between product and starting material was 1:0.16. Leaving the reaction for one and a half more hours resulted in full conversion. Even though a lower catalyst loading increased the reaction time, it is still a relatively fast reaction. In addition, both the reactions gave equal yields and purities. The data collected from these experiments indicate that the reaction is highly efficient with the formation of one product. Full conversion and good yields are obtained with both 5 mol% and 2 mol% catalyst loading. A summary of the achieved results from the two reactions is given in Table 4.

**Table 4**: Results from the synthesis of compound **6b**.

| Entry | Catalyst | Time (h) | Conversion (%)[a] | Yield (%) | State |
|---|---|---|---|---|---|
| 1 | $Pd_2(dba)_3$[b] | 0.25 | >99 | 78 | Transparent oil |
| 2 | $Pd_2(dba)_3$[c] | 3 | >99 | 79 | Yellow oil |

[a] Conversion estimated by $^1$H NMR.
[b] Catalyst loading 5 mol%.
[c] Catalyst loading 2 mol%.

### 2.2.3 Suzuki coupling of 4-hydroxyphenylboronic acid

It was of the research group's interest to synthesise compounds with different substituents on the C-6 aryl group. The further goal was to be able to compare compounds containing an ether-, methoxy-, hydroxyl-substituent or no substituent at all, to see how these variations affected the potency of the kinase inhibitor. A coupling was made with 4-hydroxyphenyl-boronic acid **5c**, using $Pd_2(dba)_3$ as catalyst. The conditions for the reaction were the same as in previous experiments and are presented in Scheme 13.

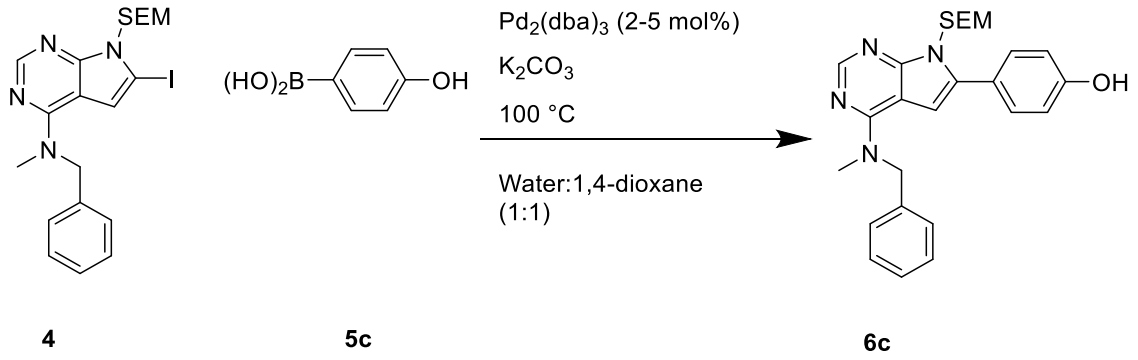


**Scheme 13**: Reaction conditions for the synthesis of compound **6c**.

The first experiment was conducted with a 5 mol% catalyst loading on a 100 mg scale. The reaction was highly efficient, and a single product was formed with complete conversion after 15 min. Conversion was monitored by $^1$H NMR and observation of the C-2 proton. It shifted from 8.29 ppm in the starting material to 8.39 ppm in the product. $^1$H NMR indicated the presence of one by-product, with a signal at 8.64 ppm, assumed to be the C-2 proton of a related pyrrolopyrimidine of some sort. After the confirmation of full conversion, the reaction was still kept at 100 °C and samples were analysed after 1.5 h and 3.5 h. No new by-products were

formed in this period of time, which indicates a stable, non-labile system. The relative amount of the impurity did not increase or decrease over time. After purification by silica-gel column chromatography, the signal at 8.64 vanished completely from the mixture. A summary of the results for the two executed experiments is presented in Table 5.

**Table 5**: Results from the synthesis of compound **6c**.

| Entry | Catalyst | Time (h) | Conversion (%)[a] | Yield (%) | State |
|---|---|---|---|---|---|
| 1 | $Pd_2(dba)_3$[b] | 0.25 | >99 | 69 | Pale yellow oil |
| 2 | $Pd_2(dba)_3$[c] | 3 | >99 | 79 | Yellow oil |

[a] Conversion estimated by $^1$H NMR.
[b] Catalyst loading 5 mol%.
[c] Catalyst loading 2 mol%.

### 2.2.4 Suzuki coupling of 3-methoxyphenylboronic acid

In Section 2.2.1, 2.2.2 and 2.2.3 all of the coupled arylboronic acids had substituents on the *para* position. It was also of the group's interest to synthesise kinase inhibitors with the same substituents on the *meta* position of the C-6 aryl group to expand the structure-activity relationship data on these substrates. A reaction scheme for the first coupling reaction is shown in Scheme 14.

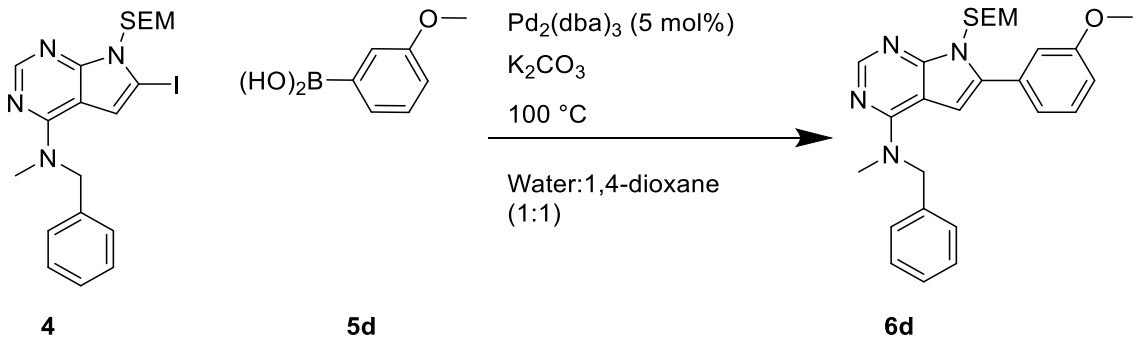


**Scheme 14**: Reaction conditions for the synthesis of compound **6d**.

The Suzuki coupling was first run on a 100 mg scale with a catalyst loading of 5 mol%. After 15 min, $^1$H NMR showed that 28% of the starting material was still present, but after 1.5 h, full conversion was indicated. Even though full conversion was reached, the reaction was left at

reflux for four more hours to evaluate the stability of the product under the given reaction conditions. No major changes were observed when comparing the $^{1}$H NMR analyses after 1.5 h and 5.5 h. This fact indicates that the product is stable under the reaction conditions. Both the extraction and purification process proceeded as planned and the yield was 71% of a yellow oil/ sticky film.

### 2.2.5 Suzuki coupling of 3-hydroxyphenylboronic acid

To continue the synthesis of compounds with *meta*-substituted aryl rings on C-6, 3-hydroxphenylboronic acid **5e** was coupled to substrate **4**. This compound was planned used in two ways. Firstly, compound **6e** would be deprotected and assayed for its CSF-1R inhibition activity. Secondly, compound **6e** was to be used in a Williamson ether synthesis where the alcohol functionality could work as a nucleophile in an $S_N2$ reaction. Three experiments were executed with three different catalyst loadings (1, 2 and 5 mol%) and different scales (100 mg and 150 mg scale). The general conditions for the executed syntheses are presented in Scheme 15.

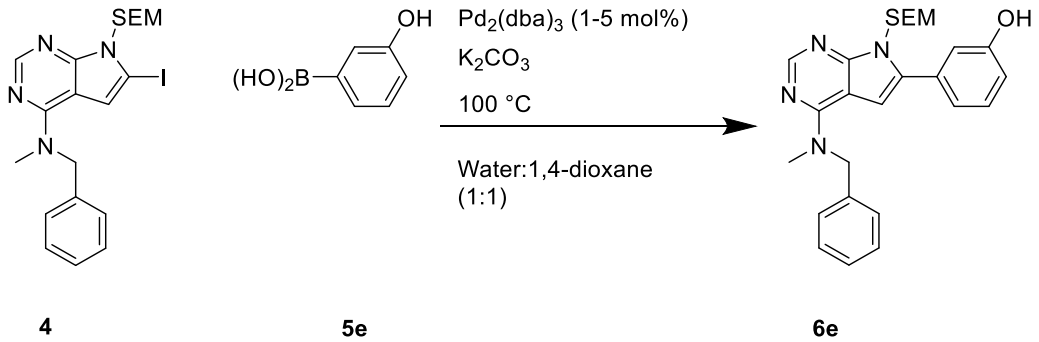


**Scheme 15**: Reaction conditions for the synthesis of compound **6e**.

A useful indicator for conversion for this reaction was colour change. Right after the catalyst and substrate were diluted with the solvents, the mixture had a strong dark colour. After some time the colour changed from black to yellow. Comparing the time of colour change with $^{1}$H NMR analysis indicated that the colour change occurred approximately at the same time as full conversion was reached. All of the three reactions were completed after 1.5 h. The analysis after 15 min showed the presence of starting material with ratios (relatively to the product) between 25:75 and 15:85 for the three experiments. The colour change from black to yellow

occurred between 30 min and 1 h and the fastest colour change occurred in the reaction with the highest catalyst loading as was expected. When full conversion was observed by $^1$H NMR, the rest of the procedure proceeded as planned. The work up appeared as effective and the solubility of **6e** in EtOAc seemed to be good. All crude mixtures were purified by silica-gel column chromatography and most of the impurities were removed. The results from the three experiments are presented in Table 6.

**Table 6**: Results from the synthesis of compound **6e**.

| Entry | Catalyst | Time (h) | Conversion (%)[a] | Yield (%) | State |
|---|---|---|---|---|---|
| 1 | $Pd_2(dba)_3$[b] | 1.5 | >99 | 59 | Transparent oil |
| 2 | $Pd_2(dba)_3$[c] | 1.5 | >99 | 81 | Transparent oil |
| 3 | $Pd_2(dba)_3$[d] | 1.5 | >99 | 66 | Transparent oil |

[a] Conversion estimated by $^1$H NMR.
[b] Catalyst loading 5 mol%.
[c] Catalyst loading 2 mol%.
[d] Catalyst loading 1 mol%.

### 2.2.6 Suzuki coupling of 2-(3-((1,3-dioxolan-2-yl)methoxy)phenyl)-4,4,5,5-tetramethyl-1,3,2-dioxaborolane

To expand the library of oxygen containing compounds even further, an effort was made to insert an aryl group with an acetal component onto C-6. Firstly, compound **6f** and its deprotected analogue was targeted to investigate how the "tail" with three oxygen would interact with the ATP binding site of the CSF-1R. All of the oxygen are potential interaction points for hydrogen bonding between the compound and the amino acids in the kinase. Secondly, the acetal group could allow for different transformations after deprotection. The Suzuki reaction was done with the same solvents and catalyst as the previous Suzuki reactions. The conditions for the reaction are presented in Scheme 16.

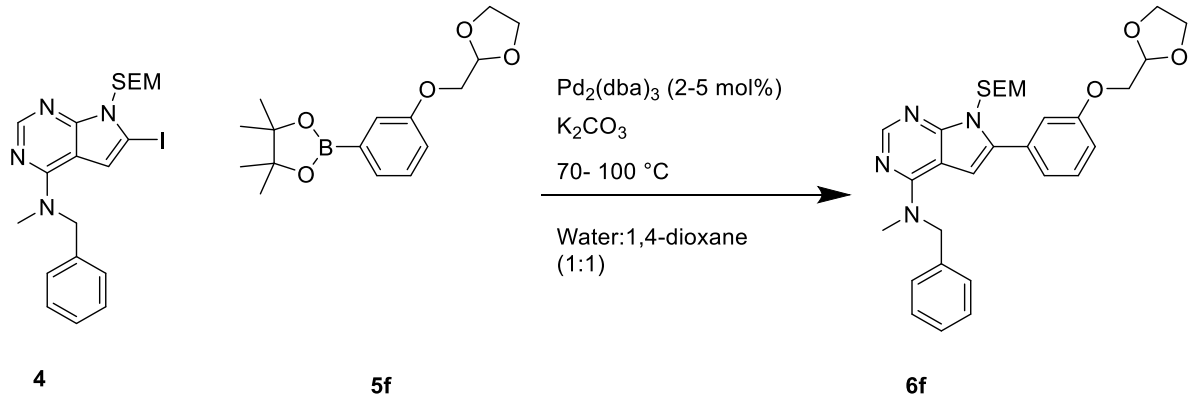


4 5f 6f

**Scheme 16**: Reaction conditions for the synthesis of compound **6f**.

For the first experiment, the temperature was set to 100 °C. The reaction was monitored with $^{1}$H NMR analyses after 15 min, 1.5 h and 3h. What was observed was that the reaction reached full conversion already after 15 min. After 3 h, two new signals had appeared in the shift region of the proton on C-2 (8.4 ppm). A suspected problem is the labile nature of the acetal ring. The acetal can be subject to a hydrolysis, which can yield an aldehyde. Still there was no aldehyde shift seen in the $^{1}$H NMR spectra. The by-product was not isolated. This fact could indicate that the by-product was highly polar and therefore adsorbed strongly to the silica gel. The wanted product was isolated in a total yield of 76% after purification. The structure was confirmed by full NMR characterisation and MS. Still the $^{1}$H NMR showed the presence of some unidentified impurities.

Due to the fast reaction observed in the first experiment (entry 1) it was decided to evaluate the effect of a lower catalyst loading (2 mol%, entry 2) and to lower the temperature while keeping the same catalyst loading (70 °C, entry 3). Analyses of these two reactions showed that it was both possible to lower the temperature and decrease the catalyst loading and still achieve full conversion and decent yields. In the second experiment, the conversion was complete after 1.5 h, but there was still some by-products present. Lowering the catalyst loading from 5- to 2 mol% increased the reaction time with 1.25 h. Still, this reaction time is relatively short and could be considered to be worth it in a cost-focused perspective. Reducing the temperature to 70 °C also gave complete conversion after 3.5 h. An advantage with these conditions was a reduced formation of by-products compared to those reactions run at 100 °C. Even though this was the most “pure” reaction, some by-products could be seen. Most of them disappeared after

purification by silica-gel column chromatography, but some are still present in the spectra that are attached in the appendix (Appendix I). A summary of the syntheses of this compound is found in Table 7.

**Table 7**: Results from the synthesis of compound **6f**.

| Entry | Catalyst | Temperature (℃) | Time (h) | Conversion (%)[a] | Yield (%) | State |
|---|---|---|---|---|---|---|
| 1 | $Pd_2(dba)_3$[b] | 100 | 0.25 | >99 | 76 | Transparent oil |
| 2 | $Pd_2(dba)_3$[c] | 100 | 1.5 | >99 | 77 | Transparent oil |
| 3 | $Pd_2(dba)_3$[b] | 70 | 3.5 | >99 | 72 | Transparent oil |

[a] Conversion estimated by $^1$H NMR.
[b] Catalyst loading 5 mol%.
[c] Catalyst loading 2 mol%.

### 2.2.7 Suzuki coupling of benzo[*d*][1,3]dioxol-5-ylboronic acid

Synthesis of compound **6g** was executed with a catalyst loading of 2- and 5 mol%. Both reactions used degassed water and 1,4-dioxane as solvent, and the temperature was 100 °C. The reaction conditions for the executed experiments are given in Scheme 17.

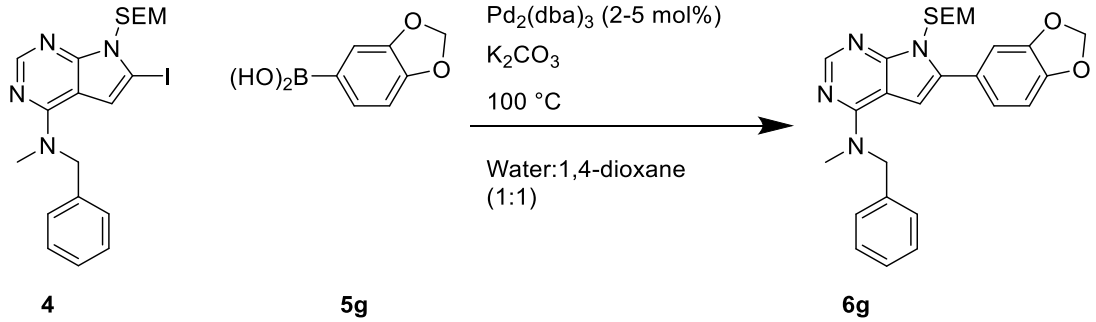


**Scheme 17**: Reaction conditions for the synthesis of compound **6g**.

Both experiments had high efficiency. One major product was formed in a low amount of time (15 min for both reactions). In the crude product of both reactions there seemed to be a

small amount of two by-products. The $^{1}$H NMR signals of these by-products were located in close proximity of the signals of the product at several points in the $^{1}$H NMR spectrum, and the multiplicities were the same. This fact indicates that the formed by-products are derivatives of the wanted product **6g**. Still the amounts of these were relatively small and the estimated ratio between product and by-product was 96:4 (estimated by $^{1}$H NMR). After purification by silica-gel column, the amount was reduced. For the first experiment (5 mol%), the reaction mixture was kept at 100 °C for 3.5 h with analyses after 15 min, 1.5 h and 3.5 h. Full conversion was reached after 15 min and the next analyses showed no significant changes in the spectra and no signs of product degradation. Both experiments gave a transparent oil and the yields were 64% for the experiment with 5 mol% catalyst loading, while the reaction that had 2 mol% catalyst loading achieved 58% yield. The results from the two experiments are given in Table 8 in Section 2.2.8.

### 2.2.8 Summary of Suzuki coupling reactions.

This thesis reports on a number of Suzuki couplings where several arylboronic acids and one arylboronic ester have been applied. Most of the reactions have been successful and excellent conversions and mediocre to good yields (58-81%) were obtained. A summary of the executed Suzuki coupling reactions with $Pd_2(dba)_3$ as catalyst is given in Table 8. In a few of the reactions, by-products were formed and this lowered the isolated yield. It is also assumed that some of the losses occurred during the work up and purification.

**Table 8**: Summary of the performed Suzuki cross-coupling reactions utilising $Pd_2(dba)_3$. Substrate **4** was the starting material in all of the coupling experiments. Catalyst amounts are marked with footnotes.

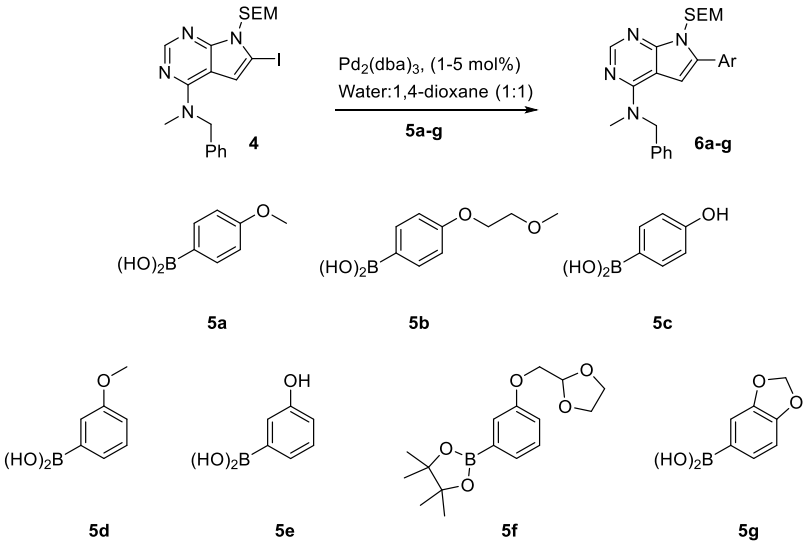


| Entry | Boronic acid/ ester | Catalyst | Scale (mg) | Time (h) | Conversion (%)[a] | Yield (%) |
|---|---|---|---|---|---|---|
| 1 | **5a** | $Pd_2(dba)_3$[c] | 100 | 0.25 | >99 | 70 |
| 2 | **5b** | $Pd_2(dba)_3$[b] | 50 | 0.25 | >99 | 78 |
| 3 | **5b** | $Pd_2(dba)_3$[c] | 150 | 0.25 | >99 | 79 |
| 4 | **5c** | $Pd_2(dba)_3$[b] | 100 | 0.25 | >99 | 64 |
| 5 | **5c** | $Pd_2(dba)_3$[c] | 150 | 1.5 | >99 | 69 |
| 6 | **5d** | $Pd_2(dba)_3$[b] | 100 | 1.5 | >99 | 71 |
| 7 | **5e** | $Pd_2(dba)_3$[b] | 100 | 1.5 | >99 | 59 |
| 8 | **5e** | $Pd_2(dba)_3$[c] | 150 | 1.5 | >99 | 81 |
| 9 | **5e** | $Pd_2(dba)_3$[d] | 150 | 1.5 | >99 | 66 |
| 10 | **5f** | $Pd_2(dba)_3$[b] | 100 | 0.25 | >99 | 76 |
| 11 | **5f** | $Pd_2(dba)_3$[c] | 100 | 1.5 | >99 | 77 |
| 12 | **5f** | $Pd_2(dba)_3$[e] | 100 | 3.0 | >99 | 72 |
| 13 | **5g** | $Pd_2(dba)_3$[b] | 100 | 0.25 | >99 | 64 |
| 14 | **5g** | $Pd_2(dba)_3$[c] | 150 | 0.25 | >99 | 58 |

[a] Calculated by $^1$H NMR.
[b] Catalyst loading 5 mol%.
[c] Catalyst loading 2 mol%.
[d] Catalyst loading 1 mol%.
[e] Catalyst loading 5 mol%, temperature 70 °C.

From the results presented in Table 8 it can be concluded that $Pd_2(dba)_3$ is a suitable catalyst system for several different arylboronic acids and esters when executing Suzuki coupling reactions with substrate **4**. Most of the arylboronic acids and esters used for this thesis have an O-R substituent in the *para* or *meta* position. This give electron-rich arylboronic acids/esters which increases reaction rates compared to electron deficient ones [71]. Since no electron deficient arylboronic acids were tested for this thesis, there is no comparison basis. The catalyst system also gave effective conversions when an OH-group was present on the arylboronic acid (**5c** and **5e**). When these arylboronic acids were used, the reaction time was 1.5 h.

Higher yields could have been achieved with more thorough extraction processes, reducing the size of the samples taken for analysis under the reaction and by upscaling the reactions. Still, most of the reactions were done with tolerable yields.

## 2.3 Post Suzuki coupling modifications

### 2.3.1 Williamson ether synthesis: Synthesis of compound 6h

As previously mentioned, it was of interest to synthesise and isolate pyrrolopyrimidines with ether tails in both the *para*- and *meta* position of the aryl group coupled on the pyrrolopyrimidine's C-6. For the *para* position, a boronic acid containing the wanted ether tail was commercially available. To synthesise a similar inhibitor with the ether tail in the *meta* position, another strategy had to be employed since the needed boronic acid was not commercially available. A Williamson ether synthesis on compound **6e** (see Section 2.2.5) was planned instead. A polar aprotic solvent combined with a strong base and addition of 1-bromo-2-methoxyethane. The experiment was based on a procedure by Eom *et al*. [86], and the reaction conditions are given in Scheme 18.

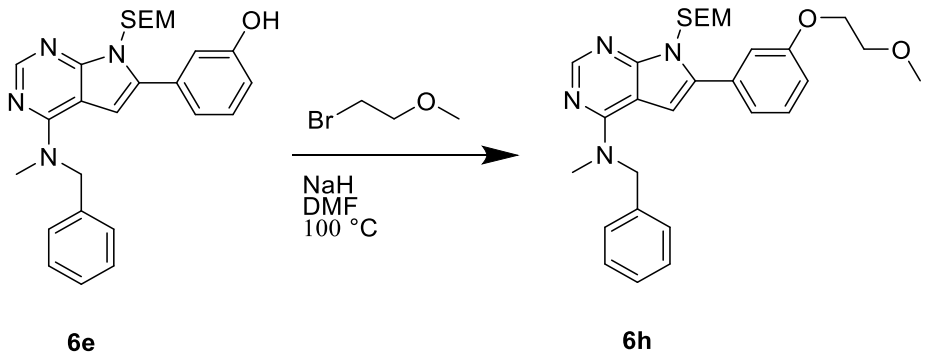


**6e** **6h**

**Scheme 18**: Reaction conditions for the synthesis of compound **6h**

The first $^{1}$H NMR analysis was done after 30 min. This analysis showed a 54% conversion (as estimated by $^{1}$H NMR). When the mixture was kept at reflux for another 1.5 h, there was no notable change in the product amount. To push the conversion further 1 eq. of 1-bromo-2-methoxyethane and base dissolved in DMF was added with a syringe. This had some effect and after 1 h of reflux, the amount of starting material was reduced to 30% (estimated by $^{1}$H NMR). Since the reaction was still incomplete, a final eq. of 1-bromo-2-methoxyethane and base was added and the final amount of starting material was estimated to be 16%. At this point, it was decided to stop the reaction and try to isolate the wanted product. The purification process proceeded as planned and the isolated yield was 45 mg (41% yield) of a transparent oil.

The outcome for this reaction was surprising since $S_N2$ reactions with strong bases and primary alkyl halides works well most of the time [87]. One of the potential issues can be that the base reacted with other components in the mixture. Solvents were fetched from the drying machine, but unfortunate handling can lead to small introductions of water, which can minimize the effect of NaH on the substrate. For the first addition, NaH was added first and the mixture was stirred for some time before the 1-bromo-2-methoxyethane was added. This was done to ensure deprotonation of the substrate **6e** instead of 1-bromo-2-methoxyethane. In the following additions, both the base and 1-bromo-2-methoxyethane was added simultaneously which could lead to deprotonation of the 1-bromo-2-methoxyethane as an alternative to hydroxyl deprotonation. Base induced elimination is a competing reaction, but is most common for secondary and tertiary alkyl halides [88]. If an elimination takes place, one potential by-product is methyl vinyl ether. A proposed mechanism for the formation of this product is presented in Scheme 19

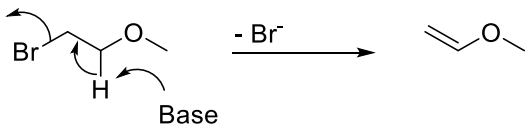


**Scheme 19**: Proposed mechanism for the competing elimination reaction and the formation of methyl vinyl ether.

If methyl vinyl ether was formed, it would not have been possible to detect since it has a boiling point of 6 °C and evaporates out of the solution. Still, the alternative reaction in Scheme 19 is not favourable for primary alkyl halides. In addition to this, deprotonation of the OH-group should be favoured due to the lower pKa-value of the OH-proton. Due to time shortage, no additional experiments were executed. If several attempts were to be made it would be advisable to consider developing a new procedure. Variations in the temperature could be tested, preferably higher temperatures to push the conversion. Different bases could be applied and an alkyl chloride could be examined as an electrophile. Still an alkyl chloride is less reactive in a Williamson ether synthesis and should not be a better option when considering reaction rate.

## 2.4 SEM removal

The final step in the synthetic route towards potential CSF-1R kinase inhibitors was a deprotection of the SEM-protected pyrrole. In most cases, these reactions gave a transformation from an oil/film, to a dry powder with a white or light yellow colour. The same procedure was used for all deprotection reactions. The SEM-protected compound was dissolved in $CH_2Cl_2$ and added an excess of trifluoroacetic acid before this mixture was heated to 50 °C. This mixture was stirred until all of the starting material had been converted (determined by $^1$H NMR). When full conversion was observed, the reaction mixture was concentrated *in vacuo* before the material was dissolved in THF and added saturated aq. $NaHCO_3$. This mixture was stirred at rt for different amounts of time before work up and purification was initiated. A general reaction scheme for the deprotection reactions can be seen in Scheme 20.

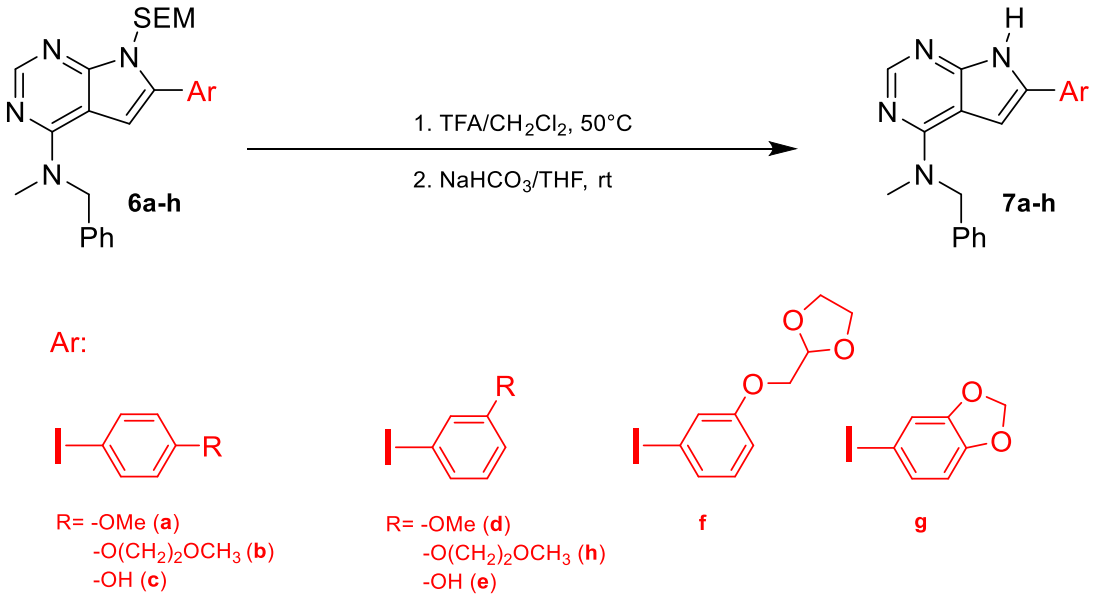


**Scheme 20**: Reaction conditions for the performed deprotection procedures and a presentation of the different aryl groups (**a-h**) present in the intermediates **6a-h** and the target compounds **7a-h**.

$^1$H NMR was used to analyse the conversion progress in the two steps of the deprotection procedure. In many cases, it was easy to monitor the conversion due to the complete disappearance of the SEM-protons, but in some cases, the chemical shifts drifted in a manner that made it more difficult to identify what originated from the starting material and which peak

that originated from the product. A summary of the results from all of the deprotection reactions are presented in Table 9.

**Table 9**: Summary of the deprotection reactions performed. The first step was performed at 50 °C while the second step was done at rt. Reported yields are after purification by one or more silica-gel columns.

| Entry | Substrate | Scale (mg) | Reaction time | | Product | Yield (%) | Mp. (℃) |
|---|---|---|---|---|---|---|---|
| | | | Step 1 | Step 2 | | | |
| 1 | **6a** | 92 | 4 | 20 | **7a** | 85 | 250-252 |
| 2 | **6b** | 123 | 6 | 24 | **7b** | 68 | 217-219 |
| 3 | **6c** | 55 | 4 | 20 | **7c** | 71 | 239-241[a] |
| 4 | **6d** | 67 | 4 | 26 | **7d** | 65 | 210-212 |
| 5 | **6e** | 93 | 10 | 20 | **7e** | 70 | 252-254 |
| 6 | **6f** | 79 | 4 | 20 | **7f** | 40 | 203-205 |
| 7 | **6g** | 56 | 24[b] | 20 | **7g** | 31 | 245-247[a] |
| 8 | **6h** | 42 | 8[b] | 20 | **7h** | 77 | 188-190 |

[a)] Decomposition.
[b)] Additional TFA added.

Early in the thesis work, the analyses of the reactions were a bit challenging due to the use of $CDCl_3$ as NMR solvent. All of the SEM-intermediates **6a-h** were soluble in $CDCl_3$ and this solvent was used for the initial analyses of these compounds. In time, it became apparent that the low solubility of **7a-h** in $CDCl_3$ gave spectra with confusing information that complicated the reaction monitoring. Another problem is that the TMS $^1$H NMR signal in $CDCl_3$ is in close proximity to the trimethylsilyl group of SEM-derivatives. This fact made it harder to decide if the SEM-group was completely removed or not. After some time, $CDCl_3$ was exchanged with DMSO-$d_6$. This gave better and more convincing information. There were different markers that were used to monitor the development of the different reaction. For compound **7a**, **7b** and **7c**, the C-6 aryl groups were *para*-substituted. This fact meant that the four aromatic protons on the aryl group appeared as two doublets in the spectra. These doublets were used to monitor the conversion in the different steps of the reaction. The disappearance of the protons from the

SEM-protecting group was also a highly useful indicator for all of the reactions. After full or partial deprotection, the appearance of the high shift N-H proton was also a conclusive indicator that the product had been formed.

For the synthesis of compound **7g** and **7h**, there were still starting material present after 4 h. To increase the conversion, more TFA was added and this pushed the conversion in the right direction. When no further development was observed, the second step of the procedure was initiated. This completed the reaction in both cases.

Initially, EtOAc was used as the extraction solvent. What became apparent in some of the extractions was that a white solid appeared in the separating funnel, which was insoluble in both the organic phase and the water phase. This solid positioned itself between the two phases. In these cases, the extraction was changed to $CH_2Cl_2$ for the fourth and fifth extraction. This increased the amount of product extracted. Most likely the yields could be even higher with more extraction. Several of the isolated products required relatively larger amount of $CH_2Cl_2$ and some methanol to be completely dissolved.

Purification was done by one or more rounds of silica-gel column chromatography for all compounds. An eluent combination of methanol and $CH_2Cl_2$ was applied, where the amount of methanol varied between 2% and 10 %. None of the crude compounds were easily dissolvable in the eluent used. In most cases, using more methanol was an effective way for dissolving the crude material. Dry loading was therefore used for all of the silica-gel columns. The purification of compound **7a**, **7b**, **7c** and **7h** required two silica-gel columns to reach a satisfying purity.

The general case for all of the deprotection experiments was an increased crystallinity when the SEM-group was cleaved off. All of the substrates were oils, and the isolated products were solids in the form of powders. Initially, the plan was to analyse all of the isolated solids by HPLC analyses. This was not done due to low solubility of the compounds in water and acetonitrile. Therefore, $^1$H NMR analyses were used to determine if the isolated compounds were pure enough to be subjects for bioactivity assays. Integrals of eventual impurities in the spectrum were used to propose the amount relative to the isolated compound.

To summarise it can be said that the deprotection procedures have given results that stretched from good (85%) to low yields (31%). Some of the poorer yields might partially be due to insufficient extractions. Generally, the compounds had high crystalline properties and some of the compound may also have stuck on the column during the purification process. Still, most of the compounds were isolated at high purities as can be seen from the spectra found in Appendix L-S.

## 2.5 Structure elucidation

During the process of confirming the structure of the synthesised products, several different characterisation methods were used. The most powerful tools have been NMR analyses and mass spectrometry. IR analyses have also been utilised, but these analyses were used more as a secondary confirmation source after a finished synthesis and not as a progressive tool during the lab work. This section will present the compounds isolated during the thesis work and their assigned $^{1}$H NMR and $^{13}$C NMR chemical shifts. To assign these shifts as precisely as possible, the following NMR spectroscopic analyses have been used: 1D $^{1}$H NMR, $^{13}$C NMR, 2D $^{1}$H-$^{1}$H COSY, $^{1}$H-$^{13}$C HSQC and $^{1}$H-$^{13}$C HMBC. All of the spectra used for the characterisations are presented in the Appendix. $^{1}$H NMR analyses have been run at 600 MHz and $^{13}$C analyses have been run at 150 MHz. ChemDraw software was used as an assisting source of shift indications. Some of the assumptions made on shielding and deshielding effects by substituents on the C-6 aryl group are based on table values published by Williams and Fleming [89] . The pyrrolopyrimidine scaffold is the base for the numbering system for all compounds. The specific numbering for each compound is presented in the figures shown above the table presenting chemical shifts.

For some of the compounds, comments are given above the table with the assigned shifts, while some are presented without comments when no further comments were found needed.

### 2.5.1 Starting materials

**Compound 2, 3 and 4.**

$^{1}$H NMR chemical shifts for compound **2**, **3** and **4** are presented in Table 10. Compound **4** is the base structure for all the synthesised kinase inhibitors. $^{1}$H NMR spectra can be found in appendix A-C. For compound **4**, $^{13}$C spectra, IR spectra and MS-analysis are also attached.

The proton on position 2 appeared in the same region for all three compound and was easy to identify. There was a shift reduction to for H-2 when the amine functionality was added. This is most like due to the inductive effect the amine nitrogen has on the scaffold. For compound **3**, the protons in position 5 and 6 appeared as two doublets. The proton in position 6 has the highest shift of the two due to the close proximity to the nitrogen and a reduced shielding effect. The protons in the SEM-group resides in almost the same region for compound **2** and **3**, while

the chemical shift also reduces in these positions after the addition of an amine functionality. Spectroscopic data for all these compounds are found in the literature, and the obtained data are consistent with previously reported data. References for the three compounds are found in Table 10.

**Table 10**: $^{1}$H NMR chemical shifts for compound **2**, **3** and **4**. All shifts are given in ppm. The shifts of compound **2** and **4** were obtained from DMSO-$d_6$, while shifts for compound **3** was obtained from $CDCl_3$.

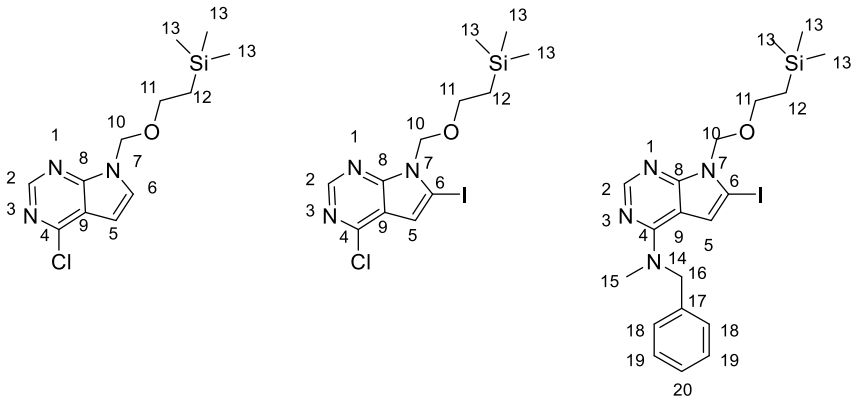

**2** **3** **4**

| | $^{1}$H [ppm] | | |
|---|---|---|---|
| **Position** | **2**[a] (7) | **3**[b] (5) | **4**[a] (83) |
| 2 | 8.68 | 8.63 | 8.14 |
| 5 | 6.71 | 7.12 | 6.94 |
| 6 | 7.87 | - | - |
| 10 | 5.64 | 5.62 | 4.99 |
| 11 | 3.52 | 3.53 | 3.52 |
| 12 | 0.82 | 0.83 | 0.80 |
| 13 | -0.11 | -0.10 | -0.08 |
| 15 | - | - | 3.30 |
| 16 | - | - | 5.50 |
| 18 | - | - | 7.26-7.22 |
| 19 | - | - | 7.33-7.31 |
| 20 | - | - | 7.26-7.22 |

[a] Solvent used: DMSO-*d6*
[b] Solvent used: $CDCl_3$

### 2.5.2 Products from Suzuki coupling reactions

**Compound 6a-c**

These three compounds all had the C-6 aryl group substituents in the *para* position. This gave a similar shift pattern for the protons in position 22 and 23 and they appeared as two doublets of which the protons in positions 22 had the highest shifts. Alteration of the C-6 aryl group substituent only gave significant changes for the protons in position 22 and 23. The remaining protons are too far away to be affected by the changed inductive effects from the substituent in the *para* position. The OH-substituent in **6c** has a lower electron donating ability compared to the O-R substituent in compound **6a** and **6b**. This gives a decreased shielding of position 24 and an increased shielding of position 23. The increased shielding of compound **6c**'s position 23 gives a lower $^{1}$H NMR shift compared to **6a** and **6b**. The assigned chemical shifts ($^{1}$H and $^{13}$C) for the different positions of **6a-c** are given in Table 11.

**Table 11**: $^{1}H$ and $^{13}C$ NMR chemical shifts for compound **6a**, **6b** and **6c**. All shifts are given in ppm. The chemical shifts were obtained from DMSO-$d_6$.

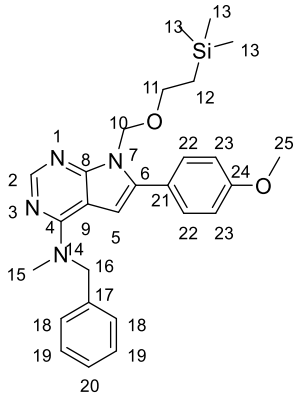

**6a**

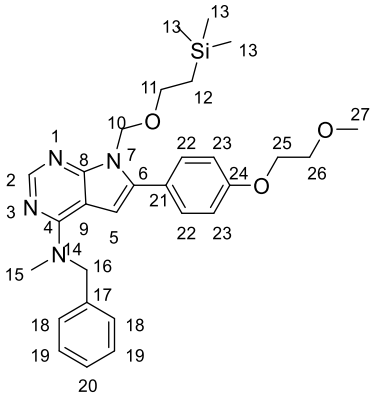

**6b**

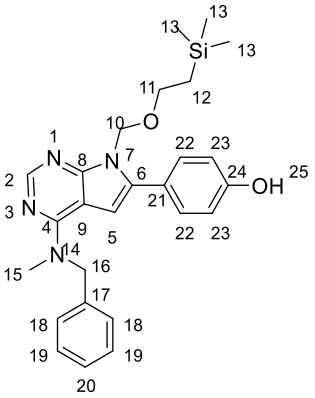

**6c**

| | $^{1}H$ [ppm] | | | $^{13}C$ [ppm] | | |
|---|---|---|---|---|---|---|
| **Position** | **6a**[a] | **6b**[a] | **6c**[a] | **6a**[a] | **6b**[a] | **6c**[a] |
| 2 | 8.23 | 8.22 | 8.21 | 151.0 | 151.0 | 150.8 |
| 4 | - | - | - | 159.2 | 158.4 | 157.6 |
| 5 | 6.70 | 6.70 | 6.64 | 101.3 | 101.3 | 100.8 |
| 6 | - | - | - | 138.3 | 138.3 | 138.3 |
| 8 | - | - | - | 152.8 | 152.8 | 152.8 |
| 9 | - | - | - | 102.1 | 102.1 | 102.1 |
| 10 | 5.51 | 5.51 | 5.49 | 70.2 | 70.2 | 70.2 |
| 11 | 3.61 | 3.61 | 3.61 | 65.6 | 65.6 | 65.6 |
| 12 | 0.84 | 0.85 | 0.84 | 17.3 | 17.3 | 17.3 |
| 13 | -0.08 | -0.08 | -0.80 | -1.5 | -1.5 | -1.4 |
| 15 | 3.35 | 3.36 | 3.35 | 37.3 | 37.3 | 37.3 |
| 16 | 5.04 | 5.05 | 5.04 | 52.8 | 52.7 | 52.7 |
| 17 | - | - | - | 136.4 | 136.3 | 136.9 |
| 18 | 7.27-7.23 | 7.27-7.23 | 7.27-7.23 | 126.9 | 126.9 | 126.9 |
| 19 | 7.34-7.31 | 7.34-7.31 | 7.33-7.31 | 128.5 | 128.5 | 128.5 |
| 20 | 7.27-7.23 | 7.27-7.23 | 7.27-7.23 | 126.9 | 126.9 | 126.9 |
| 21 | - | - | - | 123.7 | 123.8 | 122.0 |
| 22 | 7.62 | 7.62 | 7.50 | 129.9 | 129.9 | 130.0 |
| 23 | 7.02 | 7.04 | 6.84 | 114.1 | 114.1 | 115.4 |
| 24 | - | - | - | 156.3 | 156.3 | 156.3 |
| 25 | 3.80 | 4.14 | 9.69 | 55.2 | 67.0 | - |
| 26 | - | 3.67 | - | - | 70.3 | - |
| 27 | - | 3.31 | - | - | 58.1 | - |

[a] Solvent used: DMSO-*d*$_6$.

**Compound 6d-f**

Two of these compounds had O-R substituents on the C-6 aryl group which affected the system in a similar way (**6d** and **6f**), and the shifts were quite similar for all of the positions. Comparing the shifts from **6a** and **6d** shows a lower shift for H-5 in **6d**. This could indicate a long distance inductive shielding effect by the C-6 aryl methoxy substituent towards H-5. Changing the *meta* substituent to a hydroxyl functionality has the opposite effect, which is a long distance inductive deshielding effect relative to that seen for the methoxy substituent. The hydroxyl also had a higher shielding effect on H-11. This effect was not observed when the hydroxyl group was in the *para* position (**6c**). These two substituents have similar inductive effects on the compound it is attached to, but some small differences were observed. Position 24 and 26 are two other positions where it is possible to observe this difference in electron donation. The OH-group has a lesser shielding effect on H-25, but a higher shielding effect on the two neighbouring positions. This makes the chemical shift of compound **6e**'s position 24 and 26 lower compared to compounds **6d** and **6f**.

An interesting effect that was observed for compound **6f** was the splitting of the protons on position 29, which spread out as a broad multiplet between 3.99-3.86, see Figure 11. The assigned chemical shifts ($^{1}$H and $^{13}$C) for the different positions of **6d-f** are given in Table 12.

Since two different solvents were used for the NMR analyses of these compounds the discussion above can be questioned since the shift differences between solvents can be relatively large.

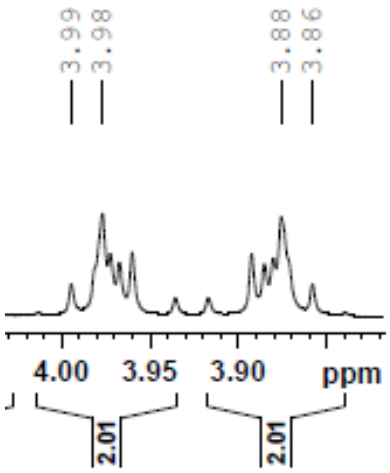


**Figure 11**: $^{1}$H NMR signals of the position 29 protons of compound **6f**.

**Table 12**: $^{1}H$ and $^{13}C$ NMR chemical shifts for compound **6d**, **6e** and **6f**. All shifts are given in ppm. The chemical shifts of **6e** were obtained from DMSO-$d_6$, while the chemical shifts of **6d** and **6f** were obtained from $CDCl_3$.

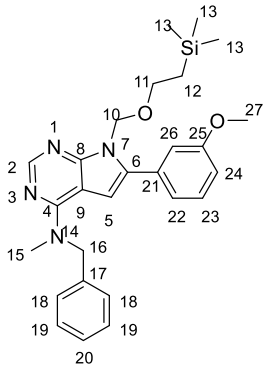

**6d**

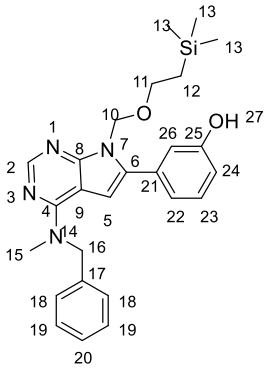

**6e**

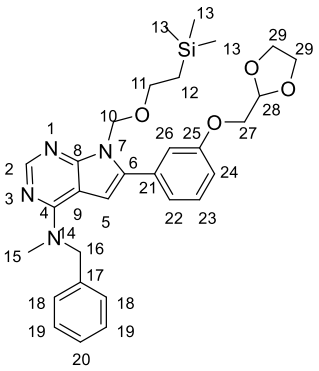

**6f**

| | $^{1}H$ [ppm] | | | $^{13}C$ [ppm] | | |
|---|---|---|---|---|---|---|
| **Position** | **6d**[a] | **6e**[b] | **6f**[a] | **6d**[a] | **6e**[b] | **6f**[a] |
| 2 | 8.40 | 8.23 | 8.40 | 151.7 | 151.2 | 151.7 |
| 4 | - | - | - | 159.7 | 157.5 | 158.7 |
| 5 | 6.56 | 6.72 | 6.55 | 102.0 | 102.0 | 102.1 |
| 6 | - | - | - | 137.3 | 138.2 | 137.8 |
| 8 | - | - | - | 153.5 | 152.3 | 153.5 |
| 9 | - | - | - | 102.0 | 101.9 | 102.8 |
| 10 | 5.59 | 5.53 | 5.58 | 70.7 | 70.3 | 70.7 |
| 11 | 3.74 | 3.59 | 3.73 | 66.4 | 65.6 | 66.4 |
| 12 | 0.97 | 0.84 | 0.97 | 18.1 | 17.3 | 18.1 |
| 13 | -0.03 | -0.09 | -0.03 | -1.5 | -1.5 | -1.4 |
| 15 | 3.37 | 3.36 | 3.37 | 37.2 | 37.4 | 37.2 |
| 16 | 5.06 | 5.05 | 5.07 | 53.8 | 52.8 | 53.3 |
| 17 | - | - | - | 137.8 | 136.6 | 137.2 |
| 18 | 7.35-7.23 | 7.27-7.23 | 7.29-7.27 | 127.1 | 126.9 | 127.1 |
| 19 | 7.35-7.23 | 7.27-7.23 | 7.34-7.31 | 128.7 | 128.5 | 128.7 |
| 20 | 7.35-7.23 | 7.34-7.31 | 7.29-2.27 | 127.2 | 126.9 | 129.7 |
| 21 | - | - | - | 133.0 | 132.6 | 133.1 |
| 22 | 7.35-7.23 | 7.12-7.11 | 7.34-7.31 | 121.4 | 119.3 | 121.9 |
| 23 | 7.35-7.23 | 7.34-7.31 | 7.20-7.15 | 129.6 | 128.5 | 128.3 |
| 24 | 6.94-6.91 | 6.82-6.80 | 6.97-6.95 | 113.9 | 115.1 | 114.7 |
| 25 | - | - | - | 157.3 | 156.5 | 157.3 |
| 26 | 7.35-7.23 | 7.06 | 7.29.7.27 | 114.4 | 115.5 | 115.0 |
| 27 | 3.83 | 9.57 | 4.06 | 55.3 | - | 68.8 |
| 28 | - | - | 5.30 | - | - | 101.9 |
| 29 | - | - | 3.99-3.86 | - | - | 65.3 |

[a] Solvent used: $CDCl_3$.

[b] Solvent used: DMSO-$d_6$.

**Compound 6g-h**

Compound **6h** has the same substituent on the C-6 aryl group as **6b**, but in a different position (*meta* instead of *para*). The ether tail is closer to the SEM-group in compound **6h** compared to **6b**. The chemical shifts of the SEM-group protons are the same in both these compounds, which shows that even though the ether group is closer, there are no significant difference in shielding effects towards the SEM-group. The chemical shifts ($^{1}$H and $^{13}$C) of the ether tail are also very similar for the *meta*-substituted **6h** to that of its *para*-substituted analogue **6b**. What can be observed is that the methylenedioxy group in compound **6g** has a significant effect on both the $^{1}$H and $^{13}$C chemical shifts of position 22, 23 and 26 compared to the other *meta*-substituted compounds. The carbon in position 26 has a $^{13}$C chemical shift at around 114 ppm in compound **6d**, **6e**, **6f**, and **6h** while it is found at 126.9 for compound **6g**. In the $^{1}$H NMR spectra of compound **6g** the coupling between the protons in position 22 and 23 become more clear since they appear as a doublet (position 23) and a doublet of doublets (position 22). The protons in these two positions appeared as multiplets for the other *meta*-substituted compounds. The assigned chemical shifts ($^{1}$H and $^{13}$C) for the different positions of **6g** and **6h** are given in Table 13.

**Table 13**: $^{1}H$ and $^{13}C$ NMR chemical shifts for compound **6g** and **6h**. All shifts are given in ppm. The chemical shifts are calibrated from DMSO-$d_6$.

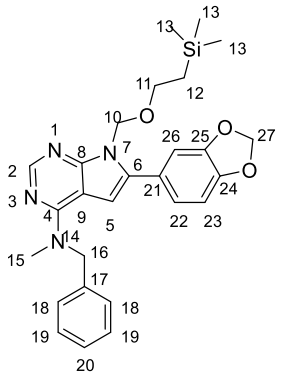

**6g**

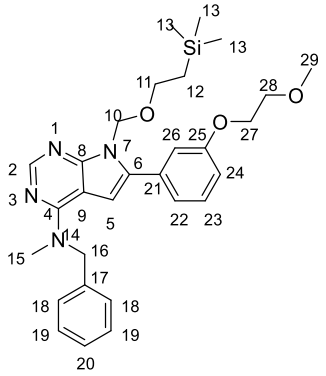

**6h**

| | $^{1}H$ [ppm] | | $^{13}C$ [ppm] | |
|---|---|---|---|---|
| **Position** | **6g**[a] | **6h**[a] | **6g**[a] | **6h**[a] |
| 2 | 8.22 | 8.25 | 151.1 | 151.1 |
| 4 | - | - | 156.4 | 158.6 |
| 5 | 6.73 | 6.83 | 101.8 | 102.5 |
| 6 | - | - | 138.2 | 138.1 |
| 8 | - | - | 152.9 | ? |
| 9 | - | - | 102.0 | 102.0 |
| 10 | 5.52 | 5.55 | 70.2 | 70.4 |
| 11 | 3.62 | 3.62 | 65.7 | 65.6 |
| 12 | 0.85 | 0.85 | 17.3 | 17.3 |
| 13 | -0.08 | -0.08 | -1.4 | -1.5 |
| 15 | 3.35 | 3.31 | 37.4 | 37.5 |
| 16 | 5.05 | 5.06 | 52.7 | 52.8 |
| 17 | - | - | 136.2 | 136.2 |
| 18 | 7.28-7.23 | 7.38-7.24 | 126.9 | 126.8 |
| 19 | 7.34-7.31 | 7.38-7.24 | 128.5 | 128.5 |
| 20 | 7.28-7.23 | 7.38-7.24 | 126.9 | 126.8 |
| 21 | - | - | 125.2 | 126.9 |
| 22 | 7.19 | 7.38-7.24 | 122.5 | 120.8 |
| 23 | 7.01 | 7.38-7.24 | 108.5 | 129.8 |
| 24 | - | 6.99-6.98 | 147.2 | 114.2 |
| 25 | - | - | 147.6 | 157.5 |
| 26 | 7.28-7.23 | 7.38-7.24 | 126.9 | 114.4 |
| 27 | 6.07 | 4.13 | 101.3 | 66.9 |
| 28 | - | 3.67 | - | 70.3 |
| 29 | - | 3.37 | - | 58.2 |

[a] Solvent used: DMSO-$d_6$.

### 2.5.3 Products from deprotection reactions

What was observed for all the deprotected products (**7a**-**7h**) was minor changes in the $^{1}H$ and $^{13}C$ chemical shifts for all the positions, except the signals from the aryl group on C-6 and the carbon and proton in position 5. The proton in positon 7 stood out with a markedly high chemical shift at around 12 ppm which made it easy to identify. Another general trend was that the compounds containing an ether substituent on the aryl group had similar chemical shifts for all positions, also the positions located on the C-6 aryl group. An OH substituent gives the same effect as was observed for the SEM-protected intermediates (**6c** and **6e**). The presence of an OH-group has a lower shielding effect on the position it is attached to (compared to an ether group), but also has a higher shielding effect on the two neighbouring positions which gives a lower chemical shift compared to the ether-substituted compounds.

HSQC was used to identify the carbon shift of all the protonated positions while a combination of deduction and ChemDraw software was used to decide the $^{13}C$ chemical shifts for the remaining carbons. Compound **7a-h** where all analysed with DMSO-$d_6$. The assigned chemical shifts ($^{1}H$ and $^{13}C$) for the different positions of **7a**-**h** are given in Table 14-16.

**Compound 7a-c**

**Table 14**: $^{1}H$ and $^{13}C$ NMR chemical shifts for compound **7a**, **7b** and **7c**. All shifts are given in ppm. The chemical shifts are calibrated from DMSO-$d_6$

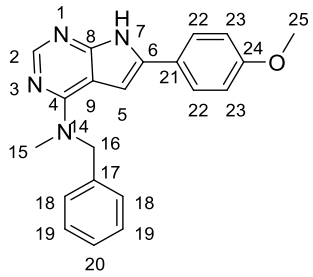

**7a**

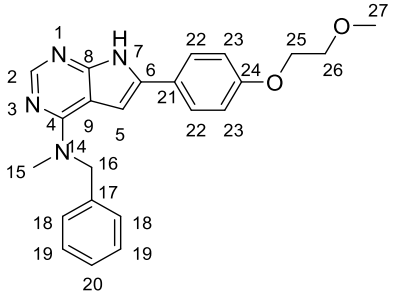

**7b**

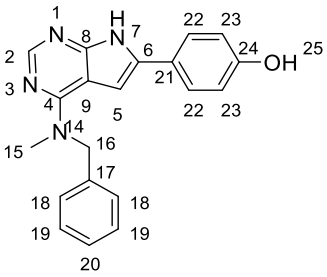

**7c**

| | $^{1}H$ [ppm] | | | $^{13}C$ [ppm] | | |
|---|---|---|---|---|---|---|
| **Position** | **7a** | **7b** | **7c** | **7a** | **7b** | **7c** |
| 2 | 8.12 | 8.13 | 8.11 | 150.7 | 150.7 | 150.5 |
| 4 | - | - | - | 158.7 | 157.9 | 157.0 |
| 5 | 6.90 | 6.90 | 6.82 | 97.3 | 97.3 | 96.6 |
| 6 | - | - | - | 133.3 | 133.3 | 133.9 |
| 7 | 12.06 | 12.06 | 11.9 | - | - | - |
| 8 | - | - | - | 152.8 | 152.7 | 152.7 |
| 9 | - | - | - | 103.3 | 103.3 | 103.3 |
| 15 | 3.36 | 3.35 | 3.34 | 37.3 | 37.1 | 37.3 |
| 16 | 5.04 | 5.04 | 5.03 | 52.7 | 52.6 | 52.6 |
| 17 | - | - | - | 138.5 | 138.7 | 138.7 |
| 18 | 7.28-7.23 | 7.28-7.23 | 7.27-7.23 | 127.0 | 127.0 | 127.0 |
| 19 | 7.34-7.31 | 7.34-7.31 | 7.34-7.31 | 128.5 | 128.5 | 128.5 |
| 20 | 7.28-7.23 | 7.28-7.23 | 7.27-7.23 | 126.8 | 126.8 | 126.8 |
| 21 | - | - | - | 124.2 | 124.2 | 122.6 |
| 22 | 7.77 | 7.76 | 7.64 | 126.1 | 126.1 | 126.2 |
| 23 | 6.97 | 6.99 | 6.78 | 114.2 | 114.7 | 115.5 |
| 24 | - | | - | 156.2 | 156.2 | 156.1 |
| 25 | 3.78 | 4.12 | 9.58 | 55.2 | 66.9 | - |
| 26 | - | 3.67 | - | - | 70.3 | - |
| 27 | - | 3.31 | - | - | 58.1 | - |

**Compound 7d-f**

**Table 15**: $^{1}H$ and $^{13}C$ NMR chemical shifts for compound **7d**, **7e** and **7f**. All shifts are given in ppm. The chemical shifts are calibrated from DMSO-$d_6$.

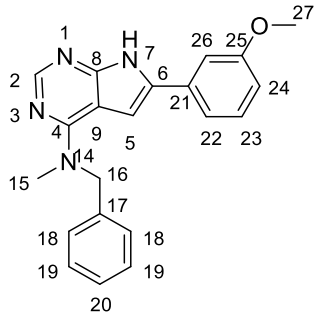


**7d**

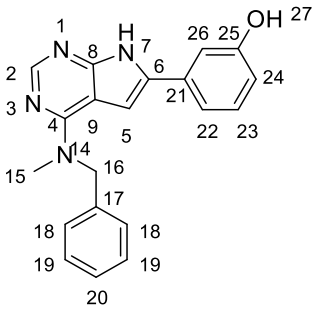


**7e**

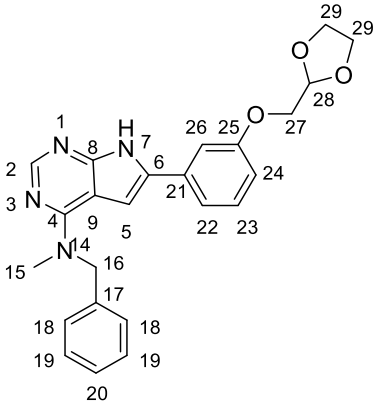


**7f**

| | $^{1}H$ [ppm] | | | $^{13}C$ [ppm] | | |
|---|---|---|---|---|---|---|
| **Position** | **7d** | **7e** | **7f** | **7d** | **7e** | **7f** |
| 2 | 8.15 | 8.14 | 8.15 | 151.2 | 151.1 | 151.3 |
| 4 | - | - | - | 159.7 | 157.6 | 158.6 |
| 5 | 7.07 | 6.92 | 7.10 | 99.2 | 98.6 | 99.3 |
| 6 | - | - | - | 132.8 | 132.8 | 132.9 |
| 7 | 12.17 | 12.09 | 12.15 | - | - | - |
| 8 | - | - | - | 152.9 | 152.8 | 152.9 |
| 9 | - | - | - | 103.2 | 103.1 | 103.2 |
| 15 | 3.37 | 3.36 | 3.37 | 37.4 | 37.3 | 37.4 |
| 16 | 5.05 | 5.04 | 5.05 | 52.7 | 52.7 | 52.6 |
| 17 | - | - | - | 138.4 | 137.4 | 138.4 |
| 18 | 7.35-7.24 | 7.28-7.23 | 7.34-7.23 | 127.0 | 127.0 | 127.0 |
| 19 | 7.35-7.24 | 7.34-7.32 | 7.34-7.23 | 128.5 | 128.4 | 128.5 |
| 20 | 7.35-7.24 | 7.28-7.23 | 7.34-7.23 | 126.9 | 126.9 | 126.9 |
| 21 | - | | | 133.1 | 133.5 | 133.0 |
| 22 | 7.43-7.41 | 7.20-7.18 | 7.47-7.43 | 110.0 | 111.7 | 110.3 |
| 23 | 7.43-7.41 | 7.28-7.23 | 7.47-7.43 | 117.1 | 115.7 | 117.4 |
| 24 | 6.85-6.83 | 6.71-6.69 | 6.87-6.84 | 113.1 | 114.4 | 113.7 |
| 25 | - | - | | 156.5 | 156.4 | 156.5 |
| 26 | 7.35-7.24 | 7.20-7.18 | 7.34-7.23 | 129.8 | 129.7 | 129.9 |
| 27 | 3.81 | 9.46 | 4.06 | 55.2 | - | 68.2 |
| 28 | - | - | 5.23 | - | - | 101.3 |
| 29 | - | - | 3.99-3.86 | - | - | 64.5 |

**Compound 7g-h**

**Table 16**: $^{1}H$ and $^{13}C$ NMR chemical shifts for compound **7g** and **7h**. All shifts are given in ppm. The chemical shifts are calibrated from DMSO-$d_6$.

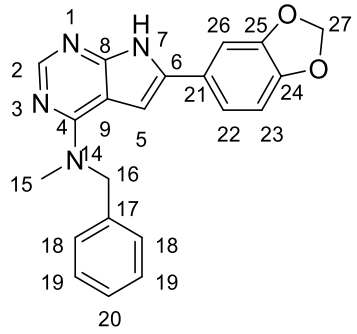


**7g**

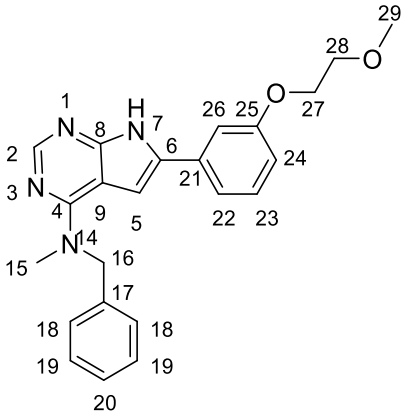


**7h**

| | $^{1}H$ [ppm] | | $^{13}C$ [ppm] | |
|---|---|---|---|---|
| **Position** | **7g** | **7h** | **7g** | **7h** |
| 2 | 8.13 | 8.15 | 150.9 | 151.2 |
| 4 | - | - | 156.3 | 158.9 |
| 5 | 6.97-6.95 | 7.09 | 98.0 | 99.2 |
| 6 | - | - | 125.8 | 133.0 |
| 7 | 12.04 | 12.14 | - | - |
| 8 | - | - | 152.8 | 152.9 |
| 9 | - | - | 103.3 | 103.2 |
| 15 | 3.35 | 3.37 | 37.3 | 37.4 |
| 16 | 5.03 | 5.05 | 52.6 | 52.6 |
| 17 | - | - | 138.5 | 138.4 |
| 18 | 7.27-7.23 | 7.34-7.23 | 127.0 | 127.0 |
| 19 | 7.36-7.31 | 7.34-7.23 | 128.5 | 128.5 |
| 20 | 7.27-7.23 | 7.34-7.23 | 126.8 | 126.9 |
| 21 | - | - | 133.2 | 132.8 |
| 22 | 7.36-7.31 | 7.41 | 118.4 | 117.2 |
| 23 | 6.97-6.95 | 7.34-7.23 | 108.6 | 129.8 |
| 24 | - | 6.84 | 146.6 | 113.7 |
| 25 | - | - | 147.8 | 156.4 |
| 26 | 7.45 | 7.46 | 105.3 | 110.5 |
| 27 | 6.04 | 3.68 | 101.1 | 70.4 |
| 28 | - | 4.16 | - | 66.8 |
| 29 | - | 3.32 | - | 58.1 |

### 2.5.4 IR spectroscopy

All of the compounds synthesised have been characterised with IR spectroscopy, and IR spectra for the novel compounds can be found in Appendix D-S. Even though IR has not been the most important source of information, it has been useful to get another confirmation on the presence of the anticipated functional groups for the isolated compounds. Both the series of SEM-protected pyrrolopyrimidines (**6a-h**) and the deprotected pyrrolopyrimidines (**7a-h**) share a lot of the same features structure wise. Because of this, all of the obtained results from IR analysis are summarised combined.

All of the IR-characterised compounds contain aromatic rings. Vibrations from these regions of the molecules can be found between 1600 $cm^{-1}$ and 1300 $cm^{-1}$. Aromatic and aliphatic C-H regions can be found in all of the analysed compounds. These C-H bonds give stretching bands which resides between 3000 $cm^{-1}$ and 2840 $cm^{-1}$ for the aliphatic, and between 3150 $cm^{-1}$ and 3000 $cm^{-1}$ for aromatic C-H stretching [90]. In all the compounds there are both C=C and C=N bonds present in the heteroaromatic part of the compounds. Stretching from these bonds often give vibrations in the 1300-1600 $cm^{-1}$ region. Another distinctive peak that was observed in all of the spectra was the strong band that appeared between 1562 and 1572. Aromatic C=C stretching modes may be the explanation for these bands [91].

After the deprotection procedures a new N-H functionality appears in the compounds (compound **7a-h**) The N-H stretching vibration generates a weak absorption band between 3200 $cm^{-1}$ and 2700 $cm^{-1}$. What was observed after deprotection was the appearance of these bands, but also a "broadening" of the signal in the region between 3200 cm-1 and 2000 cm-1. In some cases (compound **7a** and **7e**), this region almost seemed like one broad band.

## 2.6 Bio-assaying and *in vitro* evaluations

Compounds that were deemed pure enough (as decided by $^{1}$H NMR analyses) for testing were weighed, diluted in DMSO and sent to Life Technologies in the UK. Here the compounds inhibitory effect towards CSF-1R and EGFR was measured by an *in vitro* enzymatic assay. To measure the percent inhibition, two single point tests were performed. For CSF-1R, the amount of inhibitor added was 500 nM, and for EGFR the amount was 100 nM. Results showing the percent inhibitory effect of the target molecules towards CSF-1R and EGFR are presented in Table 17. Two positive controls were used, namely Dasatinib for CSF-1R and Erlotinib for EGFR.

**Table 17**: Percent inhibition of the tested kinase inhibitors towards the respective kinases. Tests are performed at 500 nM for CSF-1R and at 100 nM for EGFR.

| Entry | Compound No. | 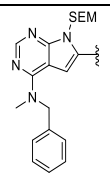 | CSF-1R (% inhibition) | EGFR (% inhibition) |
|---|---|---|---|---|
| 1 | - | Erlotonib | 12 | 100 |
| 2 | - | Dasatinib | 95 | 76 |
| 3 | - | GW2580 | 93 | - |
| 4 | **7a** | 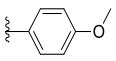 | 101 | 71 |
| 5 | **7b** | 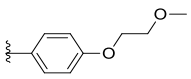 | 103 | 76 |
| 6 | **7d** | 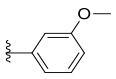 | 96 | 70 |
| 7 | **7e** |  | 96 | 78 |
| 8 | **7f** | 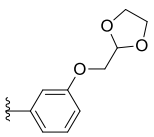 | 87 | 49 |
| 9 | **7h** | 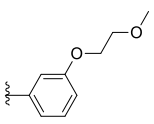 | 97 | 61 |
| 10 | **KUL01-97**[7] |  | 90 | 24 |

The results indicate several of the compounds to be potent CSF-1R inhibitors. Compound **7a**, **7b**, **7d** and **7e** all had CSF-1R inhibition of 96% or more. They also had an EGFR inhibition of 70% or more. One compound that stands out is compound **7h** containing an ether tail in the *meta* position of the C-6 aryl group. This compound has a CSF-1R inhibition of 97%, but also the lowest inhibitory effect towards EGFR (61%), which makes it a more selective inhibitor. It is more selective than for example Dasatinib, which has an EGFR inhibition of 76%. Compound **7e** containing an alcohol functionality in the *meta* position is the only tested compound containing a polar substituent on the C-6 aryl group. This inhibitor had an inhibition of 96%. Previous results from by the research group have shown that polar substituents can increase inhibition activity [5, 7]. For the data obtained, there are no indications that the hydroxyl group on **7e** gives a better inhibitory effect compared to the aryl groups with an O-R substituent. **KUL01-97** was synthesised by Larsen and is included in Table 17 for comparison [7]. This compound is even more selective towards the CSF-1R kinase then compound **7h**, but the inhibition percent is also lower.

For selected compounds, $IC_{50}$-values were determined by a 10 point titration protocol with 3-fold dilution starting at 1000 nM where enzyme activity is measured at each inhibitor concentration. This analysis includes more data points then the percent inhibition test and is therefore a more reliable measure of inhibition. Results from the $IC_{50}$ titration of **7a** is presented in Figure 12.

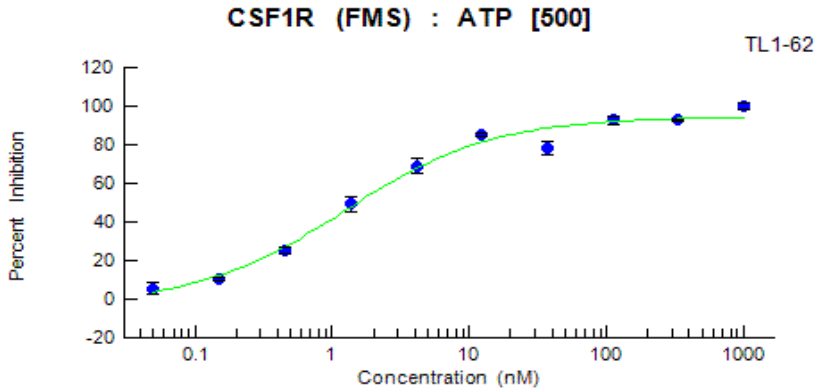


**Figure 12**: The titration curve for the $IC_{50}$ screening of compound **7a**.

When comparing the percent inhibition scores there were no significant difference, since all the compounds had an inhibition above 96%. The $IC_{50}$-values effectively differentiate the compounds with a more precise measure on which compound is most potent. Compound **7a** had the lowest $IC_{50}$-value of 1.3 nM, and is therefore the most potent inhibitor identified in this thesis. **KUL01-97** that was included in Table 17 as a reference has a relatively high $IC_{50}$-value (15 nM) compared to the new compounds assayed. A presentation of the $IC_{50}$-values is given in Figure 13. An interesting comparison between the compounds in Figure 13 is the substituents on the C-6 aryl group. **KUL01-97** is unsubstituted and show poorer activity. All of tested compounds have a substituent in the *para* or *meta* position. This indicate that all substituents on the C-6 aryl group contributes to increased potency and CSF-1R inhibition.

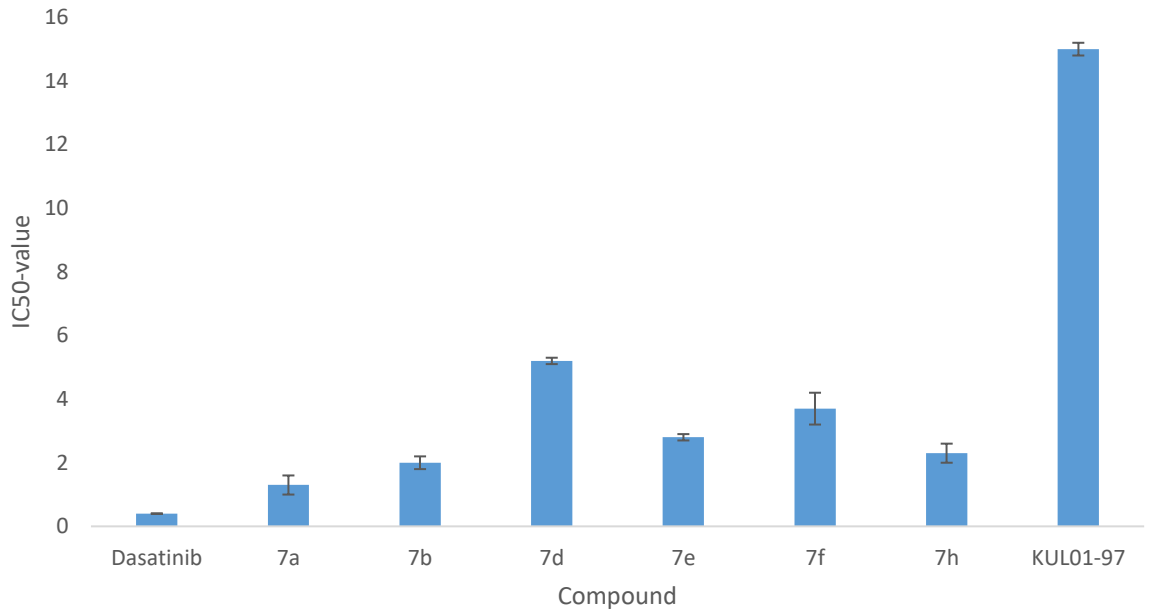


**Figure 13**: $IC_{50}$-values, with deviations for the most potent inhibitors tested for this thesis. Dasatinib is added as a positive control and KUL01-97 is used as a reference for comparison [7].

# 3 Conclusion

For this master thesis, eight novel pyrrolopyrimidine compounds have been synthesised. All of the compounds were based on the same pyrrolopyrimidine scaffold with an amine substituent on C-4. Six of the novel compounds were tested *in vitro* for their inhibition activity towards CSF-1R and EGFR.

The core building block **4** was synthesised by a thermal amination that gave 97% yield at best. A limited search for catalysts for the Suzuki cross-coupling was performed. The selected system, $Pd_2(dba)_3$ showed promising features and was used for all the executed Suzuki coupling reactions. The coupling reactions were done with a 1-5 mol% catalyst loading and the conversion was excellent in all cases. The time required to reach full conversion varied from 15 min to 3 h. Yields varied from 58-81%. Compound **6h** containing an ether tail in the *para* position of the aryl group was synthesised by a Williamson ether synthesis starting with compound **6e**. All the SEM-protected intermediates **6a-h** were deprotected using the same protocol. Most of these reactions gave yields between 65 and 85%. During the extraction process, it became clear that the solubility was low in some cases, which most likely decreased the efficiency of both the work up and the following purification.

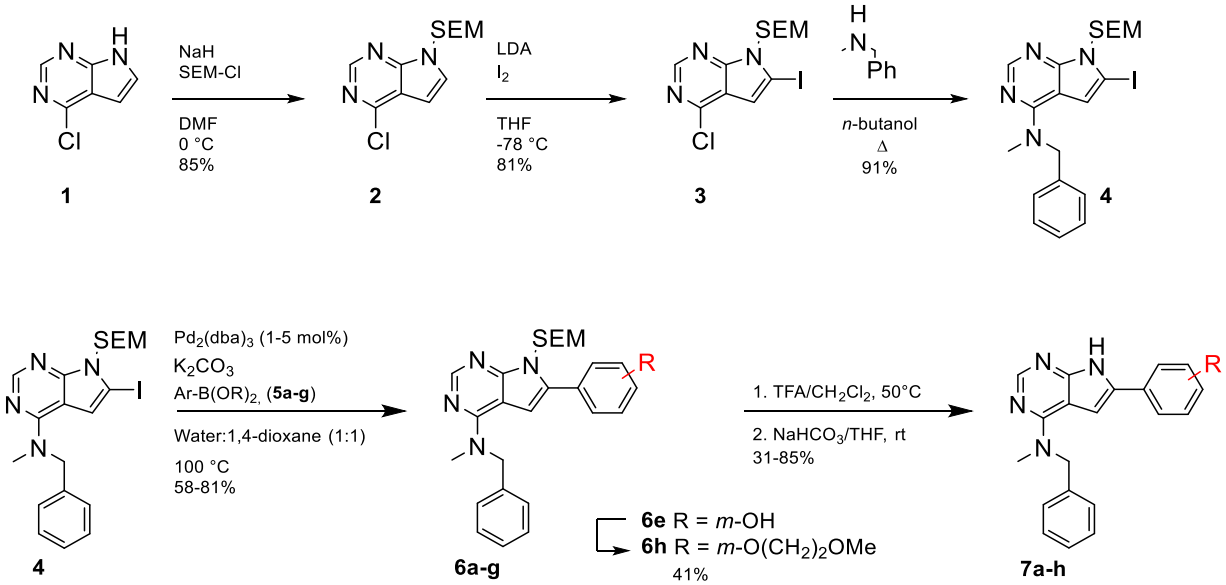

Of the eight novel compounds, six were assayed *in vitro* for their CSF-1R inhibitory activity. The obtained results from these assays indicated high biological activity for several of the compounds. Five of the tested compound had a percent inhibition higher than 96% towards CSF-1R (compound **7a**, **7b**, **7d**, **7e**, and **7h**). Inhibition of EGFR was significantly lower, varying from 49- 76%. The results did not indicate an increase in bio-activity due to extension of the ether tail on the C-6 aryl group. However, water solubility should be increased. The most potent synthesised inhibitor to be tested was compound **7a**, which had an $IC_{50}$-value of 1.3 nM on average. The other four compounds with high inhibition scores achieved $IC_{50}$-values between 2.0 and 5.3. Although none of the tested compounds could match Dasatinib for CSF-1R inhibition (IC50-value 0.4 nM), the new derivatives are highly active and could be further developed as drugs. Additionally, the reported data broaden structure-activity relationship information on CSF-1R.

# 4 Future work

The work on this master thesis have led to the discovery of several potent kinase inhibitors. None of the tested target compounds were equipotent to the commercial drug Dasatinib, but can still be considered as highly active compounds. Good results can also be an inspiration to think further and make plans for more progress. New kinase inhibitors can be made by other fragment variations on C-4 (fragment A) and C-6 (fragment B). The general structure is presented in Figure 14.

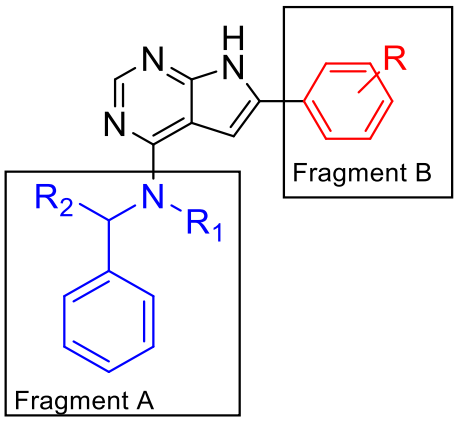


**Figure 14**: The general structure of potential new kinase inhibitors.

An approach that could lead to several new inhibitor candidates is to make alterations of the amine substituent of fragment A. A selection of the four most potent inhibitors from this thesis could be used as a base, and from that base, the amine substituent could be changed. To choose strategic amines it could be wise to look in the literature to see what amine substituents that have been present in other potent CSF-1R inhibitors. Changing the amine substituent could also have positive effects on the solubility. None of the target compounds for this thesis were analysed with HPLC due to the low solubility in water and acetonitrile. Low solubility in these solvents indicates a low solubility *in vivo*. Amine fragments that have polar substituents could increase the solubility by generating more points on the molecule for hydrogen bonding.

Alterations of the substituents on the C-6 aryl group can also increase the solubility of the pyrrolopyrimidine structures. The ether tail could be lengthened further, and other solubilising tails could be investigated. A structure that has been found to increase micelle solubility of

drugs, is the PEG-tail (polyethylene glycol) [92]. These tails can vary in length. It would have been interesting to investigate how different PEG-tails on the C-6 aryl group could affect the solubility of pyrrolopyrimidine structures. The chemical structure of PEG is given in Figure 15.

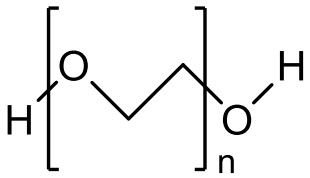


**Figure 15**: The chemical structure of polyethylene glycol (PEG).

This thesis has focused on compounds having different electron rich C-6 aryl groups. All of the performed Suzuki coupling reactions gave excellent conversion and the reaction times were generally low (0.25-3 h). It could be interesting to expand the compound library with more electron deficient aryl groups. Nitroaromatic groups can be found in some drugs and nitro substituted pyrrolopyrimidines could be an exciting addition to the kinase inhibitor library [93]. Trihalide or cyano groups are other substituents that could be investigated.

The only tests that were made for this project was inhibition percent and $IC_{50}$ analysis. These tests give valuable information on the potency of the compound, but there are still several factors that has to be examined to determine if the compounds could be used as a medical drug. Further testing that could be made is investigation of the compounds toxicity *in vivo*, its metabolic features and more solubility testing.

# 5 Experimental

## 5.1 General information

### Separation Techniques

Thin layer chromatography (TLC; silica gel on aluminum plates, $F_{254}$, Merck) was applied both to monitor several of the reactions for the thesis and for the optimization of eluent systems for silica-gel column chromatography. For plate visualization, UV-light was used (wavelength 254 nm and 365 nm). Silica gel (200-400 mesh, 60Å) was used as a stationary phase to perform silica-gel column chromatography. The mobile phases for the different silica- gel column chromatographic purifications are specified for each reaction.

### Spectroscopic analysis

Infrared absorption spectroscopy (IR) was performed with a Thermo Nicolet Nexus FT-IR Spectrometer using a Smart Endurance reflection cell. The frequencies reported are in the range of 4000-400 $cm^{-1}$. $^{1}H$ and $^{13}C$ NMR spectra were recorded on a Bruker Avance instrument, using a 14,1 Tesla Bruker Ascend magnet, operating at 600 MHz for $^{1}H$ NMR and 150 MHz for $^{13}C$ NMR. The magnet is equipped with Avance III HD electronics and a TCI CryoProbe. Information about the specific acquisition parameters can also be found in the spectra. Deuterated DMSO, DMSO-$d_6$ was the most used solvent, but some of the compounds were analysed with $CDCl_3$ to compare with reference spectra. The shifts are reported in ppm, and was calibrated based on the residual solvent peak, DMSO, which reside at 2.50 ppm in $^{1}H$ NMR and at 39.5 ppm in $^{13}C$ NMR spectrum and $CDCl_3$, which reside on 7.26 ppm for $^{1}H$ NMR and 77 ppm in $^{13}C$ NMR. Water traces can be found at 3.33 ppm in $^{1}H$ NMR, and are present in most of the spectra where DMSO was used as solvent. Peaks are described according to their multiplicity; s (singlet), d (doublet), t (triplet) and m (multiplet). Coupling constants (*J*) are reported in Hz, and unless peaks display near perfect splitting pattern they are assigned as multiplets. MS Accurate mass determination in positive and negative mode was performed on a "Synapt G2-S" Q-TOF instrument from Waters™. Samples were ionized by the use of an ASAP probe (APCI). Calculated exact masses and spectra processing was done by Waters™ Software (MassLynx V4.1 SCN871).

### Melting point

To determine melting points a Stuart automatic melting point SMP40 instrument was used.

## 5.2 Preparation of starting materials

### 5.2.1 Synthesis of 4-chloro-7-[[2-(trimethylsilyl)ethoxy]methyl]-7*H*-pyrrolo[2,3-*d*]pyrimidine (2) [78, 83].

**Synthesis in 200 mg scale**

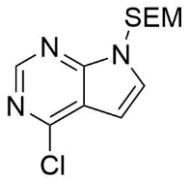


The procedure was based on similar procedures executed by Liang *et al.* [83] and Lin *et al.* [78]. Pyrrolopyrimidine **1** (200 mg, 1.30 mmol) was mixed with NaH (36 mg, 1.5 mmol) and dissolved in dry DMF (7 mL). The reaction vessel was evacuated and backfilled with nitrogen before the mixture was cooled to 0 °C on an ice bath, and stirred for 30 min. SEM-Cl (0.27 mL, 1.5 mmol) was added dropwise over 30 min. After 1.5 h, water (15 mL) was added and the mixture was extracted with EtOAc (3 x 20 mL). The combined organic phases were washed with brine (20 mL), dried over $Na_2SO_4$, filtered and concentrated *in vacuo* before the crude product was purified by silica-gel column chromatography (*n*-pentane:EtOAc, 4:1, $R_f$ = 0.74). This gave 200 mg (0.703 mmol, 54%) of a transparent oil.

**Synthesis in 3.75 g scale**

Pyrrolopyrimidine **1** (3.75 g, 24.4 mmol) was mixed with NaH (0.67 g, 28 mmol) and dissolved in dry DMF (175 mL). The reaction vessel was evacuated and backfilled with nitrogen before the mixture was cooled to 0 °C on an ice bath, and stirred for 30 min. SEM-Cl (4.97 mL, 28.1 mmol) was added dropwise over 30 min. After 1.5 h, water (100 mL) was added and the mixture was extracted with EtOAc (3 x 75 mL). The combined organic phases were washed with brine (100 mL), dried over $Na_2SO_4$, filtered and concentrated *in vacuo* before the crude product was purified by silica-gel column chromatography (*n*-pentane:EtOAc, 4:1, $R_f$ = 0.74). This gave 5.87 g (20.7 mmol, 85%) of a light yellow oil.

Spectroscopic data for compound **2** (Appendix A): $^1$H NMR (600 MHz, DMSO-$d_6$) δ: 8.68 (s, 1H), 7.87 (d, *J* = 3.6, 1H), 6.71 (d, *J* = 3.6, 1H), 5.64 (s, 2H), 3.52 (t, *J* = 8.0, 2H), 0.82 (t, *J* = 8.0, 2H), -0.11 (s, 9H). The analysis is consistent with previously reported data [83].

### 5.2.2 Synthesis of 4-chloro-6-iodo-7-[[2-(trimethylsilyl)ethoxy]methyl]-7*H*-pyrrolo[2,3-*d*]pyrimidine (3) [5]

**Synthesis in 4 g scale**

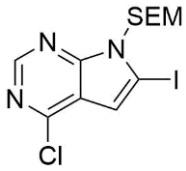


Pyrrolopyrimidine **2** (4.00 g, 14.1 mmol) was mixed with dry THF (150 mL), put under a $N_2$-atmosphere and cooled to -78 °C on a dry ice/acetone-bath. A syringe pump was used to add LDA (2M solution in THF, 14.5 mL, 21.1 mmol) dropwise over 30 min. The mixture was stirred for 1 h. Iodine (4.65 g, 18.3 mmol) was dissolved in dry THF (25 mL) and added dropwise over 30 min. After iodine addition, the mixture was stirred for an additional hour. HCl (1M, 72 mL) was added before the mixture was allowed to warm to rt before being concentrated *in vacuo*. The residue was dissolved in $CH_2Cl_2$ (100 mL) and water (75 mL). The phases were separated and the aqueous face extracted with $CH_2Cl_2$ (3 x 50 mL). The combined organic phases were washed with brine (100 mL), dried over $Na_2SO_4$, filtered and concentrated *in vacuo*. The crude product was purified by silica-gel column chromatography (*n*-pentane:EtOAc, 4:1, $R_f$ = 0.70) yielding compound **3** as a pale yellow solid in 4.69 g (11.5 mmol, 81%), mp = 101-103 °C (no mp reported in reference).

**Synthesis in 5.25 g scale**

Pyrrolopyrimidine **2** (5.25 g, 18.5 mmol) was mixed with dry THF (175 mL), put under a $N_2$-atmosphere and cooled to -78 °C on a dry ice/acetone-bath. A syringe pump was used to add LDA (2M solution in THF, 14.5 mL, 27.8 mmol) dropwise over 30 min. The mixture was stirred for 1 h. Iodine (6.10 g, 24.1 mmol) was dissolved in dry THF (30 mL) and added dropwise over 30 min before the mixture was stirred for an additional hour. HCl (1M, 80 mL) was added before the mixture was allowed to warm to rt before concentrated *in vacuo*. The residue was dissolved in $CH_2Cl_2$ (125 mL) and water (80 mL). The phases were separated and the aqueous face extracted with $CH_2Cl_2$ (3 x 60 mL). The combined organic phases were washed with brine (125 mL), dried over $Na_2SO_4$, filtered and concentrated *in vacuo*. The crude product was purified by silica-gel column chromatography (*n*-pentane:EtOAc, 4:1, $R_f$ = 0.70) yielding compound **3** in 5.20 g (12.7 mmol, 68%) as a yellow solid, mp= 101-103 °C (no mp reported in reference).

Spectroscopic data for compound **3** (Appendix B): $^{1}$H NMR (600 MHz, $CDCl_3$) δ: 8.63 (s, 1H), 7.12 (s, 1H), 5.62 (s, 2H), 3.53 (t, *J* = 7.5, 2H), 0.83 (t, *J* = 7.5, 2H), -0.10 (s, 9H). The analysis is consistent with previously reported data [5].

### 5.2.3 Synthesis of *N*-benzyl-6-iodo-*N*-methyl-7-((2-(trimethylsilyl)ethoxy)-methyl)-7*H*-pyrrolo[2,3-*d*]pyrimidin-4-amine (4) [7].

**Synthesis in 100 mg scale**

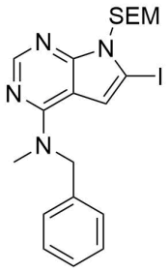


Pyrrolopyrimidine **3** (99 mg, 0.244 mmol) was dissolved in *n*-butanol (5 mL) and added *N*-benzylmethylamine (0.090 mL, 0.730 mmol) under an $N_2$-atmosphere. The reaction mixture was heated to 125 °C on an oil bath and stirred for 5 h before it was cooled to rt. The reaction mixture was added water (15 mL) and EtOAc (30 mL) and the phases were separated. The water phase was extracted with more EtOAc (2 x 10 mL). The combined organic phases were washed with brine (10 mL) and dried over $Na_2SO_4$, filtered and concentrated *in vacuo*. The crude product was purified by silica-gel column chromatography (*n*-pentane:EtOAc, 3:1, $R_f$ = 0.51). Drying gave 104 mg (0.214 mmol, 88%) of an orange oil.

**Synthesis in 1 g scale**

Pyrrolopyrimidine **3** (1.01 g, 2.47 mmol) was dissolved in *n*-butanol (30 mL) and added *N*-benzylmethylamine (0.950 mL, 7.32 mmol) under an $N_2$-atmosphere. The reaction mixture was heated to 125 °C on an oil bath and stirred for 4 h before it was cooled to rt. The reaction mixture was added water (50 mL) and EtOAc (80 mL) and the phases were separated. The water phase was extracted with more EtOAc (2 x 40 mL). The combined organic phases were washed with brine (50 mL) and dried over $Na_2SO_4$, filtered and concentrated *in vacuo*. The crude product was purified by silica-gel column chromatography (*n*-pentane:EtOAc, 3:1, $R_f$ = 0.51). Drying gave 1.10 g (0.573 mmol, 91%) of a white solid; mp. 66-68 °C (litt:[7] 67-69).

Spectroscopic data for compound **4** (Appendix C): $^{1}$H NMR (600 MHz, DMSO-$d_6$) $\delta$: 8.14 (s, 1H), 7.33-7.31 (m, 2H), 7.26-7.22 (m, 3H), 6.94 (s, 1H), 5.50 (s, 2H), 4.99 (s, 2H), 3.52 (t, *J* = 8.05, 2H), 3.30 (s, 3H), 0.80 (t, *J* = 8.05, 2H), -0.08 (s, 9H). $^{13}$C NMR (150 MHz, DMSO-$d_6$) δ: 155.3, 152.8, 151.2, 138.0, 128.5 (2C) 126.9 (2C), 126.8, 112.2, 104.1, 80.4, 72.7, 65.5, 52.7, 37.3, 17.1, -1.4 (3C). IR ($cm^{-1}$) *v*: 3113 (w), 2952 (w), 2852 (w), 1566 (s), 1448 (m), 1299 (m),

1066 (s), 831 (s) HRMS (ASAP$^+$, m/z): Detected 495.1074, calculated for $C_{20}H_{27}IN_4OSi$ $[M+H]^+$. 495.1077**.** The analyses are consistent with previously reported data [7].

## 5.3 Suzuki coupling reactions

### 5.3.1 Synthesis of N-benzyl-6-(4-methoxyphenyl)-N-methyl-7-((2-(trimethylsilyl)ethoxy)methyl)-7H-pyrrolo[2,3-d]pyrimidin-4-amine (6a)

**Xphos as catalyst (5 mol%), 100 mg scale**

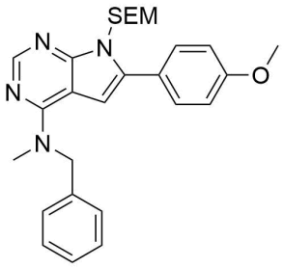


Pyrrolopyrimidine **4** (100 mg, 0.200 mmol) was added the boronic acid **5a** (33 mg, 0.24 mmol), potassium carbonate (98 mg, 0.71 mmol), XPhos (4.82 mg, 0.01 mmol) and XPhos 2$^{nd}$ generation pre catalyst (7.96 mg, 0.01 mmol) before it was put under an $N_2$-atmosphere. 1,4-Dioxane (2 mL) and water (2 mL) was degassed by flushing with $N_2$ while under ultrasonication for 30 min. After degassing, the solvents were added to the dry reagents. The mixture was heated to 100 °C on an oil bath, and full conversion was observed after 15 min. Upon completion, the reaction mixture was concentrated, diluted in water (15 mL) and added EtOAc (20 mL). The phases were separated, and the water phase was extracted with more EtOAc (2 x 20 mL). Brine (20 mL) was used to wash the combined organic phases before it was dried over $Na_2SO_4$, filtered and concentrated. The crude product was purified by silica-gel column chromatography (*n*-pentane:EtOAc 3:1, $R_f$ = 0.64). A total of 73.7 mg (0.156 mmol, 77%) of a transparent oil was isolated.

**Pd(dppf)$Cl_2$ as catalyst (5 mol%), 100 mg scale**

Pyrrolopyrimidine **4** (100 mg, 0.202 mmol) was added the boronic acid **5a** (33 mg, 0.24 mmol), potassium carbonate (98 mg, 0.71 mmol), and Pd(dppf)$Cl_2$ (7.40 mg, 10.1 µmol) before it was put under an $N_2$-atmosphere. 1,4-dioxane (2 mL) and water (2 mL) was degassed by flushing with $N_2$ while under ultrasonication for 30 min. After degassing, the solvents were added to the dry reagents. The mixture was heated to 100 °C on an oil bath, and full conversion was observed after 15 min. Upon completion, the reaction mixture was concentrated, diluted in water (15 mL) and added EtOAc (20 mL). The phases were separated, and the water phase was extracted with more EtOAc (2 x 20 mL). Brine (20 mL) was used to wash the combined organic phases before it was dried over $Na_2SO_4$, filtered and concentrated. The crude product was purified by silica-gel column chromatography (*n*-pentane:EtOAc 3:1, $R_f$ = 0.39). A total of 30 mg (0.063 mmol, 31%) of a transparent oil was isolated.

**$Pd_2(dba)_3$ as catalyst (5 mol%), 100 mg scale**

Pyrrolopyrimidine **4** (100 mg, 0.202 mmol) was added the boronic acid **5a** (33 mg, 0.24 mmol), potassium carbonate (98 mg, 0.71 mmol) and $Pd_2(dba)_3$ (9,60 mg, 10,1 µmol) before it was put under an $N_2$-atmosphere. 1,4-dioxane (2 mL) and water (2 mL) was degassed by flushing with $N_2$ while under ultrasonication for 30 min. After degassing, the solvents were added to the dry reagents. The mixture was heated to 100 °C on an oil bath, and full conversion was observed after 15 min. Upon completion, the reaction mixture was concentrated, diluted in water (15 mL) and added EtOAc (20 mL). The phases were separated, and the water phase was extracted with more EtOAc (2 x 20 mL). Brine (20 mL) was used to wash the combined organic phases before it was dried over $Na_2SO_4$, filtered and concentrated. The crude product was purified by silica-gel column chromatography (*n*-pentane:EtOAc 3:1, $R_f$ = 0.45). Drying gave compound **6a** as a transparent oil in 67.0 mg (0.141 mmol, 70%).

Spectroscopic data for compound **6a** (Appendix D): $^1$H NMR (600 MHz, DMSO-$d_6$) $\delta$: 8.23 (s, 1H), 7.62 (d, *J* = 8.9, 2H), 7.34-7.31 (m, 2H), 7.27-7.23 (m, 3H), 7.02 (d, *J* = 8.9, 2H). 6.70 (s, 1H), 5.51 (s, 2H), 5.05 (s, 2H), 3.80 (s, 3H), 3.61 (t, *J* = 8.4, 2H), 3.36 (s, 3H), 0.85 (t, *J* = 8.4, 2H), -0.08 (s, 9H). $^{13}$C NMR (150 MHz, DMSO-$d_6$) δ: 159.2, 156.3, 152.8, 151.0, 138.3, 136.4, 129.9 (2C), 128.5 (2C), 126.9 (3C), 123.7, 114.1 (2C), 102.1, 101.3, 70.2, 65.6, 55.2, 52.8, 37.3, 17.3, -1.5 (3C). IR ($cm^{-1}$) *v*: 2950 (w), 1612 (w), 1566 (s), 1452 (m), 1307 (m), 1072 (m), 833 (s). HRMS (ASAP$^+$, m/z): Detected 475.2521, calculated for $C_{27}H_{34}N_4O_2Si$ $[M+H]^+$ 475.2529.

### 5.3.2 Synthesis of N-benzyl-6-(4-methoxyphenyl)-N-methyl-7-((2-(trimethylsilyl)ethoxy)methyl)-7H-pyrrolo[2,3-d]pyrimidin-4-amine (6b)

**$Pd_2(dba)_3$ as catalyst (5 mol%), 50 mg scale**

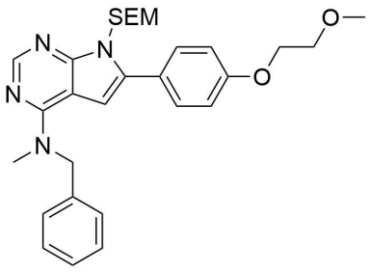


Pyrrolopyrimidine **4** (50 mg, 0.10 mmol) was added the boronic acid **5b** (24 mg, 0.12 mmol), potassium carbonate (49 mg, 0.35 mmol) and $Pd_2(dba)_3$ (4.63 mg, 5.06 µmol) before it was put under an $N_2$-atmosphere. 1,4-dioxane (1.5 mL) and water (1.5 mL) was degassed by flushing with $N_2$ while under ultrasonication for 30 min. After degassing, the solvents were added to the dry reagents. The mixture was heated to 100 °C on an oil bath, and full conversion was observed after 15 min. Upon completion the reaction mixture was concentrated, diluted in water (15 mL) and added

EtOAc (15 mL). The phases were separated, and the water phase was extracted with more EtOAc (2 x 15 mL). Brine (15 mL) was used to wash the combined organic phases before it was dried over $Na_2SO_4$, filtered and concentrated. The crude product was purified by silica-gel column chromatography (*n*-pentane:EtOAc 1:1, $R_f$ = 0.65). The isolated yield was 41 mg (78.8 mmol, 78%) of a transparent oil.

**$Pd_2(dba)_3$ as catalyst (2 mol%), 150 mg scale**

Pyrrolopyrimidine **4** (150 mg, 0.303 mmol) was added the boronic acid **5b** (71 mg, 0.36 mmol), potassium carbonate (147 mg, 1.06 mmol) and $Pd_2(dba)_3$ (5.56 mg, 6,07 µmol) before it was put under an $N_2$-atmosphere. 1,4-dioxane (3 mL) and water (3 mL) was degassed by flushing with $N_2$ while under ultrasonication 30 min. After degassing, the solvents were added to the dry reagents. The mixture was heated to 100 °C on an oil bath, and full conversion was observed after 15 min. Upon completion the reaction mixture was concentrated , diluted in water (30 mL) and added EtOAc (30 mL). The phases were separated, and the water phase was extracted with more EtOAc (2 x 30 mL). Brine (30 mL) was used to wash the combined organic phases before it was dried over $Na_2SO_4$, filtered and concentrated. The crude product was purified by silica-gel column chromatography (*n*-pentane:EtOAc 1:1, $R_f$ = 0.65). The isolated yield was 130 mg (0.239 mmol, 79%) of a transparent oil.

Spectroscopic data for compound **6b** (Appendix E): $^1$H NMR (600 MHz, DMSO-$d_6$) δ: 8.22 (s, 1H), 7.62 (d, *J* = 8.8, 2H), 7-34-7.31 (m, 2H), 7.27-7-23 (m, 3H), 7.04 (d, *J* = 8.8, 2H), 6.70 (s, 1H), 5.51 (s, 2H), 5.05 (s, 2H), 4.14 (t, *J* = 4.81, 2H), 3.67 (t, *J* = 4.81, 2H), 3.61 (t, *J* = 8.2, 2H), 3.36 (s, 3H), 3.31 (s, 3H), 0.85 (t, *J* = 8.2, 2H), -0.08 (s, 9H). $^{13}$C NMR (150 MHz, DMSO-$d_6$) δ: 158.4, 156.3, 152.8, 151.0, 138.3, 136.3, 129.9 (2C), 128.5 (2C), 126.9 (3C), 123.8, 114.6 (2C), 102.1, 101.3, 70.3, 70.2, 67.0, 65.6, 58.1, 52.7, 37.3, 17.3, -1.5 (3C). IR ($cm^{-1}$) *v*: 3029 (w), 2949 (w), 2892 (w), 1611 (s), 1561 (m), 1247 (s), 1074 (m), 857 (m). HRMS (ASAP$^+$, m/z): Detected 519.2791, calculated for $C_{29}H_{39}N_4O_3Si$ $[M+H]^+$ 519.2781.

### 5.3.3 Synthesis of 4-(4-(benzyl(methyl)amino)-7-((2-(trimethylsilyl)ethoxy)methyl)-7H-pyrrolo[2,3-d]pyrimidin-6-yl)phenol (6c)

**$Pd_2(dba)_3$ as catalyst (5 mol%), 100 mg scale**

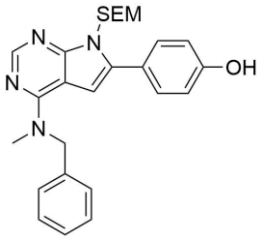


Pyrrolopyrimidine **4** (100 mg, 0.202 mmol) was added the boronic acid **5c** (33 mg, 0.24 mmol), potassium carbonate (98 mg, 0.71 mmol) and $Pd_2(dba)_3$ (9.26 mg, 10,1 µmol) before it was put under an $N_2$-atmosphere. 1,4-dioxane (2 mL) and water (2 mL) was degassed by flushing with $N_2$ while under ultrasonication for 30 min. After degassing, the solvents were added to the dry reagents. The mixture was heated to 100 °C on an oil bath, and full conversion was observed after 15 min. Upon completion, the reaction mixture was concentrated, diluted in water (20 mL) and added EtOAc (20 mL). The phases were separated, and the water phase was extracted with more EtOAc (2 x 20 mL). Brine (20 mL) was used to wash the combined organic phases before it was dried over $Na_2SO_4$, filtered and concentrated. The crude product was purified by silica-gel column chromatography (*n*-pentane:EtOAc 3:1, $R_f$ = 0.16). The isolated yield was 64.0 mg (0.139 mmol, 69%) of a pale yellow oil.

**$Pd_2(dba)_3$ as catalyst (2 mol%), 150 mg scale**

Pyrrolopyrimidine **4** (150 mg, 0.303 mmol) was added the boronic acid **5c** (50 mg, 0.36 mmol), potassium carbonate (147 mg, 1.06 mmol) and $Pd_2(dba)_3$ (5.56 mg, 6.07 µmol) before it was put under an $N_2$-atmosphere. 1,4-dioxane (3 mL) and water (3 mL) was degassed by flushing with $N_2$ while under ultrasonication for 30 min. After degassing, the solvents were added to the dry reagents. The mixture was heated to 100 °C on an oil bath, and full conversion was observed after 1.5 h. Upon completion, the reaction mixture was concentrated, diluted in water (30 mL) and added EtOAc (30 mL). The phases were separated, and the water phase was extracted with more EtOAc (2 x 30 mL). Brine (30 mL) was used to wash the combined organic phases before it was dried over $Na_2SO_4$, filtered and concentrated. The crude product was purified by silica-gel column chromatography (*n*-pentane:EtOAc 3:1, $R_f$ = 0.16). The isolated yield was 89 mg (0.194 mmol, 64%) of a transparent oil.

Spectroscopic data for compound **6c** (Appendix F): $^1$H NMR (600 MHz, DMSO-$d_6$) δ: 9.69 (s, 1H), 8.21 (s, 1H), 7.50 (d, *J* = 8.8, 2H), 7.33-7.31 (m, 2H), 7.27-7.23 (m, 3H), 6.84 (d, *J* = 8.8, 2H), 6.64 (s, 1H), 5.49 (s, 2H), 5.04 (s, 2H), 3.61 (t, *J* = 8.1, 2H), 3.35 (s, 3H), 0.84 (t, *J* =8.1,

2H), -0.80 (s, 9H). $^{13}$C NMR (150 MHz, DMSO-$d_6$) δ: 157.6, 156.3, 152.7, 150.8, 138.3, 136.9, 130.0 (2C), 128.5 (2C), 126.9 (3C), 122.0, 115.4 (2C), 102.1, 100.8, 70.2, 65.6, 52.7, 37.3, 17.3, -1.4 (3C). IR (cm$^{-1}$) *v*: 3062 (w), 2950 (w), 2895 (w), 1572 (s), 1489 (m), 1247 (m), 1076 (m), 835 (m). HRMS (ASAP$^+$, m/z): Detected 461.2373, calculated for $C_{26}H_{33}N_4O_2Si$ $[M+H]^+$ 461.2367.

### 5.3.4 Synthesis of *N*-benzyl-6-(3-methoxyphenyl)-*N*-methyl-7-((2-(trimethylsilyl)ethoxy)methyl)-7*H*-pyrrolo[2,3-*d*]pyrimidin-4-amine (6d)

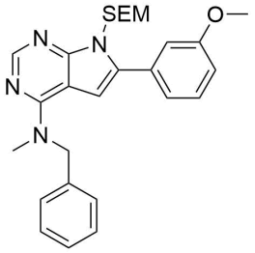


Pyrrolopyrimidine **4** (100 mg, 0.202 mmol) was added the boronic acid **5d** (37 mg, 0.24 mmol), potassium carbonate (98 mg, 0.71 mmol) and $Pd_2(dba)_3$ (9.26 mg, 10,1 µmol) before it was put under an $N_2$-atmosphere. 1,4-dioxane (2 mL) and water (2 mL) was degassed by flushing with $N_2$ while under ultrasonication for 30 min. After degassing, the solvents were added to the dry reagents. The mixture was heated to 100 °C on an oil bath, and full conversion was observed after 1.5 h. Upon completion, the reaction mixture was concentrated, diluted in water (20 mL) and added EtOAc (20 mL). The phases were separated, and the water phase was extracted with more EtOAc (2 x 20 mL). Brine (20 mL) was used to wash the combined organic phases before it was dried over $Na_2SO_4$, filtered and concentrated. The crude product was purified by silica-gel column chromatography (*n*-pentane:EtOAc 4:1, $R_f$ = 0.51). The isolated yield was 68 mg (0.143 mmol, 71%) of a yellow oil.

Spectroscopic data for compound **6d** (Appendix G): $^1$H NMR (600 MHz, $CDCl_3$) δ: 8.40 (s, 1H), 7.35-7.23 (m, 8H), 6.94-6.91 (m, 1H), 6.56 (s, 1H), 5.59 (s, 2H), 5.06 (s, 2H), 3.83 (s, 3H), 3.74 (t, *J* = 8.8, 2H), 3.37 (s, 3H), 0.97 (t, *J* = 8.8, 2H), -0.03 (s, 9H). $^{13}$C NMR (150 MHz, $CDCl_3$) δ: 159.7, 157.3, 153.5, 151.7, 137.8, 137.3, 133.0, 129.6, 128.7 (2C), 127.2, 127.1 (2C), 121.4, 114.4, 113.9, 102.8, 102.0, 70.7, 66.4, 55.3, 53.8, 37.2, 18.1, -1.5 (3C). IR (cm$^{-1}$) *v*: 3028 (w), 2950 (w), 2835 (w), 1567 (s), 1452 (m), 1308 (m), 1074 (m), 858 (m). HRMS (ASAP$^+$, m/z): Detected 475.2529, calculated for $C_{27}H_{35}N_4O_2Si$ $[M+H]^+$ 475.2530.

### 5.3.5 Synthesis of 3-(4-(benzyl(methyl)amino)-7-((2-(trimethylsilyl)ethoxy)methyl)-7H-pyrrolo[2,3-d]pyrimidin-6-yl)phenol (6e)

**$Pd_2(dba)_3$ as catalyst (5 mol%), 100 mg scale**

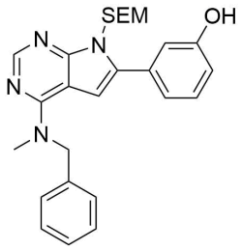


Pyrrolopyrimidine **4** (100 mg, 0.202 mmol) was added the boronic acid **5e** (33 mg, 0.24 mmol), potassium carbonate (98 mg, 0.71 mmol) and $Pd_2(dba)_3$ (9.26 mg, 10,1 µmol) before it was put under an $N_2$-atmosphere. 1,4-dioxane (2 mL) and water (2 mL) was degassed v for 30 min. After degassing, the solvents were added to the dry reagents. The mixture was heated to 100 °C on an oil bath, and full conversion was observed after 1.5 h. Upon completion, the reaction mixture was concentrated, diluted in water (20 mL) and added EtOAc (20 mL). The phases were separated, and the water phase was extracted with more EtOAc (2 x 20 mL). Brine (20 mL) was used to wash the combined organic phases before it was dried over $Na_2SO_4$, filtered and concentrated. The crude product was purified by silica-gel column chromatography (*n*-pentane:EtOAc 1:1, $R_f$ = 0.66). The isolated yield was 55.1 mg (0.119 mmol, 59%) of a transparent oil.

**$Pd_2(dba)_3$ as catalyst (2 mol%), 150 mg scale**

Pyrrolopyrimidine **4** (150 mg, 0.303 mmol) was added the boronic acid **5e** (50 mg, 0.36 mmol), potassium carbonate (147 mg, 1.06 mmol) and $Pd_2(dba)_3$ (5.56 mg, 6,07 µmol) before it was put under an $N_2$-atmosphere. 1,4-dioxane (3 mL) and water (3 mL) was degassed by flushing with $N_2$ while under ultrasonication for 30 min. After degassing, the solvents were added to the dry reagents. The mixture was heated to 100 °C on an oil bath, and full conversion was observed after 1.5 h. Upon completion, the reaction mixture was concentrated, diluted in water (30 mL) and added EtOAc (30 mL). The phases were separated, and the water phase was extracted with more EtOAc (2 x 30 mL). Brine (30 mL) was used to wash the combined organic phases before it was dried over $Na_2SO_4$, filtered and concentrated. The crude product was purified by silica-gel column chromatography (*n*-pentane:EtOAc 2:1, $R_f$ = 0.55). The isolated yield was 114 mg (0.247 mmol, 81%) of a transparent oil.

**$Pd_2(dba)_3$ as catalyst (1 mol%), 150 mg scale**

Pyrrolopyrimidine **4** (150 mg, 0.303 mmol) was added the boronic acid **5e** (50 mg, 0.36 mmol), potassium carbonate (147 mg, 1.06 mmol) and $Pd_2(dba)_3$ (5.56 mg, 6,07 µmol) before it was put under an $N_2$-atmosphere. 1,4-dioxane (3 mL) and water (3 mL) was degassed by flushing

with $N_2$ while under ultrasonication for 30 min. After degassing, the solvents were added to the dry reagents. The mixture was heated to 100 °C on an oil bath, and full conversion was observed after 1.5 h. Upon completion, the reaction mixture was concentrated, diluted in water (30 mL) and added EtOAc (30 mL). The phases were separated, and the water phase was extracted with more EtOAc (2 x 30 mL). Brine (30 mL) was used to wash the combined organic phases before it was dried over $Na_2SO_4$, filtered and concentrated. The crude product was purified by silica-gel column chromatography (*n*-pentane:EtOAc 3:1, $R_f$ = 0.28). The isolated yield was 92.7 mg (0.201 mmol, 66%) of a transparent oil.

Spectroscopic data for compound **6e** (Appendix H): $^1$H NMR (600 MHz, DMSO-$d_6$) δ: 9.57 (s , 1H), 8.23 (s, 1H), 7.34-7.31 (m, 2H), 7.27-7.23 (m, 4H), 7.12-7.11 (m, 1H), 7.06 (s, 1H), 6.82-6.80 (m 1H), 6.72 (s, 1H), 5.53 (s, 2H), 5.05 (s, 2H), 3.59 (t, *J* = 8.0, 2H), 3.36 (s, 3H), 0.84 (t, *J* = 8.0, 2H), -0.09 (s, 9H). $^{13}$C NMR (150 MHz, DMSO-$d_6$) δ: 157.5, 156.5, 152.3, 151.2, 138.2, 136.6, 132.6, 129.6, 128.5 (2C), 126.9 (3C), 119.3, 115.5, 115.1, 102.0, 101.9, 70.3, 65.6, 52.8, 37.4, 17.3, -1.5 (3C). IR (cm$^{-1}$) *v*: 3061 (w), 2951 (w), 1573 (s), 1415 (w) 1320 (w), 1246 (w), 1076 (m), 835 (w). HRMS (ASAP$^+$, m/z): Detected 461.2373, calculated for $C_{26}H_{33}N_4O_2Si$ $[M+H]^+$ 461.2373.

### 5.3.6 Synthesis of 6-(3-((1,3-dioxolan-2-yl)methoxy)phenyl)-N-benzyl-N-methyl-7-((2-(trimethylsilyl)ethoxy)methyl)-7H-pyrrolo[2,3-d]pyrimidin-4-amine (6f)

**$Pd_2(dba)_3$ as catalyst (5 mol%), 100 mg scale**

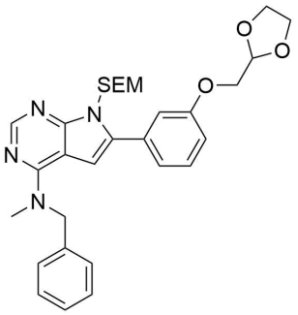


Pyrrolopyrimidine **4** (100 mg, 0.202 mmol) was added the boronic ester **5f** (74 mg, 0.24 mmol), potassium carbonate (98 mg, 0.71 mmol) and $Pd_2(dba)_3$ (9.26 mg, 10,1 µmol) before it was put under an $N_2$-atmosphere. 1,4-dioxane (2 mL) and water (2 mL) was degassed by flushing with $N_2$ while under ultrasonication for 30 min. After degassing, the solvents were added to the dry reagents. The mixture was heated to 100 °C on an oil bath, and full conversion was observed after 15 min. Upon completion, the reaction mixture was concentrated, diluted in water (20 mL) and added EtOAc (20 mL). The phases were separated, and the water phase was extracted with more EtOAc (2 x 20 mL). Brine (20 mL) was used to wash the combined organic phases before it was dried over $Na_2SO_4$, filtered and concentrated. The crude product was purified by silica-gel column

chromatography (*n*-pentane:EtOAc 1:1, $R_f$ = 0.64). The isolated yield was 84.8 mg (0.154 mmol, 77%) of a transparent oil.

**$Pd_2(dba)_3$ as catalyst (2 mol%), 100 mg scale**

Pyrrolopyrimidine **4** (150 mg, 0.303 mmol) was added the boronic ester **5f** (111 mg, 0.364 mmol), potassium carbonate (147 mg, 1.06 mmol) and $Pd_2(dba)_3$ (5.56 mg, 6,07 µmol) before it was put under an $N_2$-atmosphere. 1,4-dioxane (2 mL) and water (2 mL) was degassed by flushing with $N_2$ while under ultrasonication for 30 min. After degassing, the solvents were added to the dry reagents. The mixture was heated to 100 °C on an oil bath, and full conversion was observed after 1.5 h. Upon completion, the reaction mixture was concentrated, diluted in water (20 mL) and added EtOAc (20 mL). The phases were separated, and the water phase was extracted with more EtOAc (2 x 20mL). Brine (20 mL) was used to wash the combined organic phases before it was dried over $Na_2SO_4$, filtered and concentrated. The crude product was purified by silica-gel column chromatography (*n*-pentane:EtOAc 2:1, $R_f$ = 0.26). The isolated yield was 85 mg (0.233 mmol, 77%) of a transparent oil.

**$Pd_2(dba)_3$ as catalyst (5 mol%) , reaction temperature 70 °C, 100 mg scale**

Pyrrolopyrimidine **4** (100 mg, 0.202 mmol) was added the boronic ester **5f** (74 mg, 0.24 mmol), potassium carbonate (98 mg, 0.71 mmol) and $Pd_2(dba)_3$ (9.26 mg, 10,1 µmol) before it was put under an $N_2$-atmosphere. 1,4-dioxane (2 mL) and water (2 mL) was degassed by flushing with $N_2$ while under ultrasonication for 30 min before the solvents were added to the dry reagents. The mixture was heated to 70 °C on an oil bath, and full conversion was observed after 3 h. Upon completion, the reaction mixture was concentrated, diluted in water (20mL) and added EtOAc (20 mL). The phases were separated, and the water phase was extracted with more EtOAc (2 x 20 mL). Brine (20 mL) was used to wash the combined organic phases before it was dried over $Na_2SO_4$, filtered and concentrated. The crude product was purified by silica-gel column chromatography (*n*-pentane:EtOAc 2:1, $R_f$ = 0.26). The isolated yield was 79.1 mg (0.145 mmol, 72%) of a transparent oil.

Spectroscopic data for compound **6f** (Appendix I): $^1$H NMR (600 MHz, $CDCl_3$) δ: 8.40 (s, 1H), 7.34-7.31 (m, 3H), 7.29-7.27 (m, 4H), 7.20-7.15 (m, 1H), 6.97-6.95 (m, 1H), 6.55 (s, 1H), 5.58 (s, 1H), 5.30 (t, *J* = 4.10, 1H) 5.07 (s, 2H), 4.06 (d, *J* = 4.10, 2H), 4.06-4.04 (m, 2H), 3.98-3.95

(m, 2H), 3.73 (t, $J$ = 8.4, 2H), 3.37 (s, 3H), 0.97 (t, $J$ = 8.4, 2H), -0.03 (s, 9H) .$^{13}$C NMR (150 MHz, $CDCl_3$) δ: 158.7, 157.3, 153.5, 151.7, 137.8, 137.2, 133.1, 129.7, 128.7 (2C), 128.3, 127.1 (2C) , 121.9, 115.0, 114.7, 102.8, 102.1, 101.9, 70.7, 68.8, 66.4, 65.3 (2C), 53.3, 37.2, 18.1, -1.4 (3C). IR ($cm^{-1}$) $v$: 3028 (w), 2950 (w), 2889 (w), 1567 (s), 1414 (w), 1308 (w), 1069 (m), 858 (m). HRMS ($ASAP^+$, m/z): Detected 547.2733, calculated for $C_{30}H_{39}N_4O_2Si$ $[M+H]^+$ 547.2741.

### 5.3.7 Synthesis of 6-(benzo[d][1,3]dioxol-5-yl)-*N*-benzyl-*N*-methyl-7-((2-(trimethylsilyl)ethoxy)methyl)-7*H*-pyrrolo[2,3-*d*]pyrimidin-4-amine (6g)

**$Pd_2(dba)_3$ as catalyst (5 mol%), 100 mg scale**

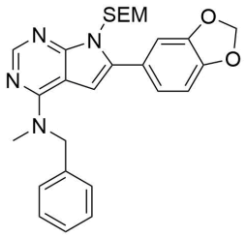


Pyrrolopyrimidine **4** (100, 0.202 mmol) was added the boronic acid **5g** (40 mg, 0.24 mmol), potassium carbonate (98 mg, 0.71 mmol) and $Pd_2(dba)_3$ (9.26 mg, 10.1 µmol) before it was put under an $N_2$-atmosphere. 1,4-dioxane (2 mL) and water (2 mL) was degassed with by flushing with $N_2$ while under ultrasonication for 30 min before the solvents were added to the dry material. The mixture was heated to 100 °C on an oil bath, and full conversion was observed after 15 min. Upon completion, the reaction mixture was concentrated, diluted in water (20 mL) and added EtOAc (20 mL). The phases were separated, and the water phase was extracted with more EtOAc (2 x 20 mL). Brine (20 mL) was used to wash the combined organic phases before it was dried over $Na_2SO_4$, filtered and concentrated. The crude product was purified by silica-gel column chromatography (*n*-pentane:EtOAc 3:1, $R_f$ = 0.21). The isolated yield was 63.7 mg (0.130 mmol, 64%) of a light yellow oil.

**$Pd_2(dba)_3$ as catalyst (2 mol%), 150 mg scale**

Pyrrolopyrimidine **4** (150 mg, 0.303 mmol) was added the boronic acid **5g** (60 mg, 0.36 mmol), potassium carbonate (147 mg, 1.06 mmol) and $Pd_2(dba)_3$ (5.56 mg, 6,07 µmol) before it was put under an $N_2$-atmosphere. 1,4-dioxane (3 mL) and water (3 mL) was degassed by flushing with $N_2$ while under ultrasonication for 30 min. After degassing, the solvents were added to the dry reagents. The mixture was heated to 100 °C on an oil bath, and full conversion was observed after 15 min. Upon completion, the reaction mixture was concentrated, diluted in water (30 mL) and added EtOAc (30 mL). The phases were separated, and the water phase was extracted with more EtOAc (2 x 30 mL). Brine (30 mL) was used to wash the combined organic phases before it was dried over $Na_2SO_4$, filtered and concentrated. The crude product was purified by silica-

gel column chromatography (*n*-pentane:EtOAc 3:1, $R_f$ = 0.21). The isolated yield was 85.2 mg (0.176 mmol, 58%) of a transparent oil.

Spectroscopic data for compound **6g** (Appendix J): $^{1}$H NMR (600 MHz, DMSO-$d_6$) δ: 8.22 (s, H), 7.34-7.31 (m, 2H), 7.28-7.23 (m, 4H), 7.19 (dd, *J* = 8.0, 1H), 7.01 (d, *J* = 8.0, 1H), 6.73 (s, 1H), 6.07 (s, 2H), 5.52 (s, 2H) 5.05 (s, 2H), 3.62 (t, *J* = 8.10, 2H), 3.35 (s, 3H), 0.85 (t, *J* = 8.10, 2H), -0.08 (s, 9H). $^{13}$C NMR (150 MHz, DMSO-$d_6$) δ: 156.4, 152.9, 151.1, 147.6, 147.2, 138.2, 136.2, 128.5 (2C), 126.9 (3C), 125.2, 122.5, 108.8, 108.5, 102.0, 101.8, 101.3, 70.2, 65,7, 52.7, 37.4, 17.3, -1.4 (3C). IR ($cm^{-1}$) *v*: 3061 (w), 2941 (w), 1570 (s), 1481 (m), 1307 (w), 1237 (m) 1075 (m), 834 (w). HRMS (ASAP$^+$, m/z): Detected 489.2316, calculated for $C_{27}H_{33}N_4O_3Si$ $[M+H]^+$ 489.2322.

## 5.4 Williamson ether synthesis

### 5.4.1 Synthesis of *N*-benzyl-6-(3-(2-methoxyethoxy)phenyl)-*N*-methyl-7-((2-(trimethylsilyl)ethoxy)methyl)-7*H*-pyrrolo[2,3-*d*]pyrimidin-4-amine (6h)

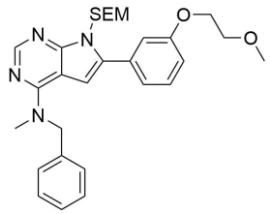


The alcohol **6e** (97.2 mg, 0.211 mmol) was added NaH (6.25 mg, 0.261 mmol) before it was put under $N_2$-atmosphere. Dry DMF (3 mL) was added, and the mixture was heated to 100 °C on an oil bath. The mixture was stirred for 15 min before 1-bromo-2-methoxyethane (36 mg, 0.26 mmol) was dissolved in DMF and added dropwise with a syringe. Stirring was continued for 4 h. Another equivalent of 1-bromo-2-methoxyethane (29.1 mg, 0.211 mmol) and NaH (5.05 mg, 0.211 mmol) was added to the mixture and it was left at 100 °C for 20 h. Another equivalent of 1-bromo-2-methoxyethane (29.1 mg, 0.211 mmol) and NaH (5.05 mg, 0.211 mmol) was added and stirring was continued for 4 h before water (30 mL) was added. The water phase was extracted with EtOAc (3 x 20 mL). The combined organic phases were washed with brine (30 mL) before being dried over $Na_2SO_4$ and concentrated *in vacuo*. The crude product was purified by silica-gel column chromatography (*n*-pentane:EtOAc, 2:1, $R_f$ = 0.04). Drying resulted in 45 mg (0.089 mmol, 41%) of a transparent oil.

Spectroscopic data for compound **6h** (Appendix K): $^1$H NMR (600 MHz, DMSO-$d_6$) δ: 8.25 (s, 1H) 7.38-7.24 (m, 8H), 6.99-6.98 (m, 1H), 6.83 (s, 1H), 5.55 (s, 2H), 5.06 (s, 2H), 4.13 (t, *J* = 4.5, 2H), 3.67 (t, *J* = 4.5, 2H), 3.62 (t, *J* = 8.4, 2H), 3.37 (s, 3H), 3.31 (s, 3H), 0.85 (t, *J* = 8.4, 2H), -0.08 (s, 9H). $^{13}$C NMR (150 MHz, DMSO-$d_6$) δ: 158.6, 157.5, 151.1, 138.1, 136.3, 132.6, 129.8, 128.5 (2C), 126.9, 126.8 (3C), 120.8, 119.4, 114.4, 114.2, 102.5, 102.0, 70.4, 70.3, 66.9, 65.6, 58.2, 52.8, 37.5, 17.3, -1.5 (3C). IR ($cm^{-1}$) *v*: 3028 (w), 2949 (w), 2890 (w), 1558 (s), 1414 (w), 1358 (w), 1247 (m), 1075 (m), 835 (m). HRMS (ASAP$^+$, m/z): Detected 519.2794, calculated for $C_{29}H_{39}N_4O_3Si$ $[M+H]^+$ 519.2791.

## 5.5 SEM removal

### 5.5.1 Synthesis of *N*-benzyl-6-(4-methoxyphenyl)-*N*-methyl-7*H*-pyrrolo[2,3-*d*]pyrimidin-4-amine (7a)

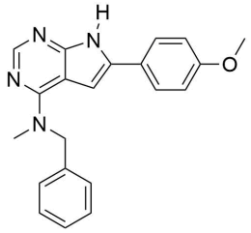

Compound **6a** (92 mg, 0.194 mmol) was dissolved in $CH_2Cl_2$ (15 mL) before TFA (3 mL). The reaction was heated to 50 °C on an oil bath and stirred for 4 h before the solvents were evaporated. The residue was added THF (15 mL) and saturated aq. $NaHCO_3$ (15 mL) before it was stirred at rt for 20 h and then concentrated *in vacuo*. Water (15 mL) and EtOAc (30 mL) were added and the phases were separated. The water phase was extracted with more EtOAc (3 x 20 mL). The combined organic phases were washed with brine (30 mL), dried over $Na_2SO_4$ and concentrated *in vacuo*. The crude product was purified by silica-gel column chromatography ($CH_2Cl_2$/MeOH, 19/1, $R_f$ = 0.30). Drying resulted in 56.9 mg (0.165 mmol, 85%) of a white powder; mp. 250-252 °C.

Spectroscopic data for compound **7a** (Appendix L): $^1$H NMR (600 MHz, DMSO-$d_6$) δ: Shift 12.06 (s, 1H), 8.13 (s, 1H), 7.77 (d, *J* = 8.9, 2H), 7.34-7.31 (m, 2H), 7.28-7.23 (m, 3H). 6.97 (d, *J*= 8.9, 2H), 6.90 (s, 1H), 5.04 (s, 2H), 3.78 (s, 3H), 3.36 (s, 3H) $^{13}$C NMR (150 MHz, DMSO-$d_6$) δ: 158.7, 156.2, 152.8, 150.7, 138.5, 133.3, 128.5 (2C), 127.0 (2C), 126.8, 126.1 (2C) 124.2, 114.2 (2C), 103.3, 97.3, 55.2, 52.7, 37.3. IR ($cm^{-1}$) *v*: 3105 (w), 2962 (w), 1732 (w), 1566 (s), 1545 (s), 1401 (m), 1248 (s), 1022 (m), 831 (m). HRMS ($ASAP^+$, m/z): Detected 345.1715, calculated for $C_{21}H_{21}N_4O$ $[M+H]^+$ 345.1715.

### 5.5.2 Synthesis of *N*-benzyl-6-(4-(2-methoxyethoxy)phenyl)-*N*-methyl-7*H*-pyrrolo[2,3-*d*]pyrimidin-4-amine (7b)

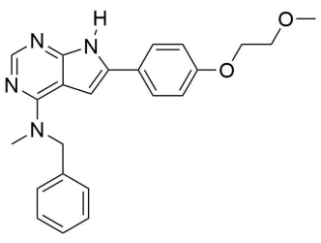

Compound **6b** (123 mg, 0.237 mmol) was dissolved in $CH_2Cl_2$ (20 mL) and TFA (3 mL). The reaction was heated to 50 °C on an oil bath and stirred for 6 h, before the solvents were evaporated. The residue was added THF (20 mL) and saturated aq. $NaHCO_3$ (20 mL) before it was stirred at rt for 20 h. Additional 5 mL of $NaHCO_3$ was added, and the mixture was stirred for 4 h before being concentrated *in vacuo*. Water (25 mL) and EtOAc (40 mL) were added and the phases were separated. The water phase was extracted with more EtOAc (3 x 30 mL). The combined organic phases were washed with brine (40 mL),

dried over $Na_2SO_4$ and concentrated *in vacuo*. The crude product was purified by silica-gel column chromatography ($CH_2Cl_2$/MeOH, 19/1, $R_f$ = 0.25). Drying resulted in 62.4 mg (0.161 mmol, 68%) of a white powder; mp. 217-219 °C.

Spectroscopic data for compound **7b** (Appendix M): $^1$H NMR (600 MHz, DMSO-$d_6$) δ: 12.06 (s, 1H), 8.13 (s, 1H), 7.76 (d, *J* = 8.9, H), 7.34-7.31 (m, 2H), 7.28-7.23 (m, 3H), 6.99 (d, *J* = 8.9, 2H), 6.90 (s, 1H), 5.04 (s, 2H), 4.12 (t, *J* = 4.2, 2H) 3.67 (t, *J* = 4.2, 2H) 3.35 (s, 3H), 3.31 (s, 3H). $^{13}$C NMR (150 MHz, DMSO-$d_6$) δ: 157.9, 156.2, 152.7, 150.7, 138.5, 133.3, 128.5 (2C), 127.0 (2C), 126.8, 126.1 (2C), 124.2, 114.7 (2C), 103.3, 97.3, 70.3, 66.9, 58.1, 52.6, 37.3. IR (cm$^{-1}$) *v*: 3108 (w), 2984 (w), 1562 (s), 1499 (m), 1248 (m), 1062 (m), 935 (w) 837 (w). HRMS (ASAP$^+$, m/z): Detected 398.1974, calculated for $C_{23}H_{25}N_4O_2$ $[M+H]^+$ 389.1978.

### 5.5.3 Synthesis of 4-(4-(benzyl(methyl)amino)-7*H*-pyrrolo[2,3-*d*]pyrimidin-6-yl)phenol (7c)

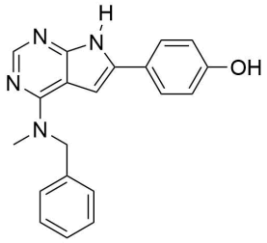


Compound **6c** (55 mg, 0.119 mmol) was dissolved in $CH_2Cl_2$ (10 mL) and TFA (2 mL). The reaction was heated to 50 °C on an oil bath and stirred for 4 h, and the solvents were evaporated. The residue was added THF (10 mL) and saturated aq. $NaHCO_3$ (10 mL) before it was stirred at rt for 20 h. Water (20 mL) and EtOAc (30 mL) were added and the phases were separated. The water phase was extracted with more EtOAc (3 x 20 mL). The combined organic phases were washed with brine (20 mL), dried over $Na_2SO_4$ and concentrated *in vacuo*. The crude product was purified by silica-gel column chromatography ($CH_2Cl_2$/MeOH, 19/1, $R_f$ = 0.27). Drying resulted in 27.8 mg (0.085 mmol, 71%) of a light yellow powder; mp. 239-241 °C (decomp.).

Spectroscopic data for compound **7c** (Appendix N): $^1$H NMR (600 MHz, DMSO-$d_6$) δ: Shifts 11.9 (s, 1H), 9.58 (s, 1H), 8.11 (s, 1H), 7.64 (d, *J* = 8.8, 2H), 7.34-7.31 (m, 2H), 7.27-7.23 (m, 3H), 6.82 (s, 1H), 6.78 (d, *J* = 8.8, 2H) 5.03 (s, 2H), 3.34 (s, 3H). $^{13}$C NMR (150 MHz, DMSO-$d_6$) δ: 157.0, 156.1, 152.7, 150.5, 138.5, 133.9, 128.5 (2C), 127.0 (2C), 126.8, 126.2 (2C), 122.6 115.5 (2C), 103.2, 96.6, 52.6, 37.3. IR (cm$^{-1}$) *v*: 3106 (w), 2959 (w), 2856 (w), 1735 (w), 1570 (s), 1405 (m), 1207 (m), 1151 (m), 862 (m). HRMS (ASAP$^+$, m/z): Detected 331.1556, calculated for $C_{20}H_{19}N_4O$ $[M+H]^+$ 331.1559.

### 5.5.4 Synthesis of *N*-benzyl-6-(3-methoxyphenyl)-*N*-methyl-7*H*-pyrrolo[2,3-*d*]pyrimidin-4-amine (7d)

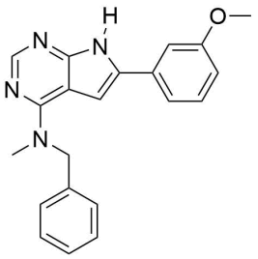

Compound **6d** (67 mg, 0.141 mmol) was dissolved in $CH_2Cl_2$ (10 mL) and TFA (1.5 mL). The reaction was heated to 50 °C on an oil bath and stirred for 4 h before the solvents were evaporated. The residue was added THF (10 mL) and saturated aq. $NaHCO_3$ (10 mL) before it was stirred at rt for 20 h. Additional 5 mL of $NaHCO_3$ was added and the mixture was stirred for 6 h. Water (20 mL) and EtOAc (30 mL) were added and the phases were separated. The water phase was extracted with more EtOAc (3 x 30 mL). The combined organic phases were washed with brine (20 mL), dried over $Na_2SO_4$ and concentrated *in vacuo*. The crude product was purified by silica-gel column chromatography ($CH_2Cl_2$/MeOH, 9/1, $R_f$ = 0.55). Drying resulted in 31.7 mg (0.917 mmol, 65%) of a pale yellow solid; mp. 210-212 °C.

Spectroscopic data for compound **7d** (Appendix O): $^1$H NMR (600 MHz, DMSO-$d_6$) δ: 12.17 (s, 1H), 8.15 (s, 1H), 7.43-7.41 (m, 2H), 7.35-7.24 (m, 6H), 7.07 (s, 1H), 6.85-6.83 (m, 1H), 5.05 (s, 2H), 3.81 (s, 3H), 3.37 (s, 3H). $^{13}$C NMR (150 MHz, DMSO-$d_6$) δ: 159.7, 156.5, 152.9, 151.2, 138.4, 133.1, 132.8, 129.8, 128.5 (2C), 127.0 (2C), 126.9, 117.1, 113.1, 110.0, 103.2, 99.2, 55.2, 52.7, 37.4 . IR (cm$^{-1}$) *v*: 3209 (w), 3106 (w), 2834 (w), 1596 (s), 1403 (w), 1240 (w), 935 (w). HRMS (ASAP$^{+,}$ m/z): Detected 345.1712, calculated for $C_{21}H_{21}N_4O$ $[M+H]^+$ 345.1715.

### 5.5.5 Synthesis of 3-(4-(benzyl(methyl)amino)-7*H*-pyrrolo[2,3-*d*]pyrimidin-6-yl)phenol (7e)

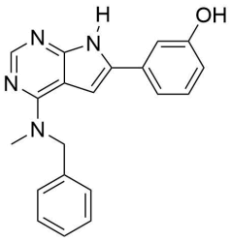

Compound **6e** (92,7 mg, 0.201 mmol) was dissolved in $CH_2Cl_2$ (15 mL) and TFA (2 mL). The reaction was heated to 50 °C on an oil bath and stirred for 10 h, before the solvents were evaporated. The residue was added THF (15 mL) and saturated aq. $NaHCO_3$ (15 mL) before it was stirred at rt for 20 h. Water (20 mL) and EtOAc (30 mL) were added and the phases were separated. The water phase was extracted with more EtOAc (3 x 20 mL) and DCM (2 x 20 mL). The combined organic phases were washed with brine (30 mL), dried over $Na_2SO_4$ and concentrated *in vacuo*. The crude product was purified by silica-gel column chromatography

($CH_2Cl_2$/MeOH, 19/1, $R_f$ = 0.20). Drying resulted in 46.5 mg (0.141 mmol, 70%) of a pale yellow powder; mp. 252-254 °C.

Spectroscopic data for compound **7e** (Appendix P): $^1$H NMR (600 MHz, DMSO-$d_6$) δ: 12.09 (s, 1H), 9.46 (s, 1H), 8.14 (s, 1H), 7.34-7.32 (m, 2H), 7.28-7.23 (m, 4H), 7.20-7.18 (m, 2H), 6.92 (s, 1H), 6.71-6.69 (m, 1H), 5.04 (s, 2H), 3.36 (s, 3H), $^{13}$C NMR (150 MHz, DMSO-$d_6$) δ: 157.6, 156.4, 152.8, 151.1, 138.4, 133.5, 132.8, 129.7, 128.4 (2C), 127.0 (2C), 126.9, 115.7, 114.4, 111.7, 103.1, 98.6, 52.7, 37.3 IR (cm$^{-1}$) *v*: 3205 (w), 3112 (w), 2922 (w), 1567 (s), 1445 (m), 1405 (m), 1237 (w), 933 (m), 693 (m). , HRMS (ASAP$^+$, m/z): Detected 331.1558, calculated for $C_{20}H_{19}N_4O$ $[M+H]^+$ 331.1559.

### 5.5.6 Synthesis of 6-(3-((1,3-dioxolan-2-yl)methoxy)phenyl)-*N*-benzyl-*N*-methyl-7*H*-pyrrolo[2,3-*d*]pyrimidin-4-amine (7f)

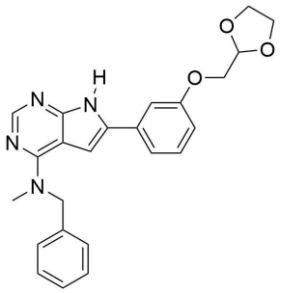

Compound **6f** (78.5 mg, 0.144 mmol) was dissolved in $CH_2Cl_2$ (15 mL) and TFA (3 mL). The reaction was heated to 50 °C on an oil bath and stirred for 4 h, before the solvents were evaporated. The residue was added THF (15 mL) and saturated aq. $NaHCO_3$ (15 mL) before it was stirred at rt for 20. Water (20 mL) and EtOAc (30 mL) were added and the phases were separated. The water phase was extracted with more EtOAc (3 x 20 mL) and DCM (2 x 20 mL). The combined organic phases were washed with brine (30 mL), dried over $Na_2SO_4$ and concentrated *in vacuo*. The crude product was purified by silica-gel column chromatography ($CH_2Cl_2$/MeOH, 9/1, $R_f$ = 0.38). Drying resulted in 23.8 mg (0.057 mmol, 40%) of a light beige powder; mp. 203-205 °C.

Spectroscopic data for compound **7f** (Appendix Q): $^1$H NMR (600 MHz, DMSO-$d_6$) δ: 12.15 (s,1H), 8.15 (s, 1H), 7.47-7.43 (m, 2H), 7.34-7.23 (m, 6H), 7.10 (s, 1H), 6.87-6.84 (m, 1H) 5.23 (t, *J* = 4.1, 1H), 5.05 (s, 2H), 4.06 (d, *J* = 4.1, 2H), 3.99-3.86 (m, 4H), 3.37 (s, 3H). $^{13}$C NMR (150 MHz, DMSO-$d_6$) δ: 158.6, 156.5, 152.9, 151.3, 138.4, 133.0, 132.9, 129.9, 128.5 (2C), 127.0 (2C), 126.9, 117.4, 113.7, 110.4, 103.2, 101.3, 99.3, 68.2, 64.5 (2C), 52.6, 37.4. IR (cm$^{-1}$) *v*: 3104 (w), 2957 (w), 2857 (w), 1572 (s), 1502 (m), 1354 (w), 1270 (m), 1068 (w), 937 (m). HRMS (ASAP$^+$, m/z): Detected 417.1927, calculated for $C_{24}H_{25}N_4O_3$ $[M+H]^+$ 417.1927.

### 5.5.7 Synthesis of 6-(benzo[*d*][1,3]dioxol-5-yl)-*N*-benzyl-*N*-methyl-7*H*-pyrrolo[2,3-*d*]pyrimidin-4-amine (7g)

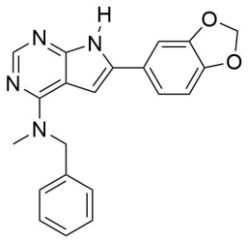

Compound **16** (56.4 mg, 0.116 mmol) was dissolved in $CH_2Cl_2$ (10 mL) and TFA (2.5 mL). The reaction was heated to 50 °C on an oil bath and stirred for 10 h. Additional 1.5 mL of TFA was added and stirring was continued for 14 h, before the solvents were evaporated. The residue was added THF (10 mL) and saturated aq. $NaHCO_3$ (10 mL) before it was stirred at rt for 20 h. Water (20 mL) and EtOAc (30 mL) were added and the phases were separated. The water phase was extracted with more EtOAc (3 x 20 mL) and DCM (2 x 20 mL). The combined organic phases were washed with brine (30 mL), dried over $Na_2SO_4$ and concentrated *in vacuo*. The crude product was purified by silica-gel column chromatography ($CH_2Cl_2$/MeOH, 19/1, $R_f$ = 0.29). Drying resulted in 12.8 mg (0.036 mmol, 31%) of a pale yellow powder; mp. 245-247 °C (decomp.).

Spectroscopic data for compound **7g** (Appendix R): $^1$H NMR (600 MHz, DMSO-$d_6$) δ: 12.04 (s, 1H), 8.13 (s, 1H), 7.45 (s, 1H), 7.36-7.31 (m, 3H), 7.27-7.23 (m, 3H), 6.97-6.95 (m, 2H), 6.04 (s, 2H), 5.03 (s, 2H), 3.35 (s, 3H). $^{13}$C NMR (150 MHz, DMSO-$d_6$) δ: 156.3, 152.8, 150.9, 147.8, 146.6, 138.5, 133.2, 128.5 (2C), 127.0 (2C), 126.8, 125.8, 118.4, 108.6, 105.3, 103.2, 101.1, 98.0, 52.6, 37.3. IR (cm$^{-1}$) *v*: 3117 (w), 2918 (w), 1570 (s), 1408 (m), 1315 (m), 1236 (s), 1003 (m), 730 (m). HRMS (ASAP$^+$, m/z): Detected 359.1507, calculated for $C_{21}H_{19}N_4O_2$ $[M+H]^+$ 359.1508.

### 5.5.8 Synthesis of compound *N*-benzyl-6-(3-(2-methoxyethoxy)phenyl)-*N*-methyl-7*H*-pyrrolo[2,3-*d*]pyrimidin-4-amine (7h)

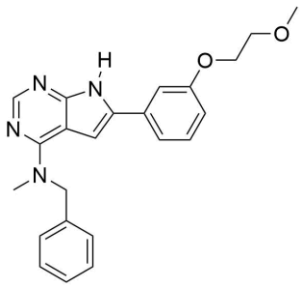

Compound **6h** (42 mg, 0.081 mmol) was dissolved in $CH_2Cl_2$ (10 mL) and TFA (2.5 mL). The reaction was heated to 50 °C on an oil bath and stirred for 6 h before additional 1.5 mL of TFA was added . After two more hours of stirring, the solvents were evaporated. The residue was added THF (10 mL) and saturated aq. $NaHCO_3$ (10 mL) before it was stirred at rt for 20 h. Water (20 mL) and EtOAc (30 mL) were added and the phases were separated. The water phase was extracted with more EtOAc (3 x 20 mL). The combined organic phases were washed with brine (20 mL), dried over $Na_2SO_4$ and

concentrated *in vacuo*. The crude product was purified by silica-gel column chromatography ($CH_2Cl_2$/MeOH, 19/1, $R_f$ = 0.20). Drying resulted in 24.1 mg (0.062 mmol, 77%) of a white powder; mp. 188-190 °C.

Spectroscopic data for compound **7h** (Appendix S): $^{1}$H NMR (600 MHz, DMSO-$d_6$) δ: 12.14 (s, 1H), 8.15 (s, 1H), 7.46 (s, 1H), 7.41 (d, *J* = 8.1, 1H), 7-34-7.23 (m, 6H), 7.09 (s, 1H), 6.84 (d, *J* = 8.1, 1H), 5.05 (s, 2H), 4.16 (t, *J* = 4.2, 2H), 3.68 (t, *J* = 4.2, 2H), 3.37 (s, 3H), 3.32 (s, 3H). $^{13}$C NMR (150 MHz, DMSO-$d_6$) δ: 158.9, 156.4, 152.9, 151.2, 138.4, 133.0, 132.8, 129.8, 128.5 (2C), 127.0 (2C), 126.9, 117.2, 113.5, 110.5, 103.2, 99.2, 70.4, 66.8, 58.1, 52.6, 37.4. IR ($cm^{-1}$) *v*: 3123 (w), 2921 (w), 2869 (w), 1568 (s), 1446 (m), 1207 (m), 1068 (m), 885 (w). HRMS ($ASAP^+$, m/z): Detected 389.1971, calculated for $C_{23}H_{25}N_4O_2$ $[M+H]^+$ 389.1978.

# References


1. Nagar, B.; Bornmann, W. G.; Pellicena, P.; Schindler, T.; Veach, D. R.; Miller, W. T.; Clarkson, B.; Kuriyan, J., Crystal structures of the kinase domain of c-Abl in complex with the small molecule inhibitors PD173955 and imatinib (STI-571). *Cancer Res.* **2002**, *62* (15), 4236-4243.
2. Bikker, J. A.; Brooijmans, N.; Wissner, A.; Mansour, T. S., Kinase domain mutations in cancer: implications for small molecule drug design strategies. *J. Med. Chem.* **2009**, *52* (6), 1493-1509.
3. Lodish, H.; Berk, A.; Zipursky, S.; Matsudaira, P.; Baltimore, D.; Darnell, J., Receptor Tyrosine Kinases and Ras. In *Molecular Cell Biology*, 4 ed.; W.H. Freeman: New York, 2000.
4. Lemmon, M. A.; Schlessinger, J., Cell signaling by receptor tyrosine kinases. *Cell* **2010**, *141* (7), 1117-1134.
5. Han, J.; Henriksen, S.; Nørsett, K. G.; Sundby, E.; Hoff, B. H., Balancing potency, metabolic stability and permeability in pyrrolopyrimidine-based EGFR inhibitors. *Eur. J. Med. Chem* **2016**, *124*, 583-607.
6. Han, J.; Kaspersen, S. J.; Nervik, S.; Norsett, K. G.; Sundby, E.; Hoff, B. H., Chiral 6-aryl-furo 2,3-d pyrimidin-4-amines as EGFR inhibitors. *E. J. Med. Chem.* **2016**, *119*, 278-299.
7. Larsen, K. U., Synthesis of Pyrrolopyrimidines as CSF-1R Kinase Inhibitors. NTNU: Trondheim, 2016; p 304.
8. Xiantao, W.; Martindale, J. L.; Yusen, L.; Holbrook, N. J., The cellular response to oxidative stress: influences of mitogen-activated protein kinase signalling pathways on cell survival. *Biochem. J.* **1998**, *333* (2), 291-300.
9. Dissen, E. Proteinkinaser. https://sml.snl.no/proteinkinase. (accessed 25.11.16).
10. Gibbs, C. S.; Zoller, M. J., Rational scanning mutagenesis of a protein kinase identifies functional regions involved in catalysis and substrate interactions. *J. Biol. Chem.* **1991**, *266* (14), 8923-8931.
11. Noble, M. E.; Endicott, J. A.; Johnson, L. N., Protein kinase inhibitors: insights into drug design from structure. *Science* **2004**, *303* (5665), 1800-1805.
12. Mergan, F.; Jaubert, F.; Sauvat, F.; Hartmann, O.; Lortat-Jacob, S.; Révillon, Y.; Nihoul-Fékété, C.; Sarnacki, S., Inflammatory myofibroblastic tumor in children: clinical review with anaplastic lymphoma kinase, Epstein-Barr virus, and human herpesvirus 8 detection analysis. *J. Pediatr. Surg.* **2005**, *40* (10), 1581-1586.
13. Herbst, R. S., Review of epidermal growth factor receptor biology. *Int. J. Radiat. Oncol. Biol. Phys.* **2004**, *59* (2), S21-S26.
14. Hubbard, S. R.; Till, J. H., Protein tyrosine kinase structure and function. *Ann. Rev. Biochem.* **2000**, *69* (1), 373-398.
15. Tefferi, A.; Lasho, T. L.; Schwager, S. M.; Steensma, D. P.; Mesa, R. A.; Li, C. Y.; Wadleigh, M.; Gary Gilliland, D., The JAK2V617F tyrosine kinase mutation in myelofibrosis with myeloid metaplasia: lineage specificity and clinical correlates. *Br. J. Haematol.* **2005**, *131* (3), 320-328.
16. Shah, N. P.; Nicoll, J. M.; Nagar, B.; Gorre, M. E.; Paquette, R. L.; Kuriyan, J.; Sawyers, C. L., Multiple BCR-ABL kinase domain mutations confer polyclonal resistance to the tyrosine kinase inhibitor imatinib (STI571) in chronic phase and blast crisis chronic myeloid leukemia. *Cancer cell* **2002**, *2* (2), 117-125.
17. Downing, J.; Rettenmier, C.; Sherr, C., Ligand-induced tyrosine kinase activity of the colony-stimulating factor 1 receptor in a murine macrophage cell line. *Mol. Cell. Biol.* **1988**, *8* (4), 1795-1799.

18. El-gamal, M. I.; Anbar, H. S.; Yoo, K. H.; Oh, C. h., FMS Kinase Inhibitors: Current Status and Future Prospects. *Med. Res. Rev.* **2013**, *33*(3), 599-636.
19. Hume, D. A.; Macdonald, K. P. A., Therapeutic applications of macrophage colony-stimulating factor-1 (CSF-1) and antagonists of CSF-1 receptor (CSF-1R) signaling. *Blood* **2012**, *119* (8), 1810.
20. Kristoffersen, E. Makrofag. https://sml.snl.no/makrofag (accessed 10.12.16).
21. Ovchinnikov, D. A., Macrophages in the embryo and beyond: much more than just giant phagocytes. *Genesis* **2008,** *46* (9), 447-462.
22. Quatromoni, J. G.; Eruslanov, E., Tumor-associated macrophages: function, phenotype, and link to prognosis in human lung cancer. *Am. J. Transl. Res.* **2012**, *4* (4), 376.
23. Bingle, L.; Brown, N.; Lewis, C., The role of tumour-associated macrophages in tumour progression: implications for new anticancer therapies. *J. Pathol.* **2002**, *196* (3), 254-265.
24. Pharmacodia Emacutzumab. http://www.pharmacodia.com/web/drug/1_9618.html (accessed 10.12.16).
25. Cassier, P. A.; Italiano, A.; Gomez-Roca, C. A.; Le Tourneau, C.; Toulmonde, M.; Cannarile, M. A.; Ries, C.; Brillouet, A.; Müller, C.; Jegg, A.-M., CSF1R inhibition with emactuzumab in locally advanced diffuse-type tenosynovial giant cell tumours of the soft tissue: a dose-escalation and dose-expansion phase 1 study. *Lancet Oncol.* **2015**, *16* (8), 949-956.
26. Ries, Carola H.; Cannarile, Michael A.; Hoves, S.; Benz, J.; Wartha, K.; Runza, V.; Rey-Giraud, F.; Pradel, Leon P.; Feuerhake, F.; Klaman, I.; Jones, T.; Jucknischke, U.; Scheiblich, S.; Kaluza, K.; Gorr, Ingo H.; Walz, A.; Abiraj, K.; Cassier, Philippe A.; Sica, A.; Gomez-Roca, C.; de Visser, Karin E.; Italiano, A.; Le Tourneau, C.; Delord, J.-P.; Levitsky, H.; Blay, J.-Y.; Rüttinger, D., Targeting Tumor-Associated Macrophages with Anti-CSF-1R Antibody Reveals a Strategy for Cancer Therapy. *Cancer Cell* **2014**, *25* (6), 846-859.
27. Tap, W. D.; Wainberg, Z. A.; Anthony, S. P.; Ibrahim, P. N.; Zhang, C.; Healey, J. H.; Chmielowski, B.; Staddon, A. P.; Cohn, A. L.; Shapiro, G. I.; Keedy, V. L.; Singh, A. S.; Puzanov, I.; Kwak, E. L.; Wagner, A. J.; Von Hoff, D. D.; Weiss, G. J.; Ramanathan, R. K.; Zhang, J.; Habets, G.; Zhang, Y.; Burton, E. A.; Visor, G.; Sanftner, L.; Severson, P.; Nguyen, H.; Kim, M. J.; Marimuthu, A.; Tsang, G.; Shellooe, R.; Gee, C.; West, B. L.; Hirth, P.; Nolop, K.; van de Rijn, M.; Hsu, H. H.; Peterfy, C.; Lin, P. S.; Tong-Starksen, S.; Bollag, G., Structure-Guided Blockade of CSF1R Kinase in Tenosynovial Giant-Cell Tumor. *N. Engl. J. Med.* **2015**, *373* (5), 428-437.
28. Conway, J. G.; McDonald, B.; Parham, J.; Keith, B.; Rusnak, D. W.; Shaw, E.; Jansen, M.; Lin, P.; Payne, A.; Crosby, R. M., Inhibition of colony-stimulating-factor-1 signaling in vivo with the orally bioavailable cFMS kinase inhibitor GW2580. *Proc. Natl. Acad. Sci. U.S.A.* **2005**, *102* (44), 16078-16083.
29. Conway, J. G.; Pink, H.; Bergquist, M. L.; Han, B.; Depee, S.; Tadepalli, S.; Lin, P.; Crumrine, R. C.; Binz, J.; Clark, R. L.; Selph, J. L.; Stimpson, S. A.; Hutchins, J. T.; Chamberlain, S. D.; Brodie, T. A., Effects of the cFMS kinase inhibitor 5-(3-methoxy-4-((4-methoxybenzyl)oxy)benzyl)pyrimidine-2,4-diamine (GW2580) in normal and arthritic rats. *J. Pharmacol. Exp. Ther.* **2008**, *326* (1), 41.
30. Kaspersen, S. J.; Han, J.; Nørsett, K. G.; Rydså, L.; Kjøbli, E.; Bugge, S.; Bjørkøy, G.; Sundby, E.; Hoff, B. H., Identification of new 4-N-substituted 6-aryl-7H-pyrrolo[2,3-d]pyrimidine-4-amines as highly potent EGFR-TK inhibitors with Src-family activity. *Eur. J. Pharm. Sci.* **2014**, *59*, 69-82.
31. Jin, H.; Sundby, E.; Hoff, B. H., Solvent selection in synthesis of 4-(1-arylfluoroethoxy)quinazolines and thienopyrimidines. *J. Fluroine. Chem.* **2013**, 7.

32. Hynes, N. E.; Lane, H. A., ERBB receptors and cancer: the complexity of targeted inhibitors. *Nat. Rev. Cancer.* **2005**, *5* (5), 341-354.
33. Paez, J. G.; Jänne, P. A.; Lee, J. C.; Tracy, S.; Greulich, H.; Gabriel, S.; Herman, P.; Kaye, F. J.; Lindeman, N.; Boggon, T. J., EGFR mutations in lung cancer: correlation with clinical response to gefitinib therapy. *Science* **2004,** *304* (5676), 1497-1500.
34. Clayden, J.; Greeves, N.; Warren, S., *Organic chemistry*. 2nd ed. ed.; Oxford University Press: Oxford, 2012.
35. Carey, F. A.; Sundberg, R. J., *Advanced Organic Chemistry : Part B : Reactions and Synthesis*. Springer US: Boston, 2007.
36. Akinyele, E. T.; Onyido, I.; Hirst, J., Mechanisms of aromatic nucleophilic substitution reactions in ethyl acetate and tetrahydrofuran. *J. Phys. Org. Chem.* **1990**, *3*, 41-47.
37. Ji, P.; Atherton, J. H.; Page, M. I., The Kinetics and Mechanisms of Aromatic Nucleophilic Substitution Reactions in Liquid Ammonia. *J. Org. Chem.* **2011**, *76* (9), 3286-3295.
38. Acevedo, O.; Jorgensen, W. L., Solvent Effects and Mechanism for a Nucleophilic Aromatic Substitution from QM/MM Simulations. *Org. Lett.* **2004**, *6* (17), 2881-2884.
39. Bunnett, J. F.; Garbisch, E. W.; Pruitt, K. M., The "Element Effect" as a Criterion of Mechanism in Activated Aromatic Nucleophilic Substitution Reactions1,2. *J. Am. Chem. Soc.* **1957**, *79* (2), 385-391.
40. Cohen, T.; Wood, J.; Dietz Jr, A. G., Organocopper intermediates in the exchange reaction of aryl halides with salts of copper(I). The possible role of copper(III). *Tetrahedron Lett.* **1974**, *15* (40), 3555-3558.
41. Kiyomori, A.; Marcoux, J.-F.; Buchwald, S. L., An efficient copper-catalyzed coupling of aryl halides with imidazoles. *Tetrahedron Lett.* **1999**, *40* (14), 2657-2660.
42. Kwong, F. Y.; Buchwald, S. L., Mild and Efficient Copper-Catalyzed Amination of Aryl Bromides with Primary Alkylamines. *Org. Lett.* **2003**, *5* (6), 793-796.
43. Genet, J. P.; Savignac, M., Recent developments of palladium (0) catalyzed reactions in aqueous medium. *J. Orgmet. Chem.* **1999**, *576* (1), 305-317.
44. Kosugi, M.; Kameyama, M.; Migita, T., Palladium-catalyzed aromatic amination of aryl bromides with N, N-di-ethylamino-tributyltin. *Chem. Lett.* **1983**, *12* (6), 927-928.
45. Paul, F.; Patt, J.; Hartwig, J. F., Palladium-catalyzed formation of carbon-nitrogen bonds. Reaction intermediates and catalyst improvements in the hetero cross-coupling of aryl halides and tin amides. *J. Am. Chem. Soc.* **1994**, *116* (13), 5969-5970.
46. Carey, J. S.; Laffan, D.; Thomson, C.; Williams, M. T., Analysis of the reactions used for the preparation of drug candidate molecules. *Org. Biomol. Chem.* **2006**, *4* (12), 2337-2347.
47. Surry, D. S.; Buchwald, S. L., Biaryl phosphane ligands in palladium-catalyzed amination. *Angew. Chem. Int. Ed.* **2008**, *47* (34), 6338-6361.
48. Kamikawa, K.; Sugimoto, S.; Uemura, M., Palladium-Catalyzed Amination of Aryl Bromides Utilizing Arene− Chromium Complexes as Ligands. *J. Org. Chem.* **1998**, *63* (23), 8407-8410.
49. Driver, M. S.; Hartwig, J. F., A rare, low-valent alkylamido complex, a diphenylamido complex, and their reductive elimination of amines by three-coordinate intermediates. *J. Am. Chem. Soc.* **1995**, *117* (16), 4708-4709.
50. Sunesson, Y.; Lime, E.; Nilsson Lill, S. O.; Meadows, R. E.; Norrby, P.-O., Role of the Base in Buchwald–Hartwig Amination. *J. Org. Chem.* **2014**, *79* (24), 11961-11969.
51. Hartwig, J. F.; Richards, S.; Barañano, D.; Paul, F., Influences on the Relative Rates for C− N Bond-Forming Reductive Elimination and β-Hydrogen Elimination of Amides. A Case Study on the Origins of Competing Reduction in the Palladium-Catalyzed Amination of Aryl Halides. *J. Am. Chem. Soc.* **1996**, *118* (15), 3626-3633.

52. Muci, A. R.; Buchwald, S. L., Practical palladium catalysts for CN and CO bond formation. In *Cross-Coupling Reactions*, Springer: 2002; pp 131-209.
53. Kaspersen, S. J. Synthesis and evaluation of pyrrolo-, thieno-and furopyrimidines as epidermal growth factor receptor tyrosine kinase inhibitors. NTNU-trykk, 2014.
54. Wagaw, S.; Rennels, R. A.; Buchwald, S. L., Palladium-catalyzed coupling of optically active amines with aryl bromides. *J. Am. Chem. Soc.* **1997**, *119* (36), 8451-8458.
55. Hammoud, H.; Schmitt, M.; Blaise, E.; Bihel, F. d. r.; Bourguignon, J.-J., N-Heteroarylation of Chiral α-Aminoesters by Means of Palladium-Catalyzed Buchwald–Hartwig Reaction. *J. Org. Chem.* **2013**, *78* (16), 7930-7937.
56. Martin, R.; Buchwald, S. L., Palladium-catalyzed Suzuki− Miyaura cross-coupling reactions employing dialkylbiaryl phosphine ligands. *Acc. Chem. Res.* **2008**, *41* (11), 1461-1473.
57. Suzuki, A., Organoboron compounds in new synthetic reactions. *Pure. Appl. Chem.* **1985**, *57* (12), 1749-1758.
58. Miyaura, N.; Yamada, K.; Suzuki, A., A new stereospecific cross-coupling by the palladium-catalyzed reaction of 1-alkenylboranes with 1-alkenyl or 1-alkynyl halides. *Tetrahedron Lett.* **1979**, *20* (36), 3437-3440.
59. Wu, X. F.; Anbarasan, P.; Neumann, H.; Beller, M., From Noble Metal to Nobel Prize: Palladium-Catalyzed Coupling Reactions as Key Methods in Organic Synthesis. *Angew. Chem. Int. Ed.* **2010**, *49* (48), 9047-9050.
60. Foundation, T. N. The Nobel Prize in Chemistry 2010. http://www.nobelprize.org/nobel_prizes/chemistry/laureates/2010/ (accessed 24.01.17).
61. Zapf, A., Coupling of Aryl and Alkyl Halides with Organoboron Reagents (Suzuki Reaction). In *Transition Metals for Organic Synthesis*, Wiley-VCH Verlag GmbH: 2008; pp 211-229.
62. Miyaura, N.; Yanagi, T.; Suzuki, A., Palladium-catalyzed cross-coupling reaction of phenylboronic acids with haloareenes in the presence of base. *Synth. Commun.* **1981**, *11* (7), 513-515.
63. García-Melchor, M.; Braga, A. A.; Lledós, A.; Ujaque, G.; Maseras, F., Computational perspective on Pd-catalyzed C–C cross-coupling reaction mechanisms. *Acc. Chem. Res.* **2013**, *46* (11), 2626-2634.
64. Lipton, M. F.; Mauragis, M. A.; Maloney, M. T.; Veley, M. F.; VanderBor, D. W.; Newby, J. J.; Appell, R. B.; Daugs, E. D., The synthesis of OSU 6162: efficient, large-scale implementation of a Suzuki coupling. *Org. Process Res. Dev.* **2003**, *7* (3), 385-392.
65. Kurti, L.; Czakó, B., *Strategic applications of named reactions in organic synthesis*. Elsevier: 2005.
66. Kotha, S.; Lahiri, K.; Kashinath, D., Recent applications of the Suzuki–Miyaura cross-coupling reaction in organic synthesis. *Tetrahedron Lett.* **2002**, *58* (48), 9633-9695.
67. Miyaura, N., Cross-coupling reaction of organoboron compounds via base-assisted transmetalation to palladium (II) complexes. *J. Organomet. Chem.* **2002**, *653* (1), 54-57.
68. Amatore, C.; Le Duc, G.; Jutand, A., Mechanism of Palladium-Catalyzed Suzuki–Miyaura Reactions: Multiple and Antagonistic Roles of Anionic “Bases” and Their Countercations. *Chem. Eur. J.* **2013**, *19* (31), 10082-10093.
69. Surry, D. S.; Buchwald, S. L., Dialkylbiaryl phosphines in Pd-catalyzed amination: a user's guide. *Chem. Sci* **2011,** *2* (1), 27-50.
70. Maluenda, I.; Navarro, O., Recent Developments in the Suzuki-Miyaura Reaction: 2010–2014. *Molecules* **2015,** *20* (5), 7528-7557.

71. Yang, J.; Liu, S.; Zheng, J. F.; Zhou, J. S., Room-Temperature Suzuki–Miyaura Coupling of Heteroaryl Chlorides and Tosylates. *Eur. J. Org.* **2012**, *2012* (31), 6248-6259.
72. Kenner, G. W.; McCombie, S. W.; Smith, K. M., Pyrroles and related compounds. Part XXIV. Separation and oxidative degradation of chlorophyll derivatives. *J. Chem. Soc., Perkin Trans. 1*. **1973**, 2517-2523.
73. Joule, J. A.; Mills, K., *Heterocyclic Chemistry*. 5 ed.; John Wiley & Sons, Ltd: Chichester, UK, 2012; p 78-85.
74. Jolicoeur, B.; Chapman, E. E.; Thompson, A.; Lubell, W. D., Pyrrole protection. *Tetrahedron Lett.* **2006**, *62* (50), 11531-11563.
75. Merrill, B. A.; Legoff, E., A general synthetic route to 2,2':5',2"-terpyrrole, 2,5-di(2-pyrryl)thiophene, and alkyl-substituted analogs. *J. Org. Chem.* **1990**, *55* (9), 2904-2908.
76. Bray, B. L.; Mathies, P. H.; Naef, R.; Solas, D. R.; Tidwell, T. T.; Artis, D. R.; Muchowski, J. M., N-(Triisopropylsilyl)pyrrole. A progenitor "par excellence" of 3-substituted pyrroles. *J. Org. Chem.* **1990**, *55* (26), 6317-6328.
77. Edwards, M. P.; Doherty, A. M.; Ley, S. V.; Organ, H. M., Preparation of 2-substituted pyrroles and indoles by regioselective alkylation and deprotection of 1-(2-trimethylsilylethoxymethyl)pyrrole and 1-(2-trimethylsilylethoxymethyl) indole. *Tetrahedron Lett.* **1986**, *42* (13), 3723-3729.
78. Lin, Q.; Meloni, D.; Pan, Y.; Xia, M.; Rodgers, J.; Shepard, S.; Li, M.; Galya, L.; Metcalf, B.; Yue, T.-Y., Enantioselective synthesis of Janus kinase inhibitor INCB018424 via an organocatalytic aza-Michael reaction. *Org. Lett.* **2009**, *11* (9), 1999-2002.
79. Henderson, J. L.; Kormos, B. L.; Hayward, M. M.; Coffman, K. J.; Jasti, J.; Kurumbail, R. G.; Wager, T. T.; Verhoest, P. R.; Noell, G. S.; Chen, Y., Discovery and preclinical profiling of 3-[4-(Morpholin-4-yl)-7 H-pyrrolo [2, 3-d] pyrimidin-5-yl] benzonitrile (PF-06447475), a highly potent, selective, brain penetrant, and in vivo active LRRK2 Kinase inhibitor. *J. Med. Chem.* **2014**, *58* (1), 419-432.
80. Rodgers, J. D.; Shepard, S.; Li, Y.-L.; Zhou, J.; Liu, P.; Meloni, D.; Xia, M., Azetidine and cyclobutane derivatives as JAK inhibitors. Google Patents: 2013.
81. Chandra, T.; Broderick, W. E.; Broderick, J. B., An Efficient Deprotection of N-Trimethylsilylethoxymethyl (SEM) Groups From Dinucleosides and Dinucleotides. *Nucleos. Nucleot. Nucl.* **2010**, *29* (2), 132-143.
82. Kan, T.; Hashimoto, M.; Yanagiya, M.; Shirahama, H., Effective deprotection of 2-(trimethylsilylethoxy) methylated alcohols (SEM ethers). Synthesis of thyrsiferyl-23 acetate. *Tetrahedron lett.* **1988**, *29* (42), 5417-5418.
83. Liang, X.; Huang, Y.; Zang, J.; Gao, Q.; Wang, B.; Xu, W.; Zhang, Y., Design, synthesis and preliminary biological evaluation of 4-aminopyrazole derivatives as novel and potent JAKs inhibitors. *Bioorg. Med. Chem.* **2016,** *24* (12), 2660-2672.
84. Leithaug, T., Vanillin based building blocks for the synthesis of CSF1R-inhibitors. **2016**.
85. Bugge, S.; Kaspersen, S. J.; Sundby, E.; Hoff, B. H., Route selection in the synthesis of C-4 and C-6 substituted thienopyrimidines. *Tetrahedron Lett.* **2012**, *68* (45), 9226-9233.
86. Eom, M. S.; Noh, J.; Kim, H.-S.; Yoo, S.; Han, M. S.; Lee, S., High-throughput screening protocol for the coupling reactions of aryl halides using a colorimetric chemosensor for halide ions. *Org. lett.* **2016**, *18* (8), 1720-1723.
87. Carey, F. A.; Sundberg, R. J., *Advanced Organic Chemistry: Part A: Structure and Mechanisms*. Springer Science & Business Media: 2007.
88. Patai, S., Chemistry of the Ether linkage. **1967**.

89. Williams, D. H.; Fleming, I., *Spectroscopic methods in organic chemistry*. McGraw-Hill: 1980.
90. Silverstein, R. M.; Webster, F. X.; Kiemle, D. J.; Bryce, D. L., *Spectrometric identification of organic compounds*. John wiley & sons: 2014.
91. Kumar, S. S.; Priyadarsini, K. I.; Sainis, K. B., Inhibition of peroxynitrite-mediated reactions by vanillin. *J. Agric. Food. Chem.* **2004**, *52* (1), 139.
92. Ashok, B.; Arleth, L.; Hjelm, R. P.; Rubinstein, I.; Önyüksel, H., In vitro characterization of PEGylated phospholipid micelles for improved drug solubilization: effects of PEG chain length and PC incorporation. *J. Pharm. Sci.* **2004**, *93* (10), 2476-2487.
93. Strauss, M. J., The nitroaromatic group in drug design. Pharmacology and toxicology (for nonpharmacologists). *Ind. Eng. Chem. Prod. Res. Dev.* **1979**, *18* (3), 158-166.

# Appendix

# A Spectroscopic data for compound 2

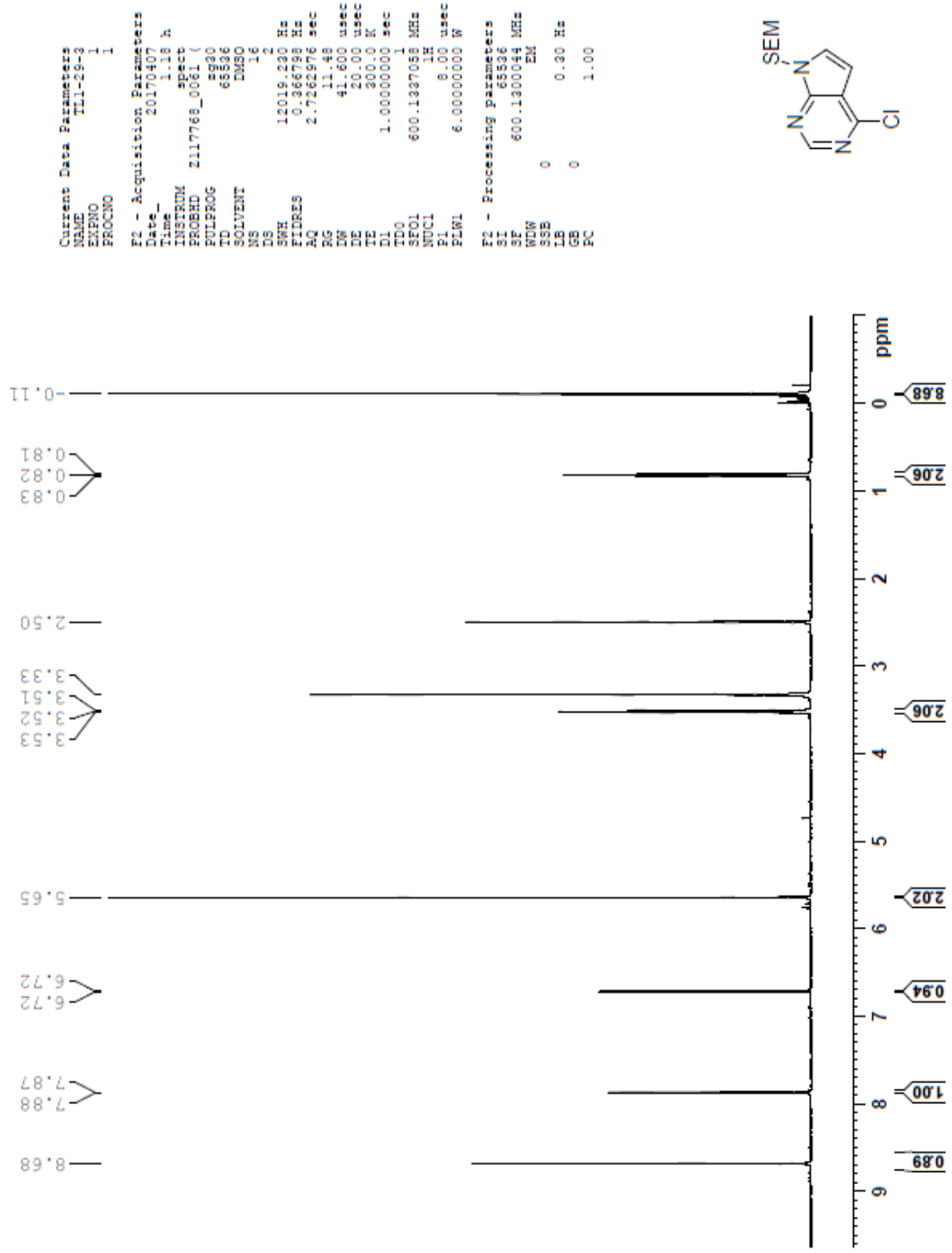


**Figure A.1**: $^{1}$H NMR spectrum of compound **2.**

# B Spectroscopic data for compound 3

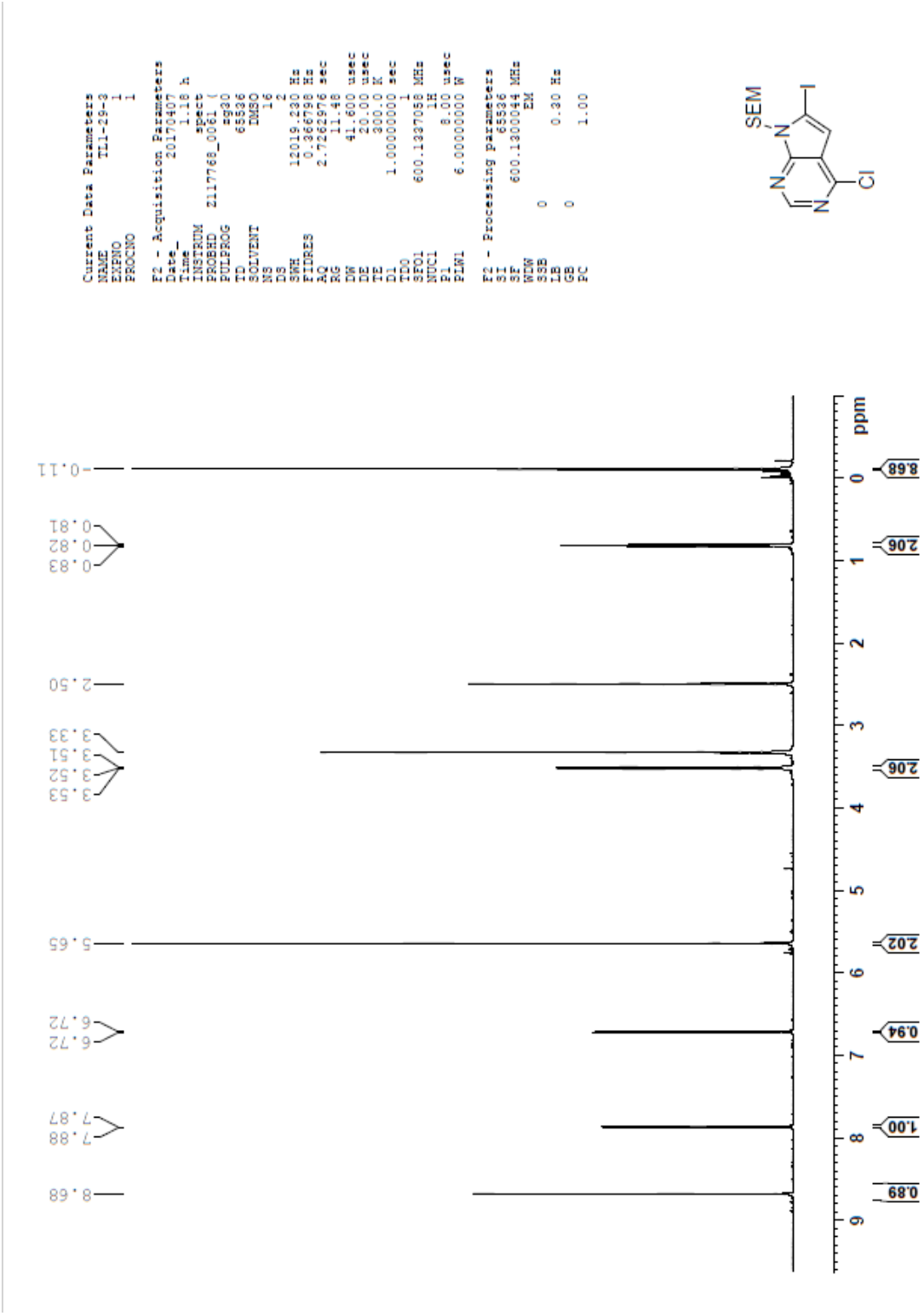


**Figure B.1**: $^{1}$H NMR spectrum of compound **3.**

# C Spectroscopic data for compound 4

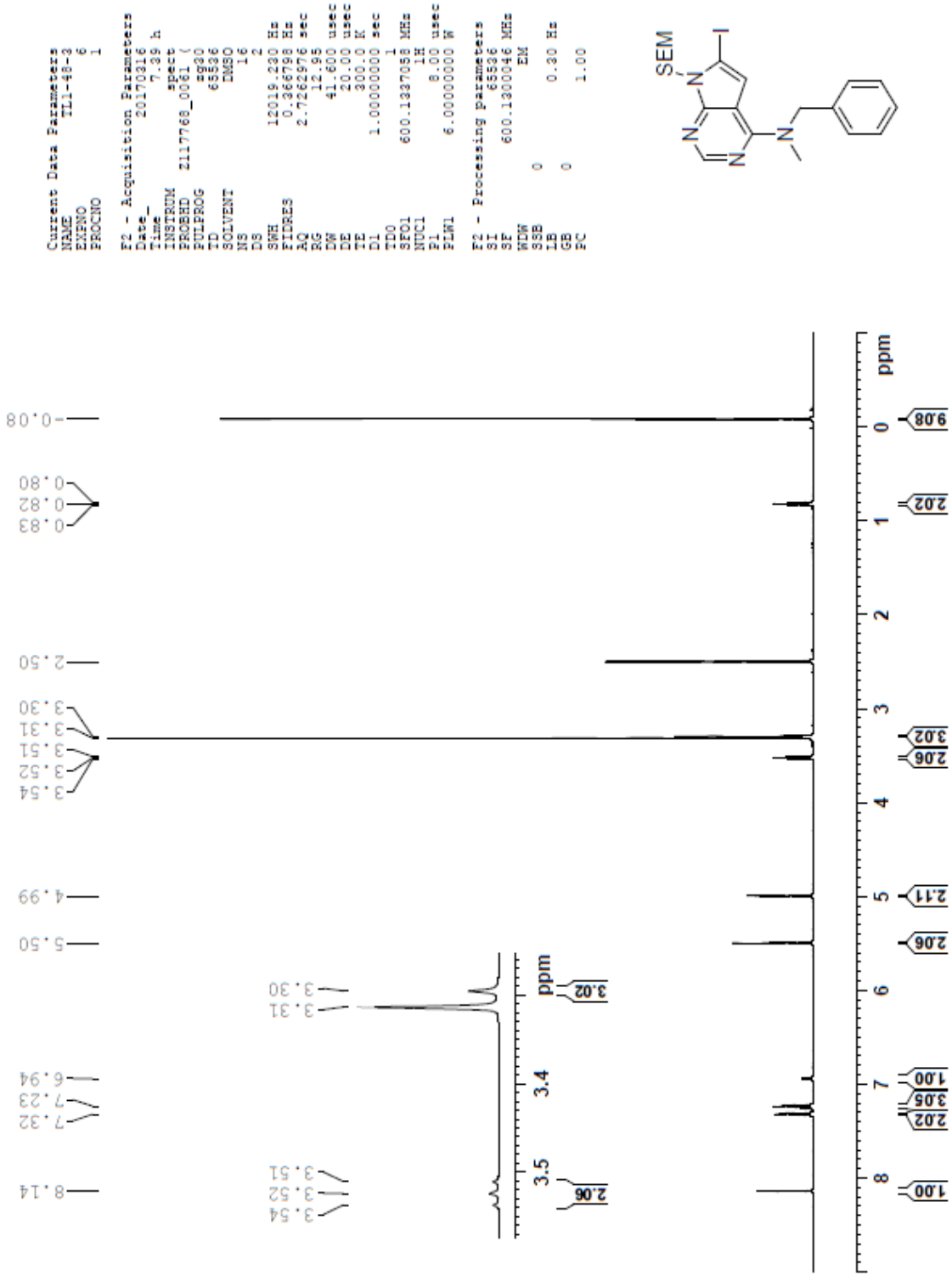


**Figure C.1**: $^{1}$H NMR spectrum of compound **4.**

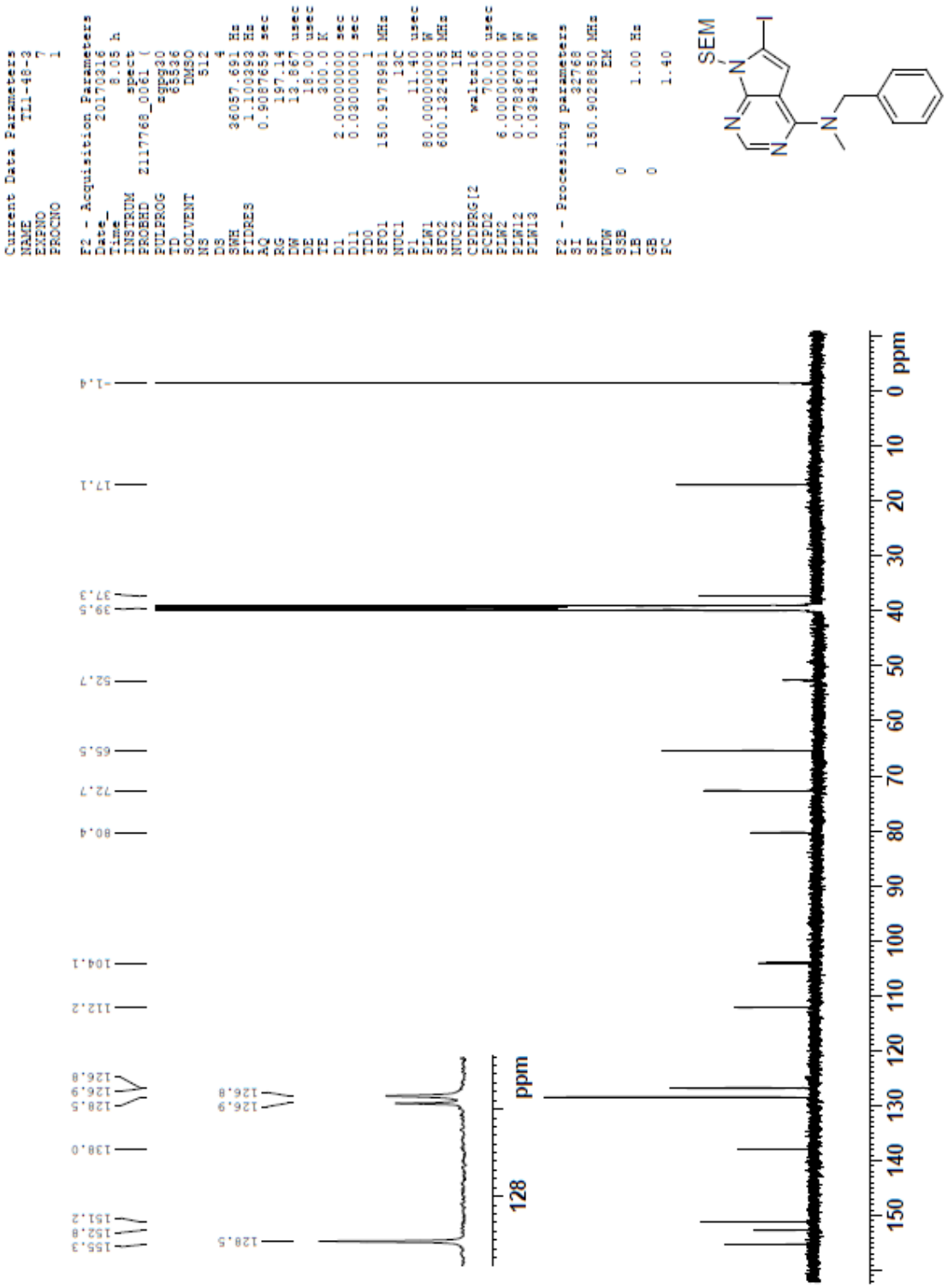


**Figure C.2**: $^{13}C$ NMR spectrum of compound **4.**

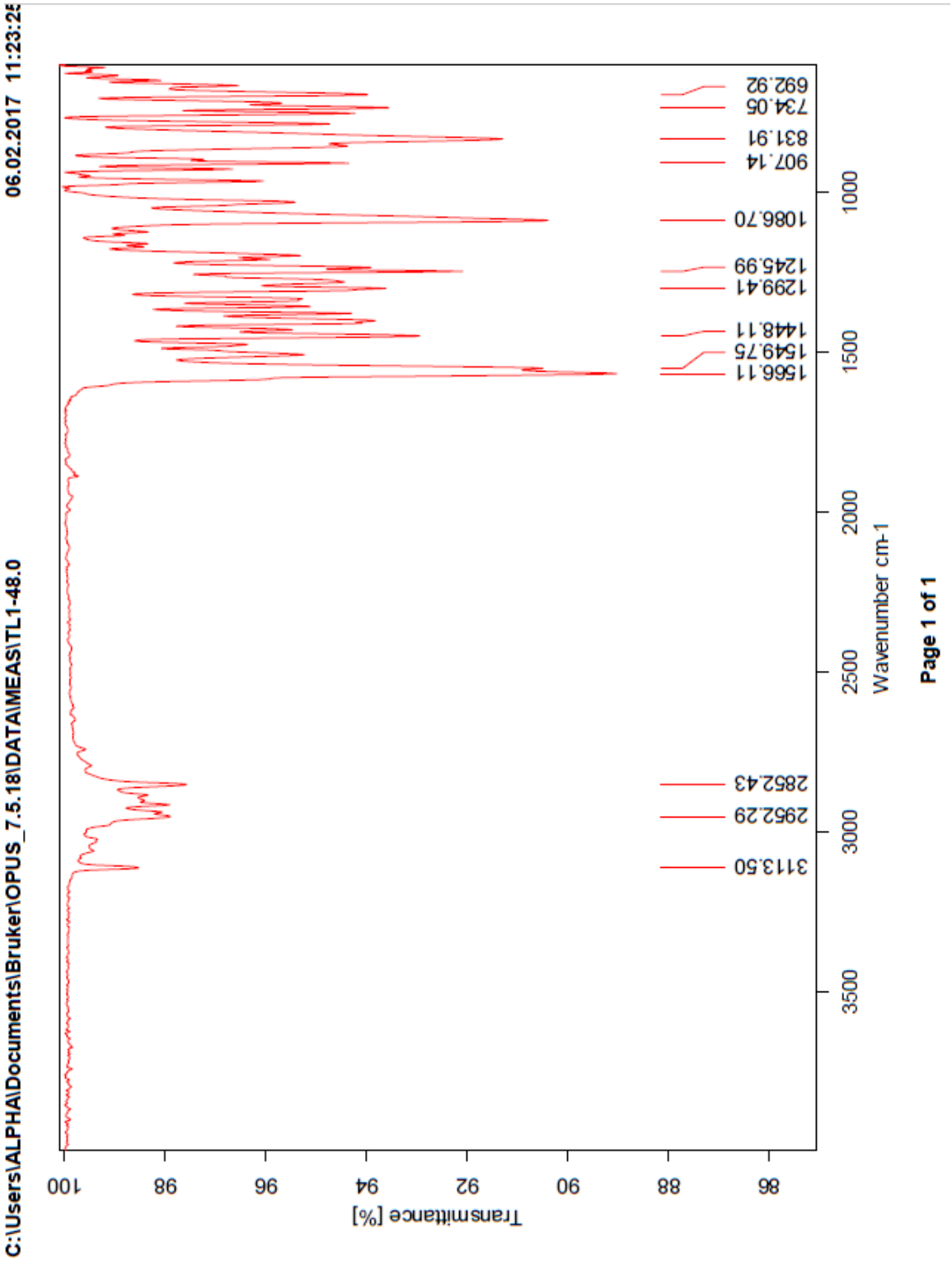


**Figure C.3**: IR spectrum of compound **4.**

## Elemental Composition Report



### Single Mass Analysis

Tolerance = 2.0 PPM / DBE: min = -1.5, max = 50.0
Element prediction: Off
Number of isotope peaks used for i-FIT = 3

Monoisotopic Mass, Even Electron Ions
10165 formula(e) evaluated with 18 results within limits (all results (up to 1000) for each mass)
Elements Used:
C: 1-500 H: 0-1000 N: 0-20 O: 0-25 Si: 0-3 I: 0-2

NT-MSLAB-Operator-SVG
2017-61 302 (5.876) AM2 (Ar,35000.0,0.00,0.00); Cm (302:314)

1: TOF MS ASAP+
3.64e+006

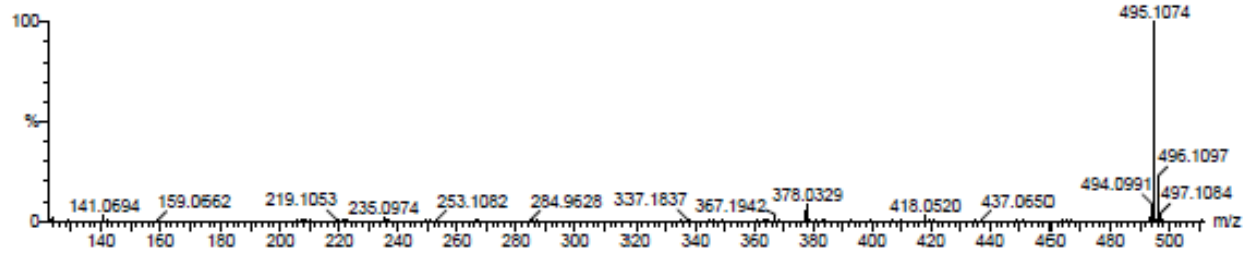


| | | | | | | | | |
|---|---|---|---|---|---|---|---|---|
| Minimum: | | | | -1.5 | | | | |
| Maximum: | | 5.0 | 2.0 | 50.0 | | | | |
| Mass | Calc. Mass | mDa | PPM | DBE | i-FIT | Norm | Conf(%) | Formula |
| 495.1074 | 495.1077 | -0.3 | -0.6 | 9.5 | 165.7 | 0.252 | 77.75 | C20 H28 N4 O Si I |
| | 495.1071 | 0.3 | 0.6 | 22.5 | 167.9 | 2.403 | 9.04 | C18 H11 N16 O Si |
| | 495.1071 | 0.3 | 0.6 | 11.5 | 168.1 | 2.609 | 7.36 | C20 H23 N2 O11 Si |
| | 495.1072 | 0.2 | 0.4 | 8.5 | 169.7 | 4.207 | 1.49 | C13 H19 N8 O13 |
| | 495.1082 | -0.8 | -1.6 | 2.5 | 169.7 | 4.264 | 1.41 | C5 H24 N16 O2 Si I |
| | 495.1076 | -0.2 | -0.4 | 4.5 | 170.1 | 4.575 | 1.03 | C5 H19 N14 O12 Si |
| | 495.1076 | -0.2 | -0.4 | 7.5 | 170.9 | 5.382 | 0.46 | C12 H23 N8 O10 Si2 |
| | 495.1078 | -0.4 | -0.8 | 6.5 | 170.9 | 5.411 | 0.45 | C13 H24 N10 O3 I |
| | 495.1082 | -0.8 | -1.6 | 5.5 | 171.5 | 5.998 | 0.25 | C12 H28 N10 Si2 I |
| | 495.1064 | 1.0 | 2.0 | 1.5 | 171.5 | 6.033 | 0.24 | C12 H28 N6 O7 I |
| | 495.1075 | -0.1 | -0.2 | 10.5 | 171.8 | 6.305 | 0.18 | C19 H27 N2 O8 Si3 |
| | 495.1068 | 0.6 | 1.2 | 0.5 | 172.2 | 6.686 | 0.12 | C11 H32 N6 O4 Si2 I |
| | 495.1066 | 0.8 | 1.6 | 26.5 | 172.4 | 6.961 | 0.09 | C26 H11 N10 O2 |
| | 495.1066 | 0.8 | 1.6 | 29.5 | 172.8 | 7.359 | 0.06 | C33 H15 N4 Si |
| | 495.1068 | 0.6 | 1.2 | 3.5 | 173.7 | 8.178 | 0.03 | C18 H36 O2 Si3 I |
| | 495.1080 | -0.6 | -1.2 | 20.5 | 174.0 | 8.502 | 0.02 | C29 H19 O8 |
| | 495.1080 | -0.6 | -1.2 | 3.5 | 174.8 | 9.310 | 0.01 | C4 H23 N14 O9 Si3 |
| | 495.1067 | 0.7 | 1.4 | -1.5 | 175.7 | 10.238 | 0.00 | C3 H27 N10 O13 Si3 |

Ion observed [M+H]

**Figure C.4**: MS spectrum of compound **4.**

# D Spectroscopic data for compound 6a

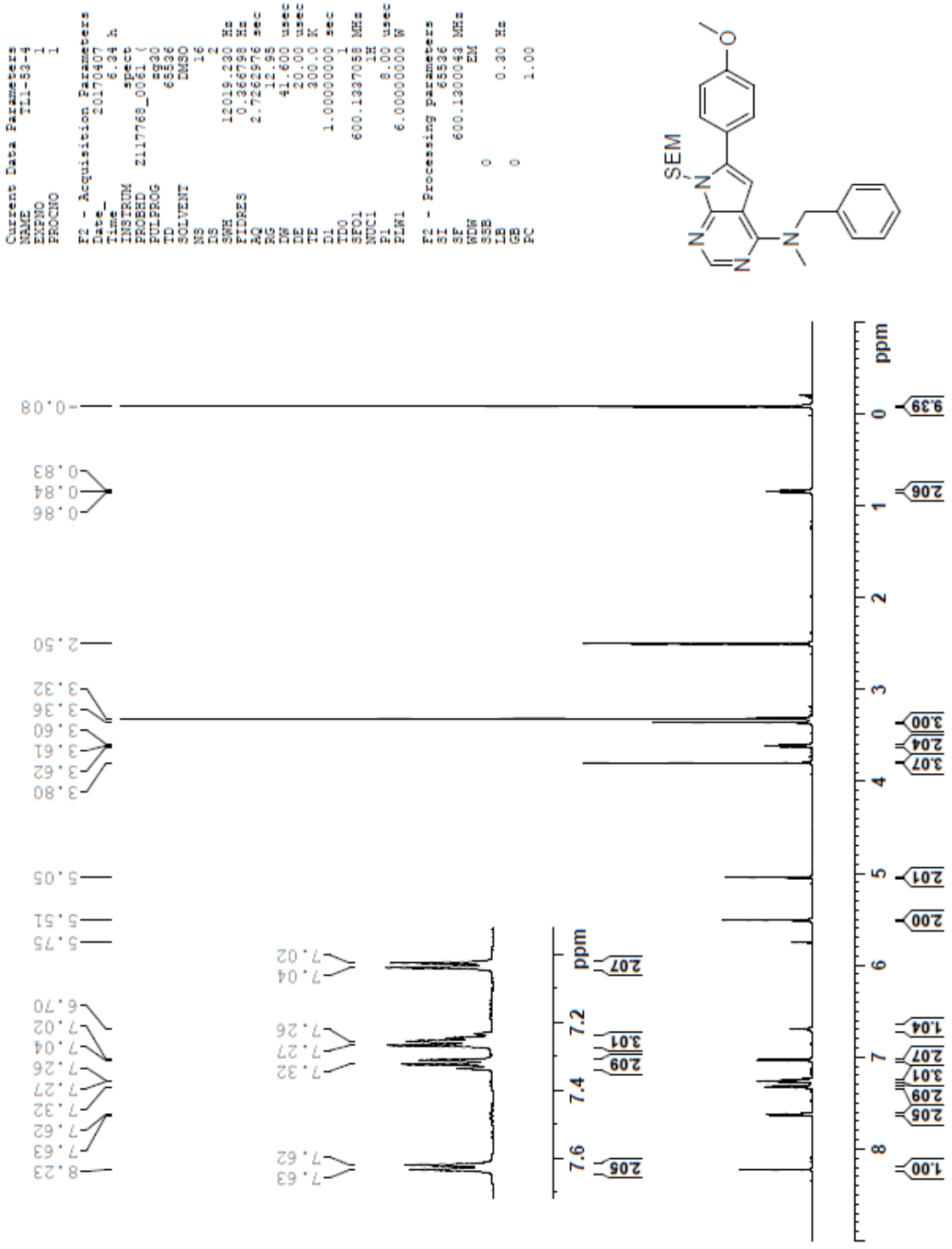


**Figure D.1**: $^{1}$H NMR spectrum of compound **6a.**

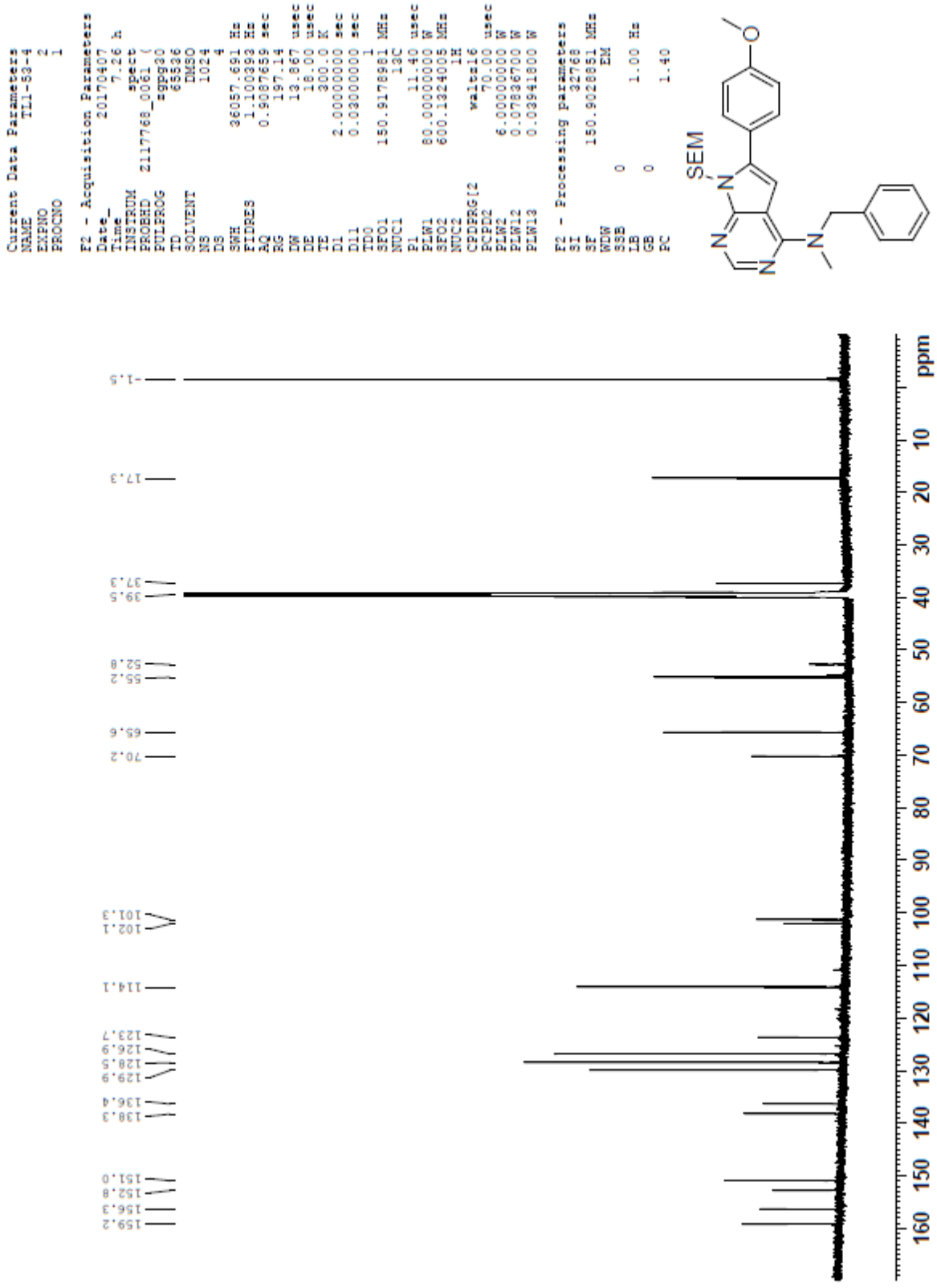


**Figure D.2**: $^{13}C$ NMR spectrum of compound **6a.**

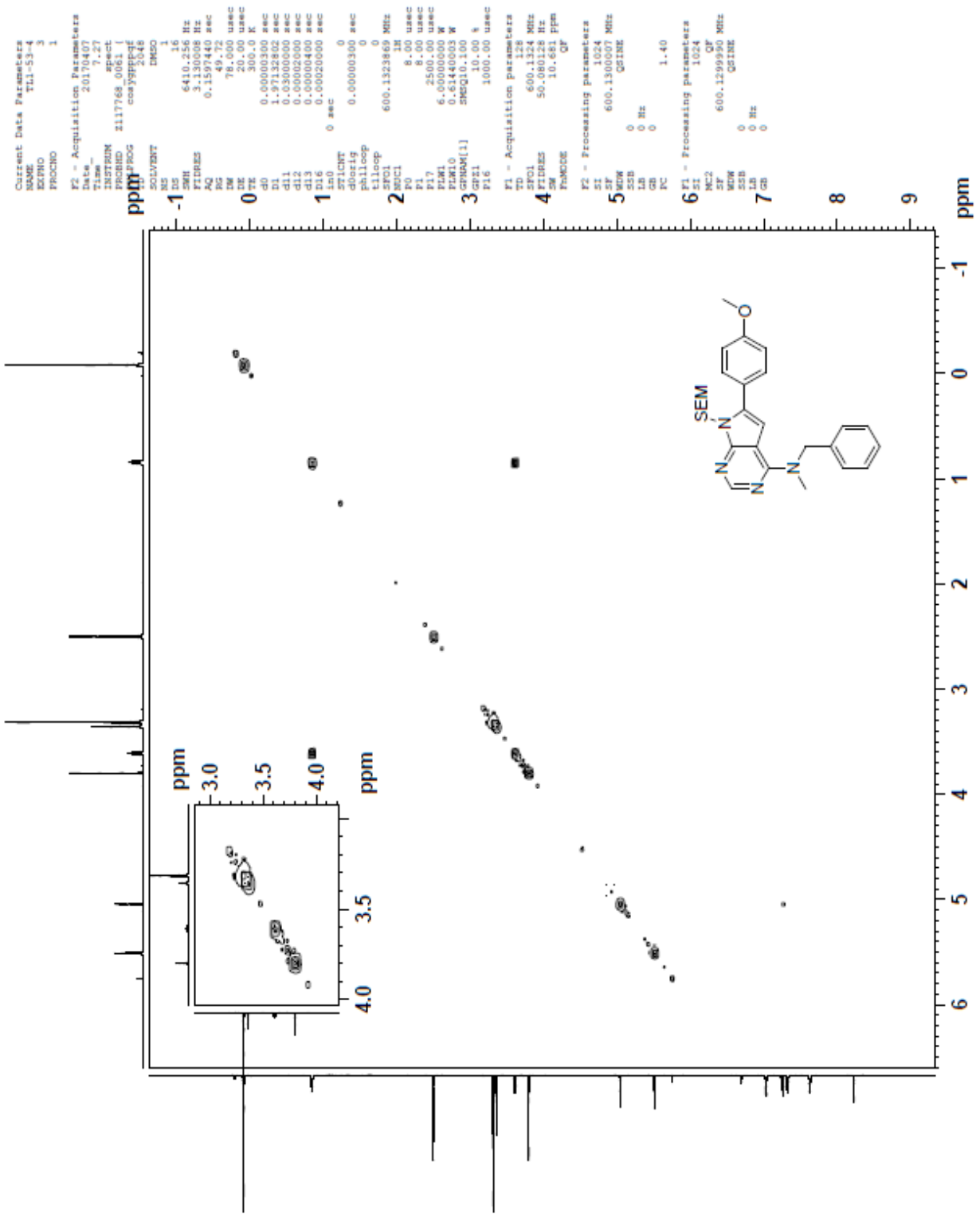


**Figure D.3**: COSY spectrum of compound **6a.**

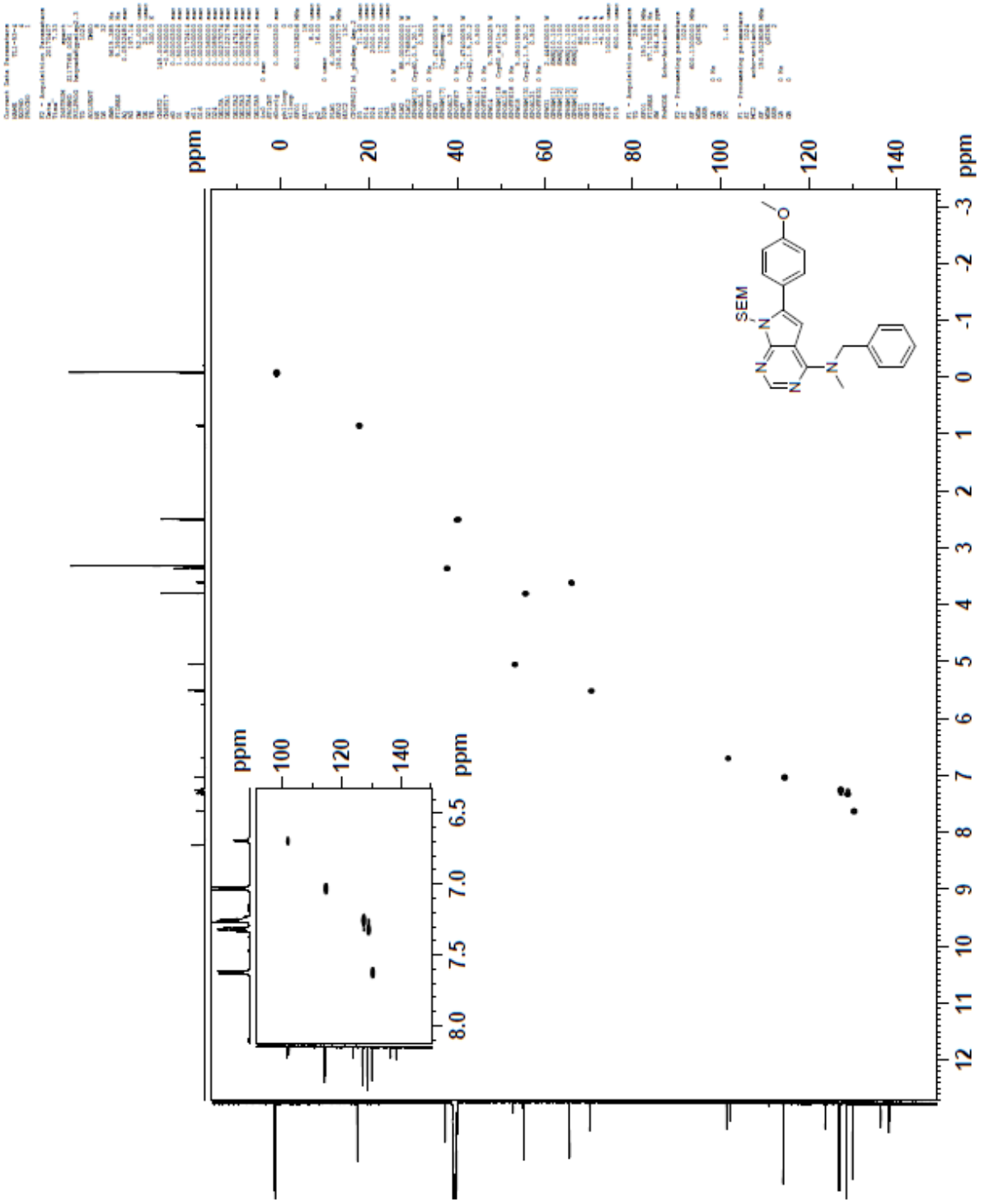


**Figure D.4**: HSQC spectrum of compound **6a.**

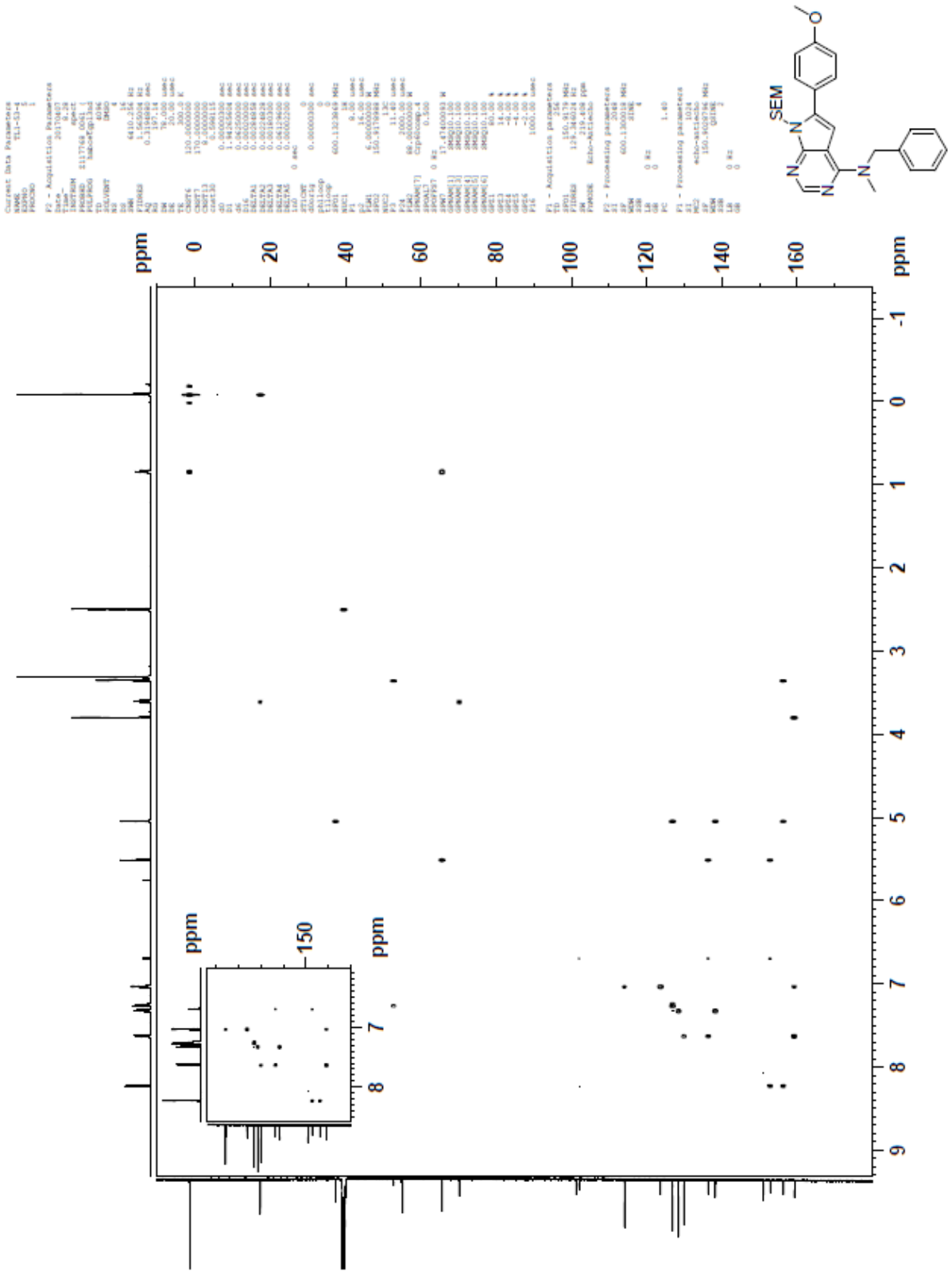


**Figure D.5**: HMBC spectrum of compound **6a**.

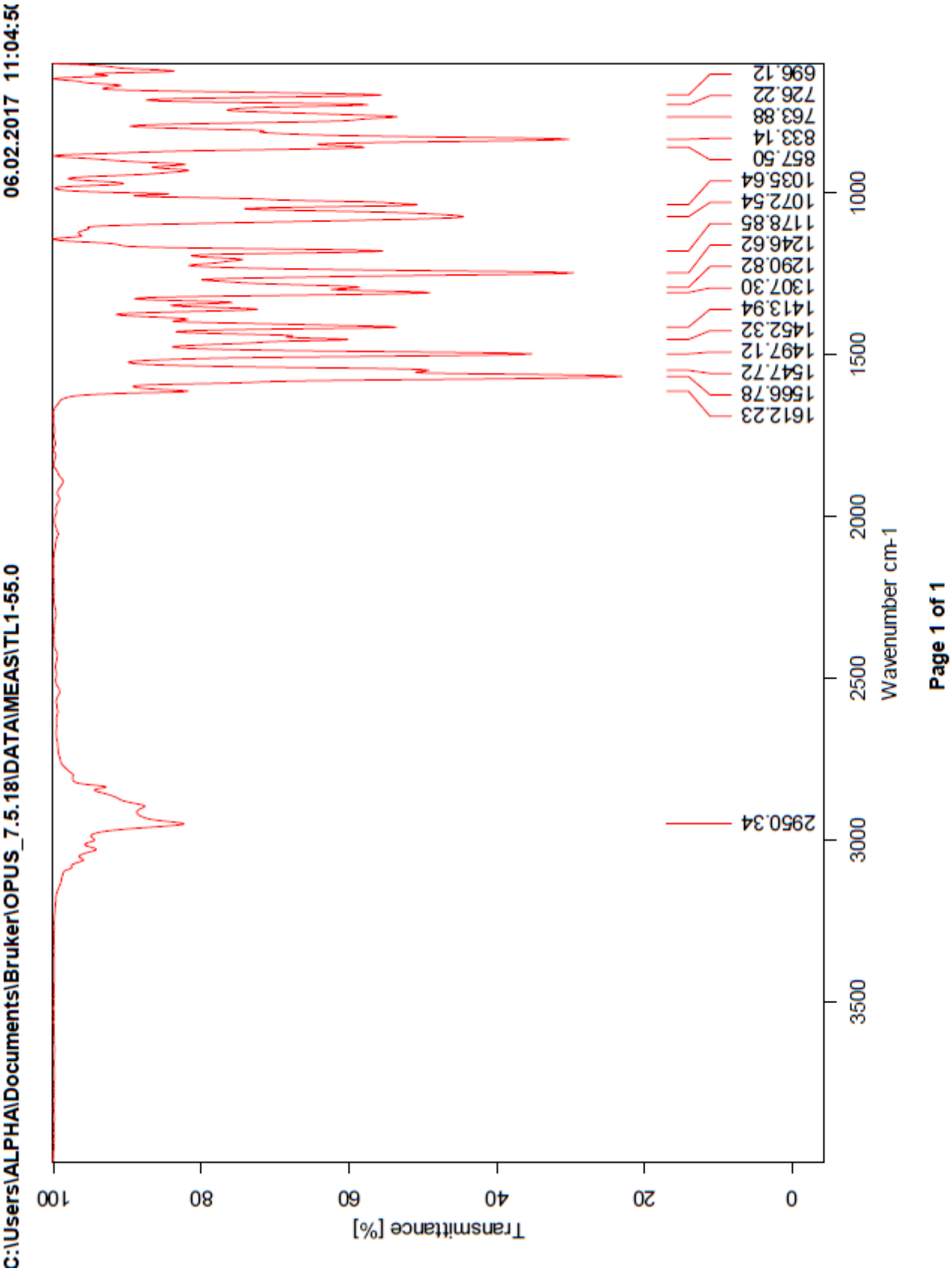


**Figure D.6**: IR spectrum of compound **6a.**

**Elemental Composition Report** Page 1

**Single Mass Analysis**
Tolerance = 2.0 PPM / DBE: min = -1.5, max = 50.0
Element prediction: Off
Number of isotope peaks used for i-FIT = 3

Monoisotopic Mass, Even Electron Ions
5779 formula(e) evaluated with 9 results within limits (all results (up to 1000) for each mass)
Elements Used:
C: 1-500 H: 0-1000 N: 0-20 O: 0-25 Si: 0-3

NT-MSLAB-Operator-SVG
2017-74 206 (4.015) AM2 (Ar,35000.0,0.00,0.00); Cm (201:206)

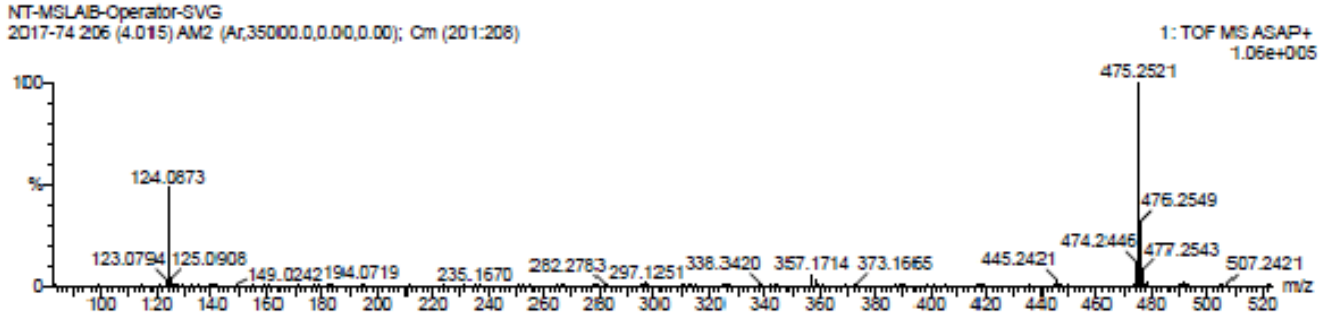


| | | | | | | | | |
|---|---|---|---|---|---|---|---|---|
| Minimum: | | | | -1.5 | | | | |
| Maximum: | | 5.0 | 2.0 | 50.0 | | | | |
| Mass | Calc. Mass | mDa | PPM | DBE | i-FIT | Norm | Conf(%) | Formula |
| 475.2521 | 475.2516 | 0.5 | 1.1 | 8.5 | 279.6 | 0.092 | 91.20 | C26 H39 O6 Si |
| | 475.2529 | -0.8 | -1.7 | 13.5 | 282.0 | 2.440 | 8.72 | C27 H35 N4 O2 Si |
| | 475.2520 | 0.1 | 0.2 | 4.5 | 287.2 | 7.633 | 0.05 | C18 H39 N6 O5 Si2 |
| | 475.2521 | 0.0 | 0.0 | 1.5 | 288.2 | 8.630 | 0.02 | C11 H35 N12 O7 Si |
| | 475.2516 | 0.5 | 1.1 | 5.5 | 289.9 | 10.393 | 0.00 | C19 H35 N6 O8 |
| | 475.2530 | -0.9 | -1.9 | 10.5 | 290.0 | 10.469 | 0.00 | C20 H31 N10 O4 |
| | 475.2520 | 0.1 | 0.2 | 7.5 | 290.1 | 10.563 | 0.00 | C25 H43 O3 Si3 |
| | 475.2525 | -0.4 | -0.8 | 0.5 | 291.2 | 11.620 | 0.00 | C10 H39 N12 O4 Si3 |
| | 475.2521 | 0.0 | 0.0 | -1.5 | 293.7 | 14.128 | 0.00 | C4 H31 N18 O9 |

iON OBSERVED M+H

**Figure D.7**: MS spectrum of compound **6a.**

# E Spectroscopic data for compound 6b

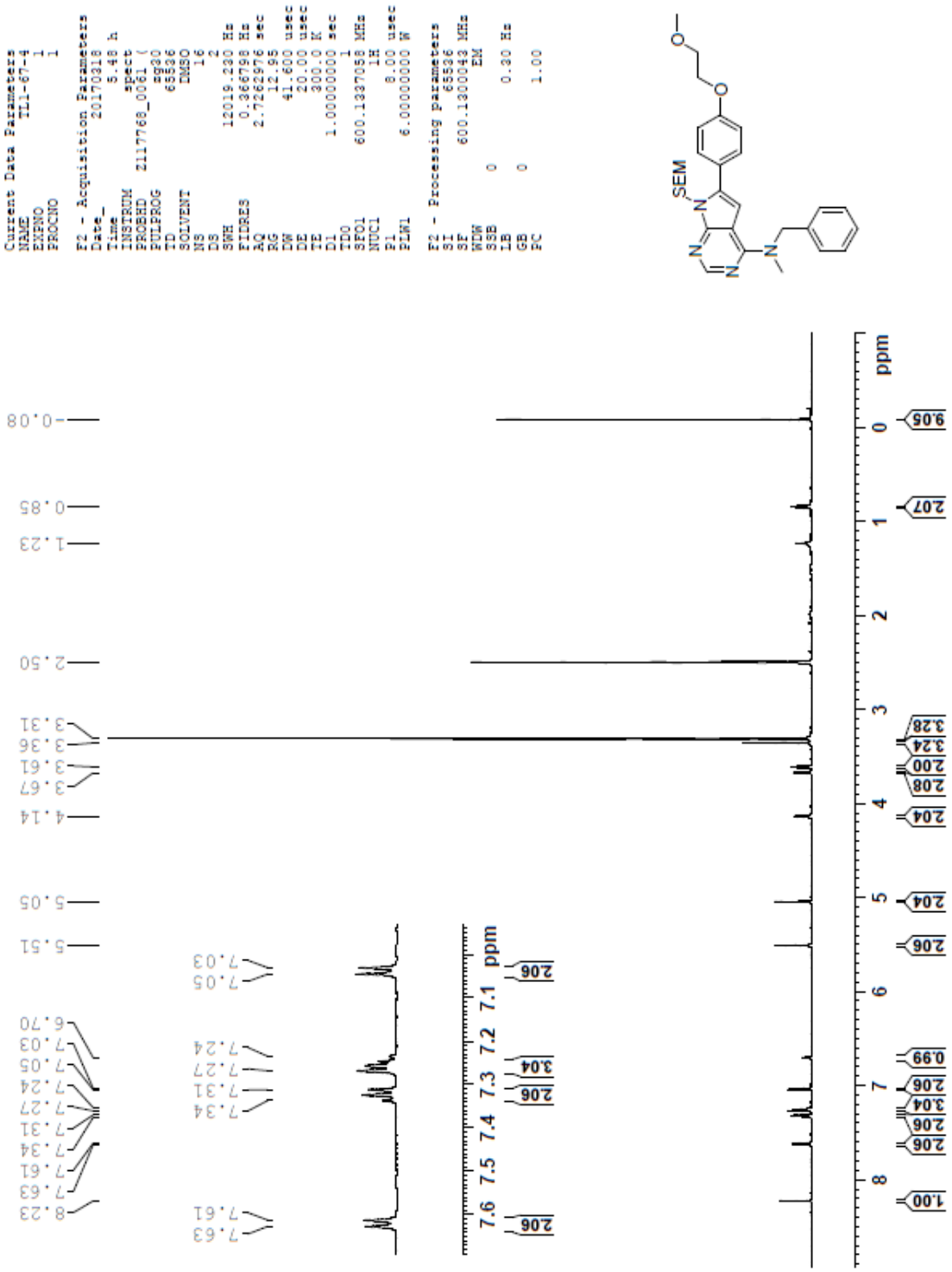


**Figure E.1**: $^{1}$H NMR spectrum of compound **6b.**

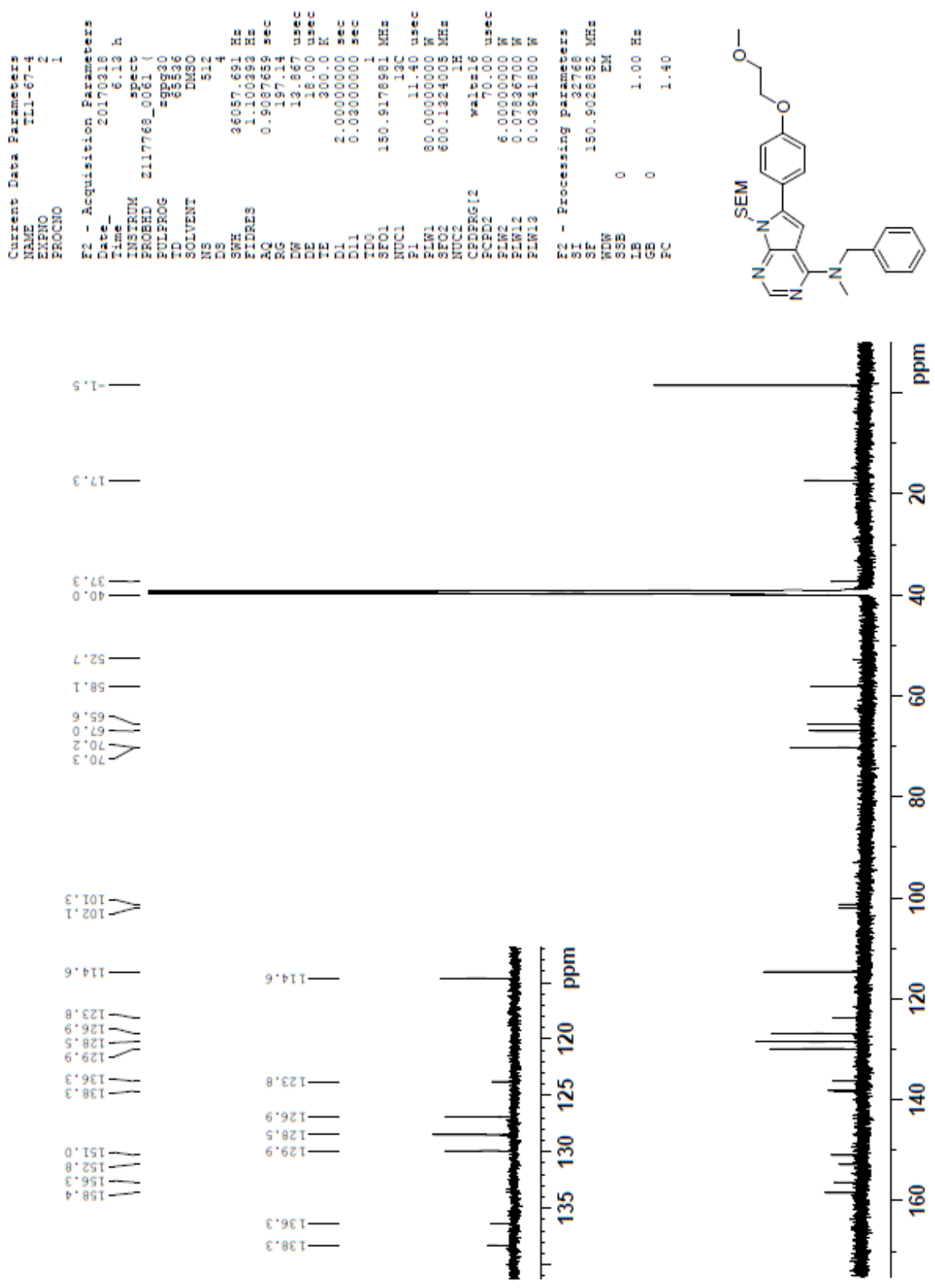


**Figure E.2**: $^{13}C$ NMR spectrum of compound **6b.**

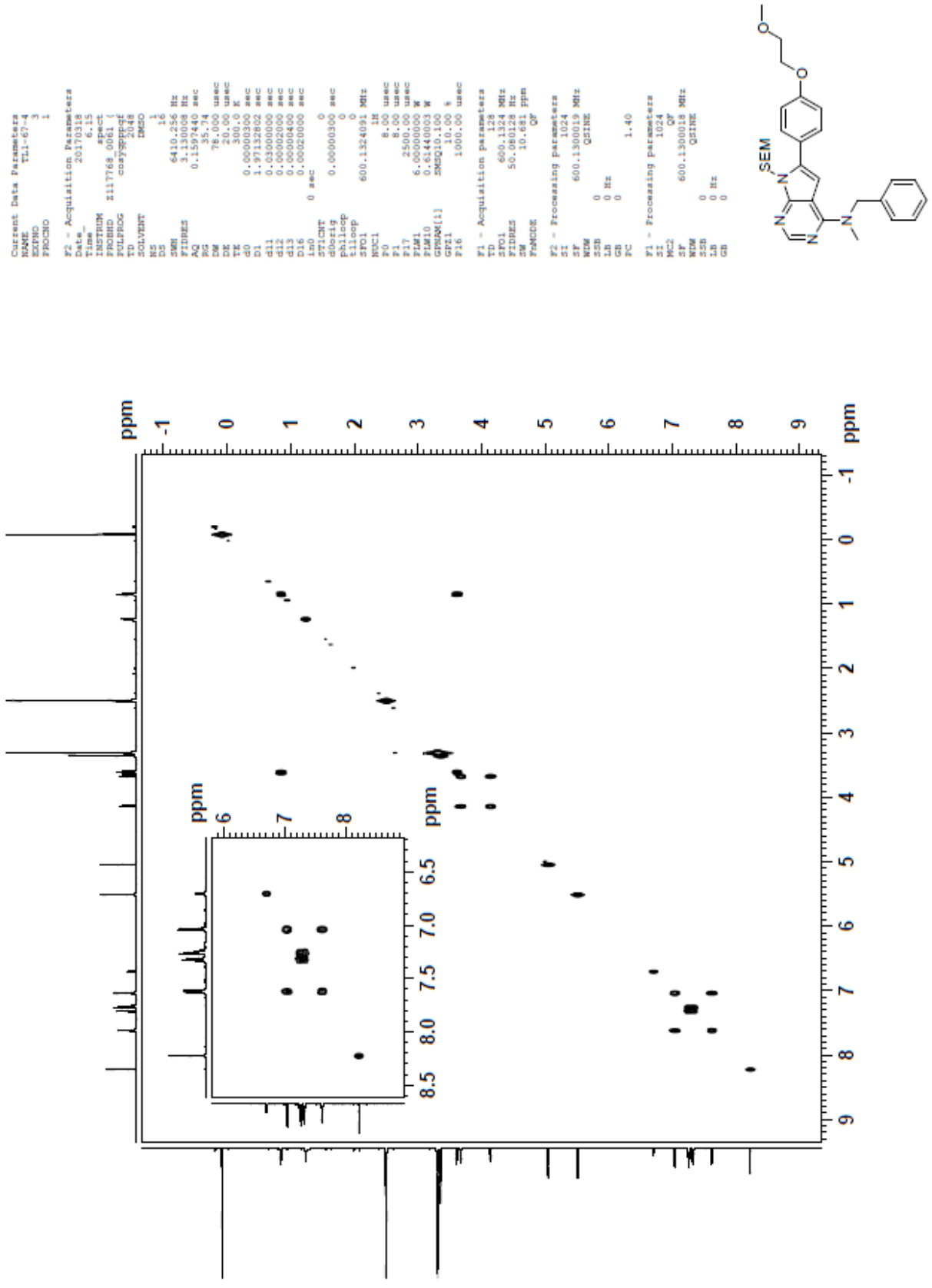


**Figure E.3**: COSY spectrum of compound **6b.**

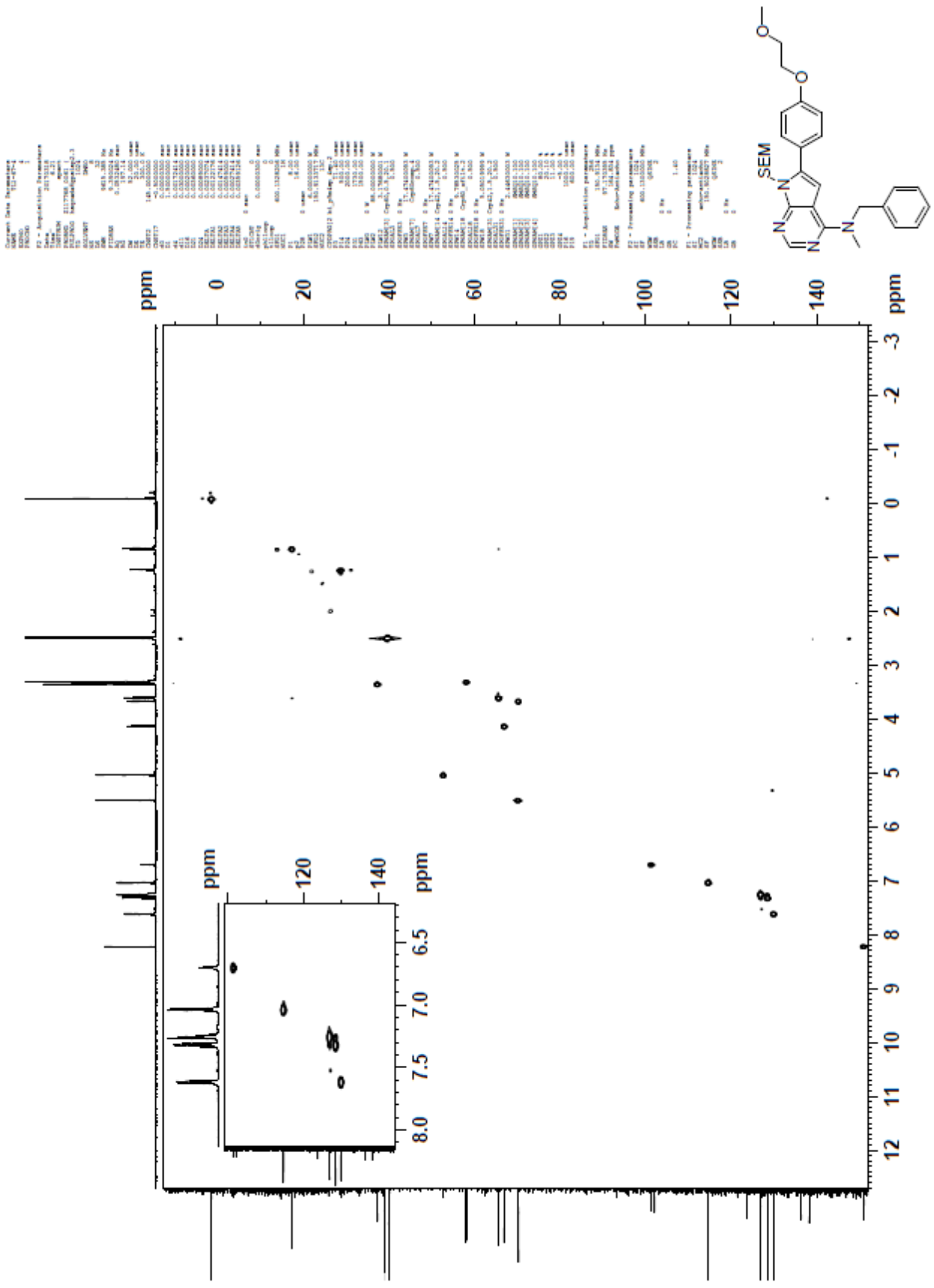


**Figure E.4**: HSQC spectrum of compound **6b.**

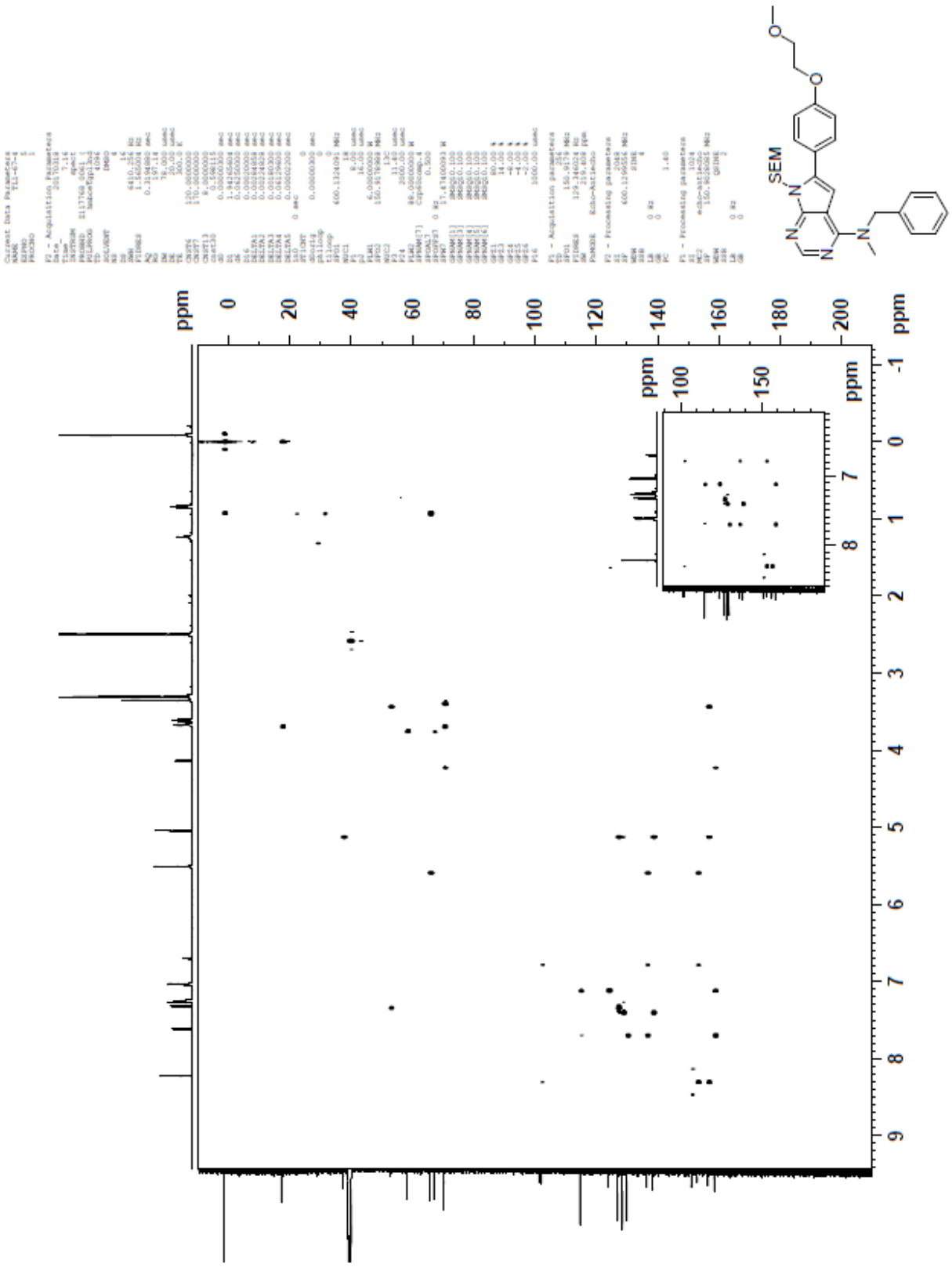


**Figure E.5**: HMBC spectrum for compound **6b**.

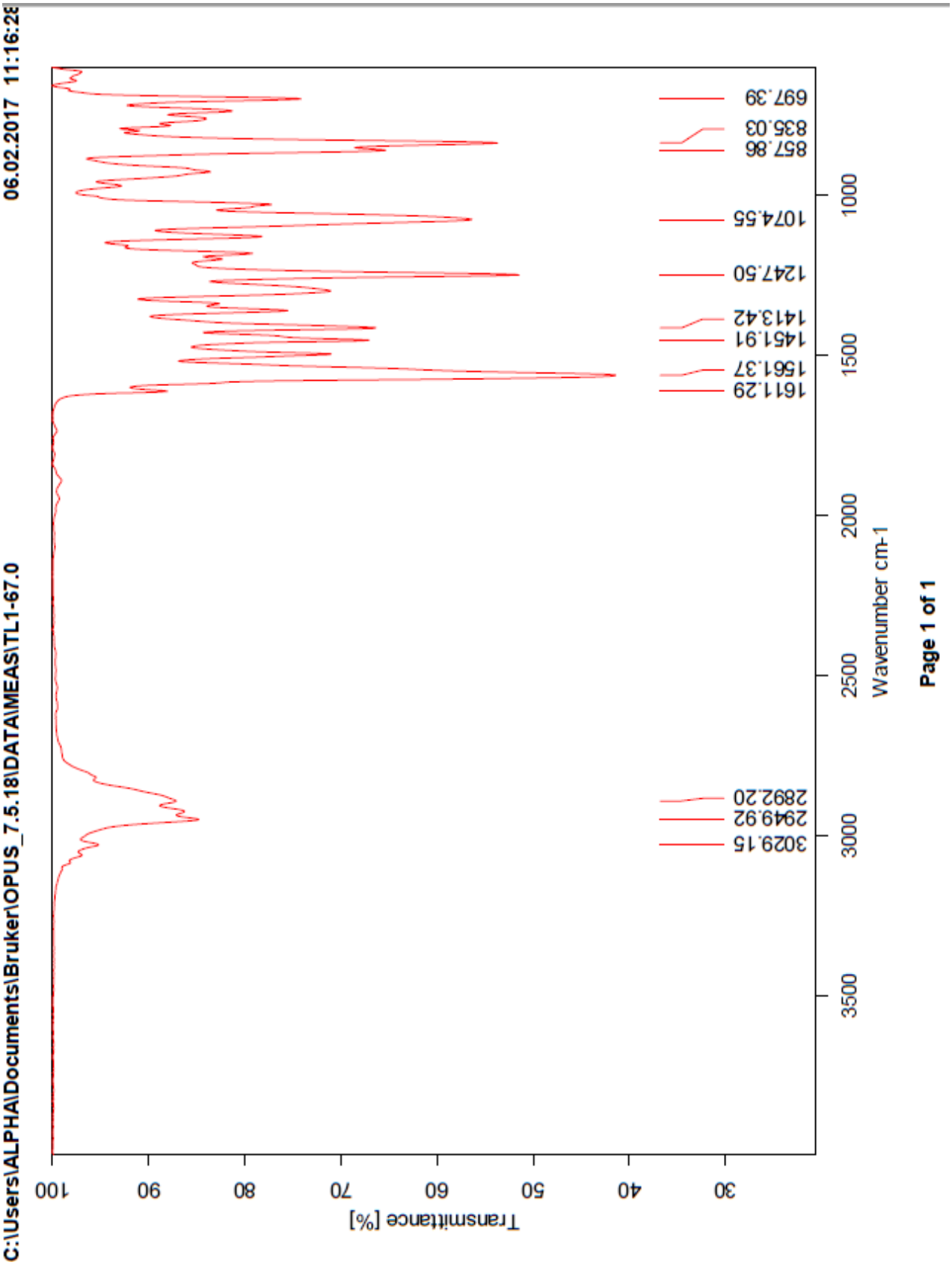


**Figure E.6**: IR spectrum of compound **6b.**

**Elemental Composition Report** Page 1

**Single Mass Analysis**
Tolerance = 3.0 PPM / DBE: min = -1.5, max = 50.0
Element prediction: Off
Number of isotope peaks used for i-FIT = 3

Monoisotopic Mass, Even Electron Ions
7055 formula(e) evaluated with 14 results within limits (all results (up to 1000) for each mass)
Elements Used:
C: 1-500 H: 0-1000 N: 0-20 O: 0-25 Si: 0-3
NT-MSLAB-Operator-SVG
2017-75 222 (4.325) AM2 (Ar,35000.0,0.00,0.00); Cm (214:223) 1: TOF MS ASAP+ 8.27e+004

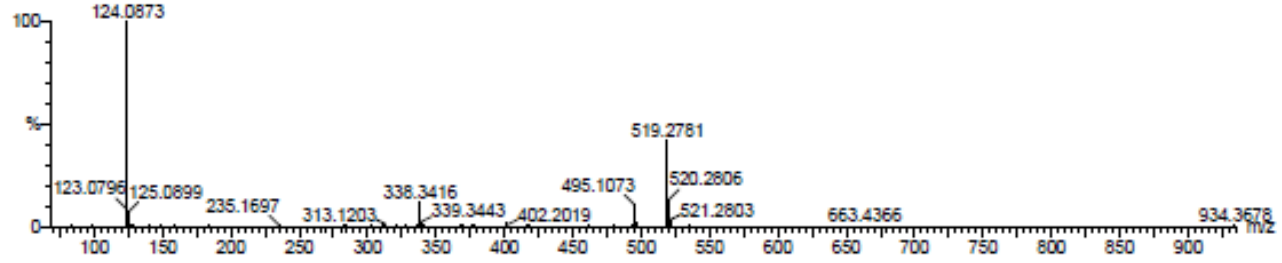


| | | | | | | | | |
|---|---|---|---|---|---|---|---|---|
| Minimum: | | | | -1.5 | | | | |
| Maximum: | | 5.0 | 3.0 | 50.0 | | | | |
| Mass | Calc. Mass | mDa | PPM | DBE | i-FIT | Norm | Conf(%) | Formula |
| 519.2781 | 519.2778 | 0.3 | 0.6 | 8.5 | 130.4 | 0.207 | 81.34 | C28 H43 O7 Si |
| | 519.2796 | -1.5 | -2.9 | 6.5 | 132.8 | 2.615 | 7.32 | C14 H35 N16 O4 Si |
| | 519.2791 | -1.0 | -1.9 | 13.5 | 133.1 | 2.851 | 5.76 | C29 H39 N4 O3 Si Ion observed M+H |
| | 519.2783 | -0.2 | -0.4 | 1.5 | 133.6 | 3.343 | 3.53 | C13 H39 N12 O8 Si |
| | 519.2783 | -0.2 | -0.4 | 4.5 | 135.0 | 4.752 | 0.86 | C20 H43 N6 O6 Si2 |
| | 519.2796 | -1.5 | -2.9 | 9.5 | 135.6 | 5.401 | 0.45 | C21 H39 N10 O2 Si2 |
| | 519.2769 | 1.2 | 2.3 | -0.5 | 136.4 | 6.120 | 0.22 | C19 H47 N2 O10 Si2 |
| | 519.2779 | 0.2 | 0.4 | 5.5 | 136.8 | 6.599 | 0.14 | C21 H39 N6 O9 |
| | 519.2792 | -1.1 | -2.1 | 10.5 | 136.9 | 6.692 | 0.12 | C22 H35 N10 O5 |
| | 519.2769 | 1.2 | 2.3 | 10.5 | 137.1 | 6.826 | 0.11 | C17 H35 N16 Si2 |
| | 519.2782 | -0.1 | -0.2 | 7.5 | 137.5 | 7.277 | 0.07 | C27 H47 O4 Si3 |
| | 519.2796 | -1.5 | -2.9 | 12.5 | 138.2 | 7.967 | 0.03 | C28 H43 N4 Si3 |
| | 519.2787 | -0.6 | -1.2 | 0.5 | 139.1 | 8.860 | 0.01 | C12 H43 N12 O5 Si3 |
| | 519.2784 | -0.3 | -0.6 | -1.5 | 140.2 | 9.970 | 0.00 | C6 H35 N18 O10 |

**Figure E.7**: MS spectrum of compound **6b.**

# F Spectroscopic data for compound 6c

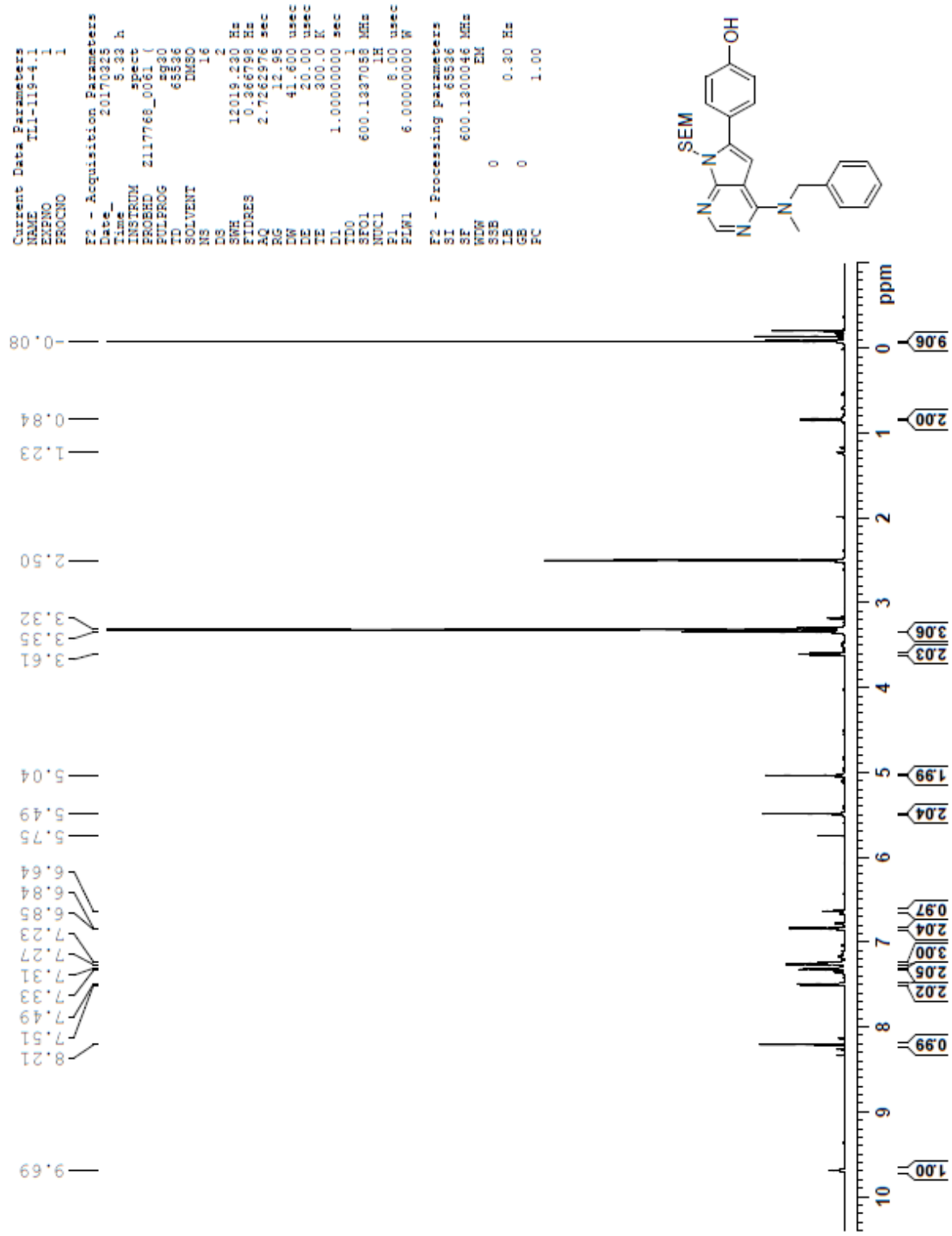


**Figure F.1**: $^{1}$H NMR spectrum of compound **6c.**

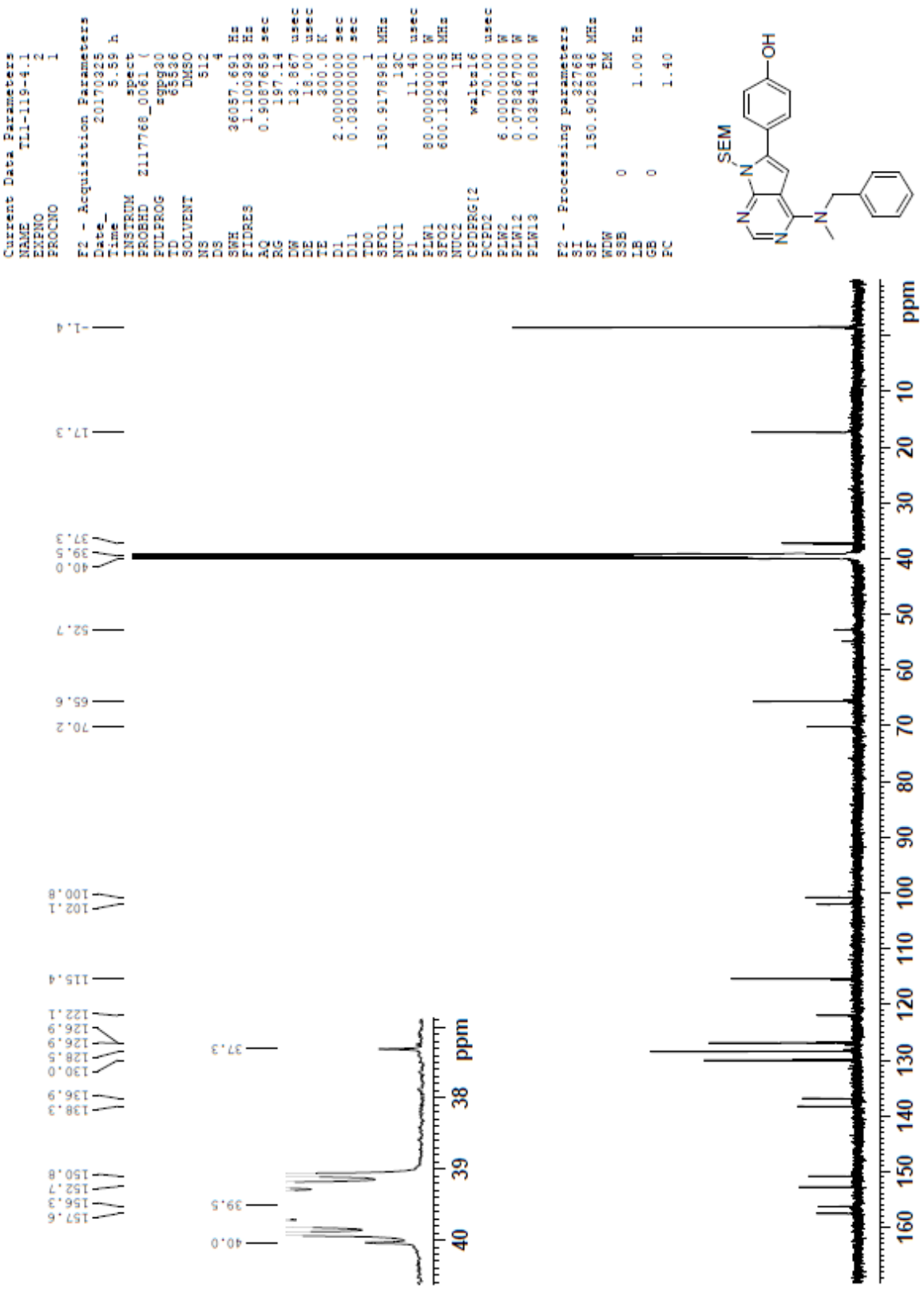


**Figure F.2**: $^{13}C$ NMR spectrum of compound **6c.**

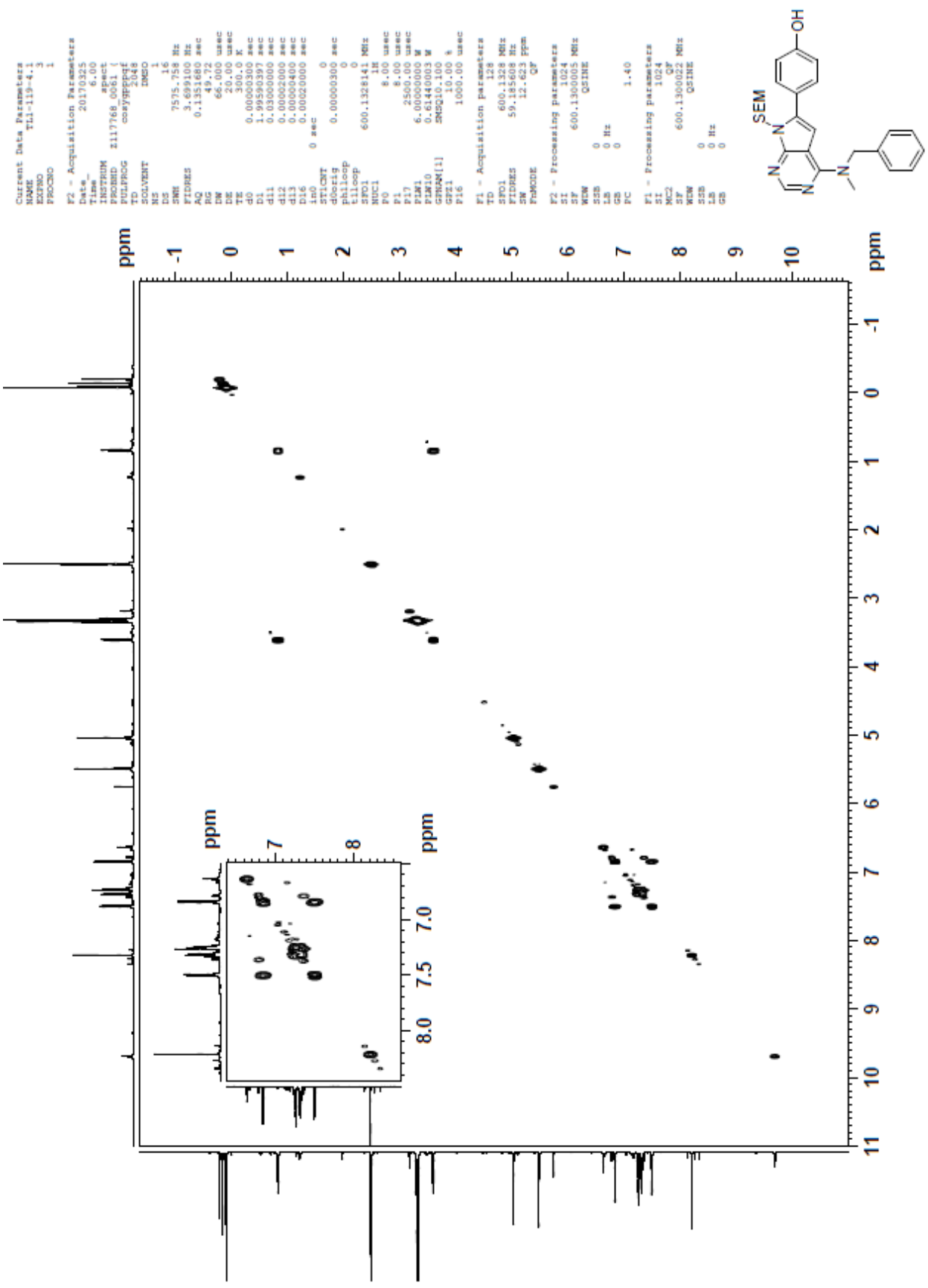


**Figure F.3**: COSY spectrum of compound **6c.**

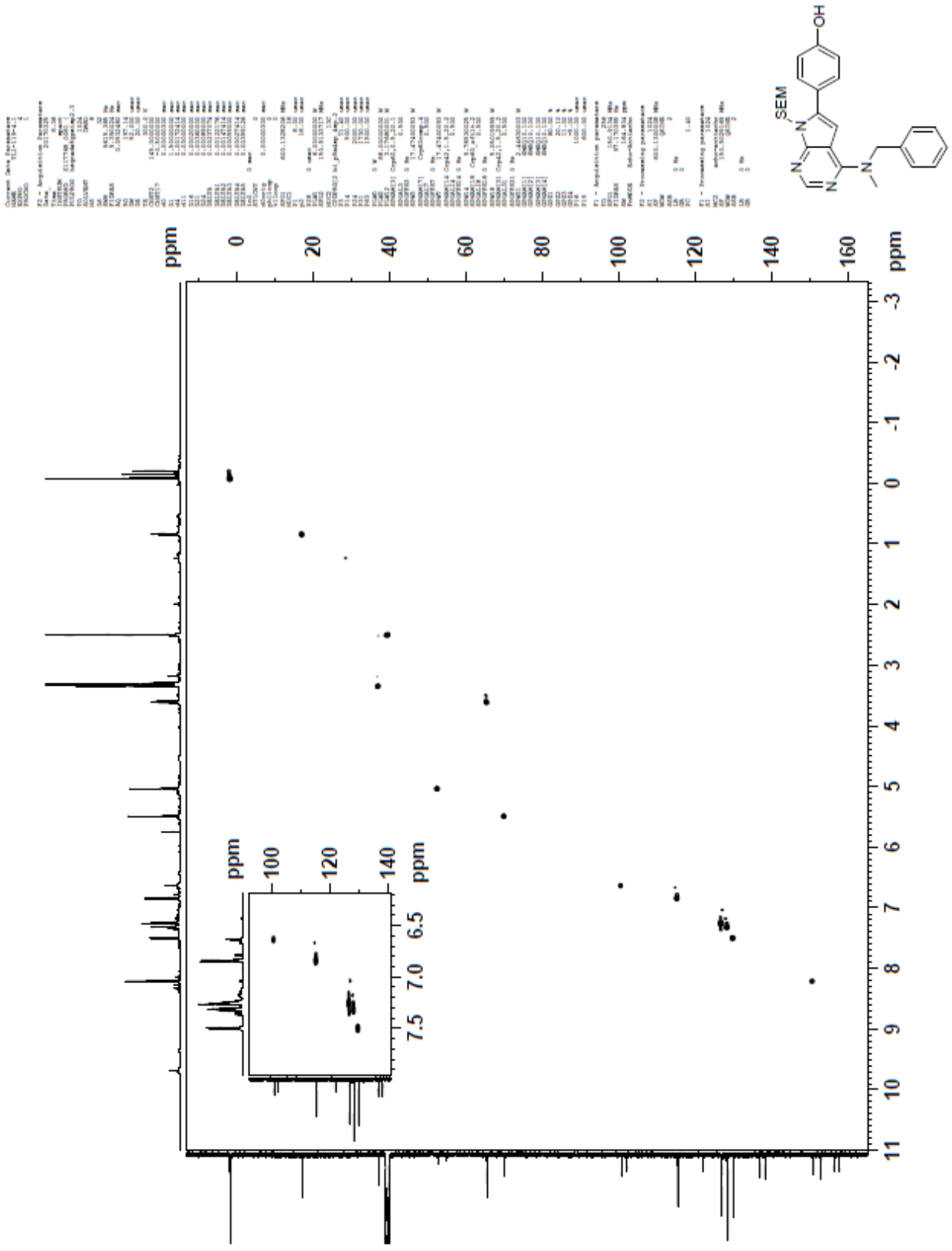


**Figure F.4**: HSQC spectrum of compound **6c.**

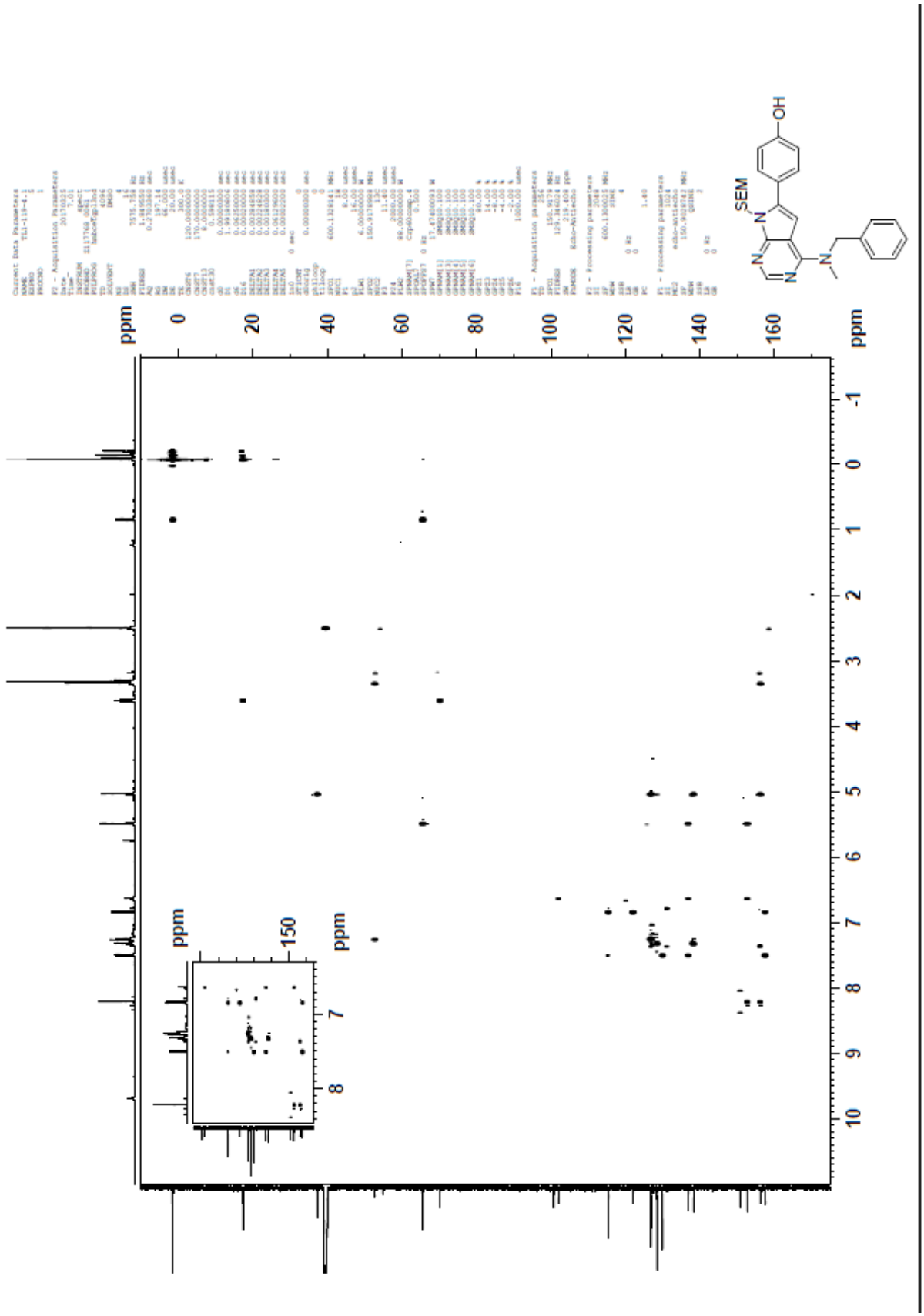


**Figure F.5**: HMBC spectrum of compound **6c**.

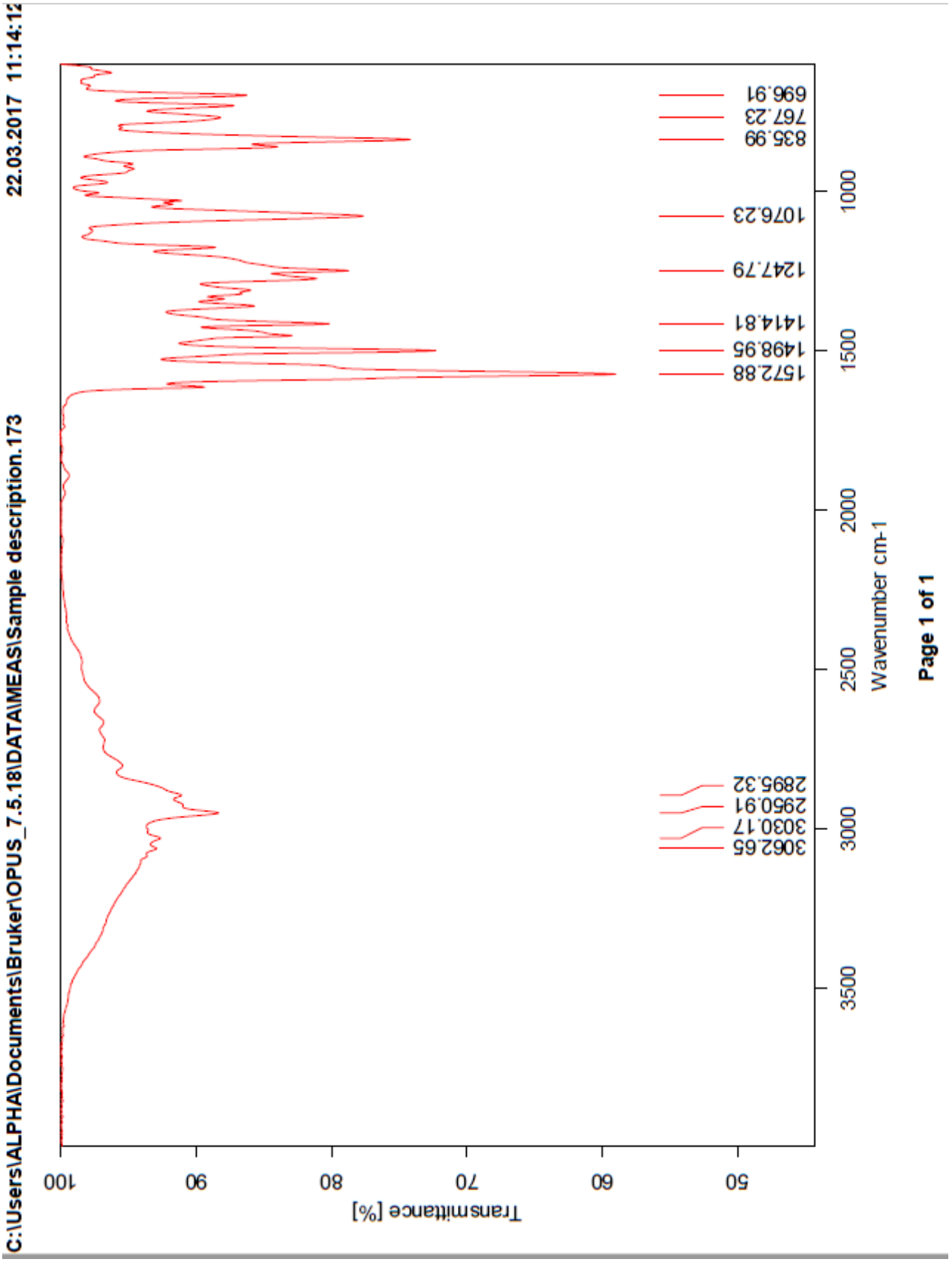


**Figure F.6**: IR spectrum of compound **6c.**

## Elemental Composition Report



### Single Mass Analysis

Tolerance = 2.0 PPM / DBE: min = -1.5, max = 50.0
Element prediction: Off
Number of isotope peaks used for i-FIT = 3

Monoisotopic Mass, Even Electron Ions
5293 formula(e) evaluated with 9 results within limits (all results (up to 1000) for each mass)
Elements Used:
C: 2-40 H: 0-1000 N: 0-20 O: 0-25 Si: 0-3

NT-MSLAB-Operator-SVG
2017-167 68 (1.344) AM2 (Ar,35000.0,0.00,0.00); Cm (62:68)

1: TOF MS ASAP+
1.33e+005

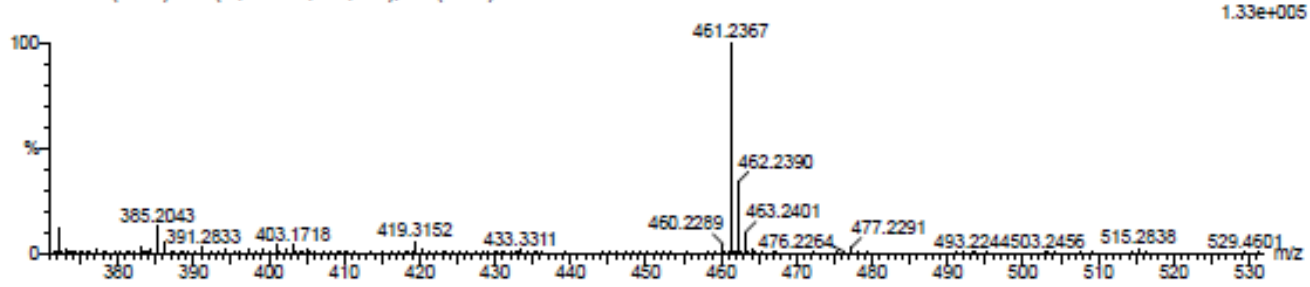


| | | | | | | | | |
|---|---|---|---|---|---|---|---|---|
| Minimum: | | | | -1.5 | | | | |
| Maximum: | | 5.0 | 2.0 | 50.0 | | | | |
| Mass | Calc. Mass | mDa | PPM | DBE | i-FIT | Norm | Conf(%) | Formula |
| 461.2367 | 461.2359 | 0.8 | 1.7 | 8.5 | 344.2 | 0.234 | 79.17 | C25 H37 O6 Si ION OBSERVED [M+H] |
| | 461.2373 | -0.6 | -1.3 | 13.5 | 345.5 | 1.569 | 20.83 | C26 H33 N4 O2 Si |
| | 461.2364 | 0.3 | 0.7 | 4.5 | 353.9 | 9.948 | 0.00 | C17 H37 N6 O5 Si2 |
| | 461.2360 | 0.7 | 1.5 | 5.5 | 354.8 | 10.860 | 0.00 | C18 H33 N6 O8 |
| | 461.2373 | -0.6 | -1.3 | 10.5 | 355.3 | 11.352 | 0.00 | C19 H29 N10 O4 |
| | 461.2364 | 0.3 | 0.7 | 1.5 | 357.9 | 13.908 | 0.00 | C10 H33 N12 O7 Si |
| | 461.2369 | -0.2 | -0.4 | 0.5 | 358.0 | 13.994 | 0.00 | C9 H37 N12 O4 Si3 |
| | 461.2363 | 0.4 | 0.9 | 7.5 | 358.1 | 14.130 | 0.00 | C24 H41 O3 Si3 |
| | 461.2365 | 0.2 | 0.4 | -1.5 | 360.2 | 16.233 | 0.00 | C3 H29 N18 O9 |

**Figure F.7**: MS spectrum of compound **6c.**

# G Spectroscopic data for compound 6d

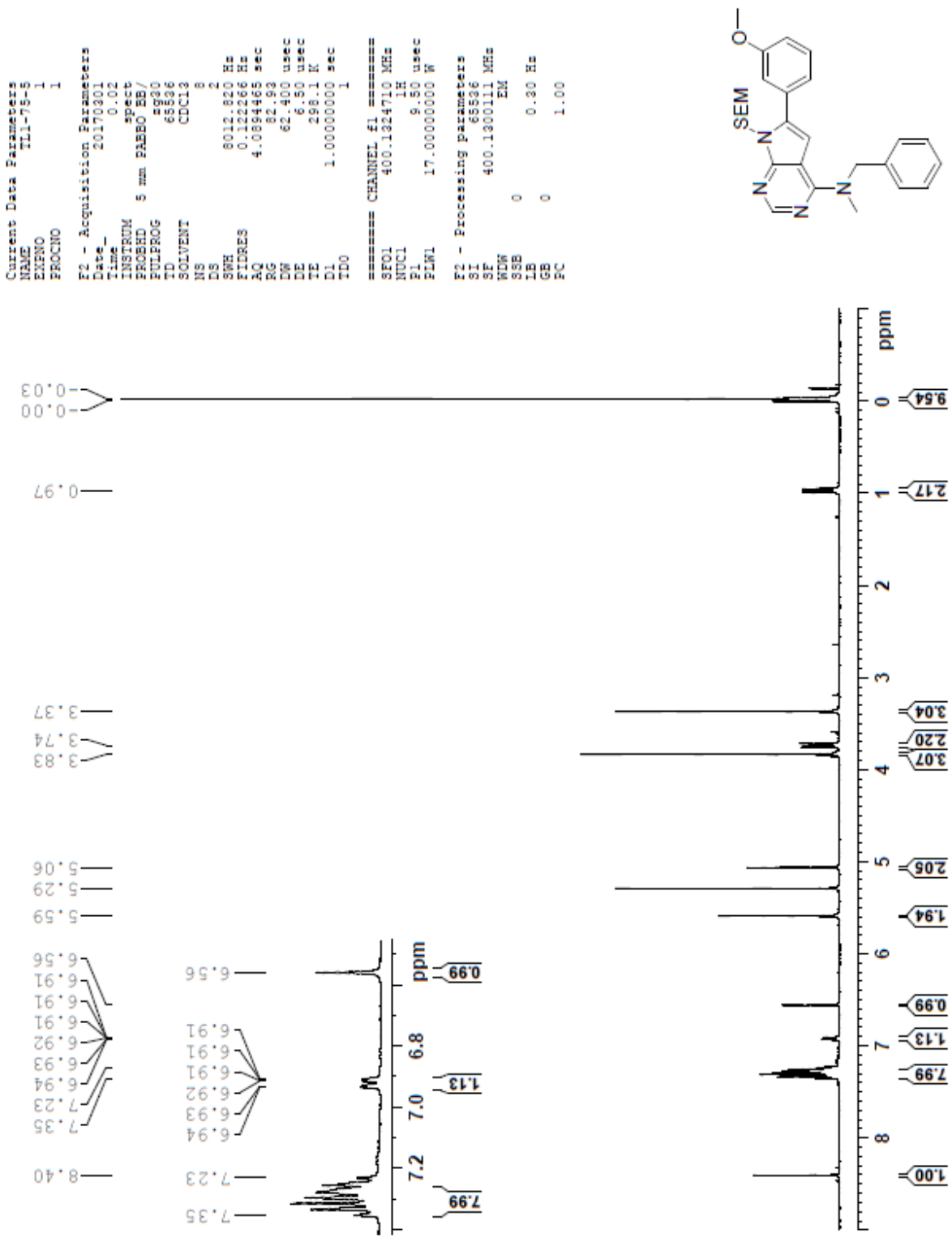


**Figure G.1**: $^{1}$H NMR spectrum of compound **6d.**

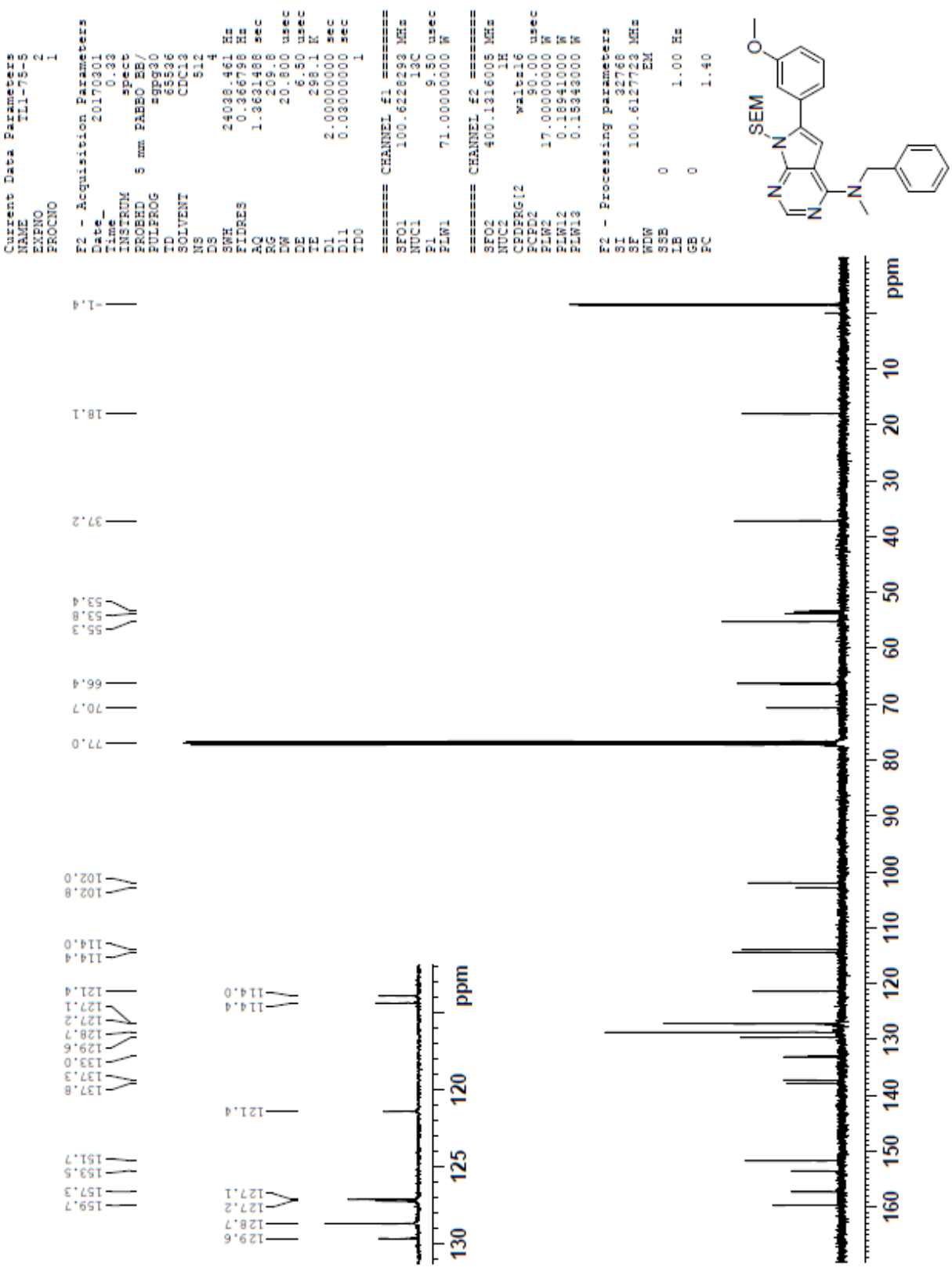


**Figure G.2**: $^{13}C$ NMR spectrum of compound **6d.**

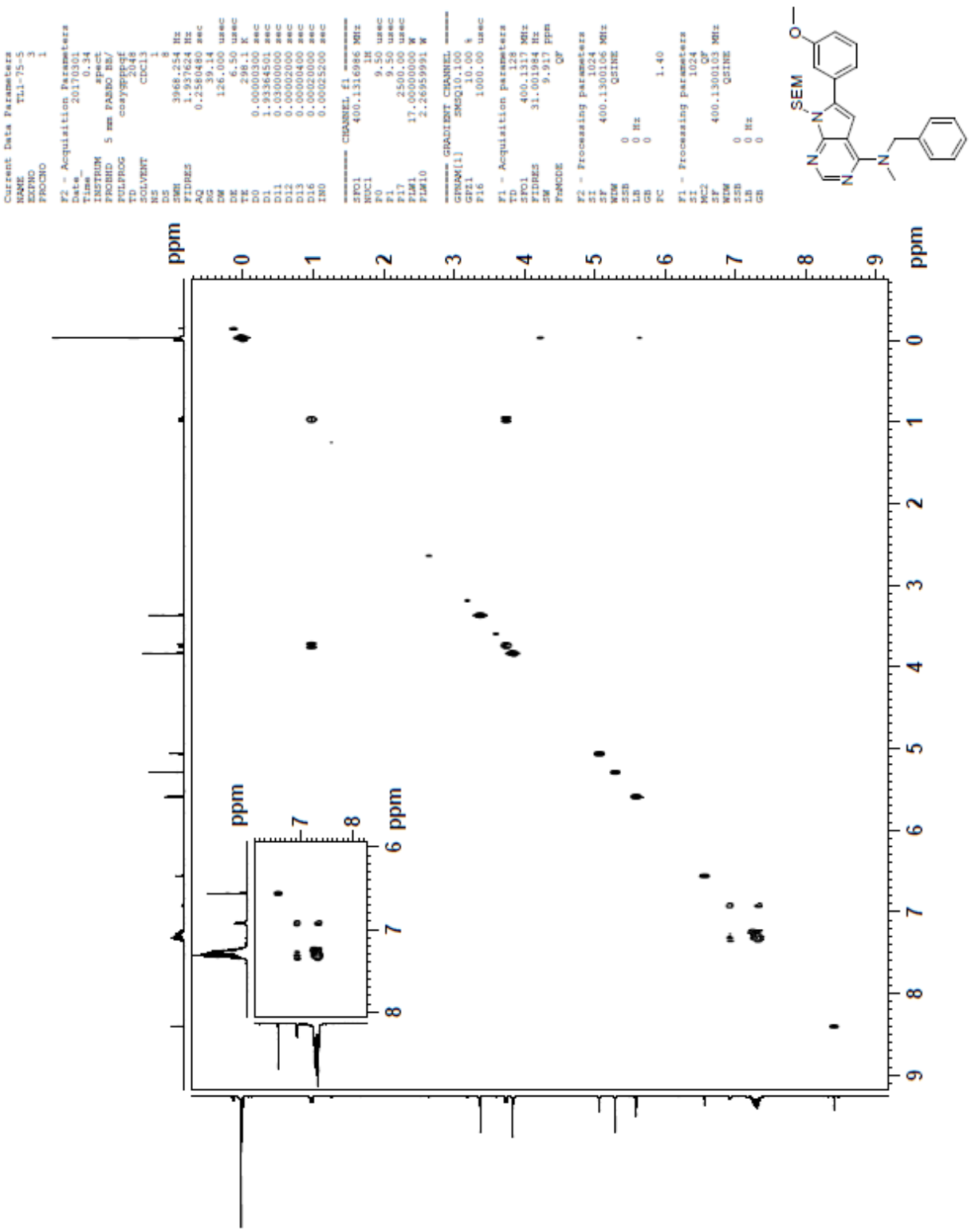


**Figure G.3**: COSY spectrum of compound **6d.**

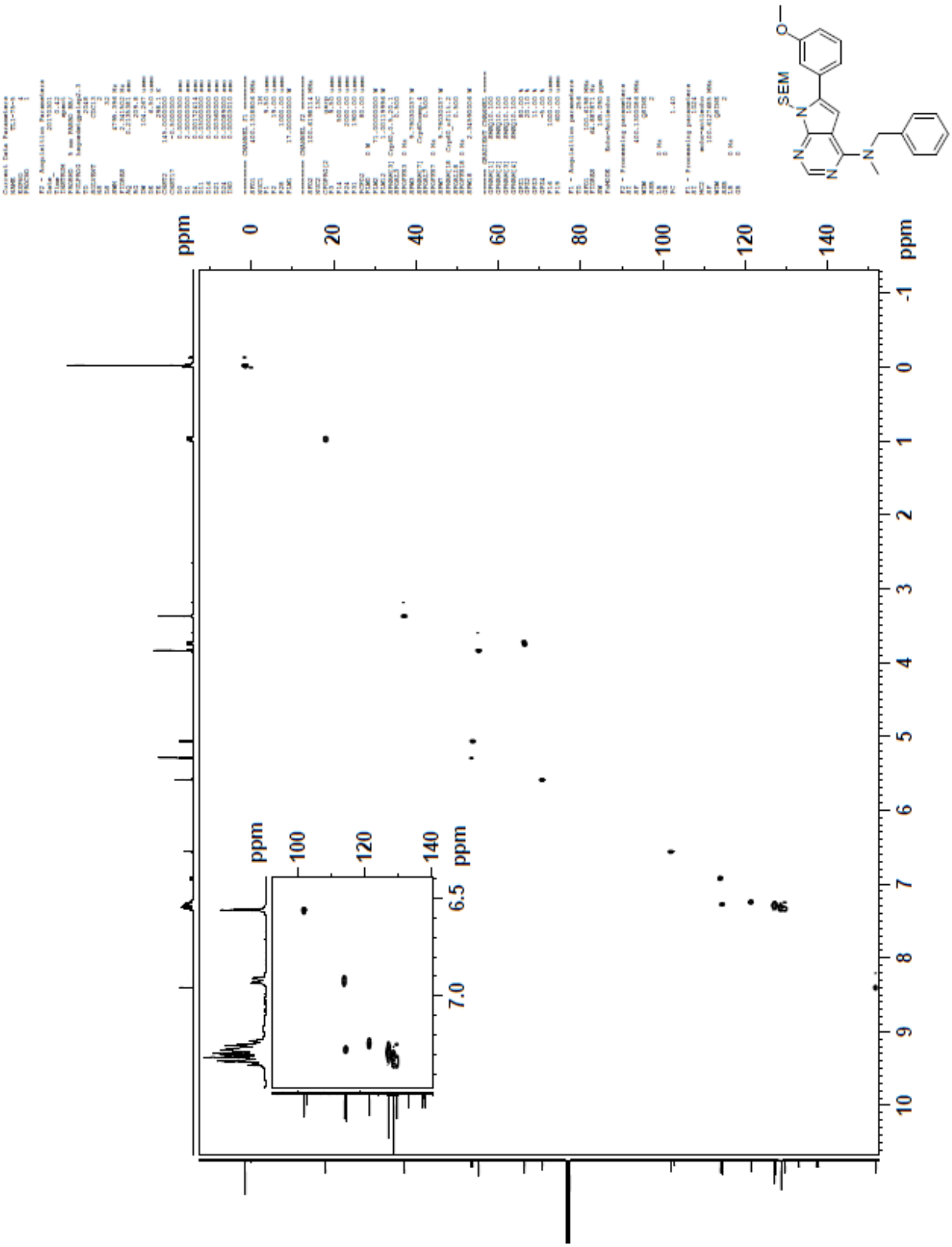


**Figure G.4**: HSQC spectrum of compound **6d.**

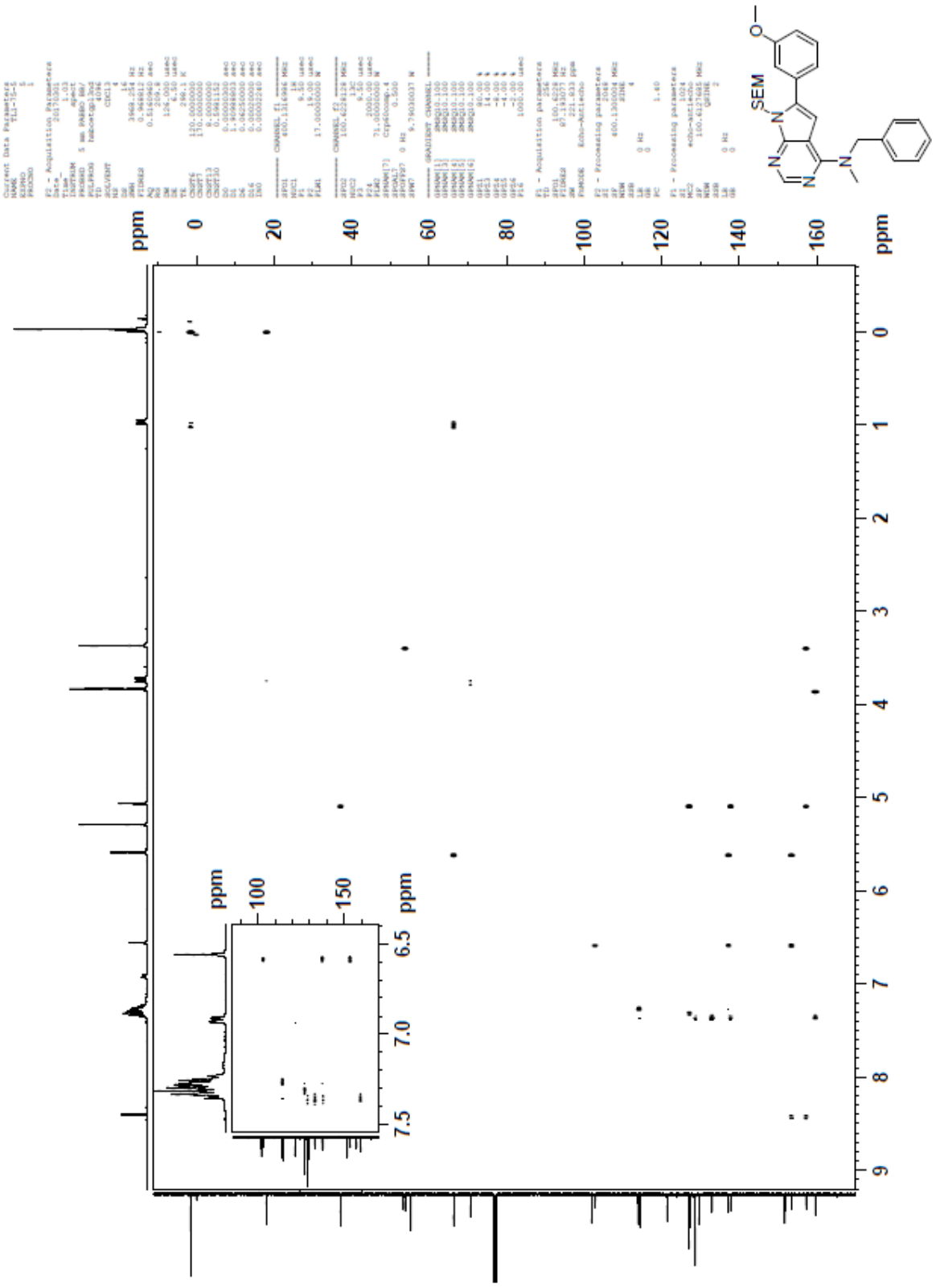


**Figure G.5**: HMBC spectrum of compound **6d**.

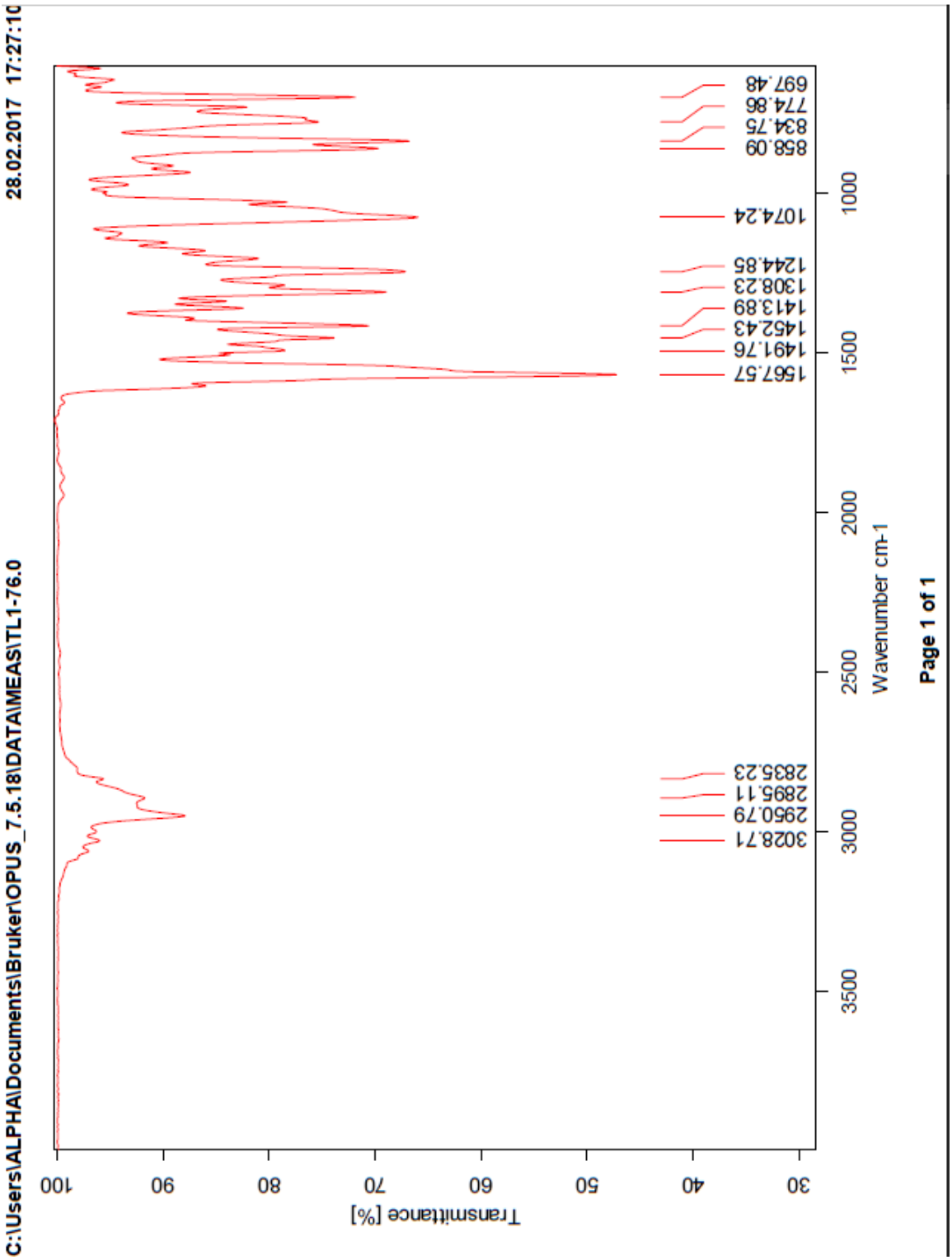


**Figure G.5**: IR spectrum of compound **6d.**

**Elemental Composition Report** Page 1

**Single Mass Analysis**
Tolerance = 2.0 PPM / DBE: min = -1.5, max = 50.0
Element prediction: Off
Number of isotope peaks used for i-FIT = 3

Monoisotopic Mass, Even Electron Ions
5693 formula(e) evaluated with 8 results within limits (all results (up to 1000) for each mass)
Elements Used:
C: 2-500 H: 0-1000 N: 0-20 O: 0-25 Si: 0-3

NT-MSLAB-Operator-SVG
2017-134 90 (1.776) AM2 (Ar,35000.0,0.00,0.00); Cm (84:93)

1: TOF MS ASAP+
8.02e+004

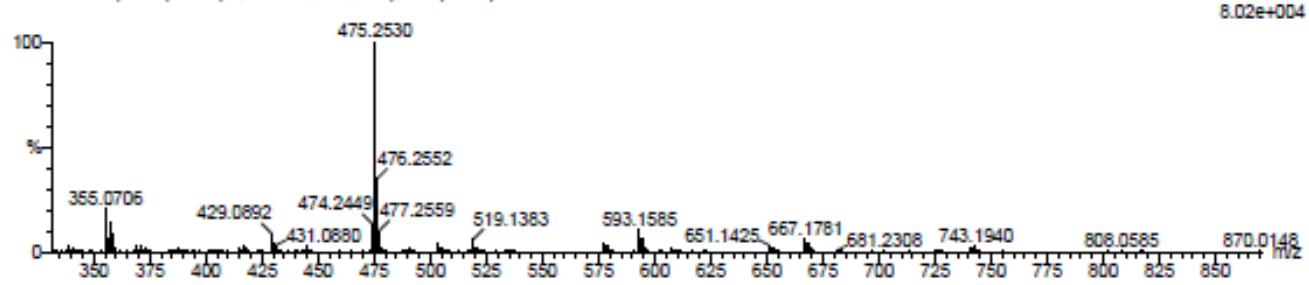


| | | | | | | | | |
|---|---|---|---|---|---|---|---|---|
| Minimum: | | | | -1.5 | | | | |
| Maximum: | | 5.0 | 2.0 | 50.0 | | | | |
| Mass | Calc. Mass | mDa | PPM | DBE | i-FIT | Norm | Conf(%) | Formula |
| 475.2530 | 475.2530 | 0.0 | 0.0 | 10.5 | 255.8 | 12.877 | 0.00 | C20 H31 N10 O4 |
| | 475.2529 | 0.1 | 0.2 | 13.5 | 242.9 | 0.000 | 100.00 | C27 H35 N4 O2 Si ION OBSERVED M+H |
| | 475.2534 | -0.4 | -0.8 | 9.5 | 253.0 | 10.075 | 0.00 | C19 H35 N10 O Si2 |
| | 475.2534 | -0.4 | -0.8 | 6.5 | 256.6 | 13.673 | 0.00 | C12 H31 N16 O3 Si |
| | 475.2525 | 0.5 | 1.1 | 0.5 | 258.1 | 15.194 | 0.00 | C10 H39 N12 O4 Si3 |
| | 475.2538 | -0.8 | -1.7 | 5.5 | 257.3 | 14.434 | 0.00 | C11 H35 N16 Si3 |
| | 475.2521 | 0.9 | 1.9 | 1.5 | 257.6 | 14.672 | 0.00 | C11 H35 N12 O7 Si |
| | 475.2521 | 0.9 | 1.9 | -1.5 | 260.2 | 17.283 | 0.00 | C4 H31 N18 O9 |

**Figure G.6**: MS spectrum of compound **6d.**

# H Spectroscopic data for compound 6e

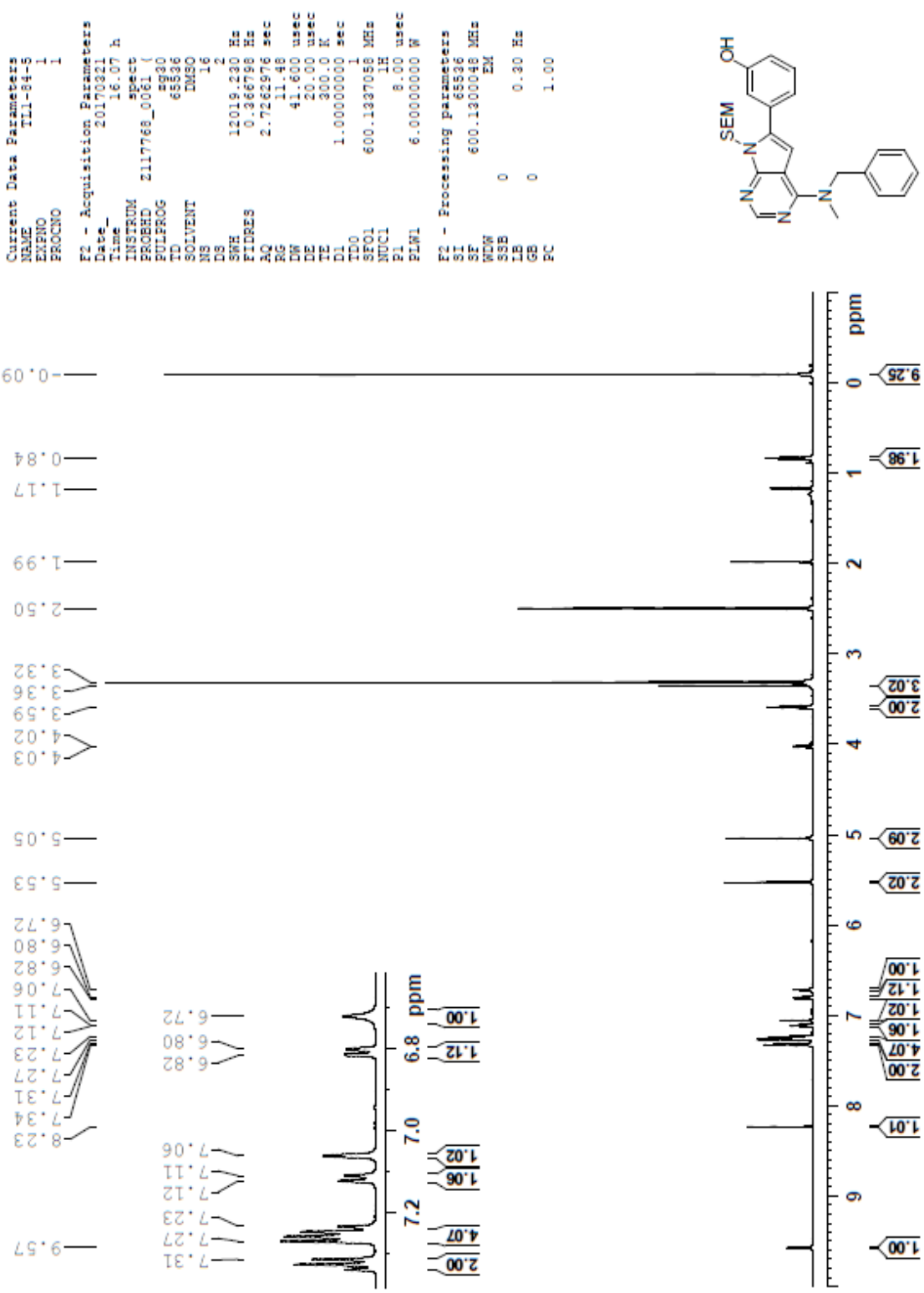


**Figure H.1**: $^{1}$H NMR spectrum of compound **6e.**

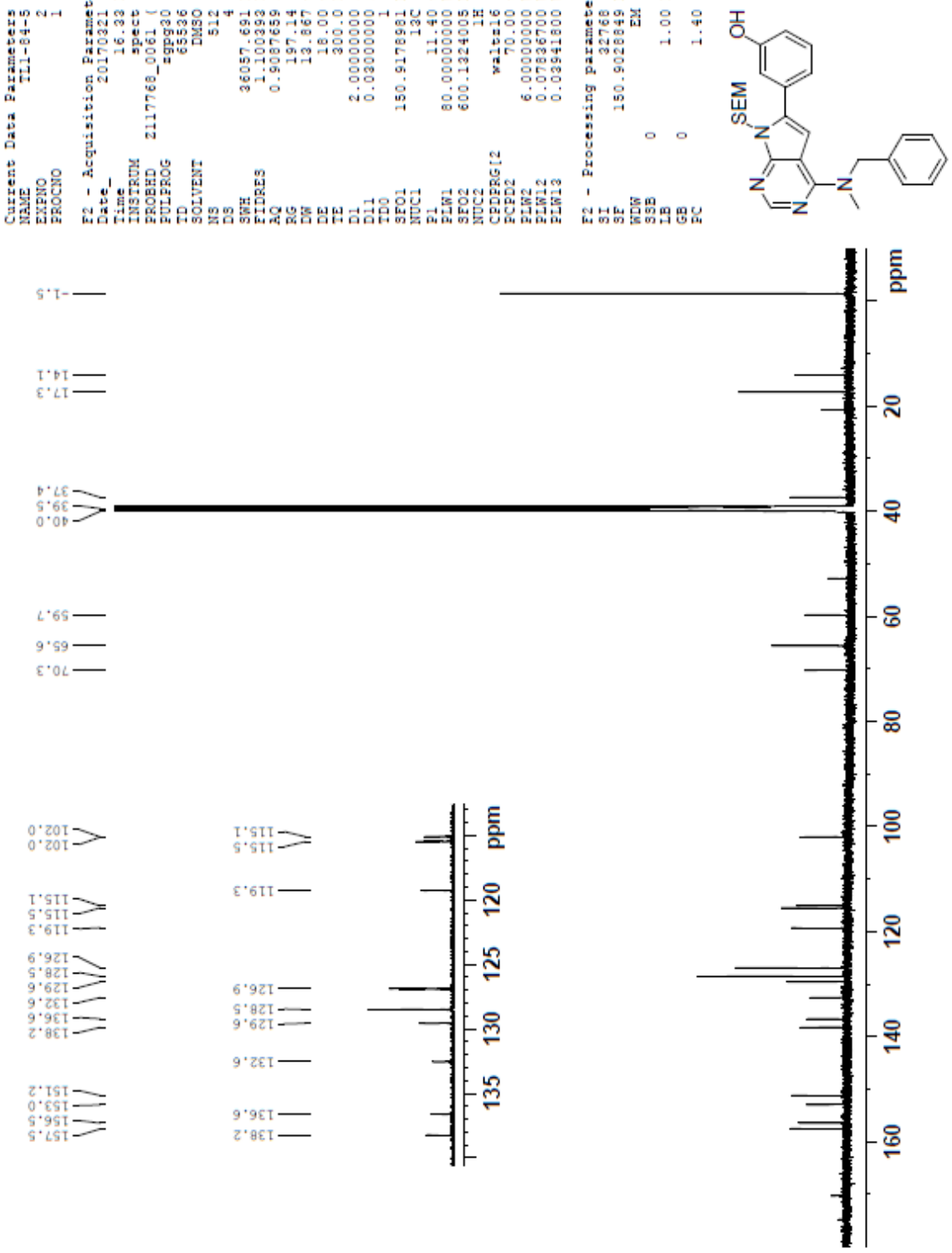


**Figure H.2**: $^{13}C$ NMR spectrum of compound **6e.**

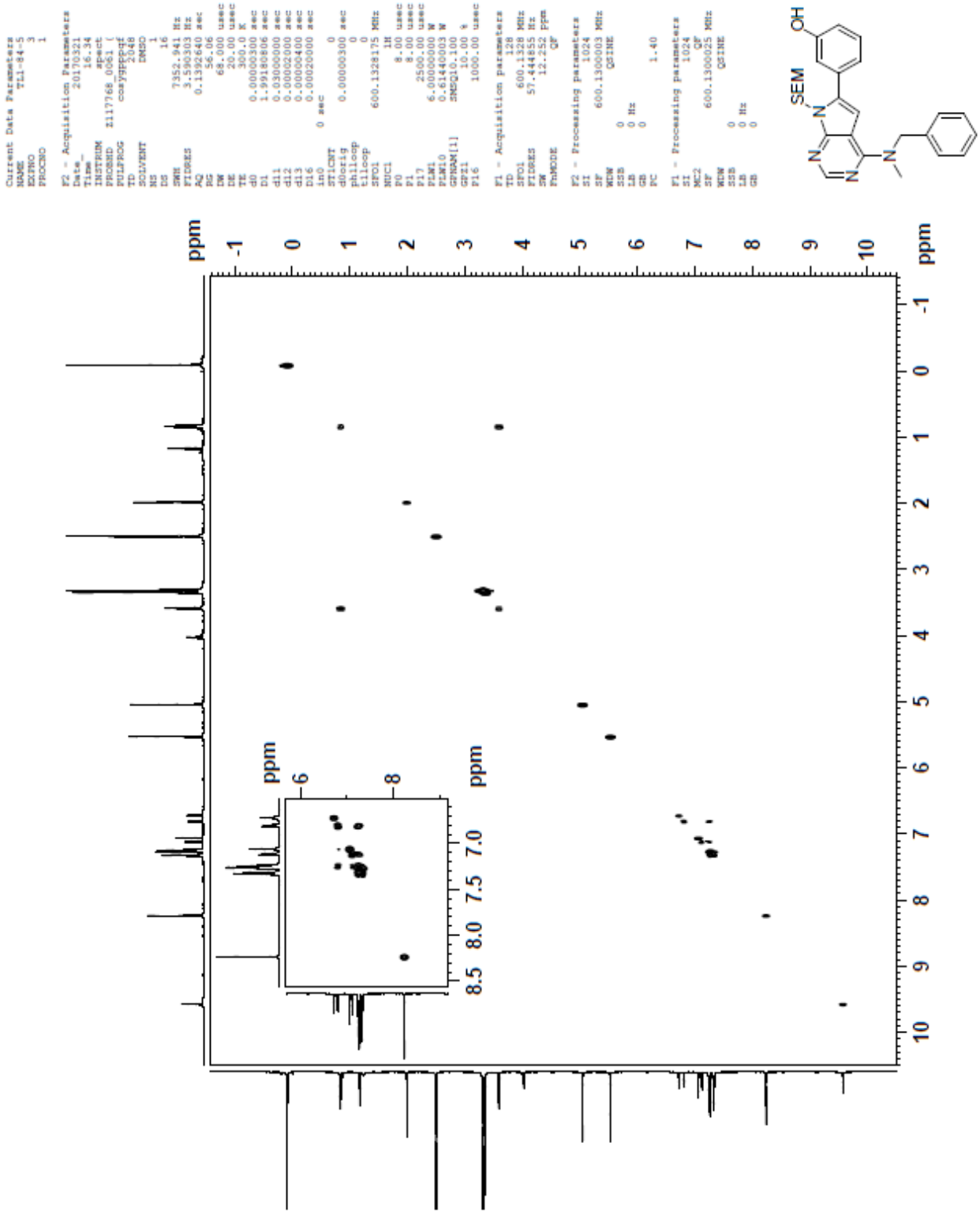


**Figure H.3**: COSY spectrum of compound **6e.**

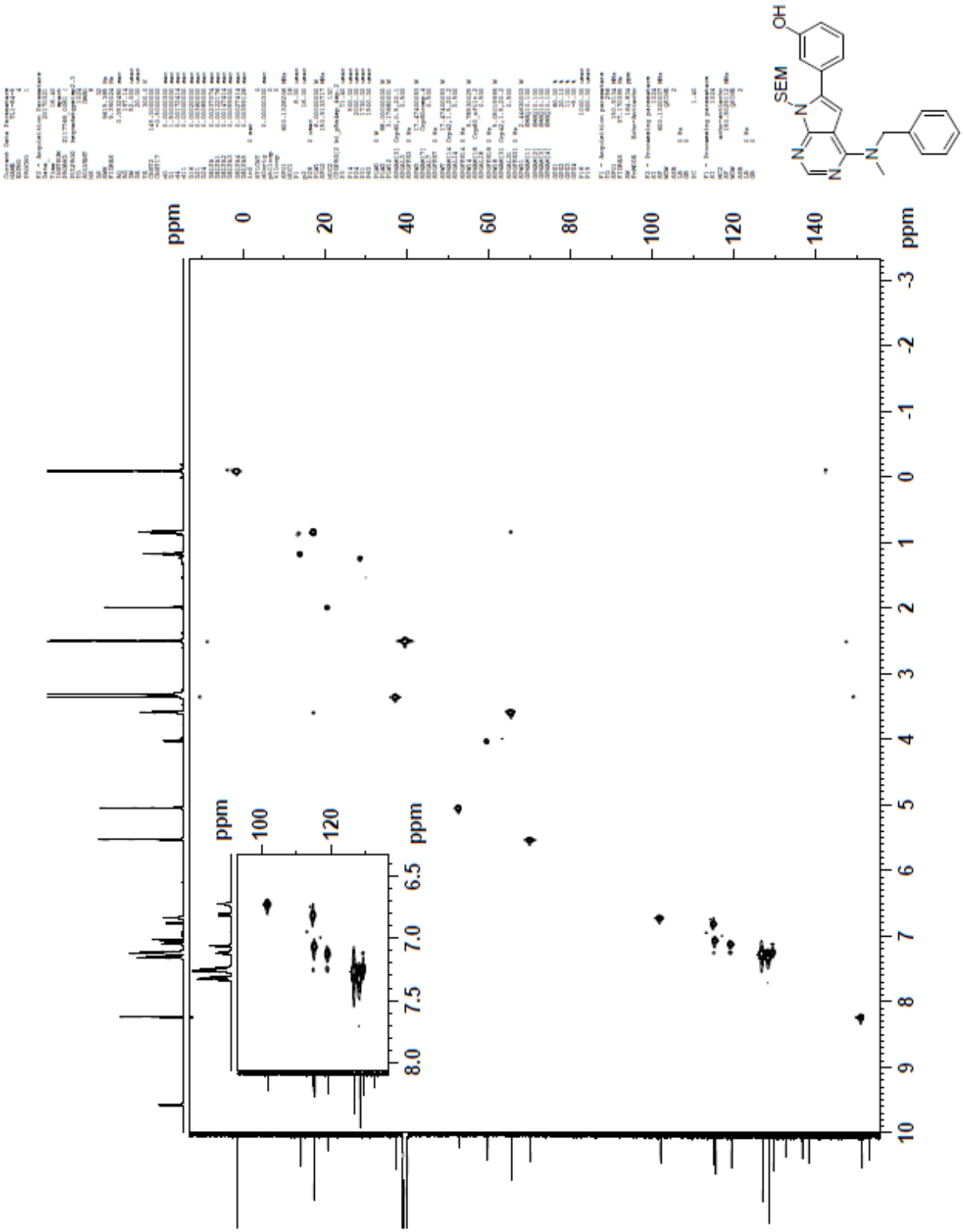


**Figure H.4**: HSQC spectrum of compound **6e.**

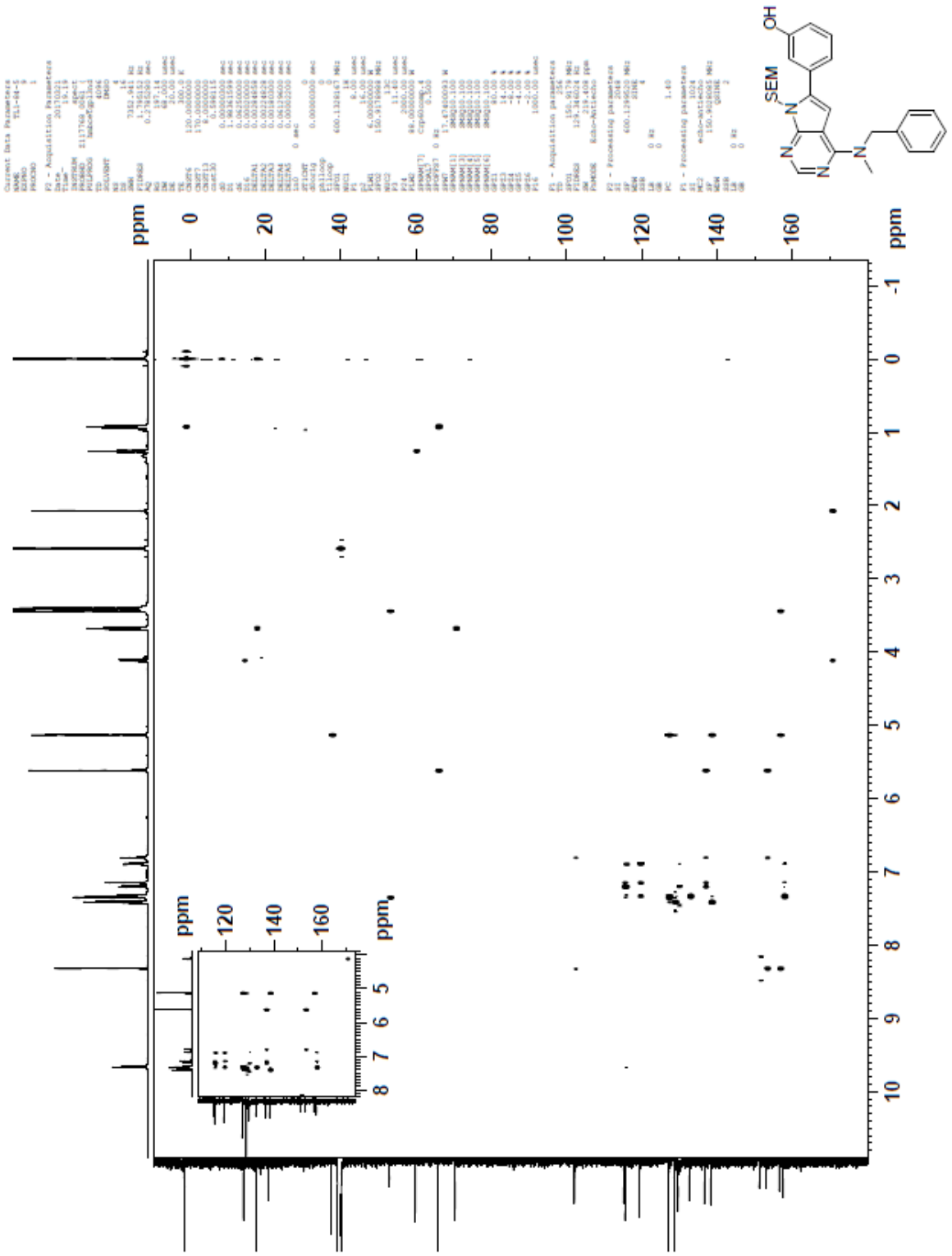


**Figure H.5**: HMBC spectrum of compound **6e**.

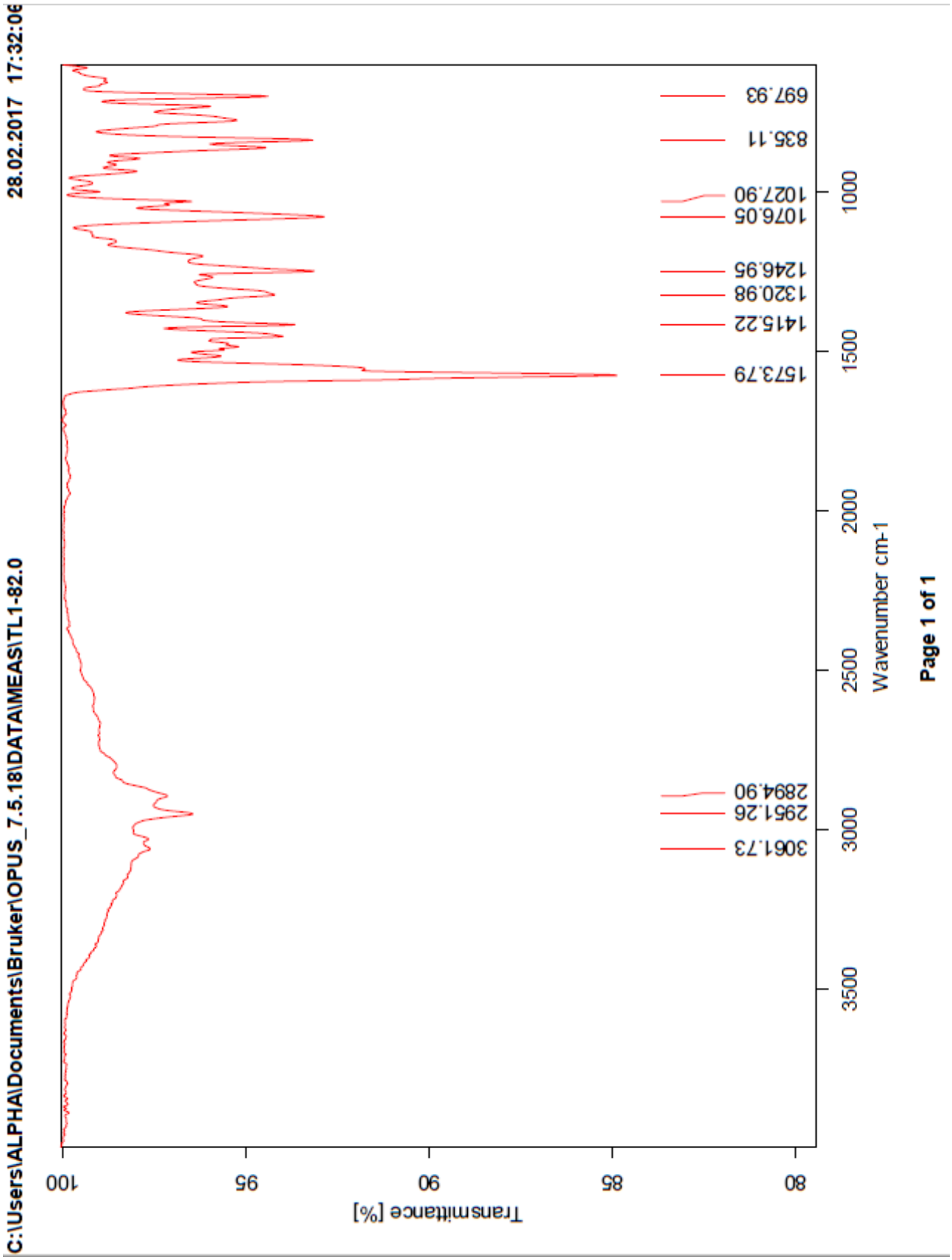


**Figure H.6**: IR spectrum of compound **6e.**

**Elemental Composition Report** Page 1

**Single Mass Analysis**
Tolerance = 2.0 PPM / DBE: min = -1.5, max = 50.0
Element prediction: Off
Number of isotope peaks used for i-FIT = 3

Monoisotopic Mass, Even Electron Ions
5292 formula(e) evaluated with 9 results within limits (all results (up to 1000) for each mass)
Elements Used:
C: 2-500 H: 0-1000 N: 0-20 O: 0-25 Si: 0-3

NT-MSLAB-Operator-SVG
2017-135 256 (4.979) AM2 (Ar,35000.0,0.00,0.00); Cm (247:257)

1: TOF MS ASAP+
9.01e+006

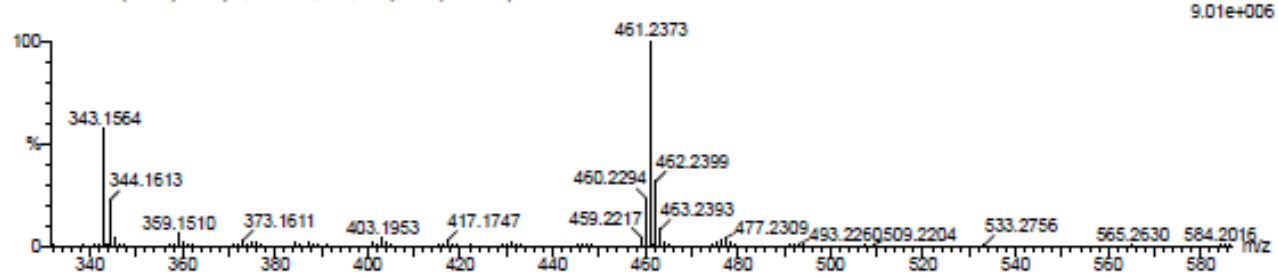


| | | | | | | | | |
|---|---|---|---|---|---|---|---|---|
| Minimum: | | | | -1.5 | | | | |
| Maximum: | | 5.0 | 2.0 | 50.0 | | | | |
| Mass | Calc. Mass | mDa | PPM | DBE | i-FIT | Norm | Conf(%) | Formula |
| 461.2373 | 461.2373 | 0.0 | 0.0 | 13.5 | 159.6 | 0.002 | 99.81 | C26 H33 N4 O2 Si |
| | 461.2373 | 0.0 | 0.0 | 10.5 | 169.1 | 9.564 | 0.01 | C19 H29 N10 O4 |
| | 461.2369 | 0.4 | 0.9 | 0.5 | 171.3 | 11.686 | 0.00 | C9 H37 N12 O4 Si3 |
| | 461.2377 | -0.4 | -0.9 | 9.5 | 166.6 | 7.060 | 0.09 | C18 H33 N10 O Si2 |
| | 461.2378 | -0.5 | -1.1 | 6.5 | 167.2 | 7.581 | 0.05 | C11 H29 N16 O3 Si |
| | 461.2365 | 0.8 | 1.7 | -1.5 | 173.8 | 14.219 | 0.00 | C3 H29 N18 O9 |
| | 461.2364 | 0.9 | 2.0 | 1.5 | 168.7 | 9.131 | 0.01 | C10 H33 N12 O7 Si |
| | 461.2364 | 0.9 | 2.0 | 4.5 | 167.7 | 8.162 | 0.03 | C17 H37 N6 O5 Si2 |
| | 461.2382 | -0.9 | -2.0 | 5.5 | 170.6 | 11.022 | 0.00 | C10 H33 N16 Si3 |

Ion observed M+H

**Figure H.7**: MS spectrum of compound **6e.**

# I Spectroscopic data for compound 6f

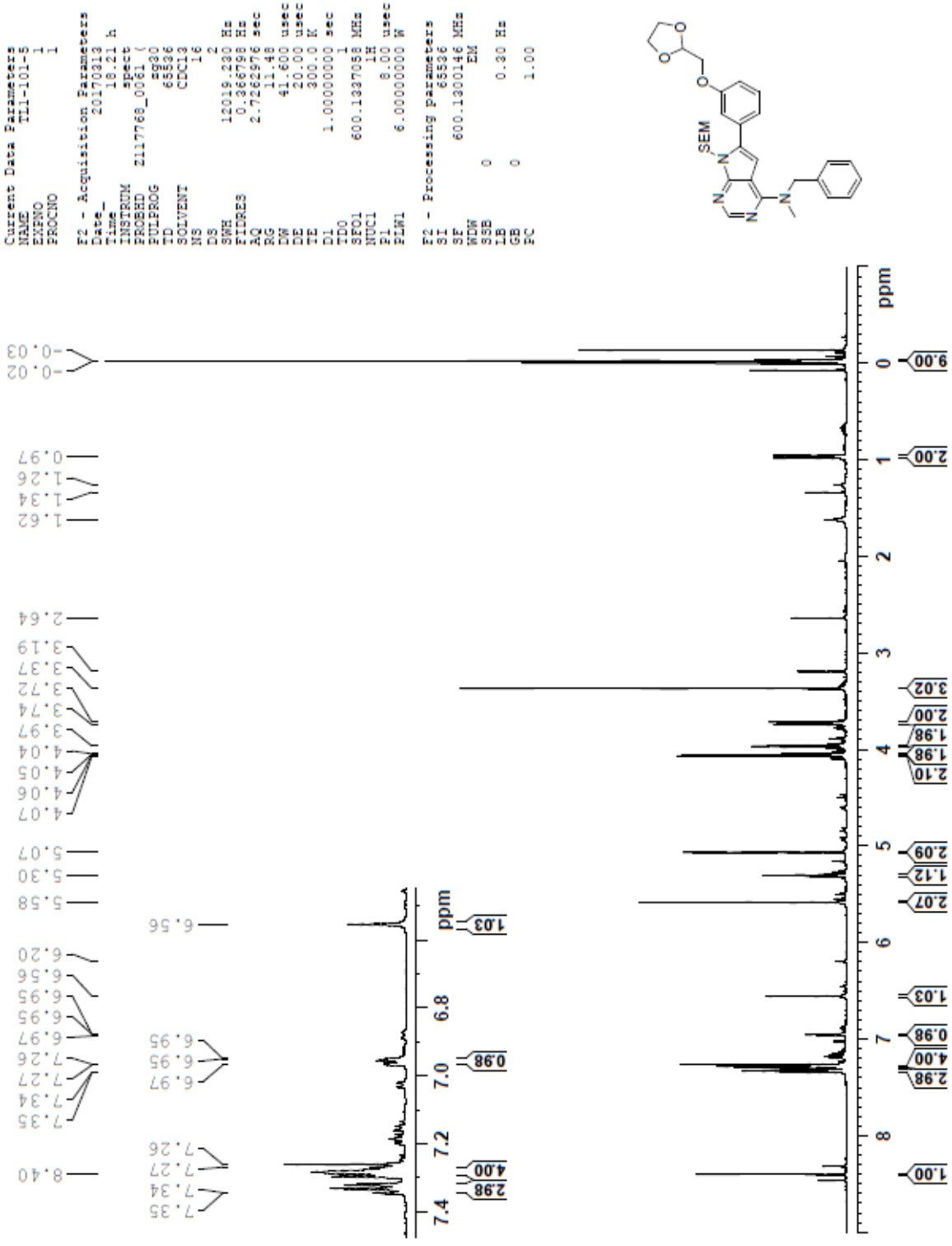


**Figure I.1**: $^{1}$H NMR spectrum of compound **6f.**

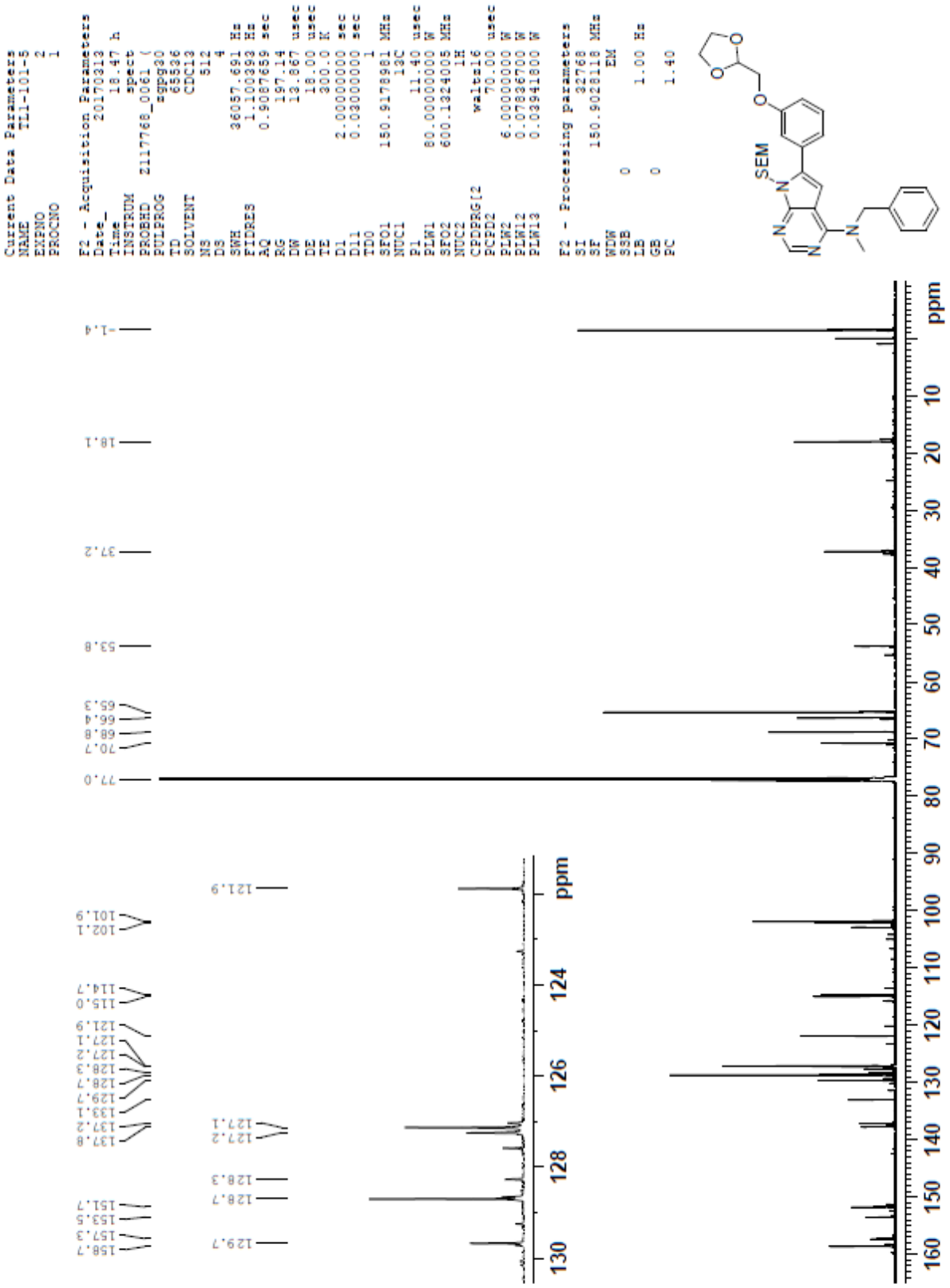


**Figure I.2**: C NMR spectrum of compound **6f.**

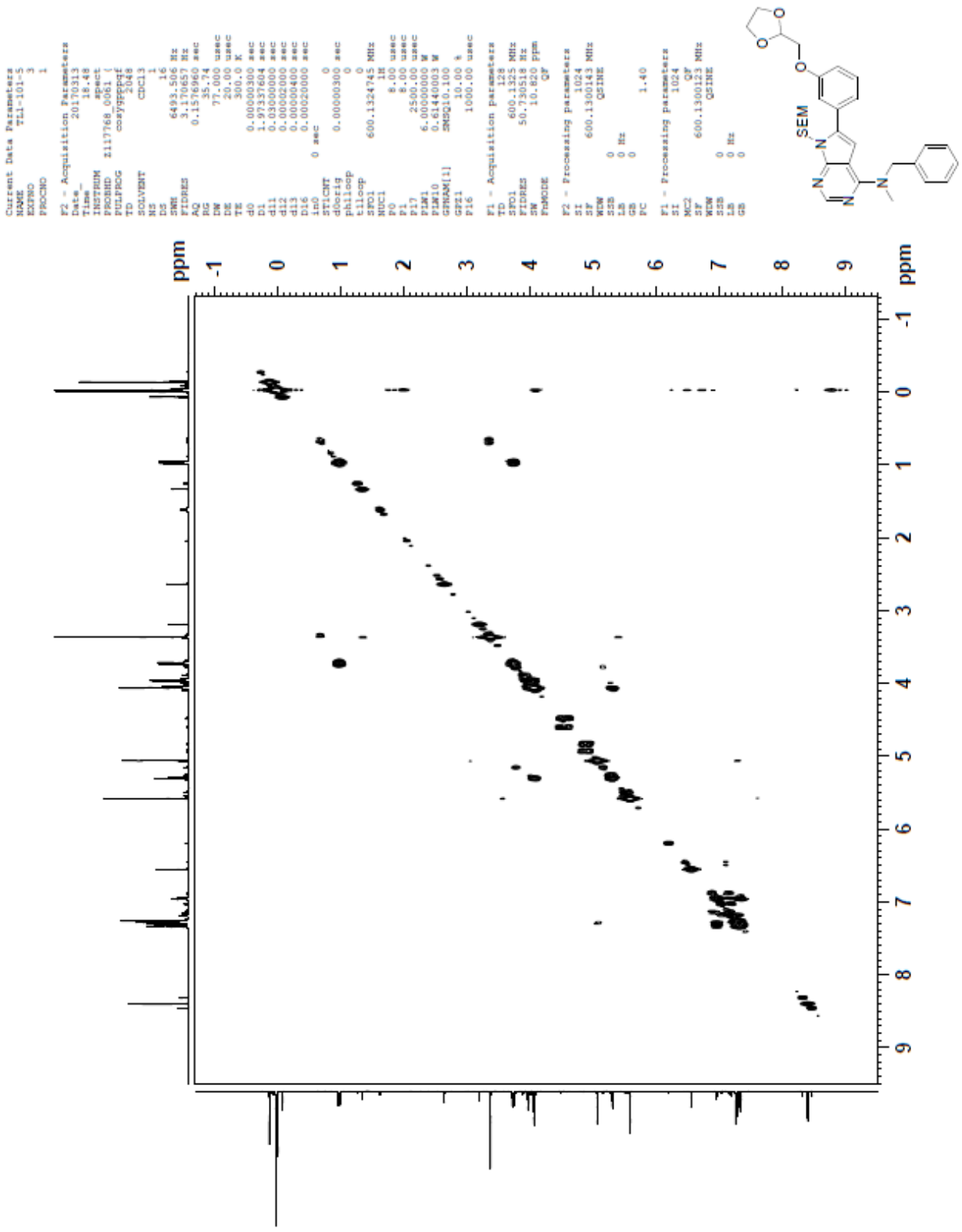


**Figure I.3**: COSY spectrum of compound **6f.**

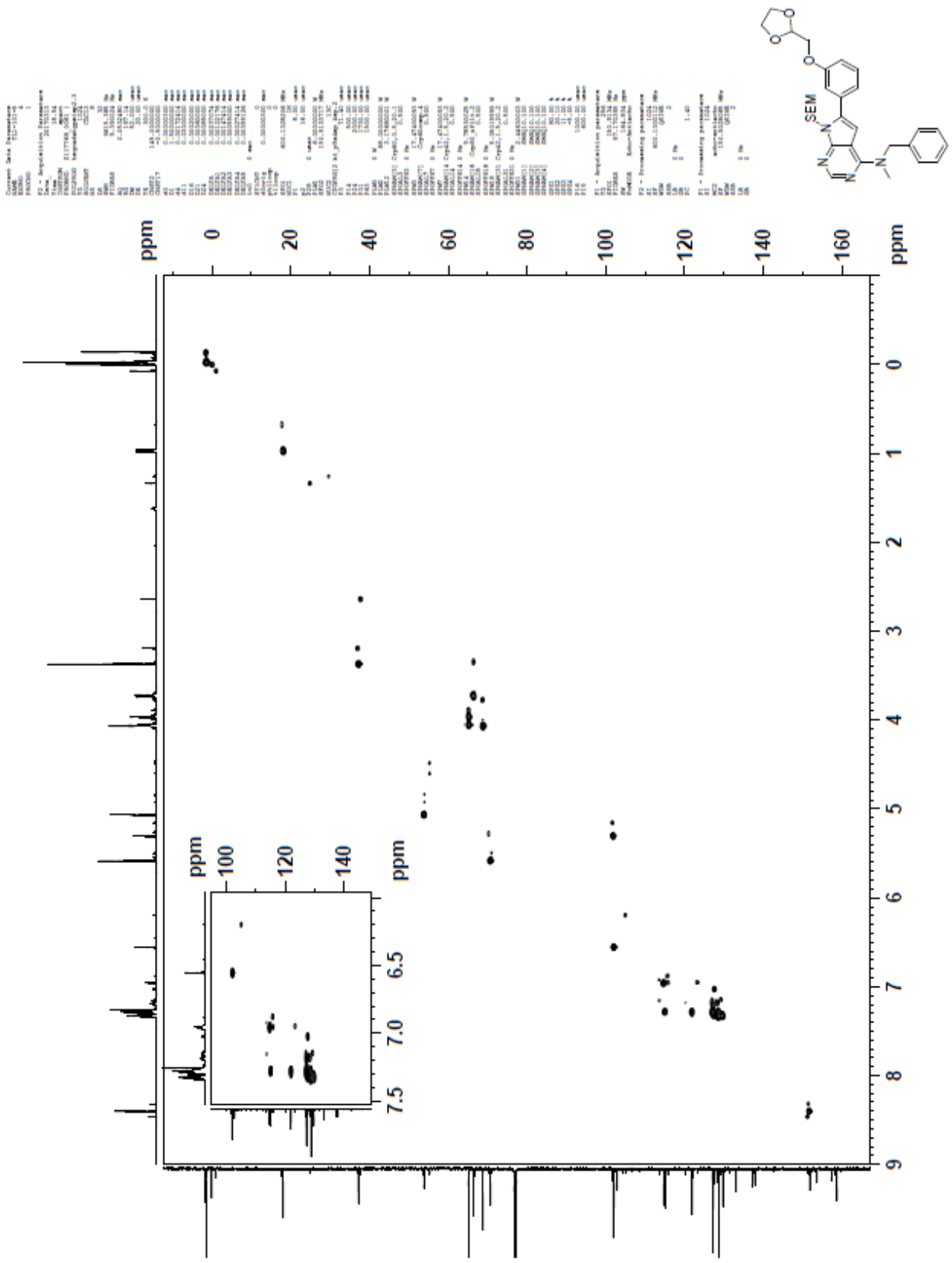


**Figure I.4**: HSQC spectrum of compound **6f.**

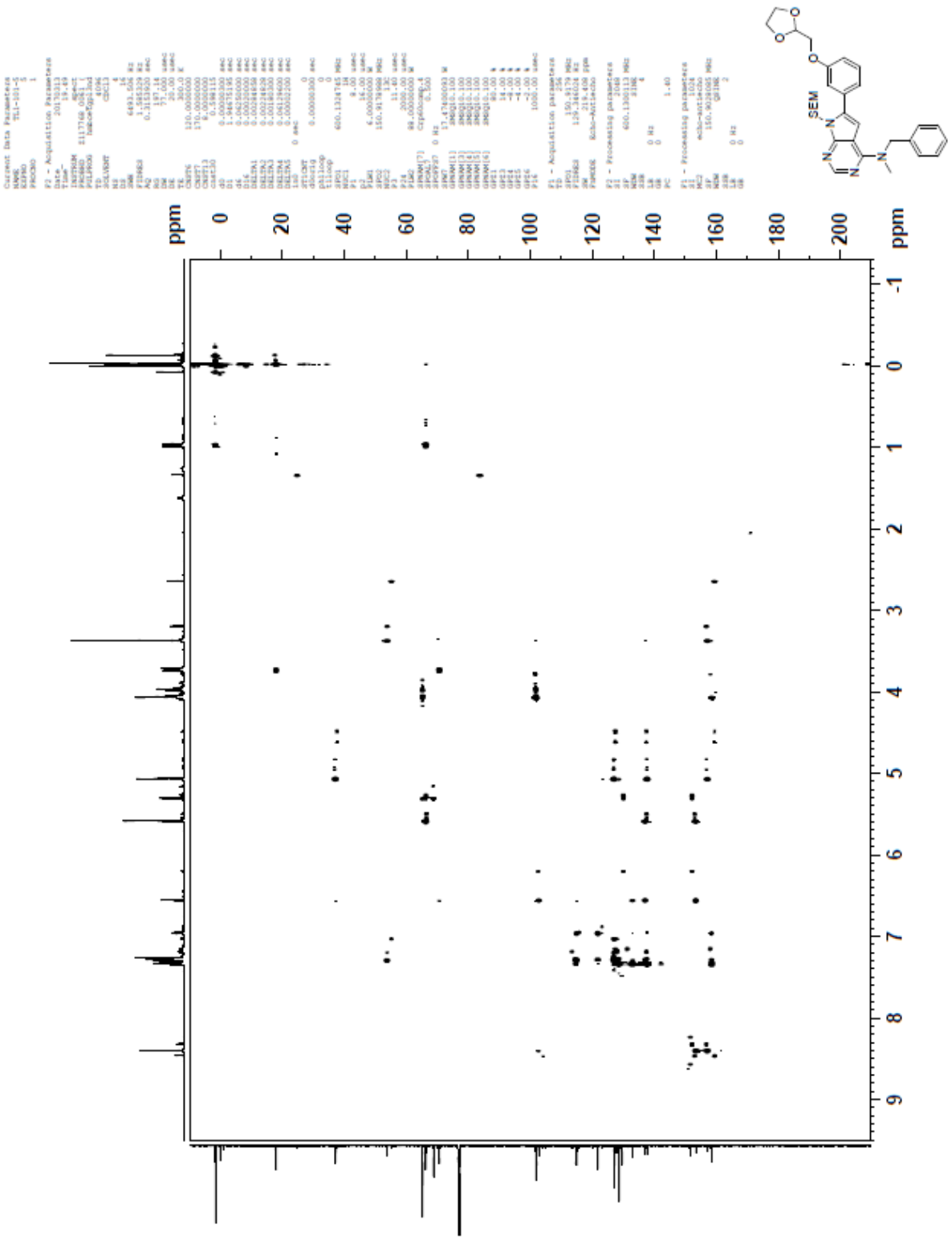


**Figure I.5**: HMBC spectrum of compound **6f**.

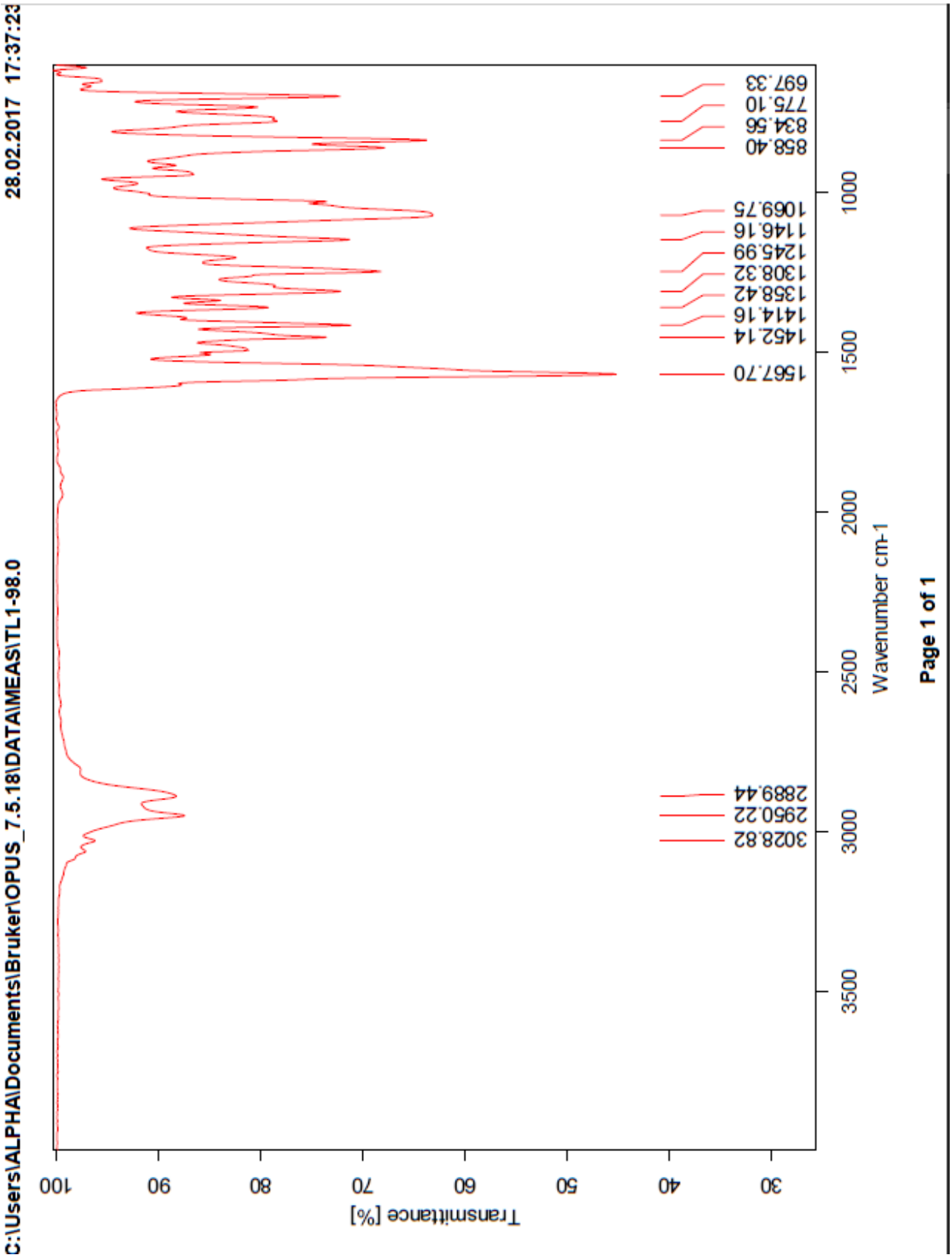


**Figure I.6**: IR spectrum of compound **6f.**

## Elemental Composition Report



### Single Mass Analysis

Tolerance = 2.0 PPM / DBE: min = -1.5, max = 50.0
Element prediction: Off
Number of isotope peaks used for i-FIT = 3

Monoisotopic Mass, Even Electron Ions
7823 formula(e) evaluated with 11 results within limits (all results (up to 1000) for each mass)
Elements Used:
C: 2-500 H: 0-1000 N: 0-20 O: 0-25 Si: 0-3

NT-MSLAB-Operator-SVG
2017-136 99 (1.948) AM2 (Ar,35000.0,0.00,0.00); Cm (89:105)

1: TOF MS ASAP+
8.44e+004

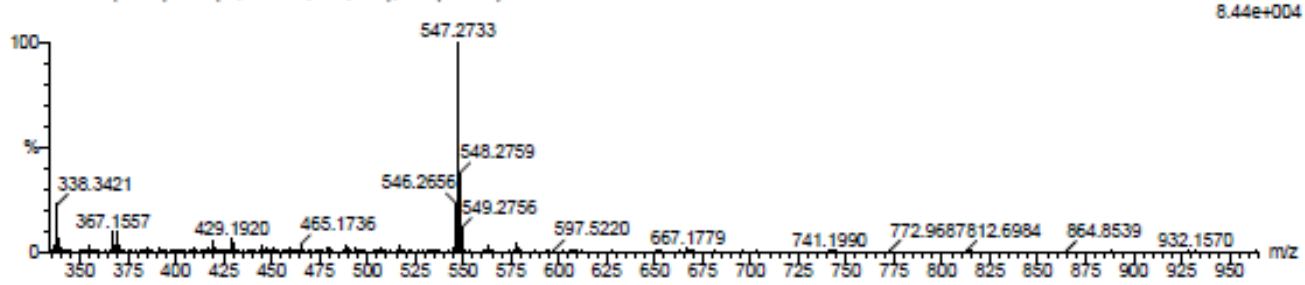


| | | | | | | | | |
|---|---|---|---|---|---|---|---|---|
| Minimum: | | | | -1.5 | | | | |
| Maximum: | | 5.0 | 2.0 | 50.0 | | | | |
| Mass | Calc. Mass | mDa | PPM | DBE | i-FIT | Norm | Conf(%) | Formula |
| 547.2733 | 547.2727 | 0.6 | 1.1 | 9.5 | 194.2 | 0.003 | 99.65 | C29 H43 O8 Si |
| | 547.2741 | -0.8 | -1.5 | 14.5 | 199.9 | 5.667 | 0.35 | C30 H39 N4 O4 Si Ion observed M+H |
| | 547.2732 | 0.1 | 0.2 | 5.5 | 205.6 | 11.337 | 0.00 | C21 H43 N6 O7 Si2 |
| | 547.2732 | 0.1 | 0.2 | 2.5 | 208.6 | 14.327 | 0.00 | C14 H39 N12 O9 Si |
| | 547.2731 | 0.2 | 0.4 | 8.5 | 209.3 | 15.100 | 0.00 | C28 H47 O5 Si3 |
| | 547.2728 | 0.5 | 0.9 | 17.5 | 210.0 | 15.749 | 0.00 | C20 H27 N20 |
| | 547.2736 | -0.3 | -0.5 | 1.5 | 210.4 | 16.197 | 0.00 | C13 H43 N12 O6 Si3 |
| | 547.2728 | 0.5 | 0.9 | 6.5 | 211.4 | 17.186 | 0.00 | C22 H39 N6 O10 |
| | 547.2741 | -0.8 | -1.5 | 11.5 | 211.6 | 17.363 | 0.00 | C23 H35 N10 O6 |
| | 547.2737 | -0.4 | -0.7 | -1.5 | 212.0 | 17.787 | 0.00 | C6 H39 N18 O8 Si2 |
| | 547.2733 | 0.0 | 0.0 | -0.5 | 213.7 | 19.427 | 0.00 | C7 H35 N18 O11 |

**Figure I.7**: MS spectrum of compound **6f.**

# J Spectroscopic data for compound 6g

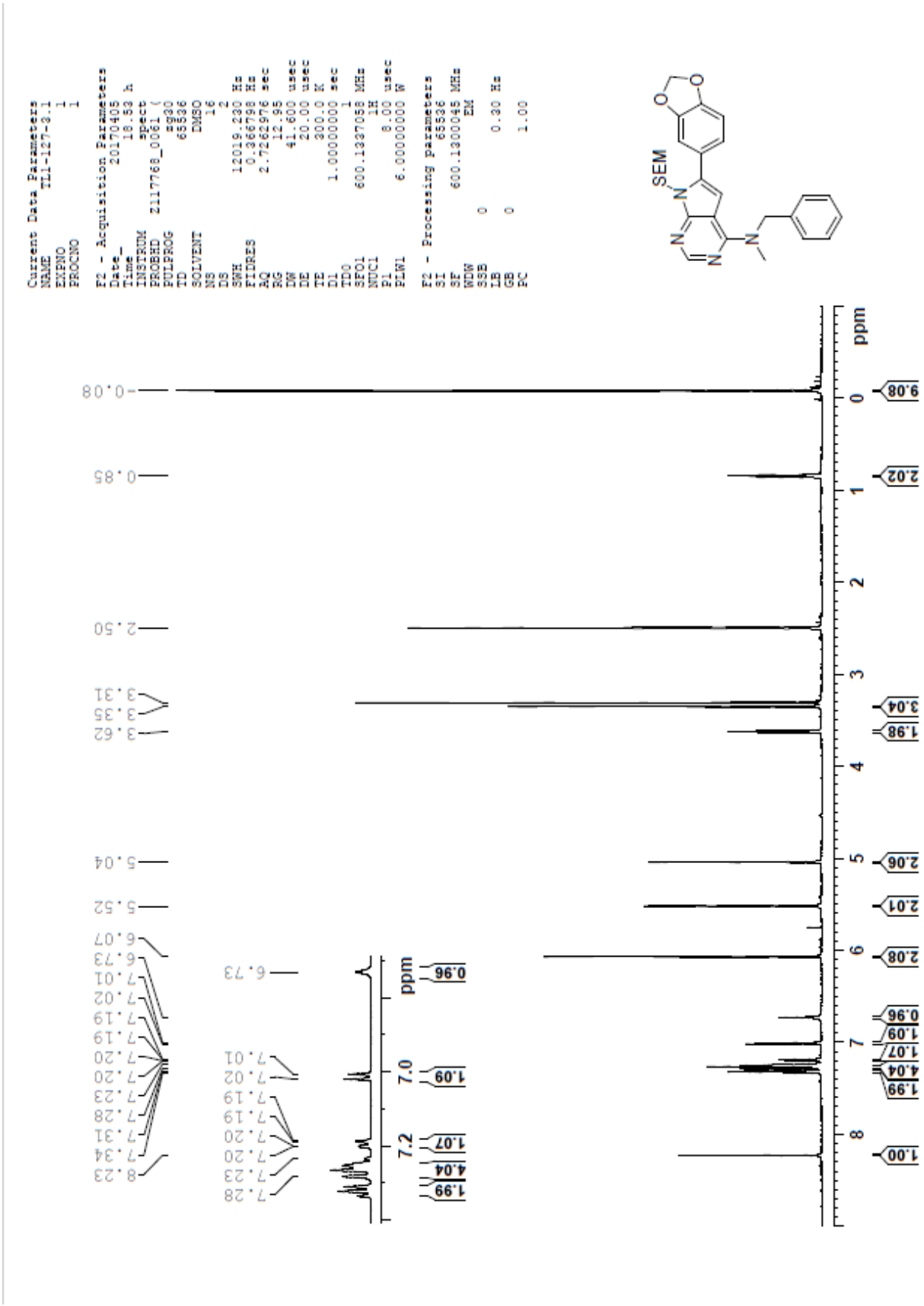


**Figure J.1**: $^{1}$H NMR spectrum of compound **6g.**

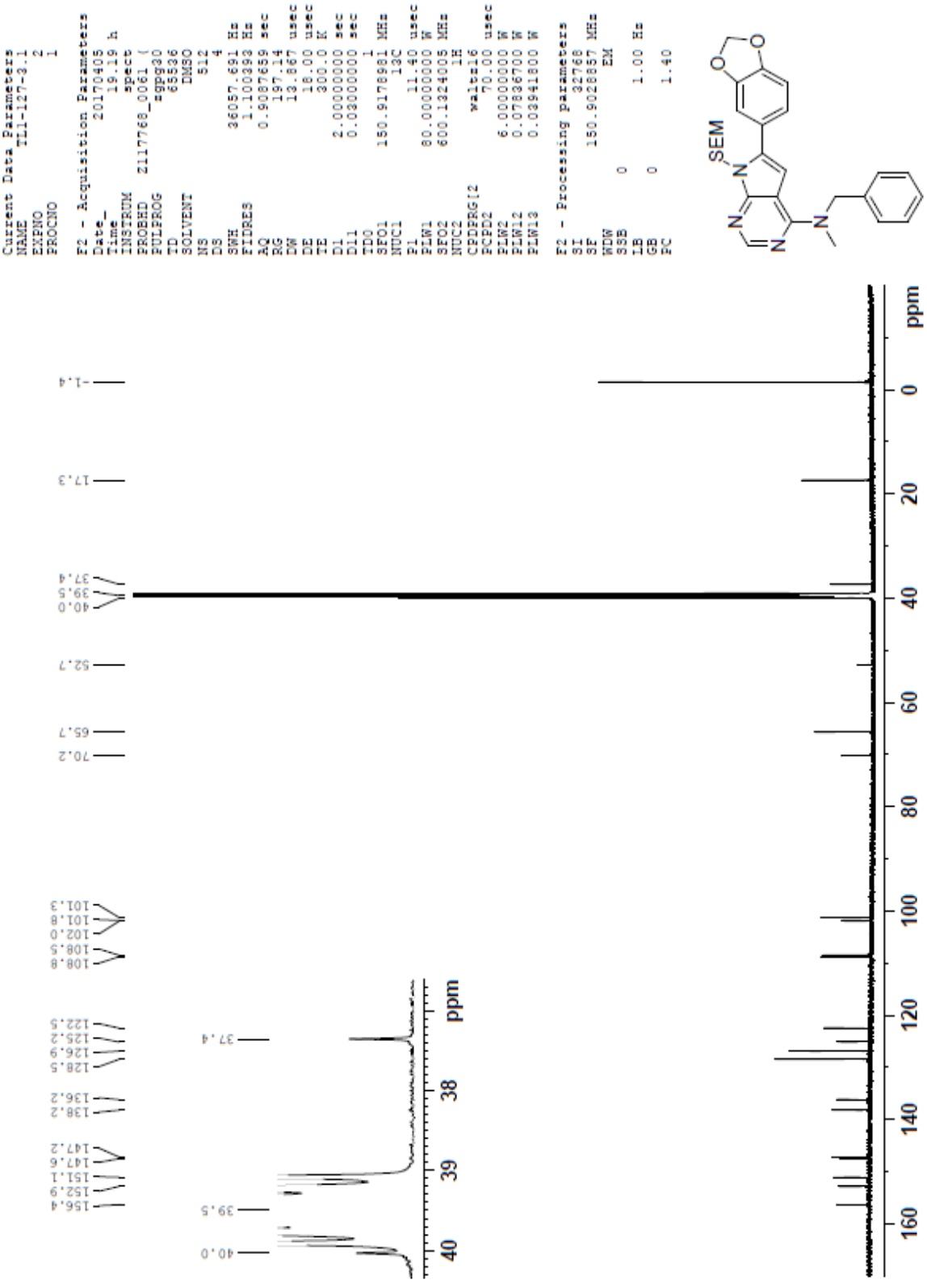


**Figure J.2**: $^{13}C$ NMR spectrum of compound **6g.**

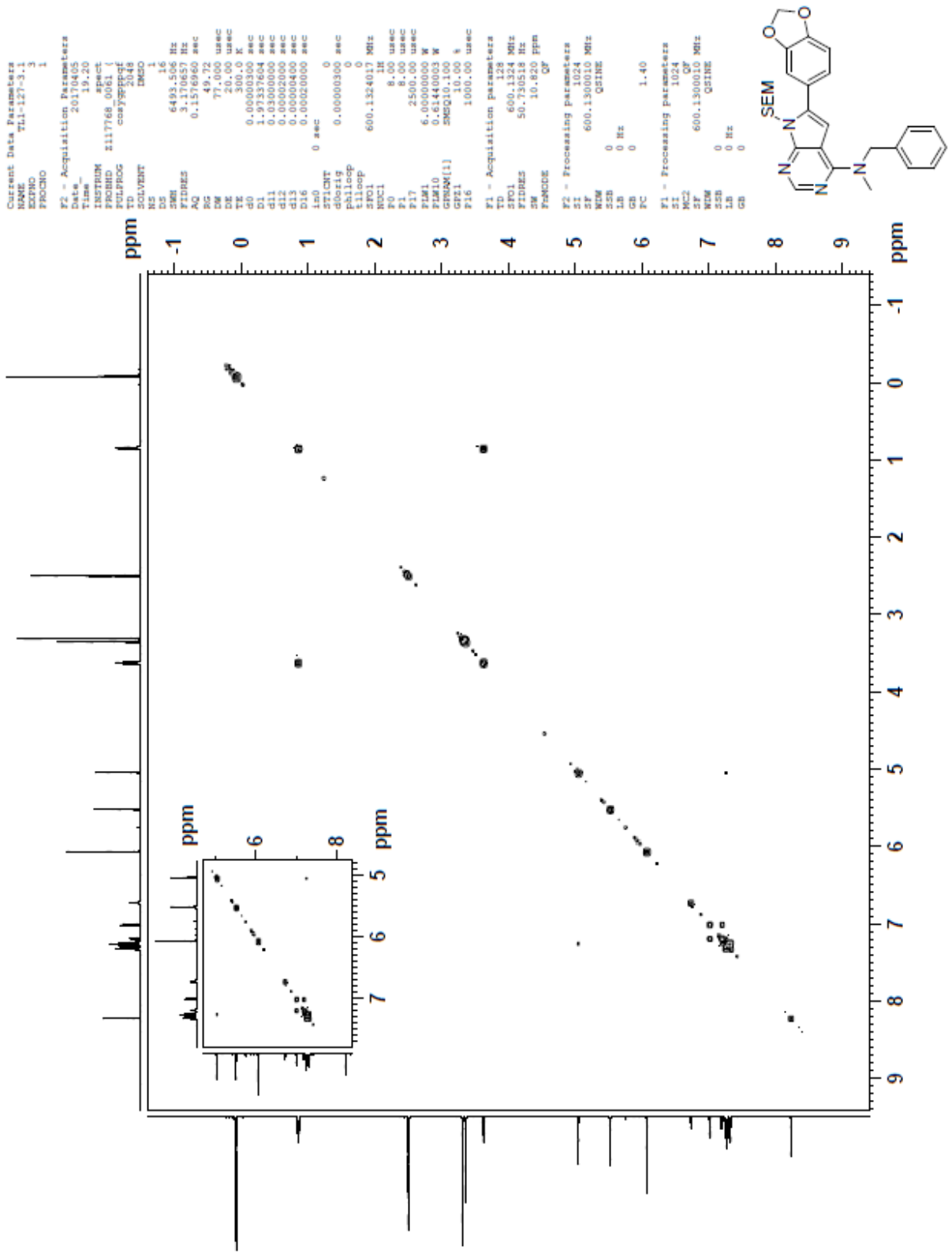


**Figure J.3**: COSY spectrum of compound **6g.**

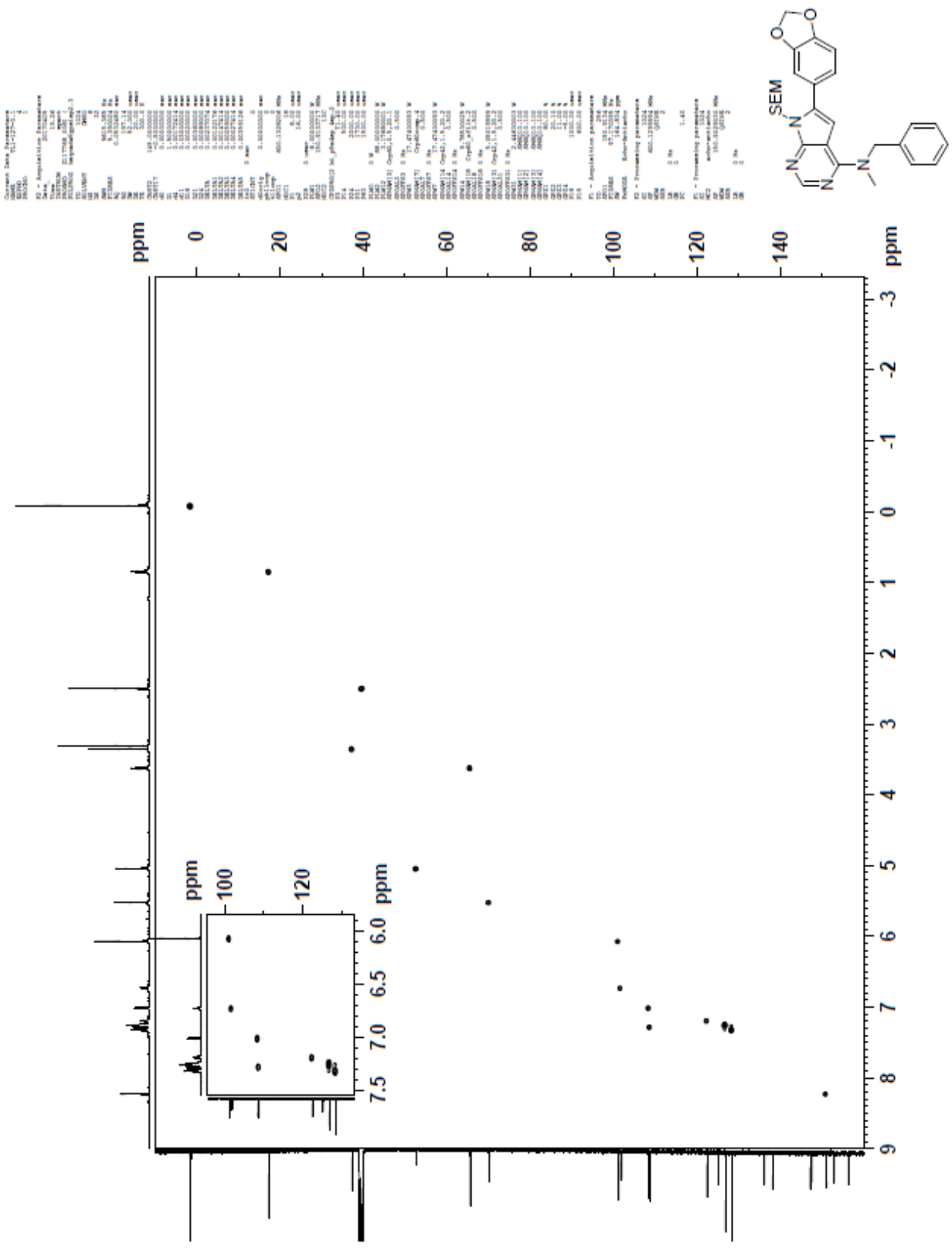


**Figure J.4**: HSQC spectrum of compound **6g.**

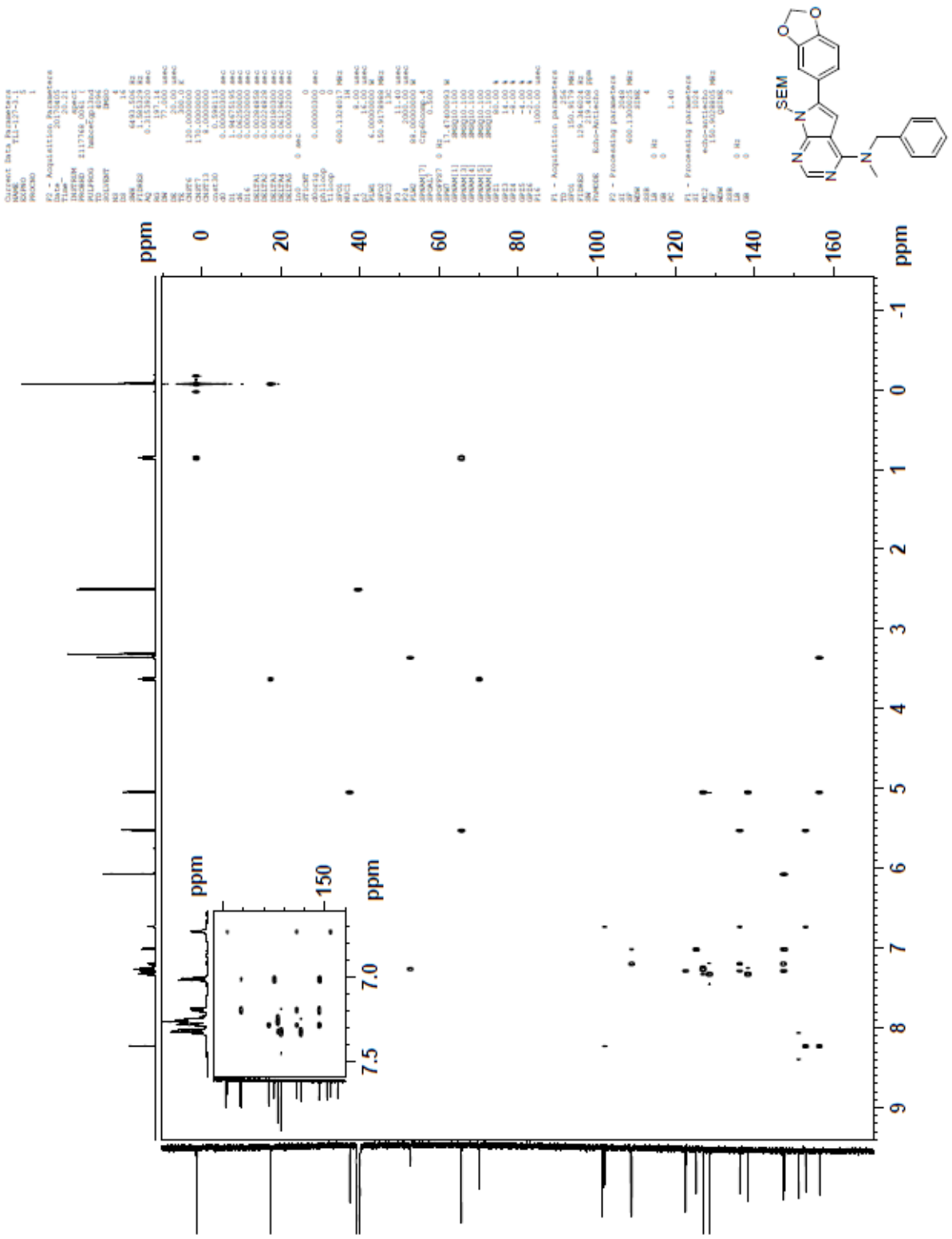


**Figure J.5**: HMBC spectrum of compound **6g**.

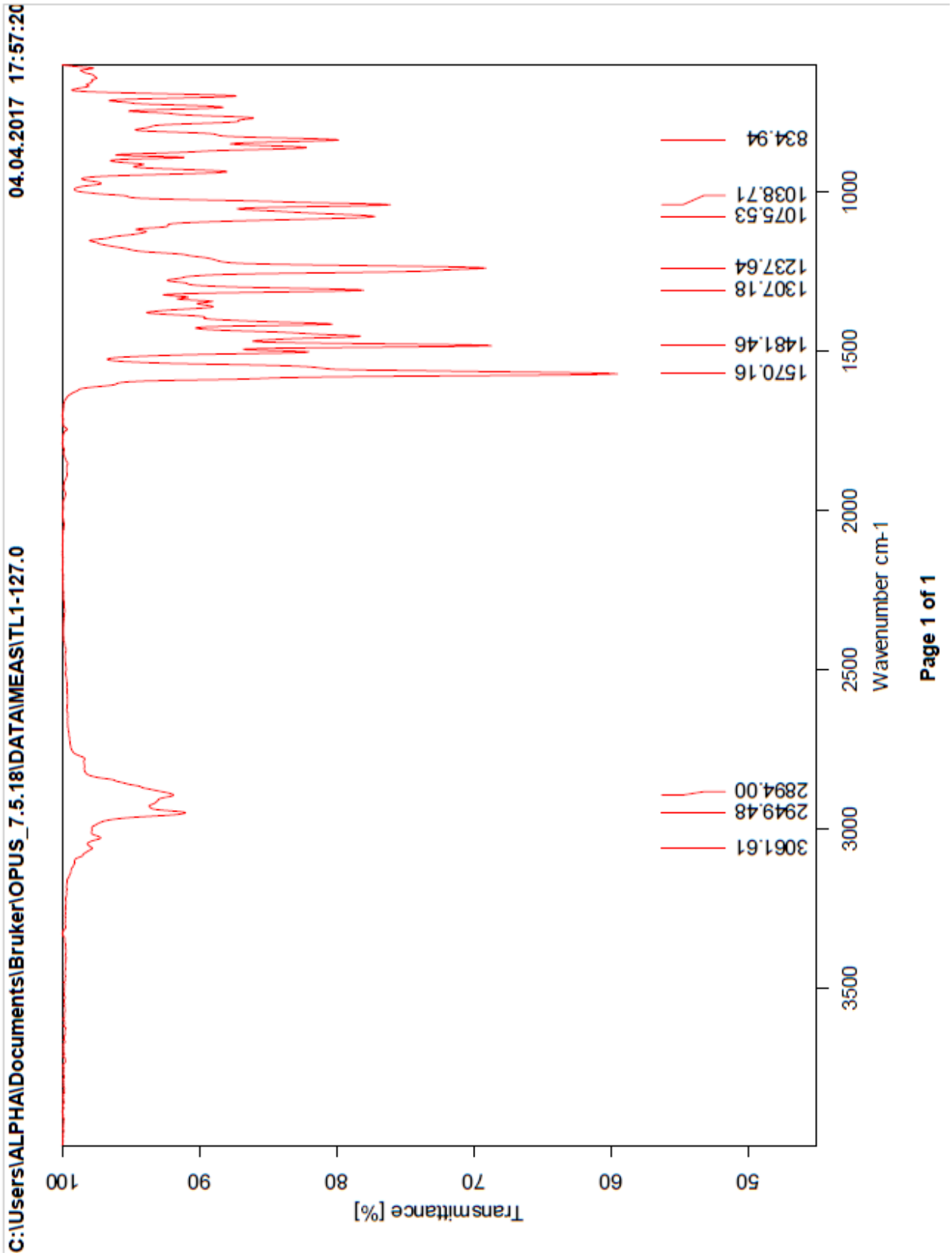


**Figure J.6**: IR spectrum of compound **6g.**

**Elemental Composition Report** Page 1

**Single Mass Analysis**
Tolerance = 2.0 PPM / DBE: min = -1.5, max = 50.0
Element prediction: Off
Number of isotope peaks used for i-FIT = 3

Monoisotopic Mass, Even Electron Ions
3880 formula(e) evaluated with 6 results within limits (all results (up to 1000) for each mass)
Elements Used:
C: 1-500 H: 1-1000 N: 0-10 O: 0-25 Si: 0-3
2017-195 120 (2.343) AM2 (Ar,35000.0,0.00,0.00); Cm (117:120)
1: TOF MS ASAP+

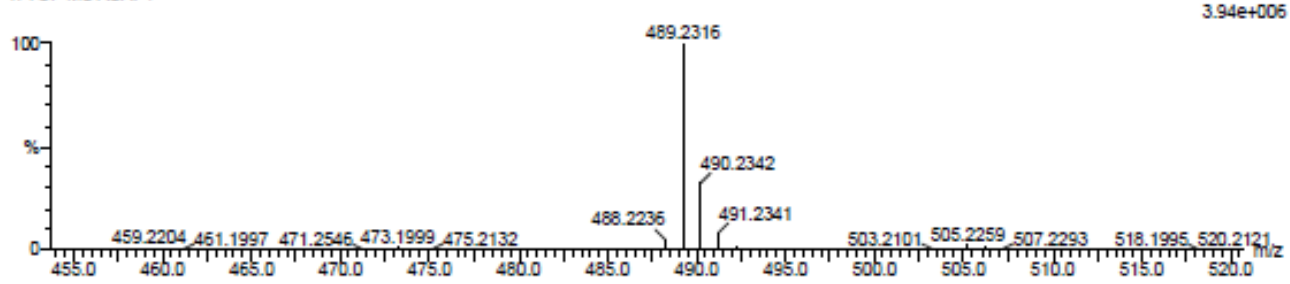


| | | | | | | | | |
|---|---|---|---|---|---|---|---|---|
| Minimum: | | | | -1.5 | | | | |
| Maximum: | | 2.0 | 2.0 | 50.0 | | | | |
| Mass | Calc. Mass | mDa | PPM | DBE | i-FIT | Norm | Conf(%) | Formula |
| 489.2316 | 489.2322 | -0.6 | -1.2 | 14.5 | 1124.4 | 0.937 | 39.16 | C27 H33 N4 O3 Si ion observed [M+H] |
| | 489.2309 | 0.7 | 1.4 | 9.5 | 1124.0 | 0.499 | 60.74 | C26 H37 O7 Si |
| | 489.2313 | 0.3 | 0.6 | 8.5 | 1133.9 | 10.385 | 0.00 | C25 H41 O4 Si3 |
| | 489.2322 | -0.6 | -1.2 | 11.5 | 1131.7 | 8.198 | 0.03 | C20 H29 N10 O5 |
| | 489.2309 | 0.7 | 1.4 | 6.5 | 1131.7 | 8.235 | 0.03 | C19 H33 N6 O9 |
| | 489.2313 | 0.3 | 0.6 | 5.5 | 1131.2 | 7.742 | 0.04 | C18 H37 N6 O6 Si2 |

**Figure J.7**: MS spectrum of compound **6g.**

# K Spectroscopic data for compound 6h

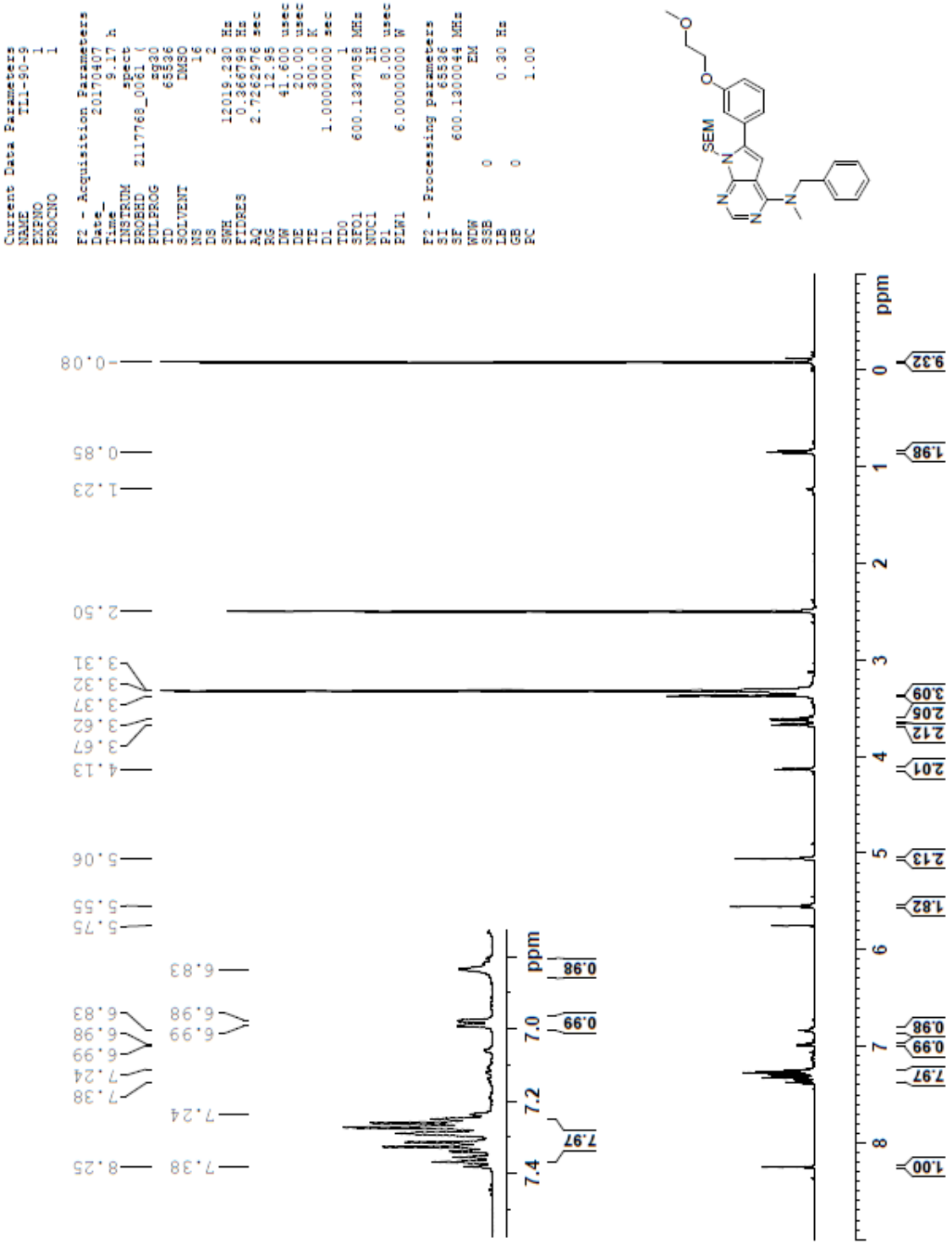


**Figure K.1**: $^{1}$H NMR spectrum of compound **6h.**

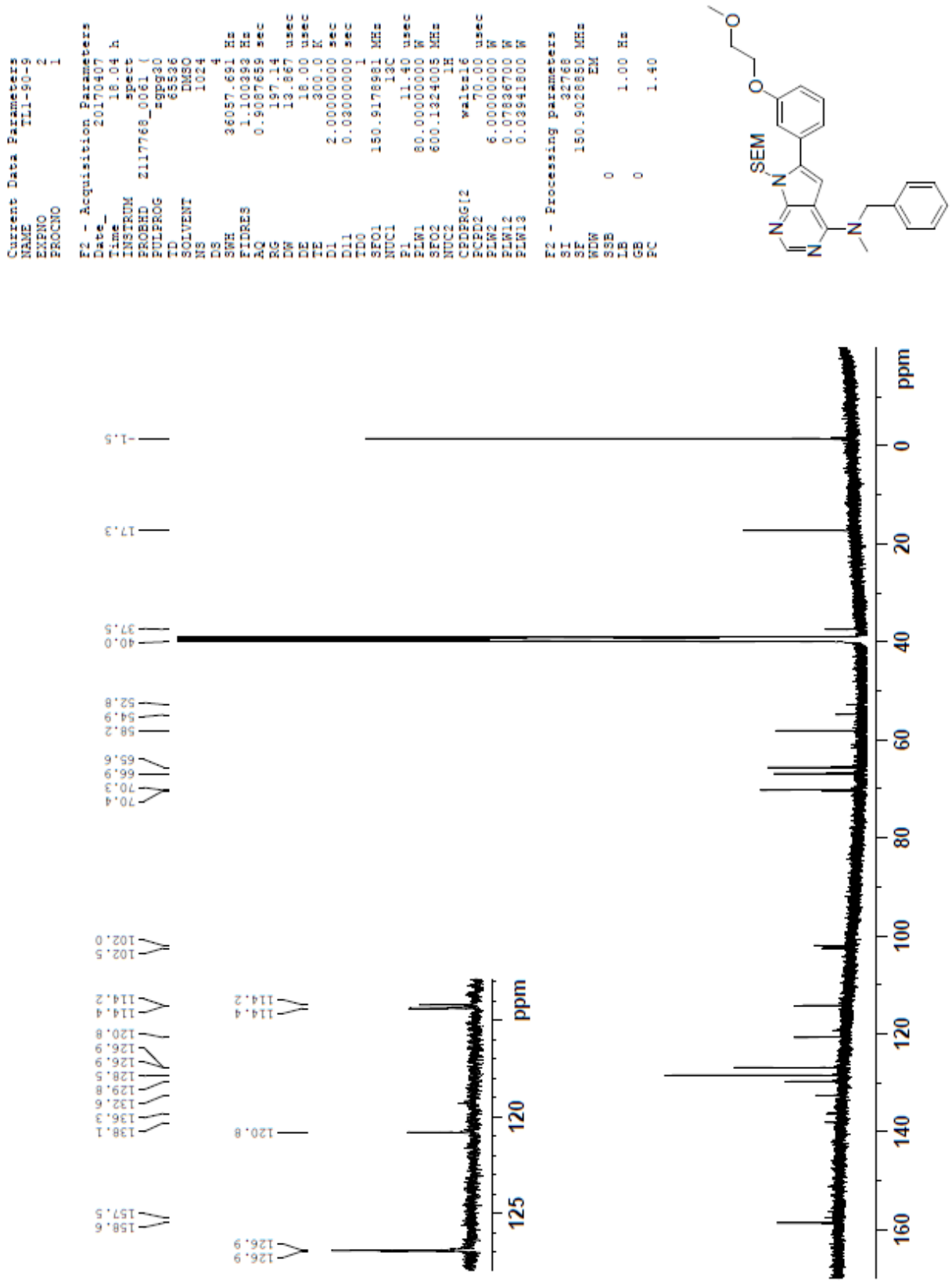


**Figure K.2**: $^{13}C$ NMR spectrum of compound **6h.**

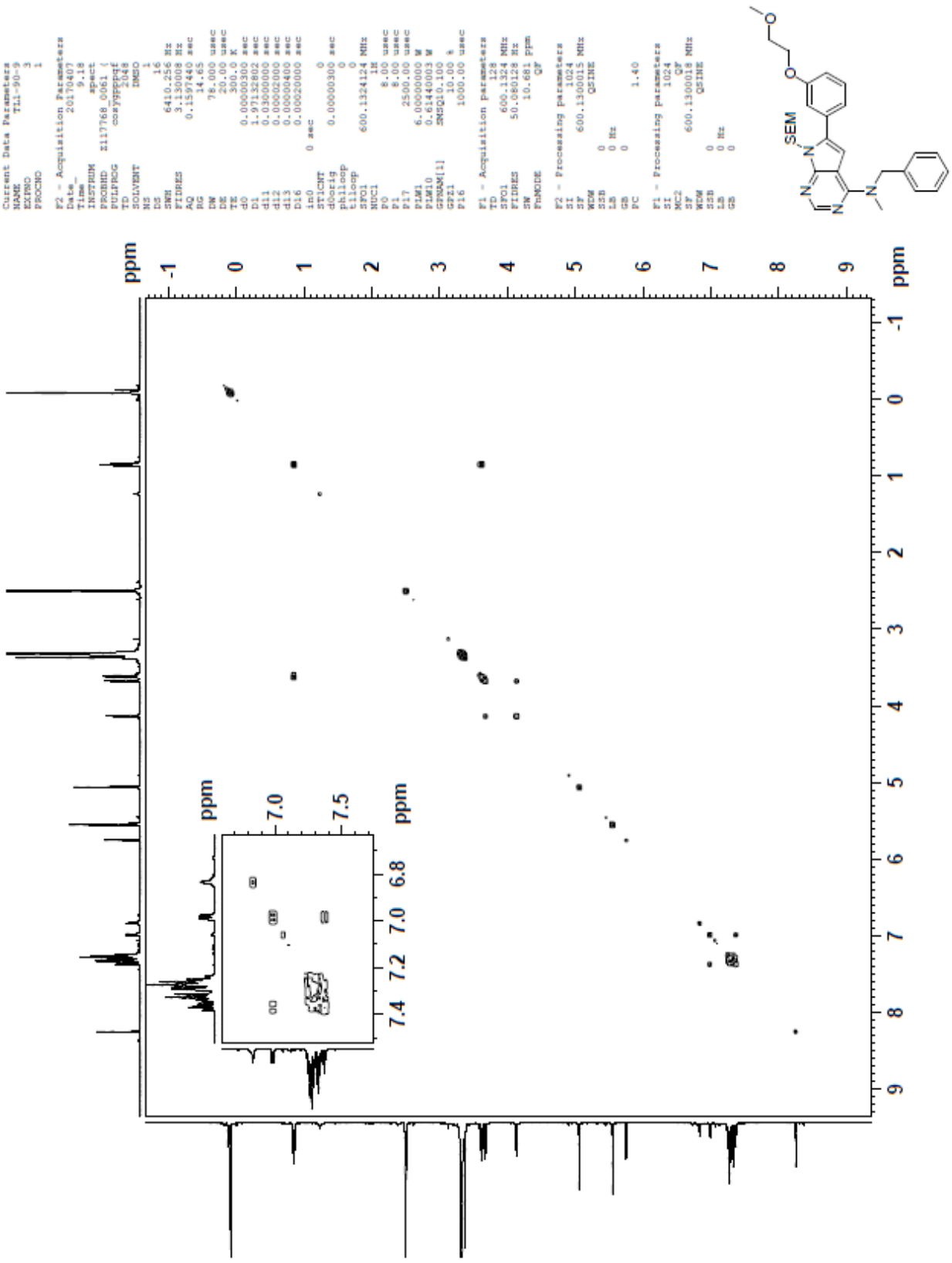


**Figure K.3**: COSY spectrum of compound **6h.**

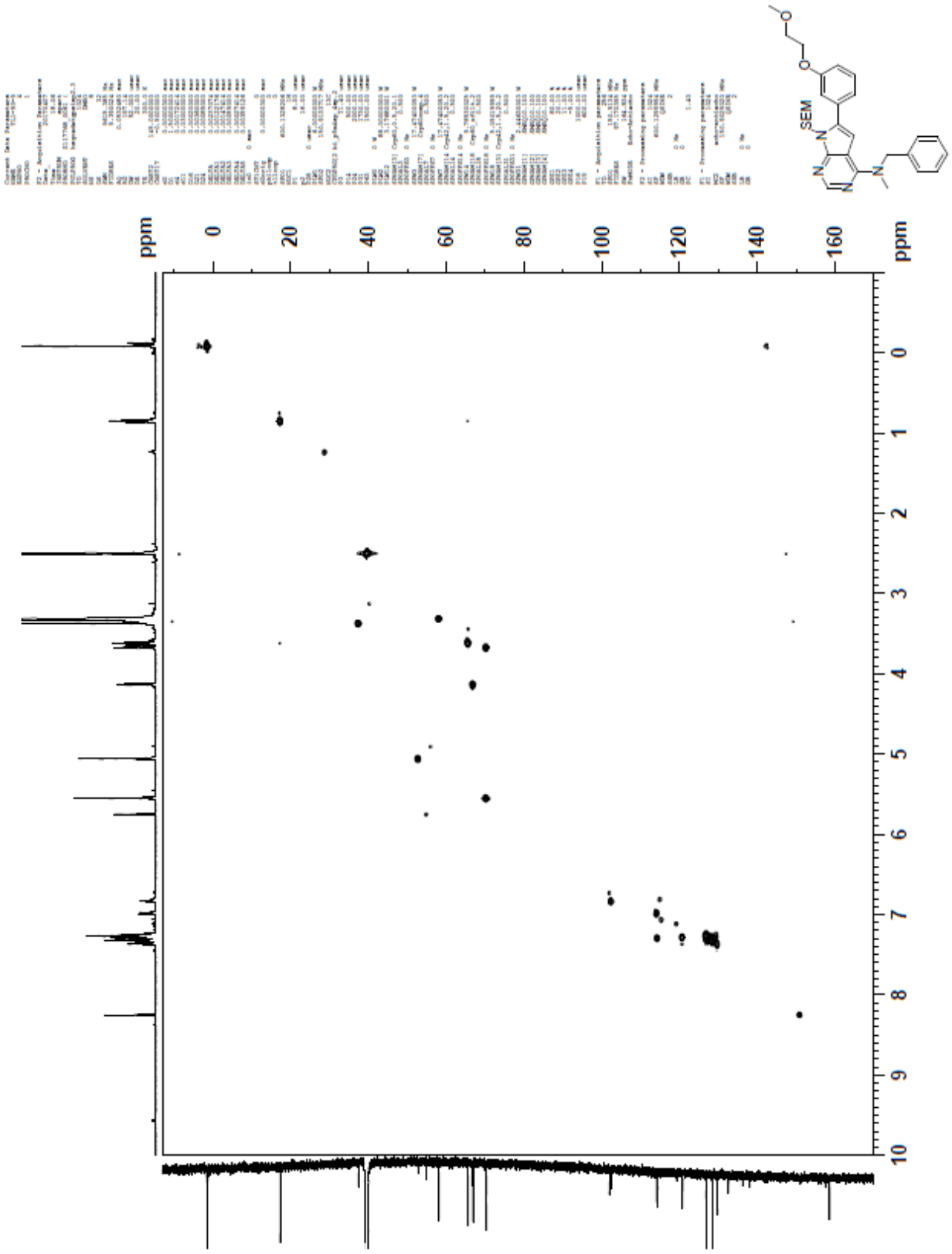


**Figure K.4**: HSQC spectrum of compound **6h.**

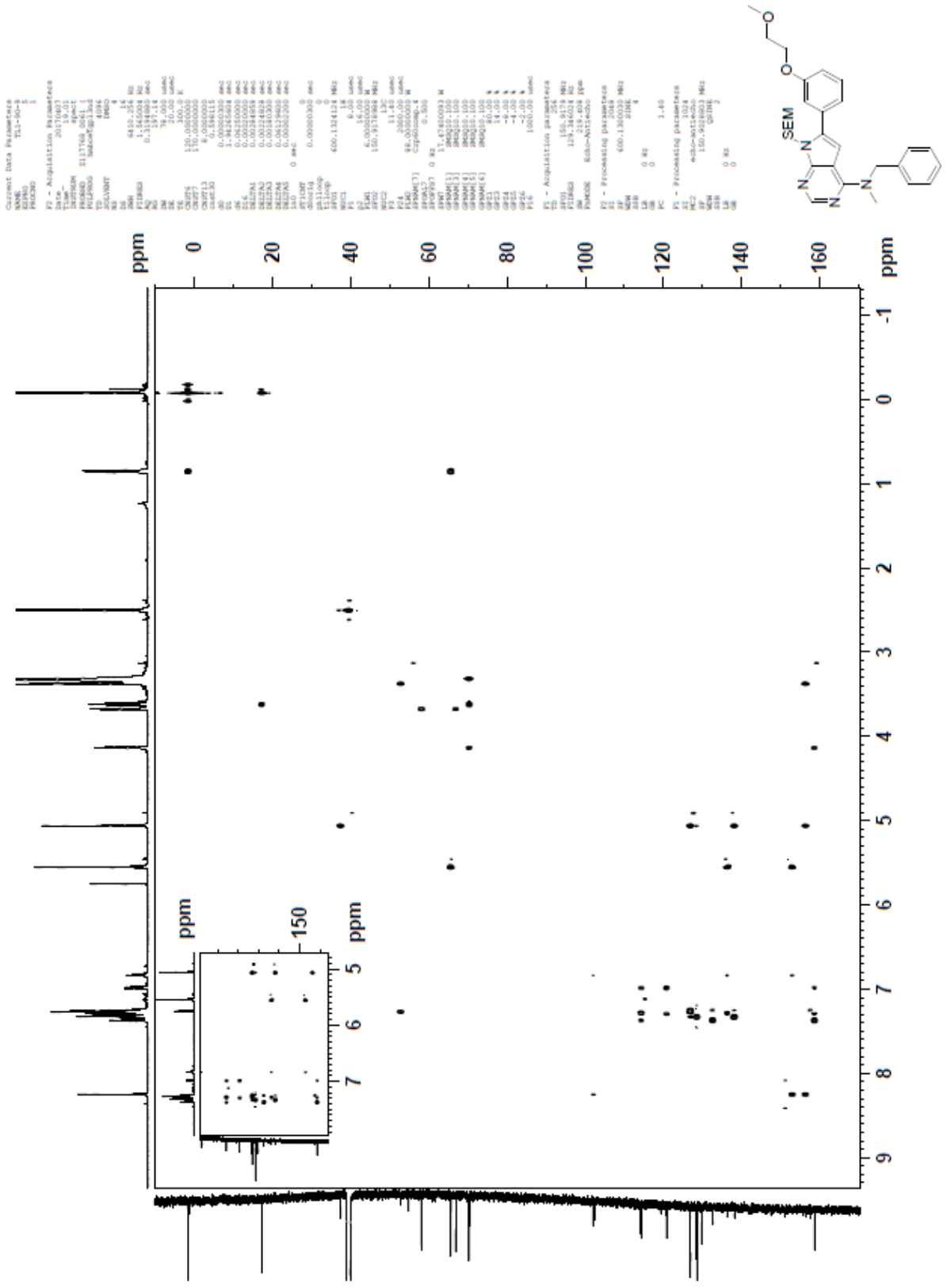


**Figure K.5**: HMBC spectrum of compound **6h**.

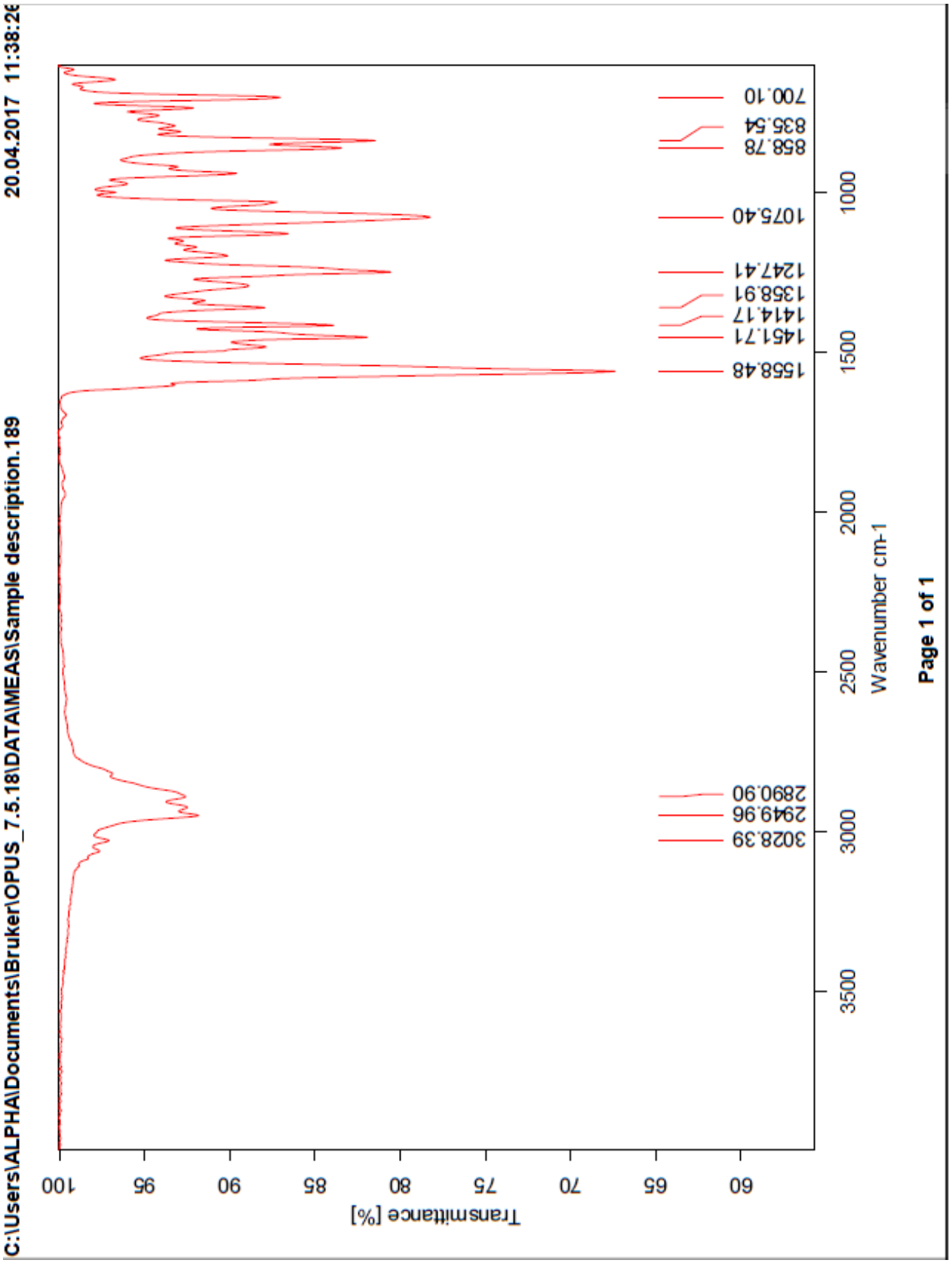


**Figure K.6**: IR spectrum of compound **6h.**

## Elemental Composition Report



### Single Mass Analysis

Tolerance = 2.0 PPM / DBE: min = -1.5, max = 50.0
Element prediction: Off
Number of isotope peaks used for i-FIT = 3

Monoisotopic Mass, Even Electron Ions
13414 formula(e) evaluated with 18 results within limits (all results (up to 1000) for each mass)
Elements Used:
C: 3-100 H: 0-1000 11B: 0-1 N: 0-20 O: 0-25 Si: 0-3

NT-MSLAB-Operator-SVG
2017-218 293 (5.703) AM2 (Ar,35000.0,0.00,0.00); Cm (293:296)

1: TOF MS ASAP+
1.73e+007

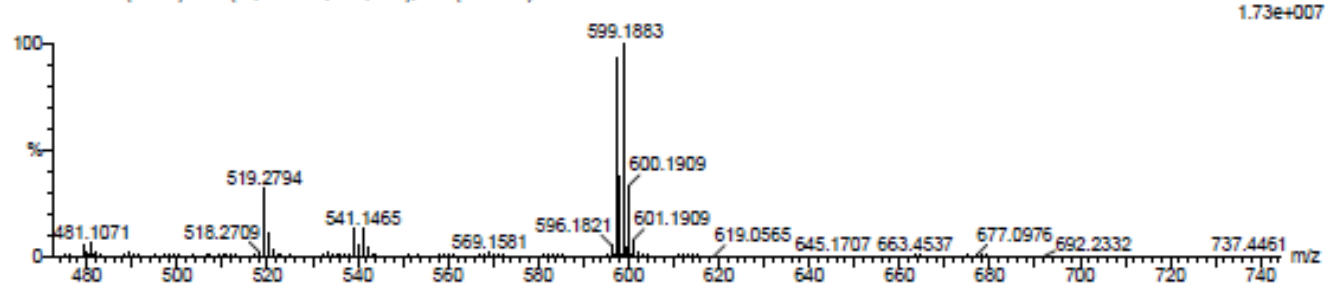


| | | | | | | | | |
|---|---|---|---|---|---|---|---|---|
| Minimum: | | | | -1.5 | | | | |
| Maximum: | | 5.0 | 2.0 | 50.0 | | | | |
| Mass | Calc. Mass | mDa | PPM | DBE | i-FIT | Norm | Conf(%) | Formula |
| 519.2794 | 519.2797 | -0.3 | -0.6 | 14.5 | 1073.8 | 0.039 | 96.16 | C21 H32 11B N14 Si |
| | 519.2797 | -0.3 | -0.6 | 3.5 | 1077.4 | 3.667 | 2.55 | C23 H44 11B O10 Si |
| | 519.2791 | 0.3 | 0.6 | 13.5 | 1078.2 | 4.376 | 1.26 | C29 H39 N4 O3 Si Ion observed [M+H] |
| | 519.2796 | -0.2 | -0.4 | 6.5 | 1083.3 | 9.571 | 0.01 | C14 H35 N16 O4 Si |
| | 519.2792 | 0.2 | 0.4 | 18.5 | 1083.4 | 9.630 | 0.01 | C29 H32 11B N8 O |
| | 519.2796 | -0.2 | -0.4 | 9.5 | 1084.3 | 10.553 | 0.00 | C21 H39 N10 O2 Si2 |
| | 519.2801 | -0.7 | -1.3 | -0.5 | 1084.5 | 10.741 | 0.00 | C15 H44 11B N6 O9 Si2 |
| | 519.2797 | -0.3 | -0.6 | 11.5 | 1085.0 | 11.248 | 0.00 | C14 H28 11B N20 O2 |
| | 519.2792 | 0.2 | 0.4 | 10.5 | 1085.0 | 11.272 | 0.00 | C22 H35 N10 O5 |
| | 519.2800 | -0.6 | -1.2 | 22.5 | 1085.9 | 12.119 | 0.00 | C38 H35 N2 |
| | 519.2788 | 0.6 | 1.2 | 5.5 | 1086.0 | 12.218 | 0.00 | C12 H36 11B N16 O3 Si2 |
| | 519.2801 | -0.7 | -1.3 | 2.5 | 1086.6 | 12.839 | 0.00 | C22 H48 11B O7 Si3 |
| | 519.2784 | 1.0 | 1.9 | 6.5 | 1086.7 | 12.893 | 0.00 | C13 H32 11B N16 O6 |
| | 519.2796 | -0.2 | -0.4 | 12.5 | 1086.7 | 12.954 | 0.00 | C28 H43 N4 Si3 |
| | 519.2797 | -0.3 | -0.6 | 0.5 | 1087.2 | 13.446 | 0.00 | C16 H40 11B N6 O12 |
| | 519.2801 | -0.7 | -1.3 | 5.5 | 1088.0 | 14.196 | 0.00 | C13 H39 N16 O Si3 |
| | 519.2787 | 0.7 | 1.3 | 8.5 | 1088.4 | 14.641 | 0.00 | C19 H40 11B N10 O Si3 |
| | 519.2787 | 0.7 | 1.3 | 0.5 | 1088.7 | 14.902 | 0.00 | C12 H43 N12 O5 Si3 |

**Figure K.7**: MS spectrum of compound **6h.**

# L Spectroscopic data for compound 7a

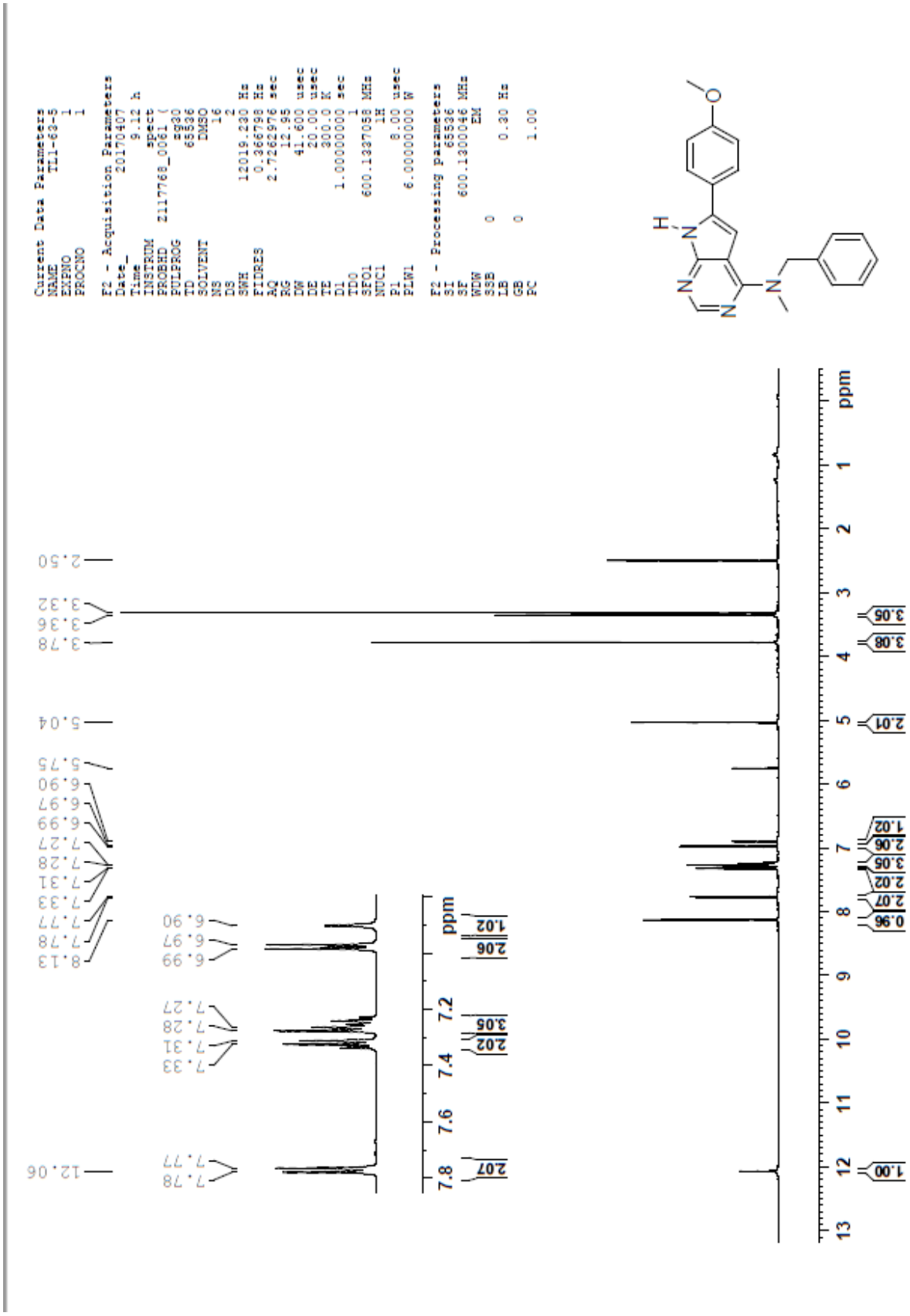

**Figure L.1**: $^{1}$H NMR spectrum of compound **7a.**

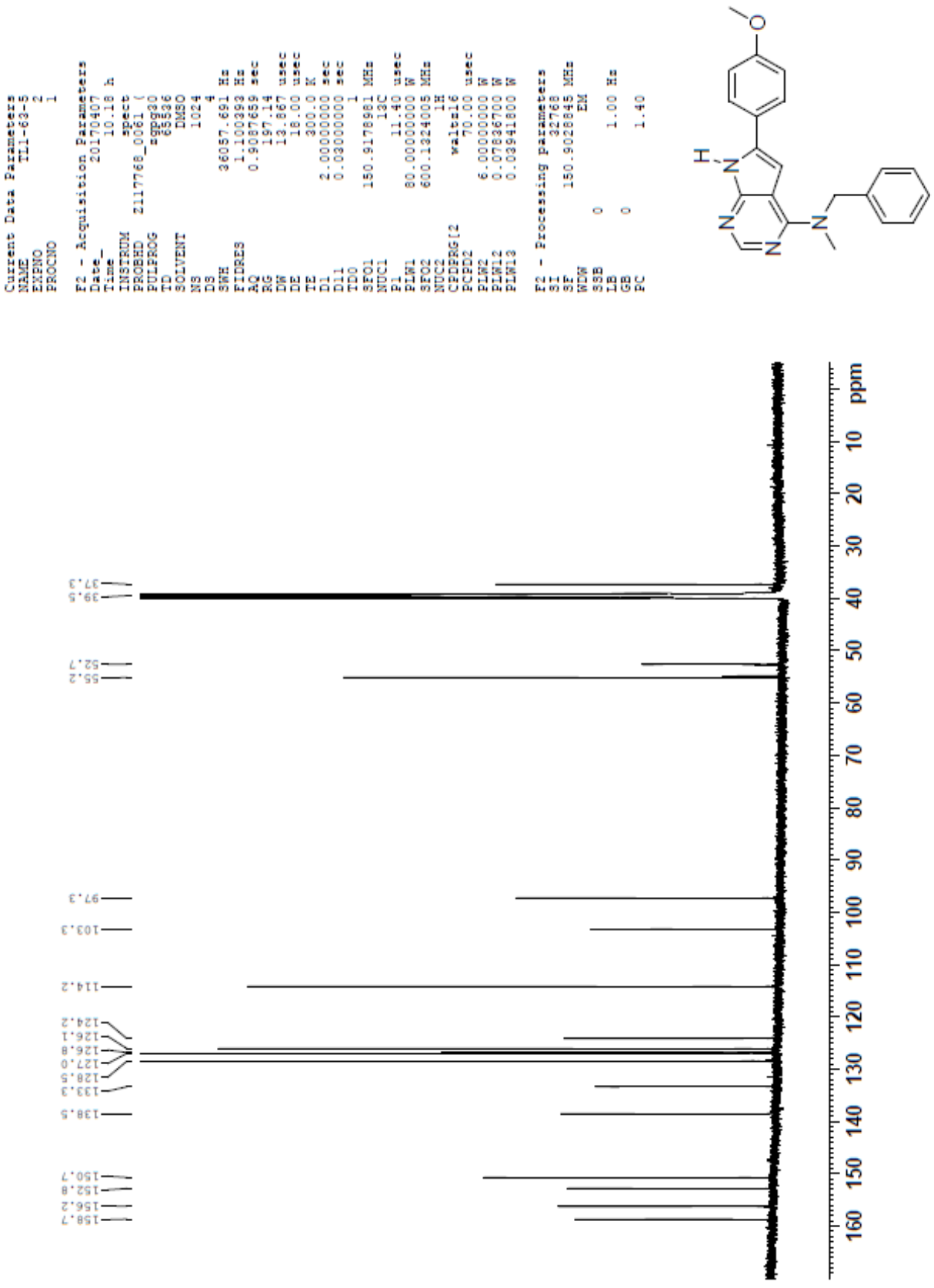


**Figure L.2**: $^{13}C$ NMR spectrum of compound **7a.**

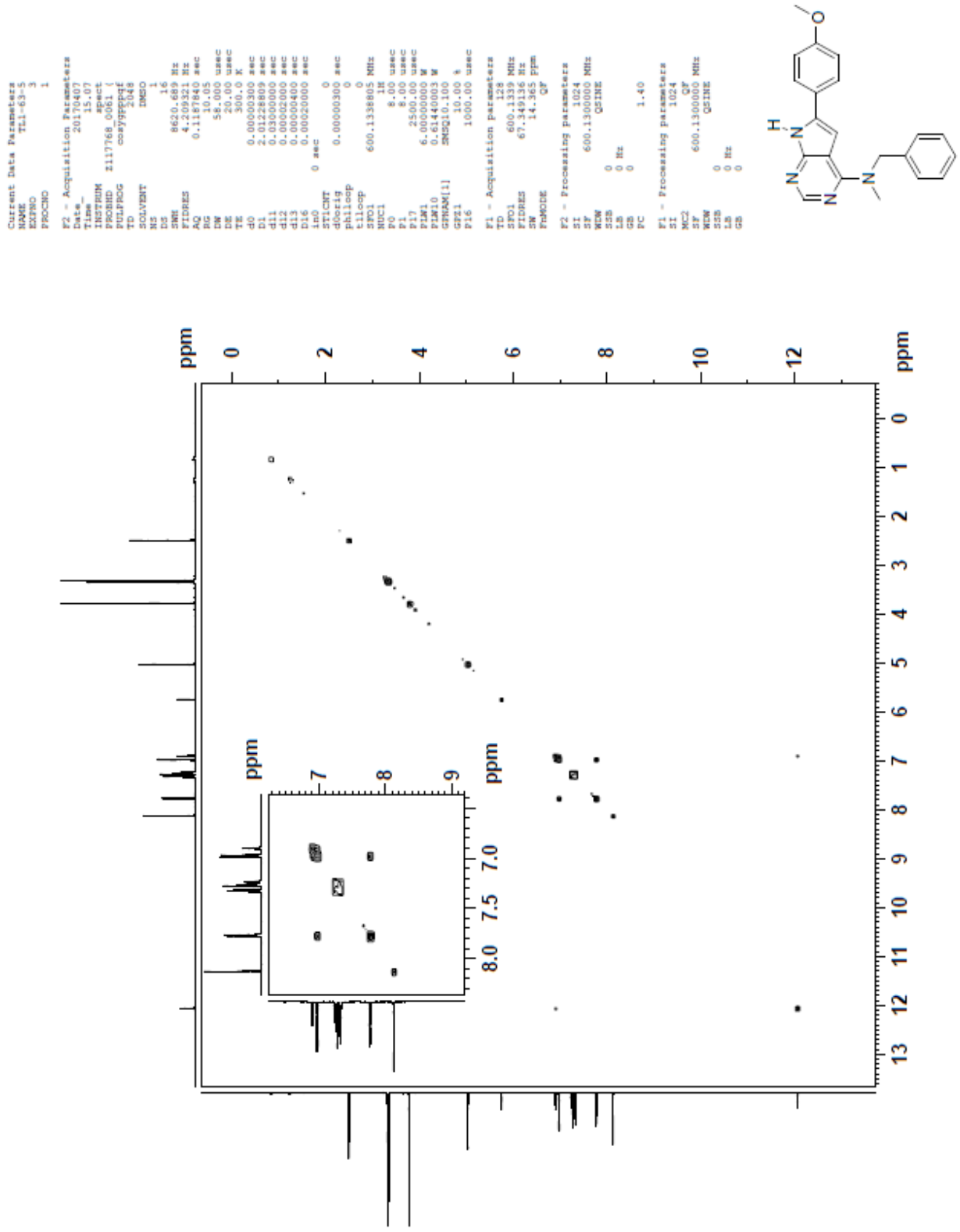

**Figure L.3**: COSY spectrum of compound **7a.**

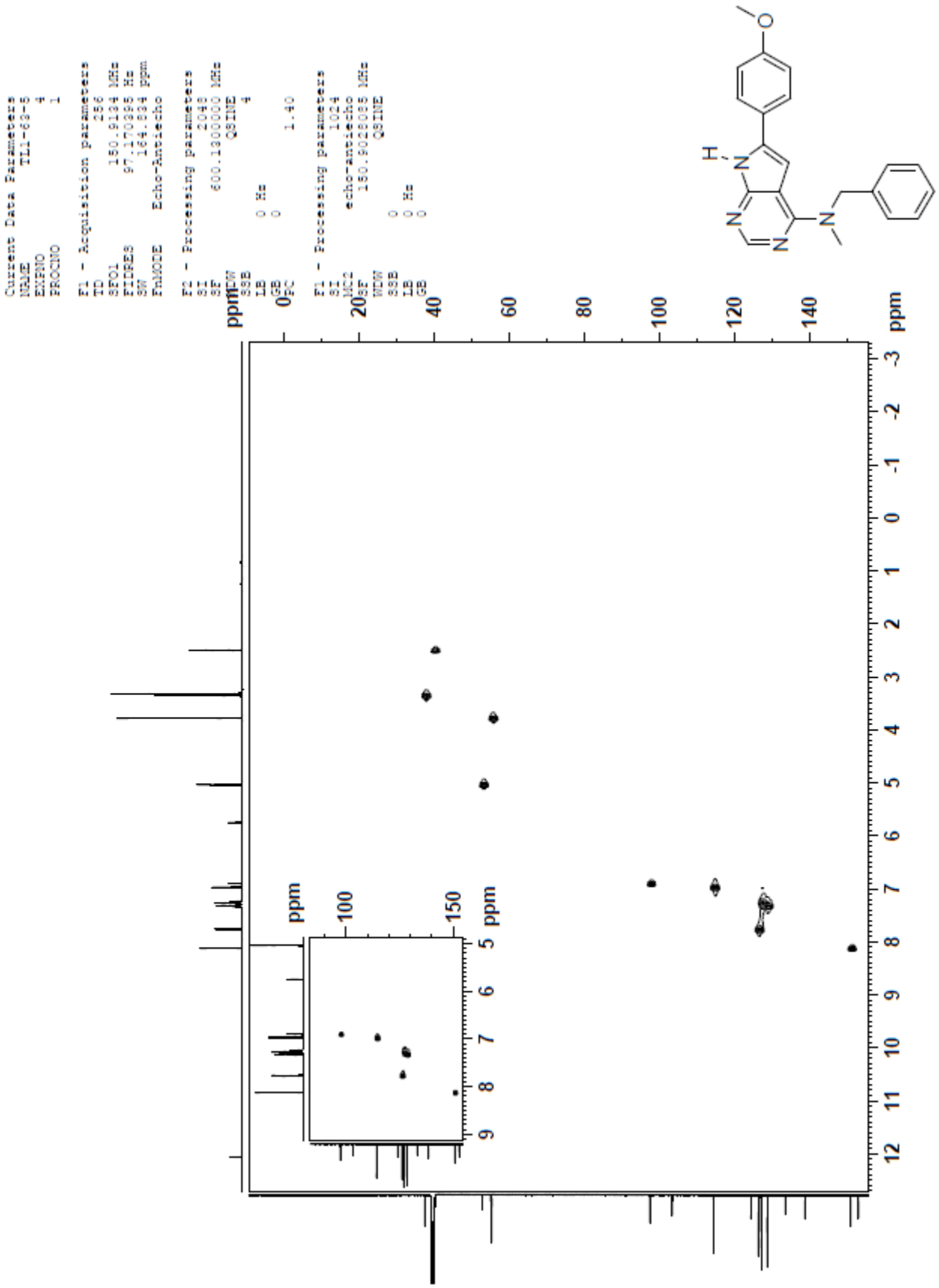


**Figure L.4**: HSQC spectrum of compound **7a.**

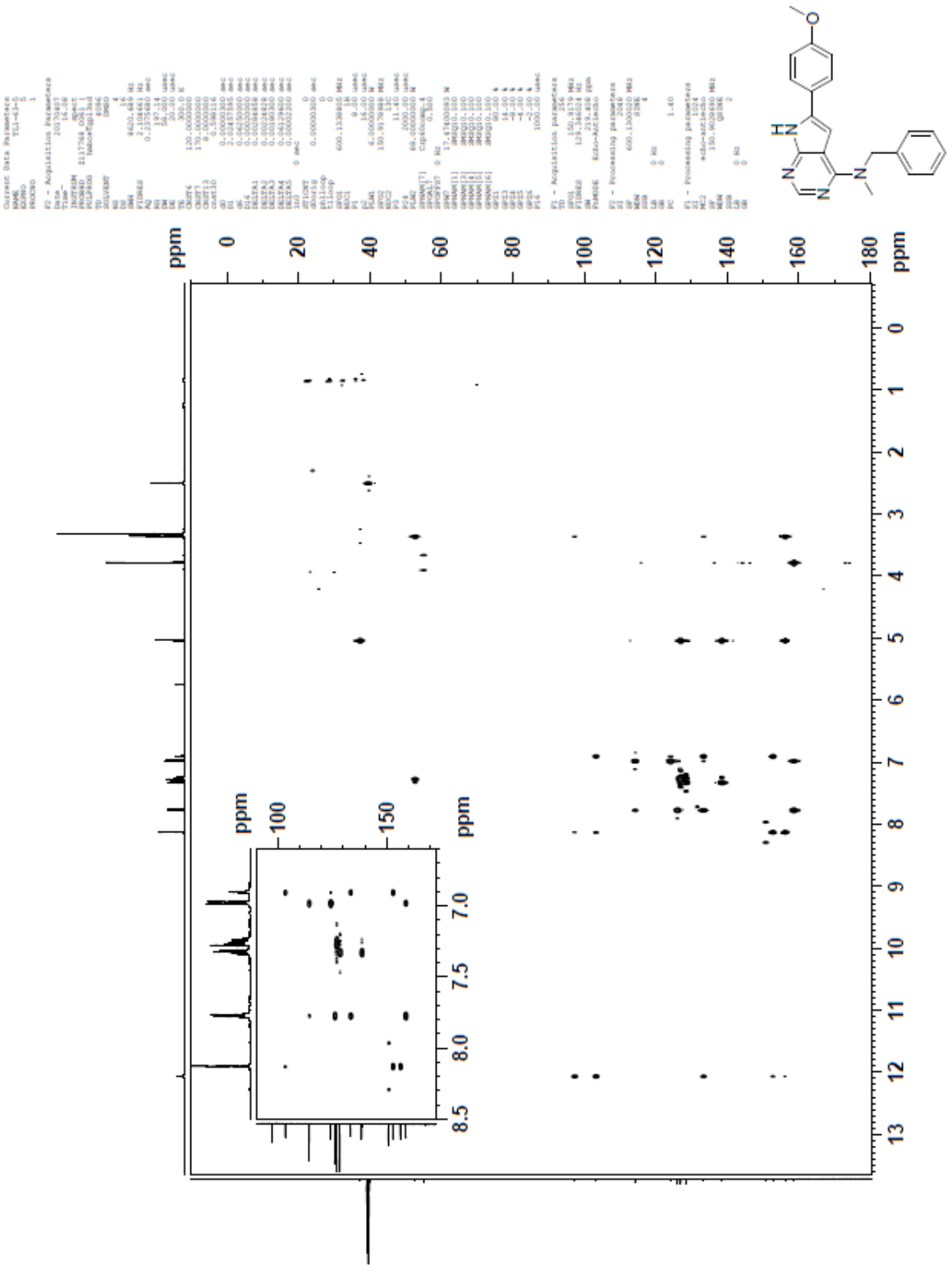

**Figure L.5**: HMBC spectrum of compound **7a**.

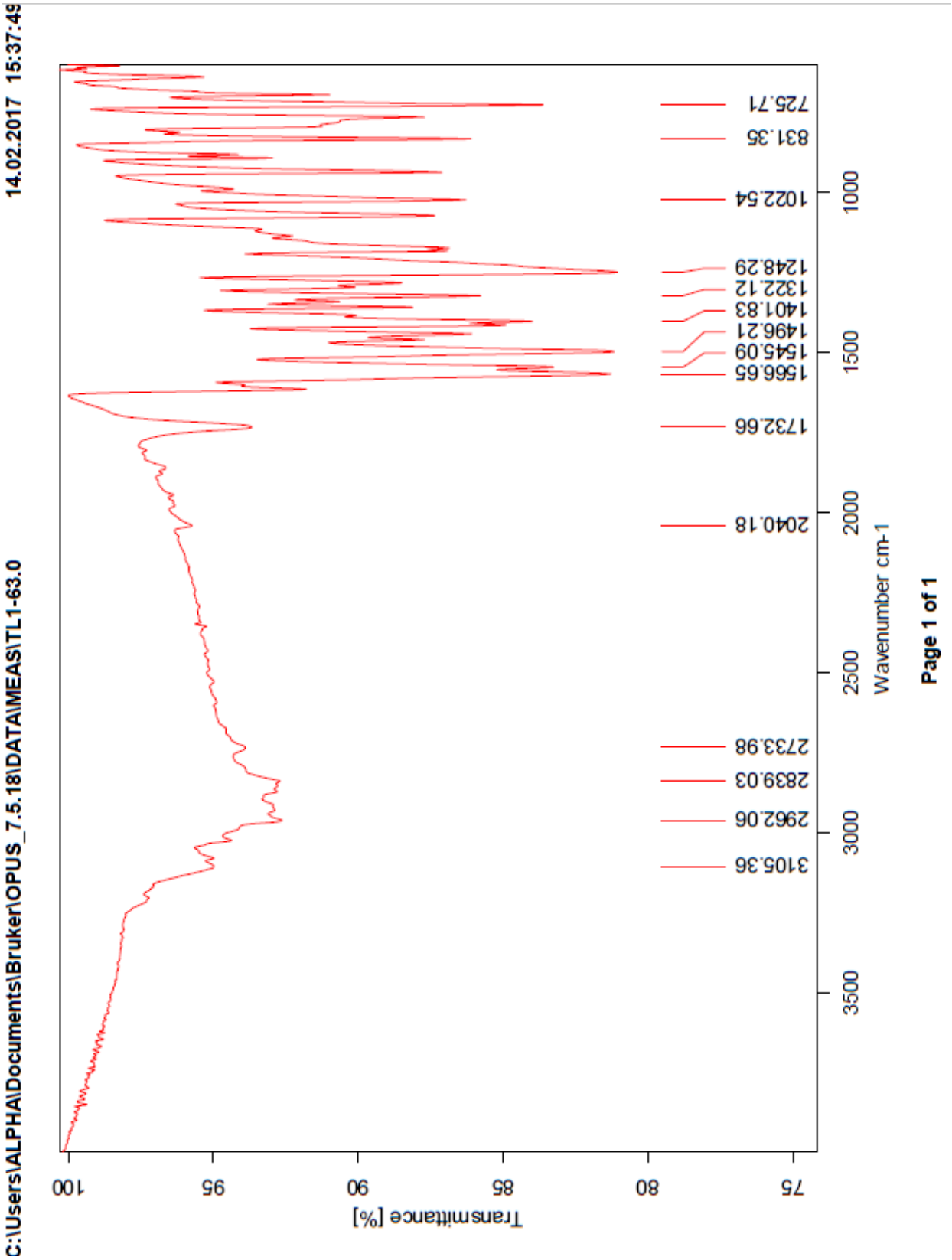


**Figure L.6**: IR spectrum of compound **7a.**

**Elemental Composition Report** Page 1

**Single Mass Analysis**
Tolerance = 2.0 PPM / DBE: min = -1.5, max = 50.0
Element prediction: Off
Number of isotope peaks used for i-FIT = 3

Monoisotopic Mass, Even Electron Ions
445 formula(e) evaluated with 1 results within limits (all results (up to 1000) for each mass)
Elements Used:
C: 1-500 H: 1-1000 N: 1-10 O: 1-25
2017-91 178 (3.482) AM2 (Ar,35000.0,0.00,0.00); Cm (178:180)
1: TOF MS ASAP+

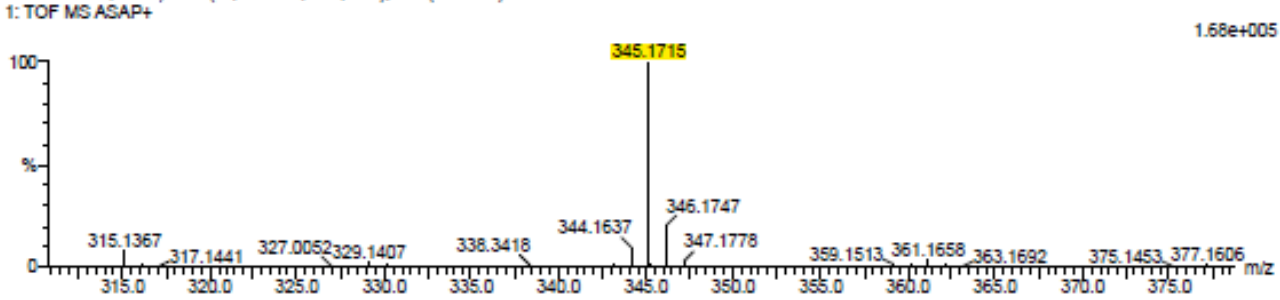


| | | | | | | | | |
|---|---|---|---|---|---|---|---|---|
| Minimum: | | | | -1.5 | | | | |
| Maximum: | | 2.0 | 2.0 | 50.0 | | | | |
| Mass | Calc. Mass | mDa | PPM | DBE | i-FIT | Norm | Conf(%) | Formula |
| 345.1715 | 345.1715 | 0.0 | 0.0 | 13.5 | 755.7 | n/a | n/a | C21 H21 N4 O ion observed [M+H] |

**Figure L.7**: MS spectrum of compound **7a.**

# M Spectroscopic data for compound 7b

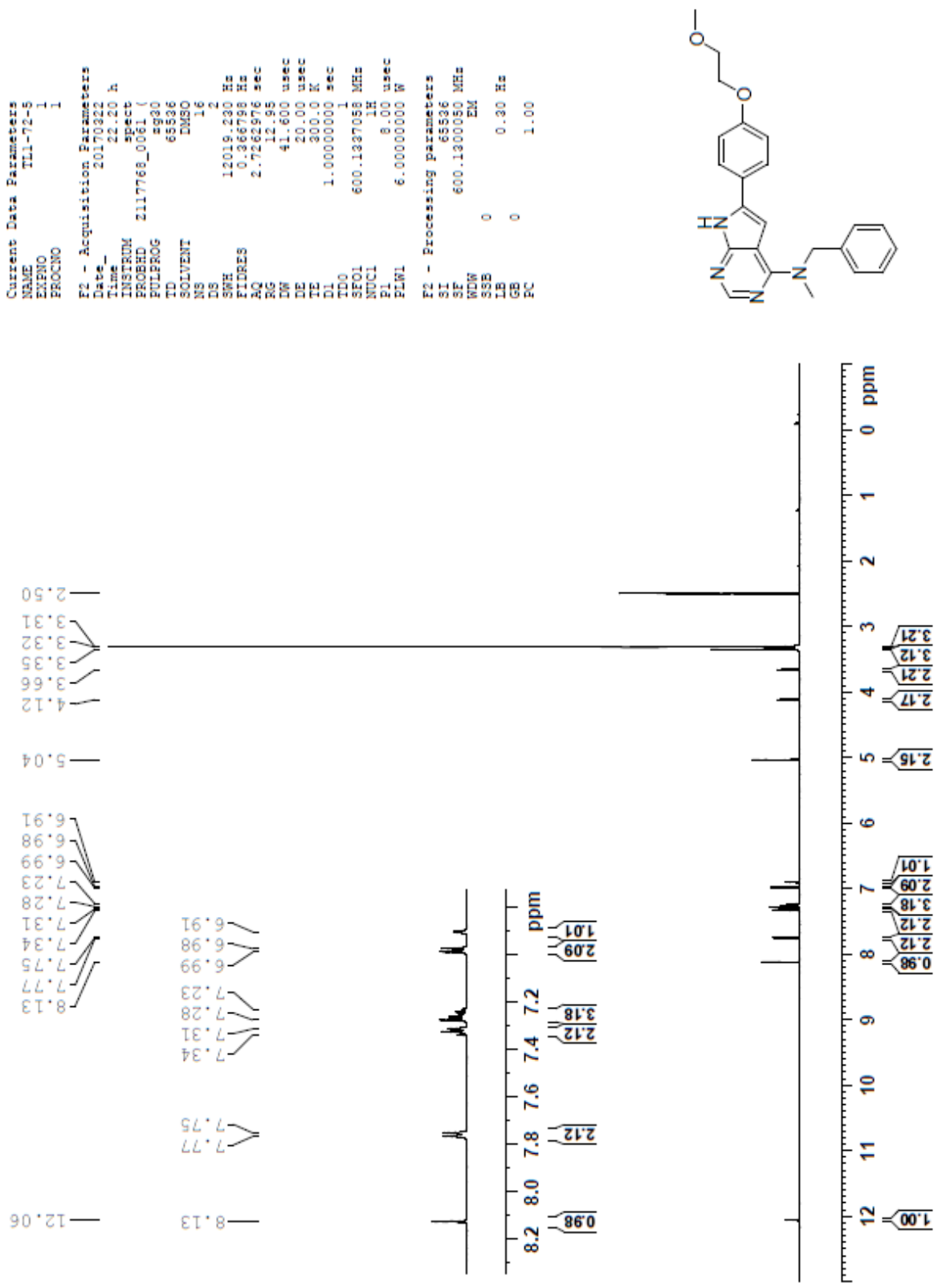


**Figure M.1**: $^{1}$H NMR spectrum of compound **7b.**

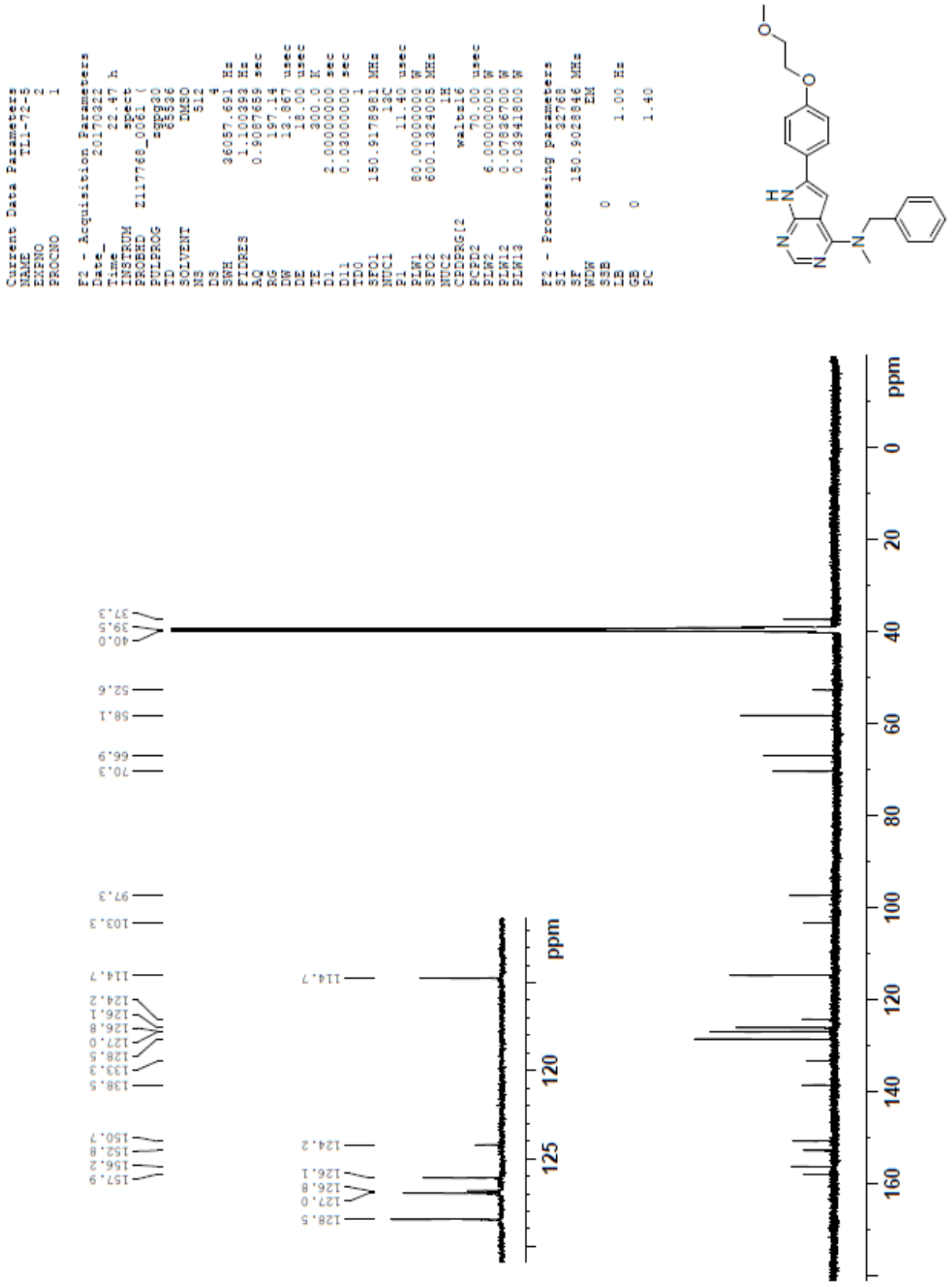


**Figure M.2**: $^{13}$C NMR spectrum of compound **7b.**

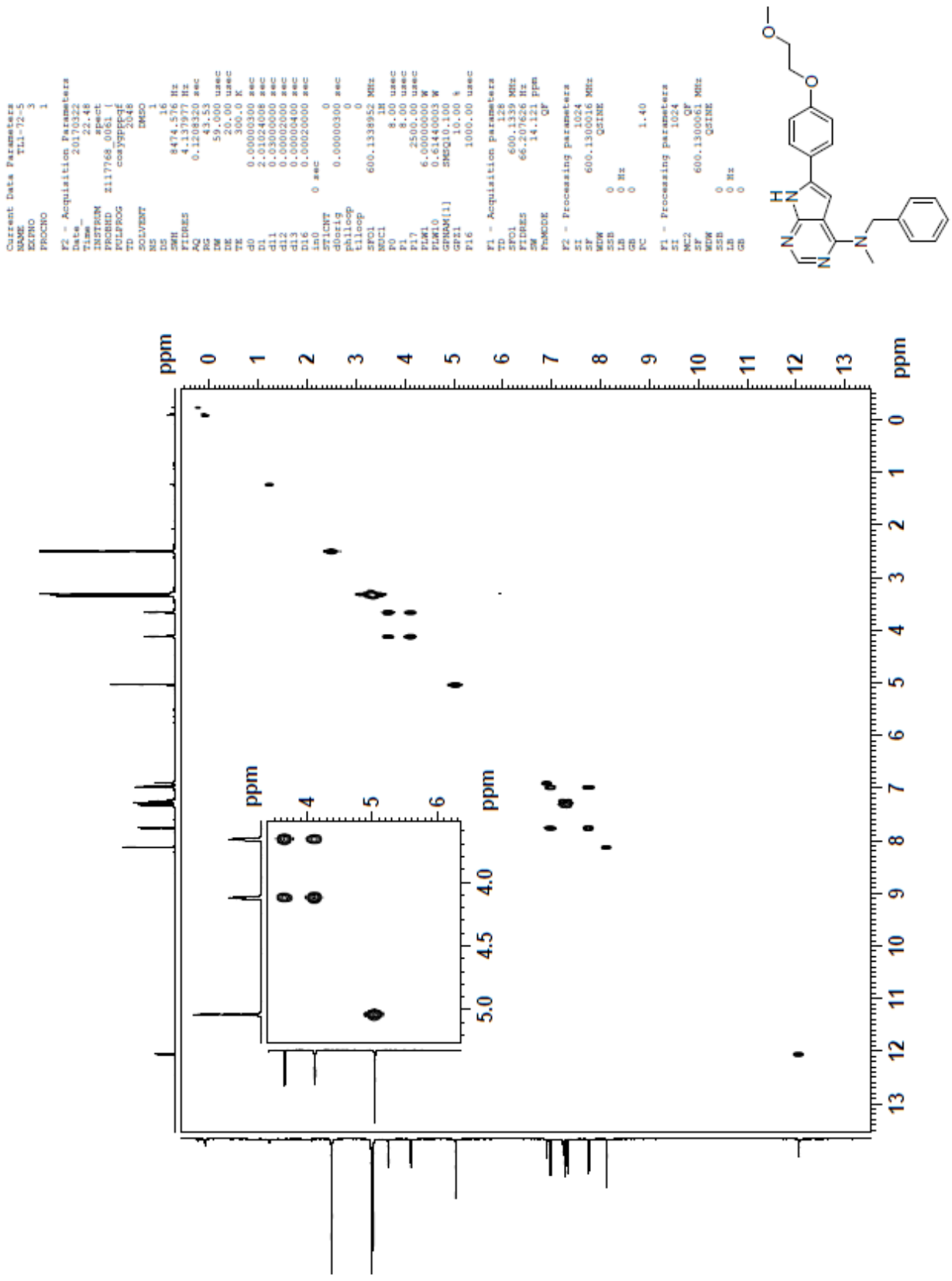


**Figure M.3**: COSY spectrum of compound **7b.**

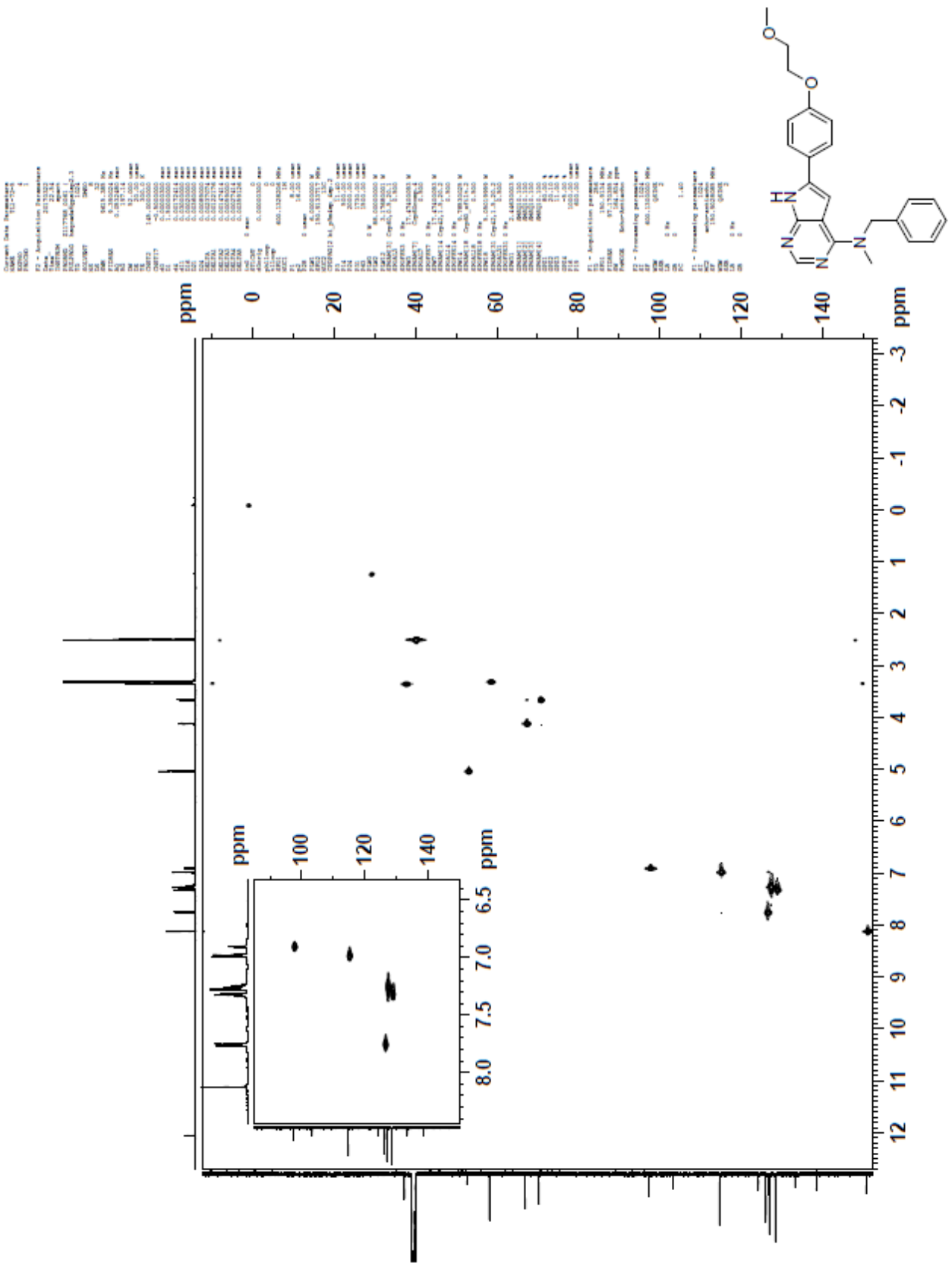


**Figure M.4**: HSQC spectrum of compound **7b.**

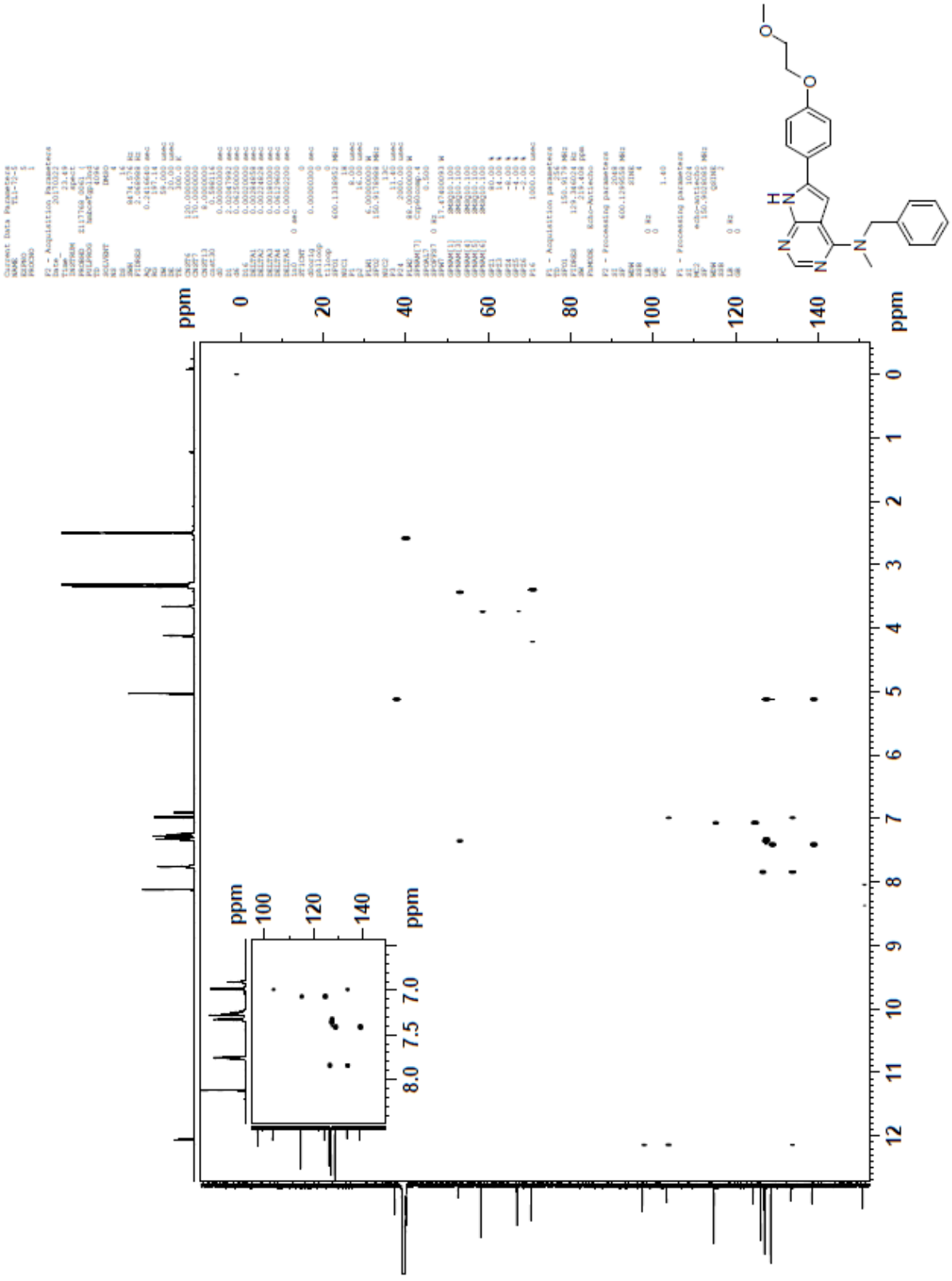

**Figure M.5**: HMBC spectrum of compound **7b**.

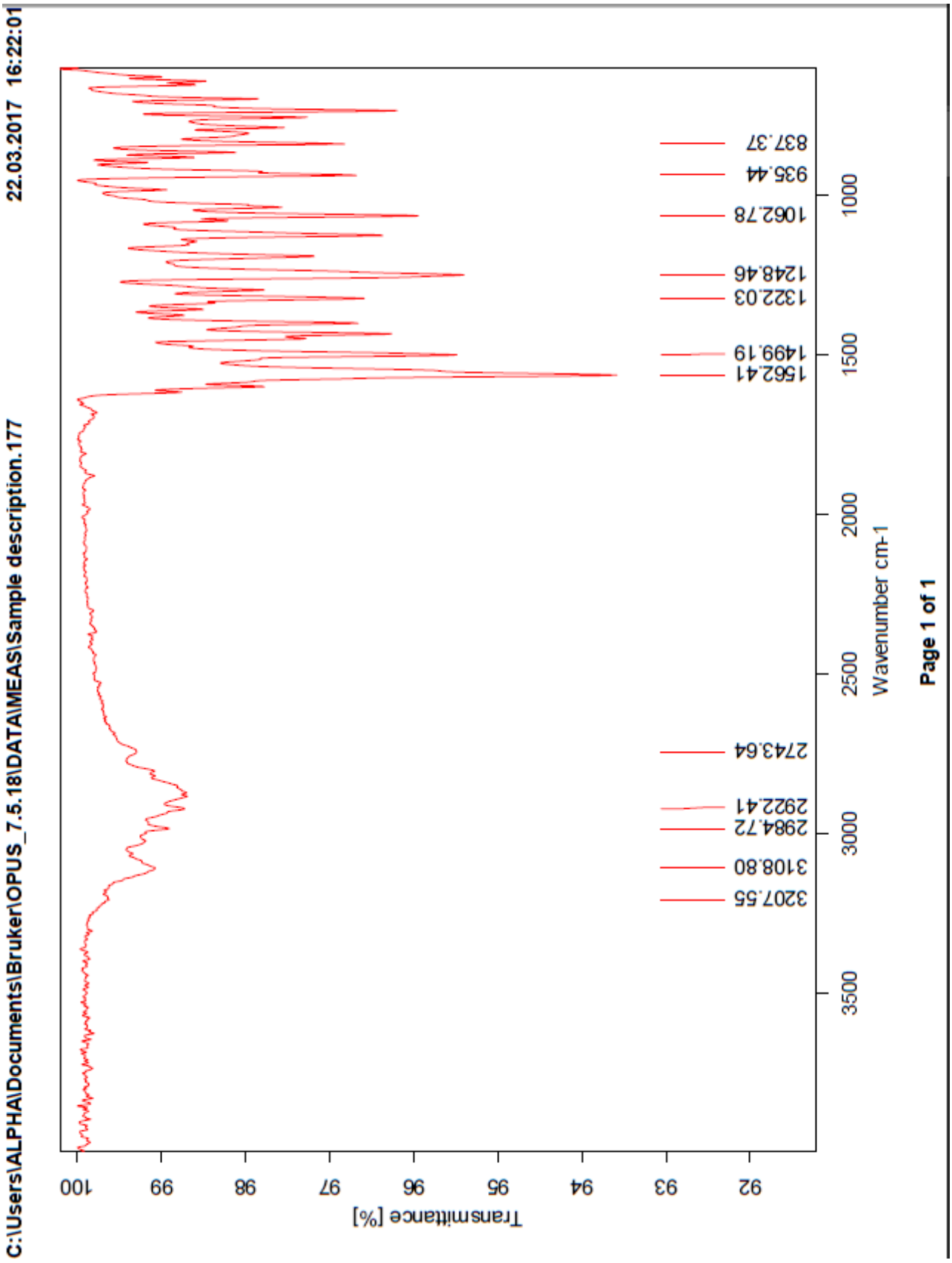


**Figure M.6**: IR spectrum of compound **7b.**

**Elemental Composition Report** Page 1

**Single Mass Analysis**
Tolerance = 2.0 PPM / DBE: min = -1.5, max = 50.0
Element prediction: Off
Number of isotope peaks used for i-FIT = 3

Monoisotopic Mass, Even Electron Ions
569 formula(e) evaluated with 1 results within limits (all results (up to 1000) for each mass)
Elements Used:
C: 1-500 H: 1-1000 N: 1-10 O: 1-25
2017-92 165 (3.223) AM2 (Ar,35000.0,0.00,0.00); Cm (165:167)
1: TOF MS ASAP+

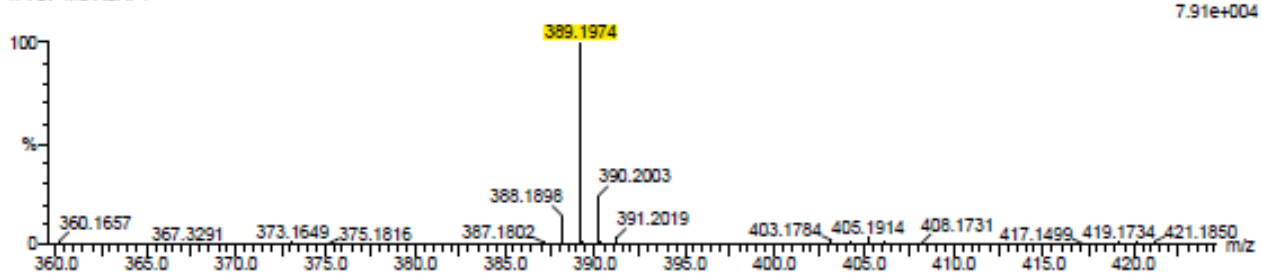


| | | | | | | | | |
|---|---|---|---|---|---|---|---|---|
| Minimum: | | | | -1.5 | | | | |
| Maximum: | | 2.0 | 2.0 | 50.0 | | | | |
| Mass | Calc. Mass | mDa | PPM | DBE | i-FIT | Norm | Conf(%) | Formula |
| 389.1974 | 389.1978 | -0.4 | -1.0 | 13.5 | 598.7 | n/a | n/a | C23 H25 N4 O2 ion observed [M+H] |

**Figure M.7**: MS spectrum of compound **7b.**

# N Spectroscopic data for compound 7c

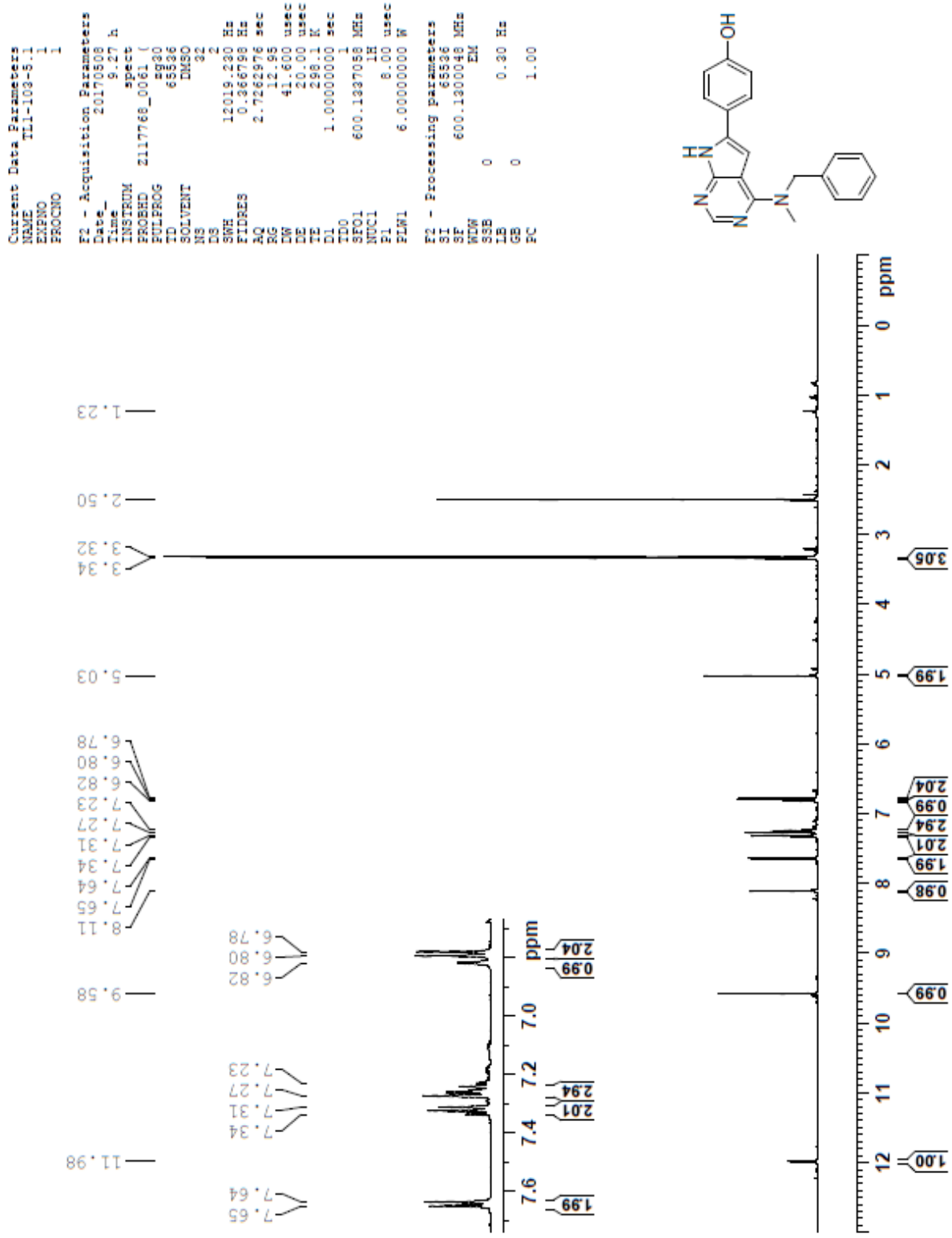


**Figure N.1**: $^{1}$H NMR spectrum of compound **7c.**

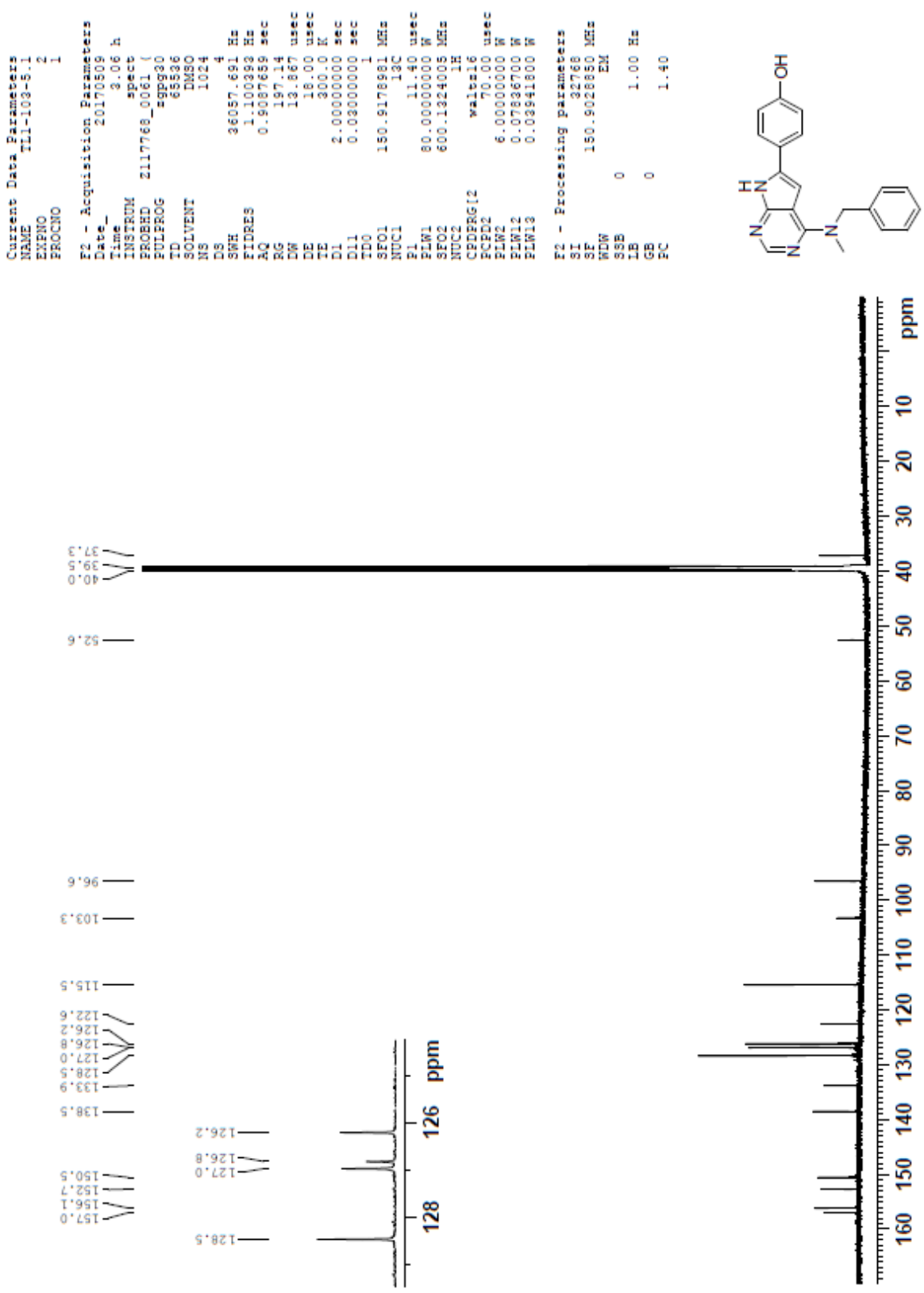


**Figure N.2**: $^{13}C$ NMR spectrum of compound **7c.**

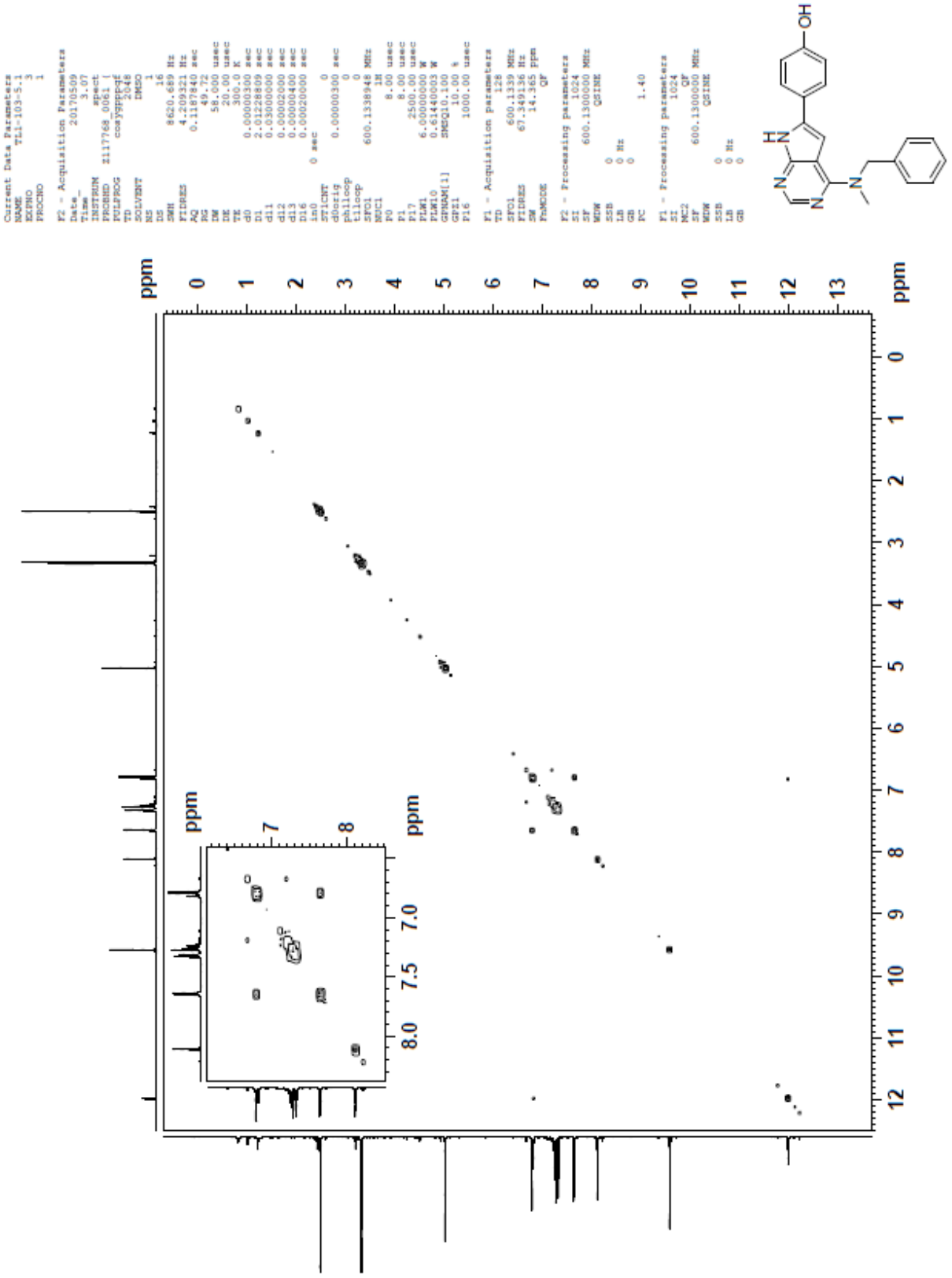

**Figure N.3**: COSY spectrum of compound **7c.**

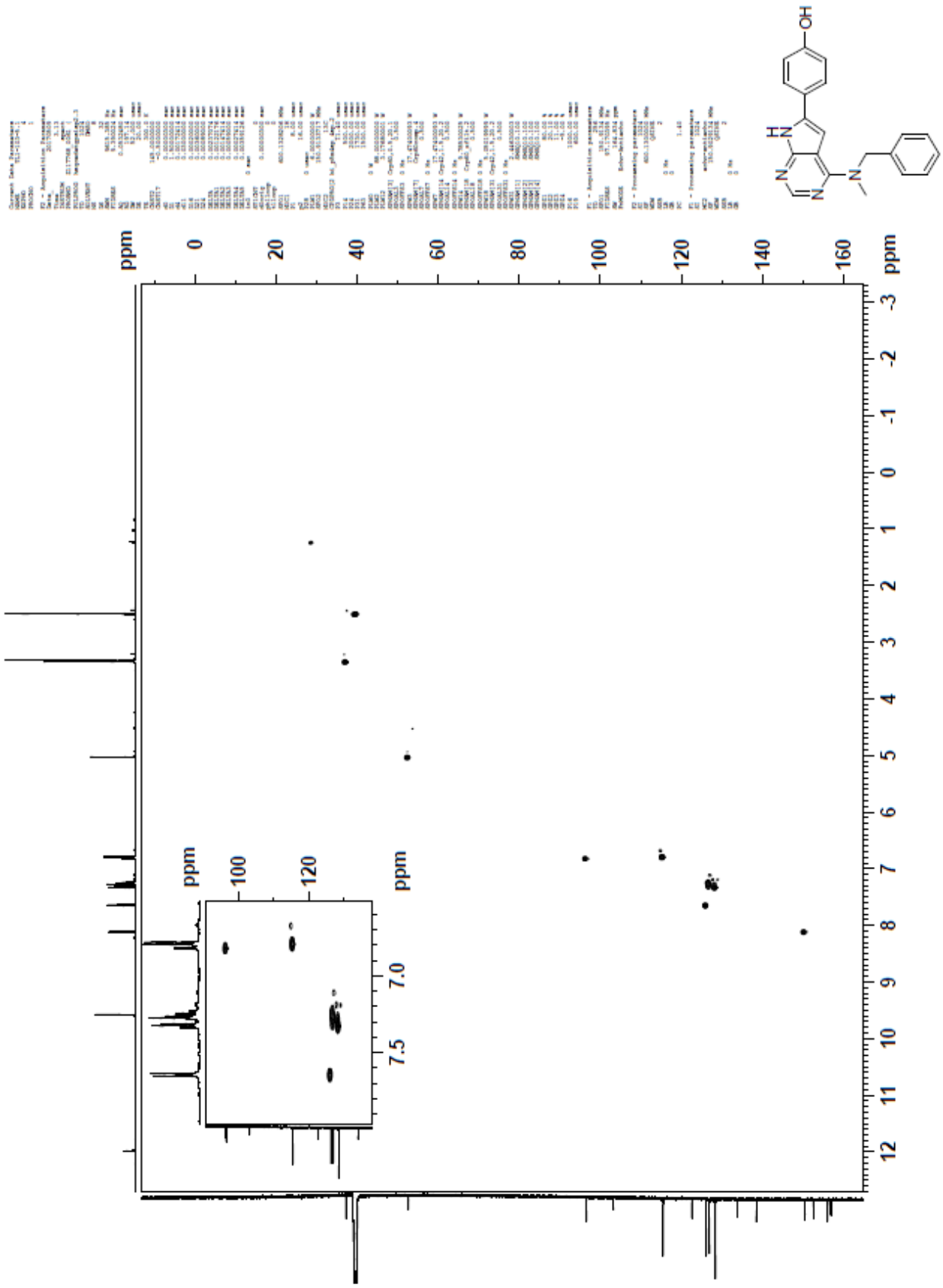


**Figure N.4**: HSQC spectrum of compound **7c.**

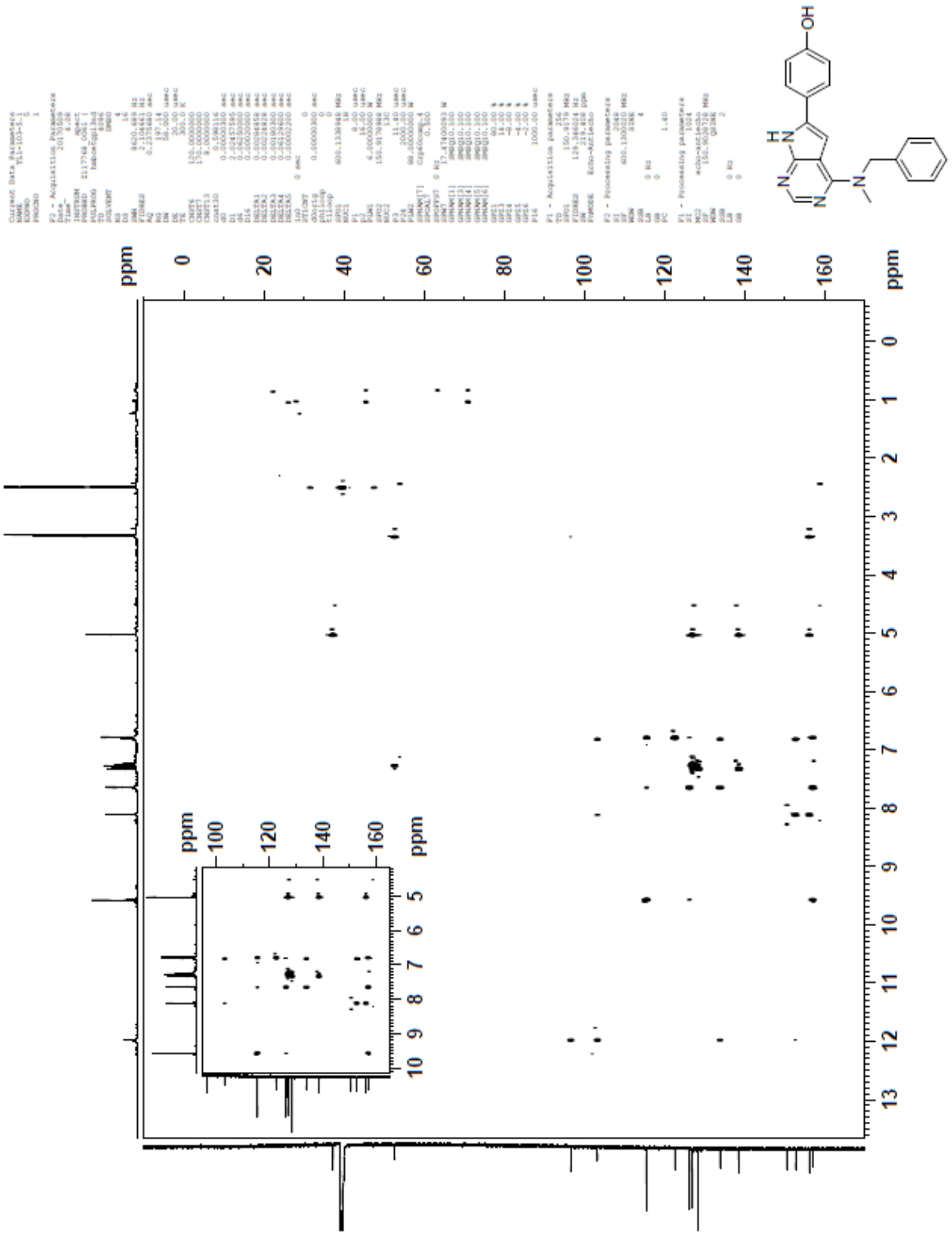

**Figure N.5**: HMBC spectrum of compound **7c**.

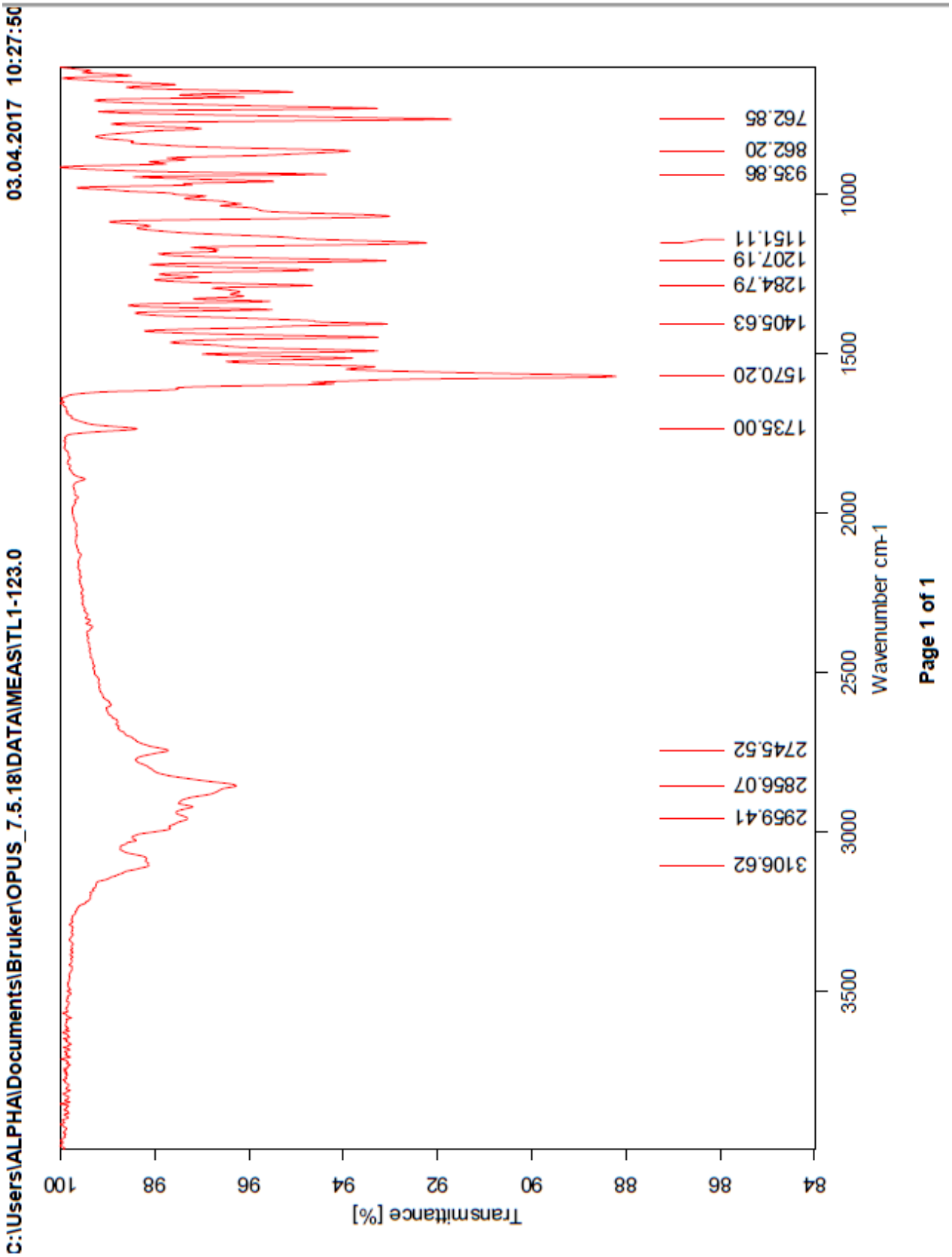


**Figure N.6**: IR spectrum of compound **7c.**

**Elemental Composition Report** Page 1

**Single Mass Analysis**
Tolerance = 5.0 PPM / DBE: min = -1.5, max = 50.0
Element prediction: Off
Number of isotope peaks used for i-FIT = 3

Monoisotopic Mass, Even Electron Ions
512 formula(e) evaluated with 2 results within limits (all results (up to 1000) for each mass)
Elements Used:
C: 1-500 H: 1-1000 N: 0-10 O: 0-25
2017-176 266 (5.186) AM2 (Ar,35000.0,0.00,0.00); Cm (256:272)
1: TOF MS ASAP+

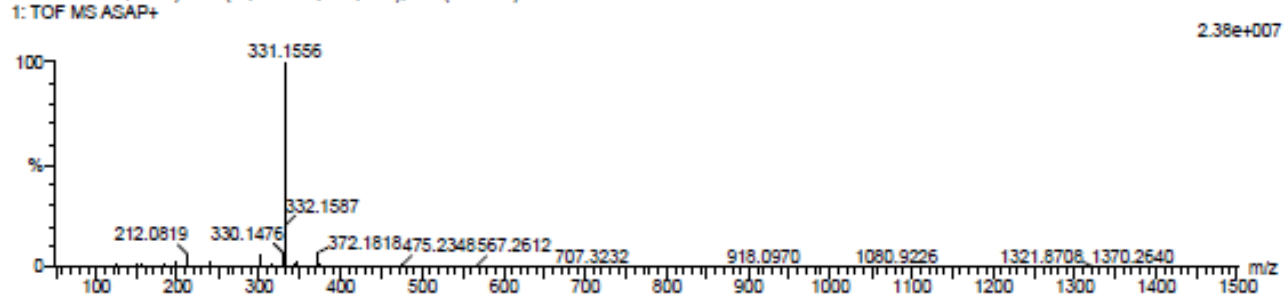


| | | | | | | | | |
|---|---|---|---|---|---|---|---|---|
| Minimum: | | | | -1.5 | | | | |
| Maximum: | | 2.0 | 5.0 | 50.0 | | | | |
| Mass | Calc. Mass | mDa | PPM | DBE | i-FIT | Norm | Conf(%) | Formula |
| 331.1556 | 331.1559 | -0.3 | -0.9 | 13.5 | 1752.9 | 0.273 | 76.07 | C20 H19 N4 O ion observed [M+H] |
| | 331.1545 | 1.1 | 3.3 | 8.5 | 1754.1 | 1.430 | 23.93 | C19 H23 O5 |

**Figure N.7**: MS spectrum of compound **7c.**

# O Spectroscopic data for compound 7d

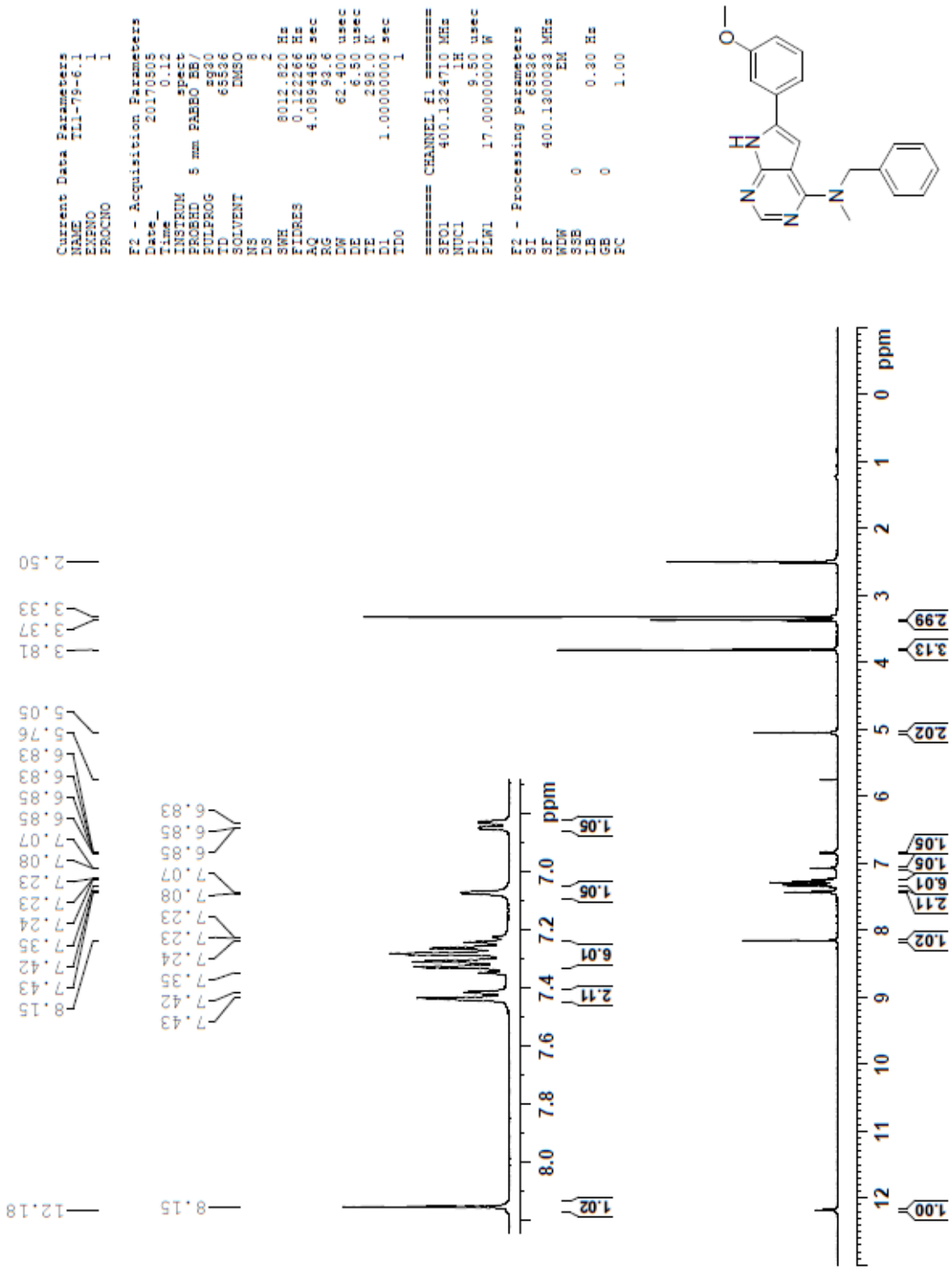


**Figure O.1**: $^{1}$H NMR spectrum of compound **7d.**

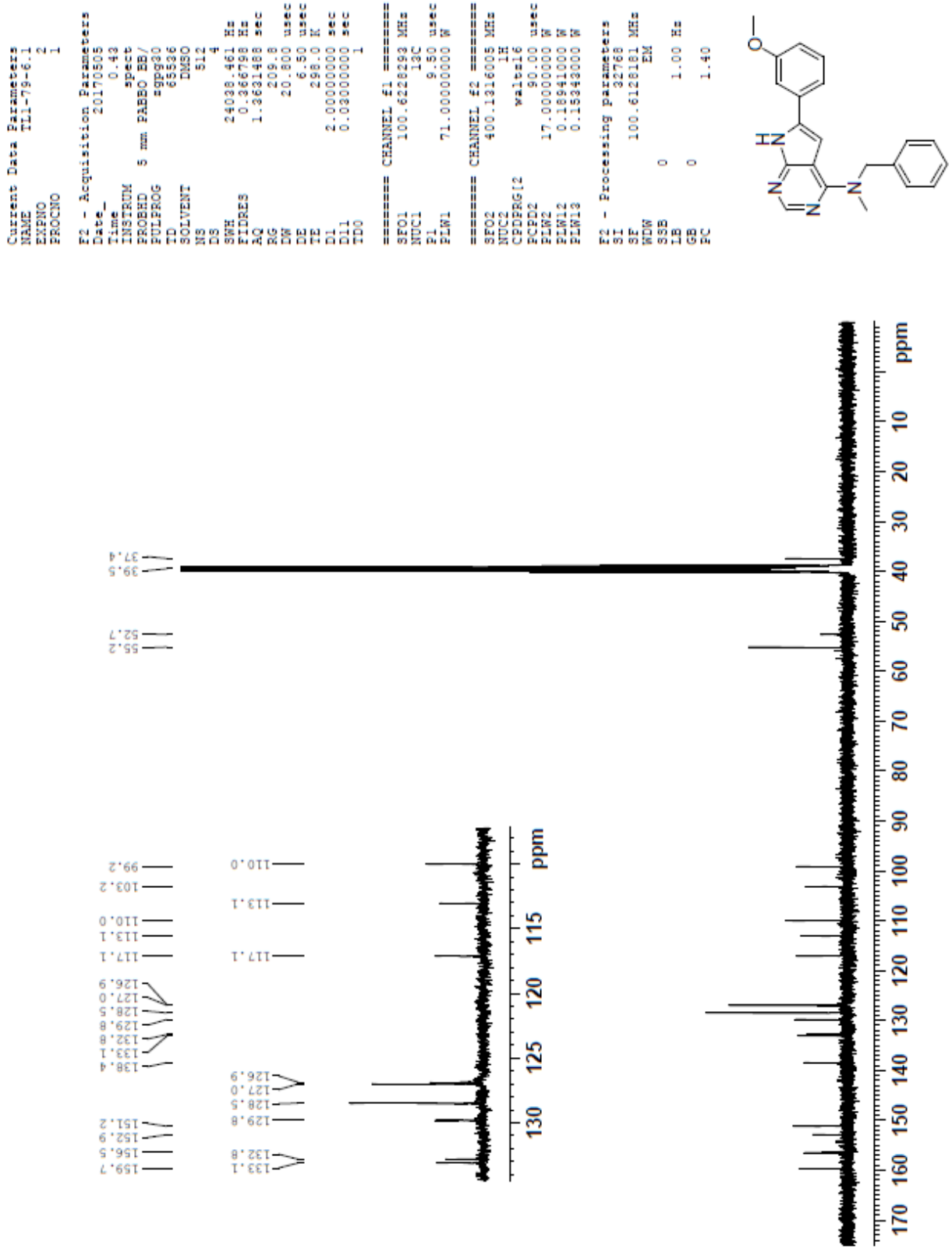


**Figure O.2**: $^{13}$C NMR spectrum of compound **7d.**

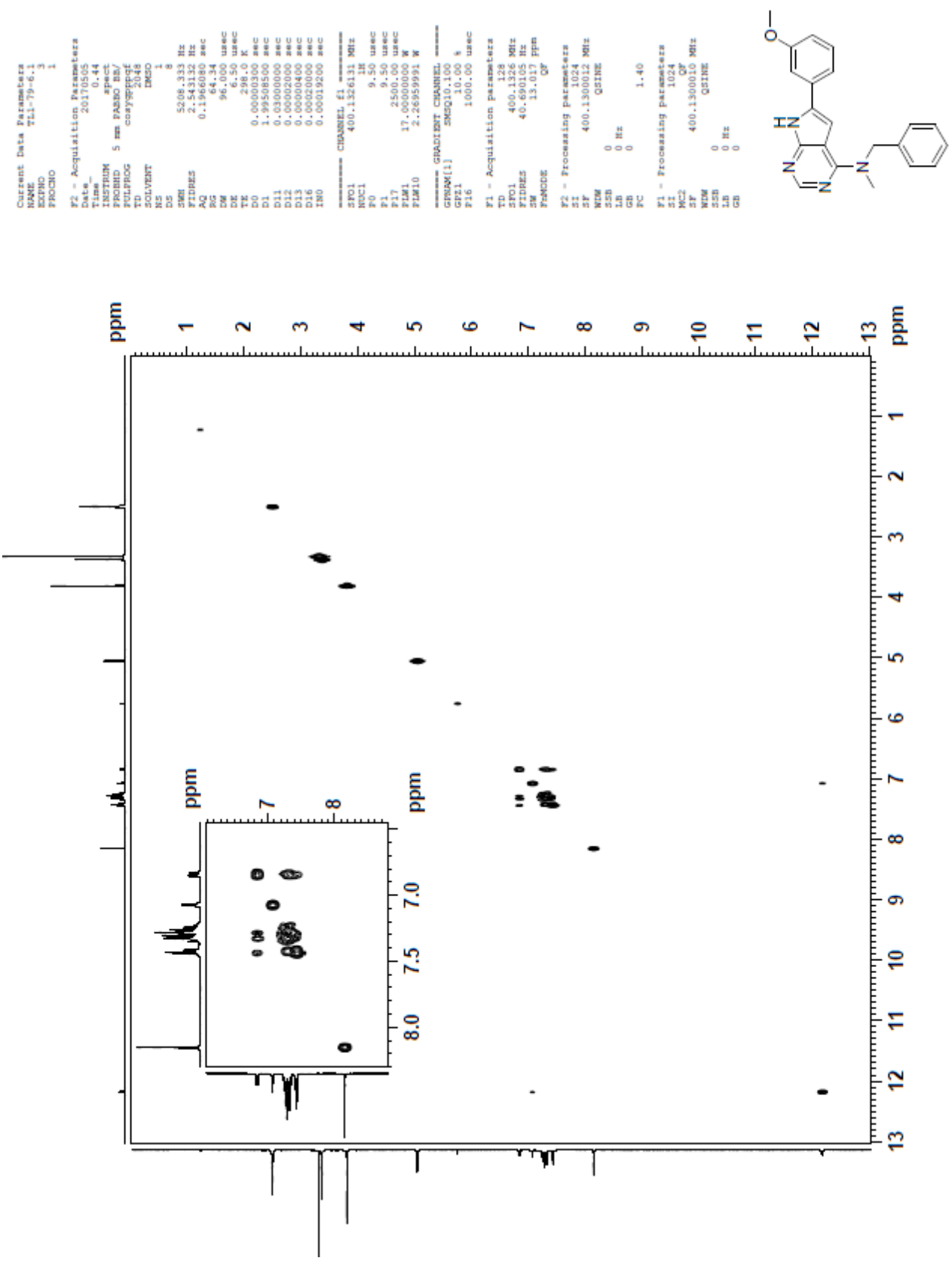


**Figure O.3**: COSY spectrum of compound **7d.**

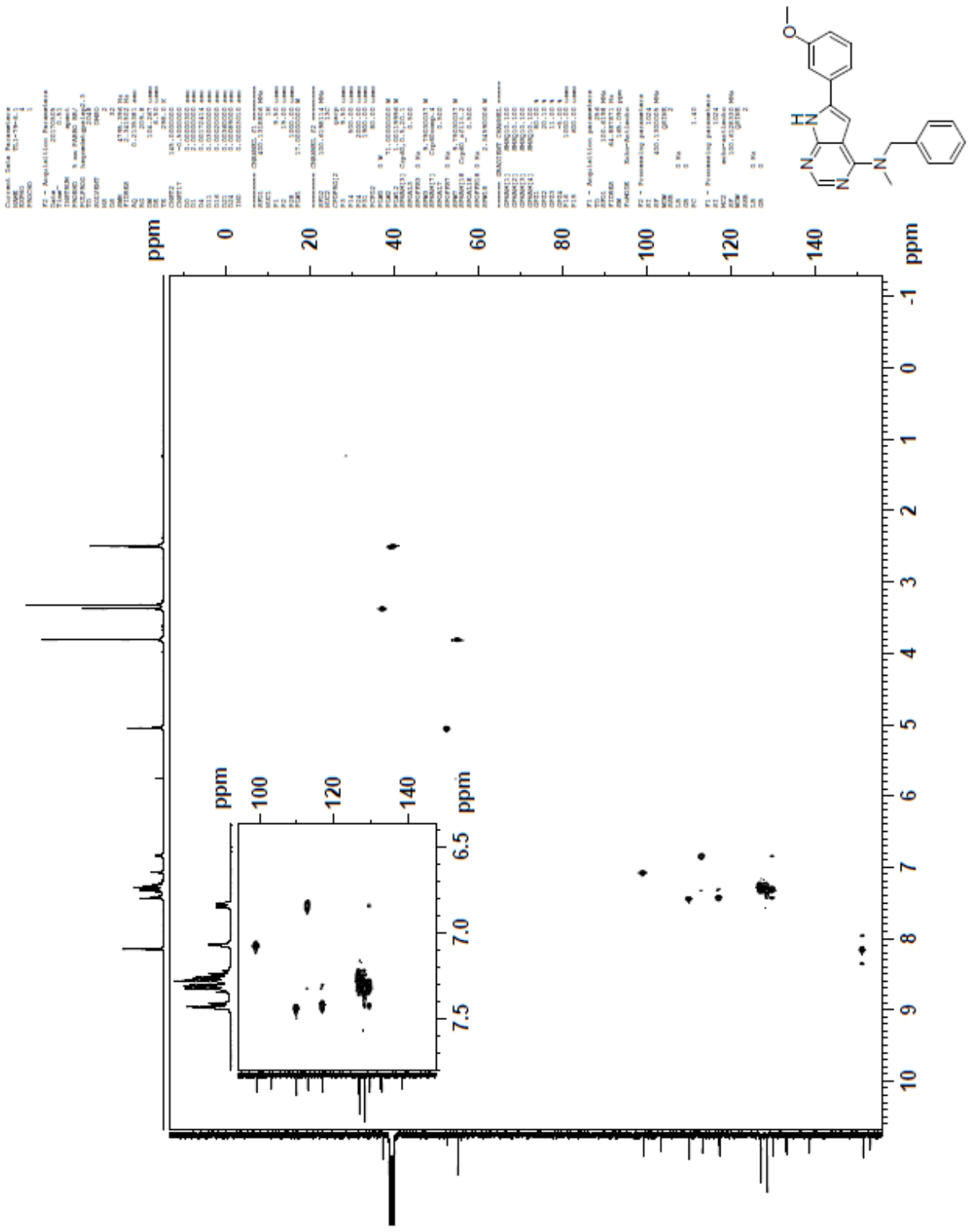

**Figure O.4**: HSQC spectrum of compound **7d.**

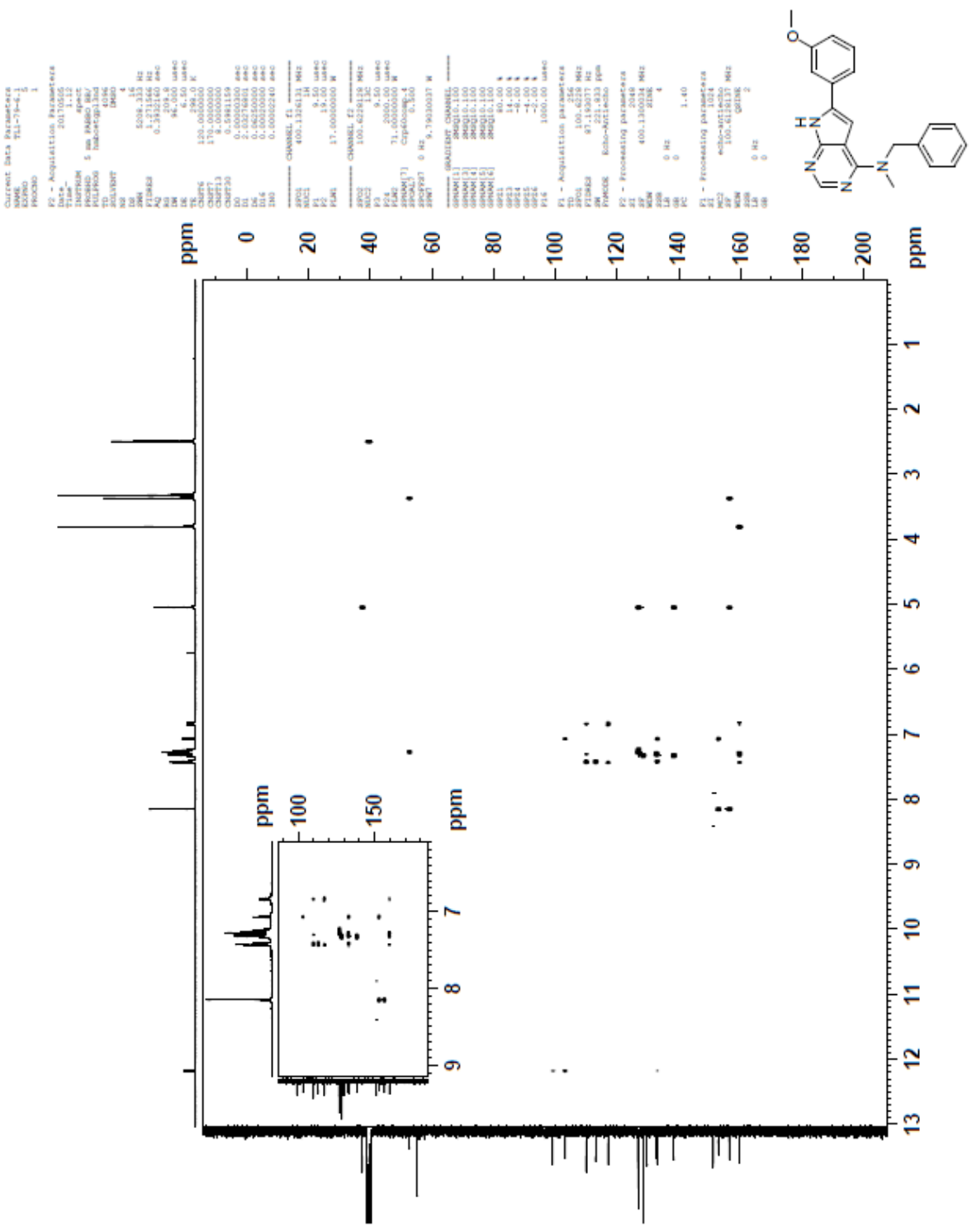

**Figure O.5**: HMBC spectrum of compound **7d**.

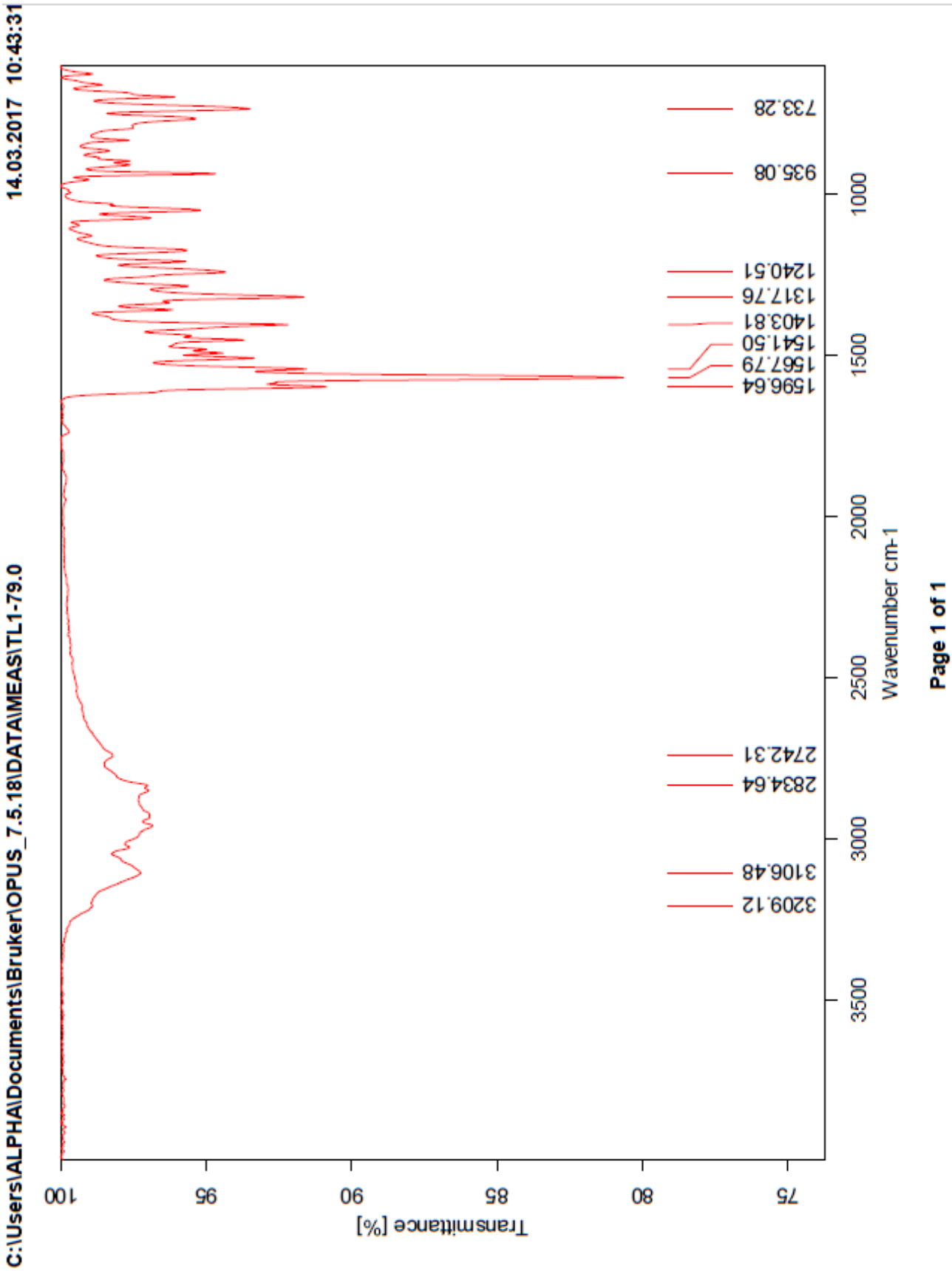


**Figure O.6**: IR spectrum of compound **7d.**

**Elemental Composition Report** Page 1

**Single Mass Analysis**
Tolerance = 2.0 PPM / DBE: min = -1.5, max = 50.0
Element prediction: Off
Number of isotope peaks used for i-FIT = 3

Monoisotopic Mass, Even Electron Ions
446 formula(e) evaluated with 1 results within limits (all results (up to 1000) for each mass)
Elements Used:
C: 1-500 H: 1-1000 N: 1-10 O: 1-25
2017-155 123 (2.414) AM2 (Ar,35000.0,0.00,0.00); Cm (121:123)
1: TOF MS ASAP+

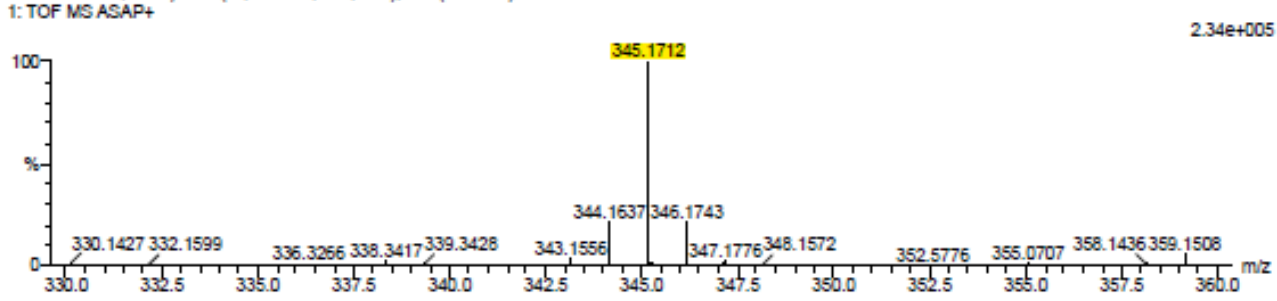


| | | | | | | | | |
|---|---|---|---|---|---|---|---|---|
| Minimum: | | | | -1.5 | | | | |
| Maximum: | | 2.0 | 2.0 | 50.0 | | | | |
| Mass | Calc. Mass | mDa | PPM | DBE | i-FIT | Norm | Conf(%) | Formula |
| 345.1712 | 345.1715 | -0.3 | -0.9 | 13.5 | 865.3 | n/a | n/a | C21 H21 N4 O [ion observed M+H] |

**Figure A.7**: MS spectrum of compound **7d.**

# P Spectroscopic data for compound 7e

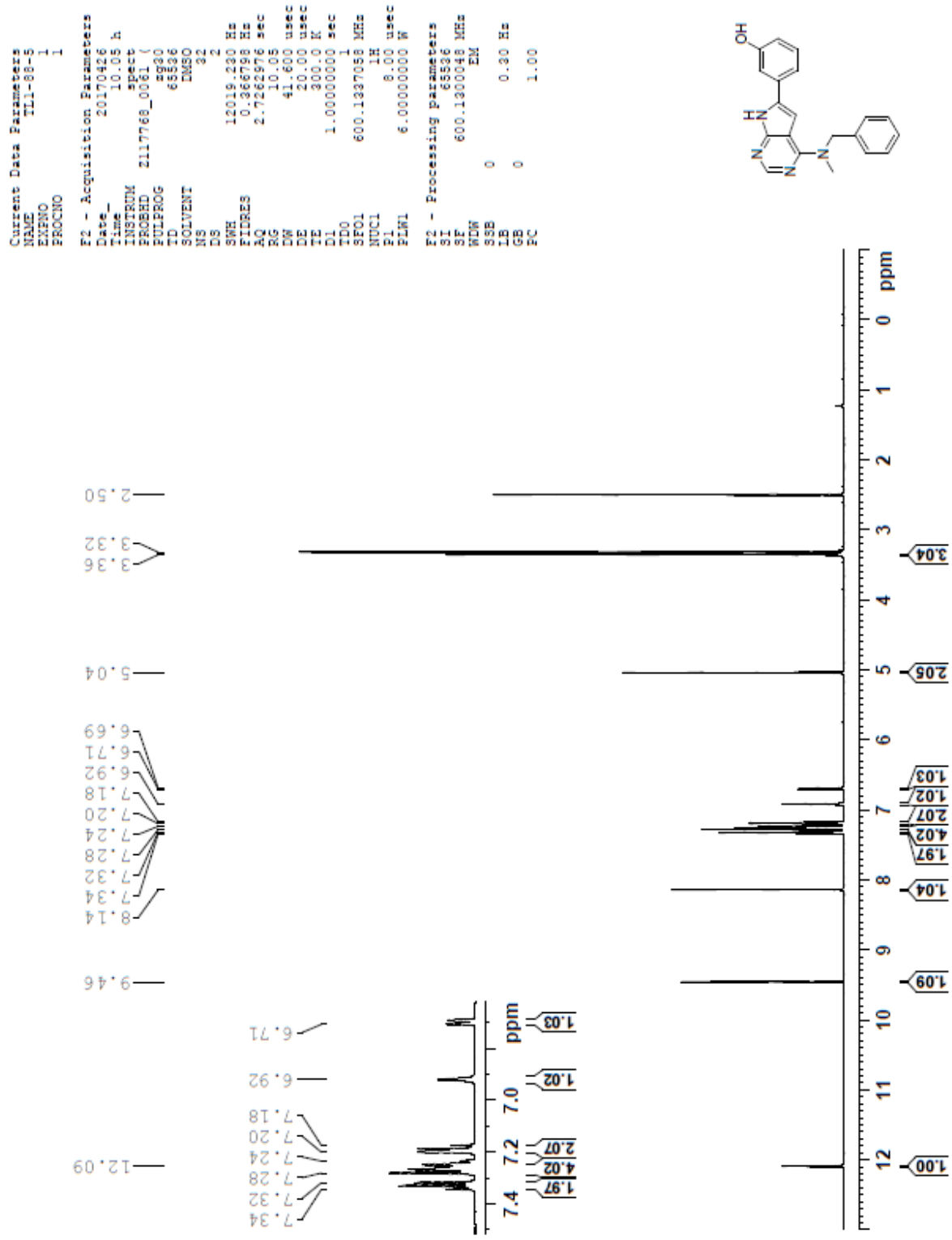


**Figure P.1**: $^{1}$H NMR spectrum of compound **7e.**

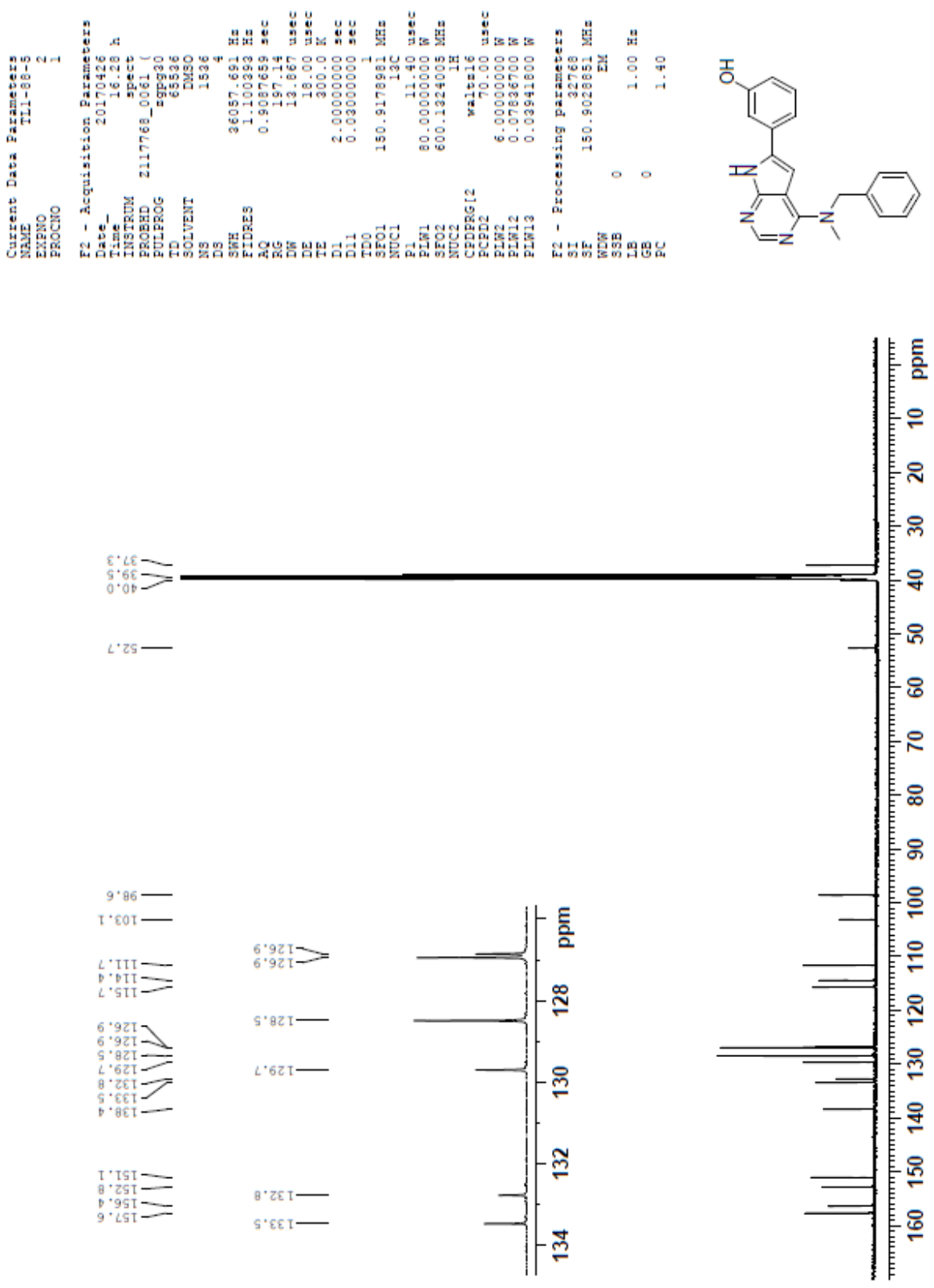


**Figure P.2**: $^{13}C$ NMR spectrum of compound **7e.**

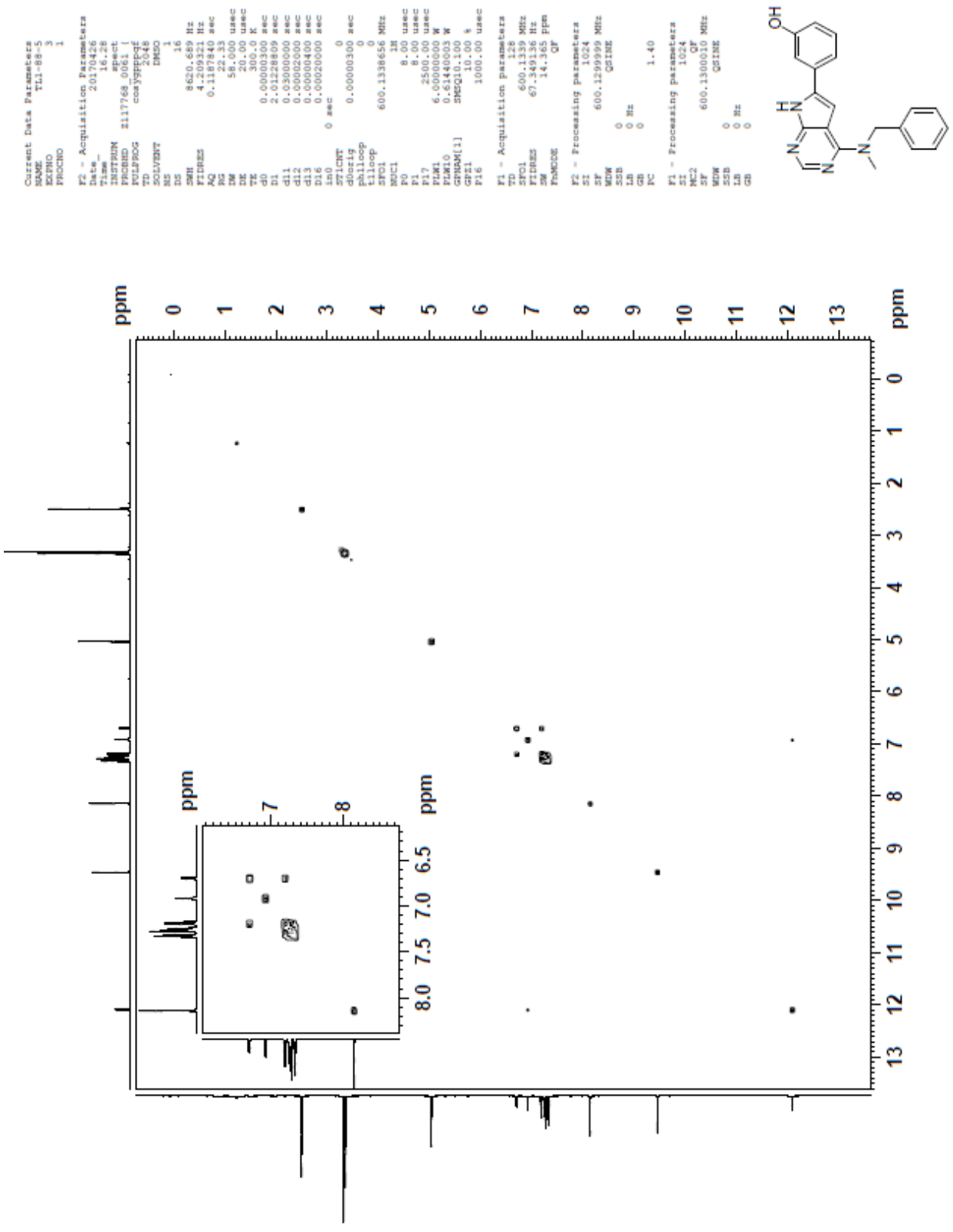

**Figure P.3**: COSY spectrum of compound **7e.**

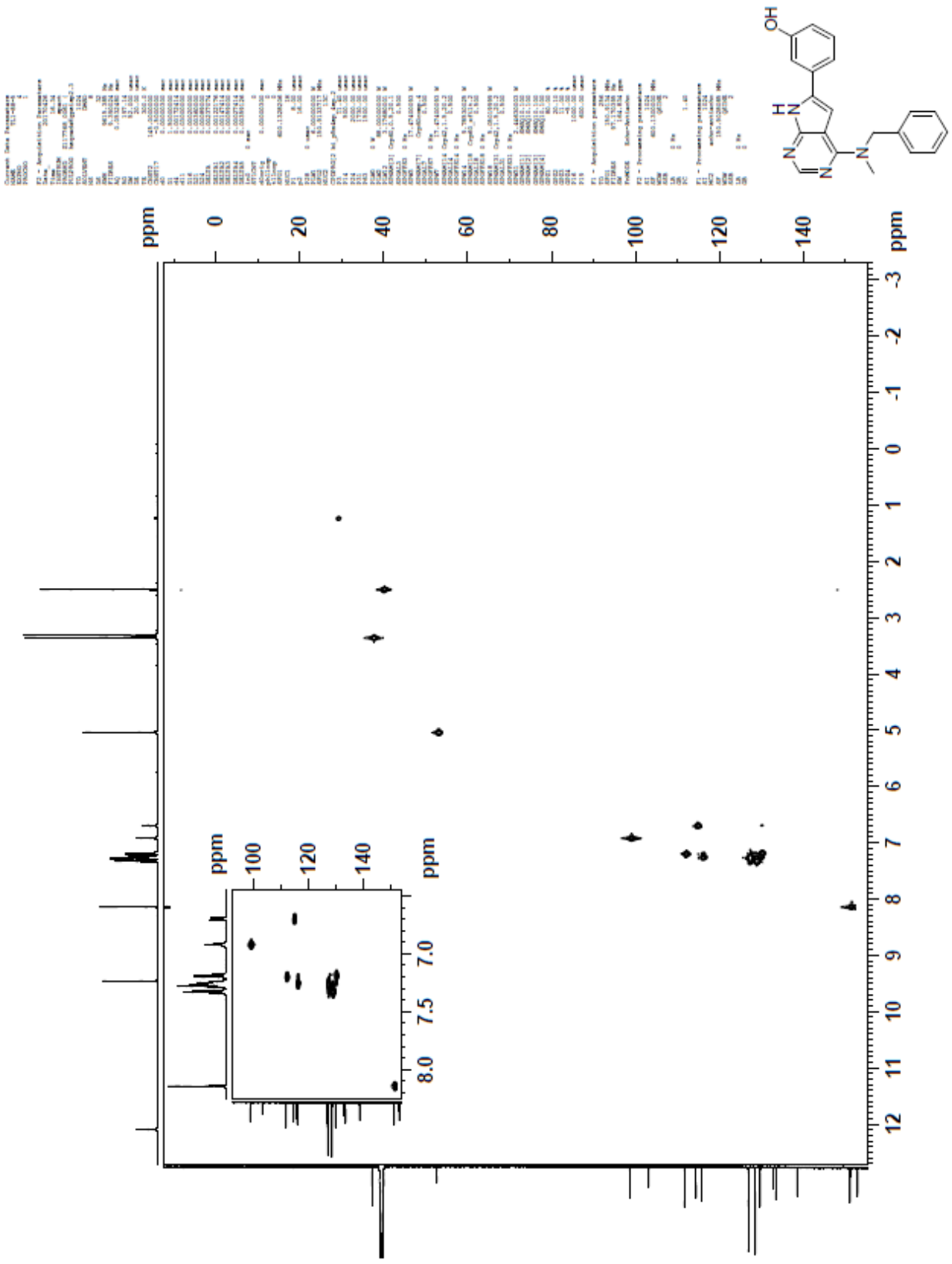


**Figure P.4**: HSQC spectrum of compound **7e.**

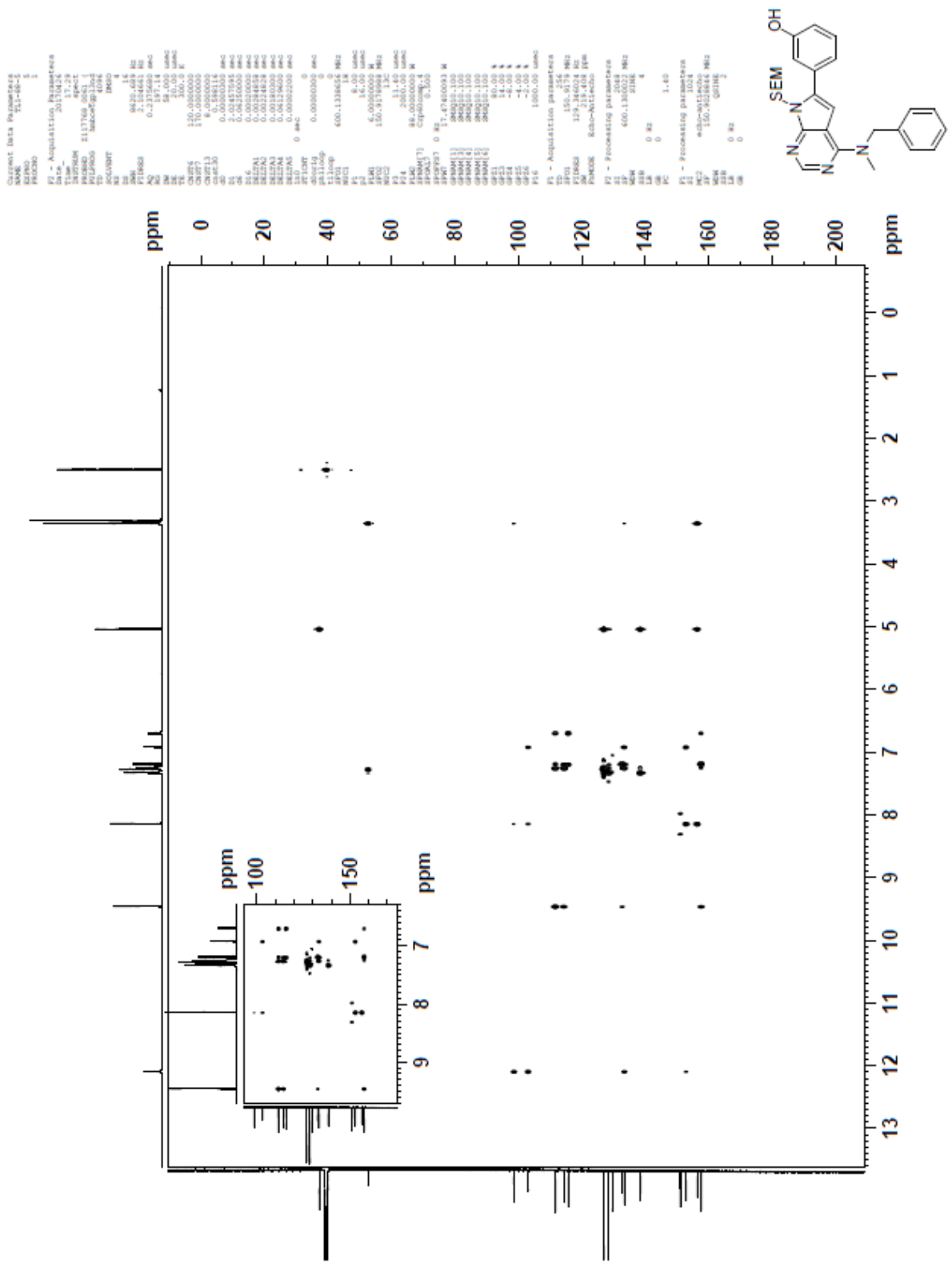


**Figure P.5**: HMBC spectrum of compound **7e**.

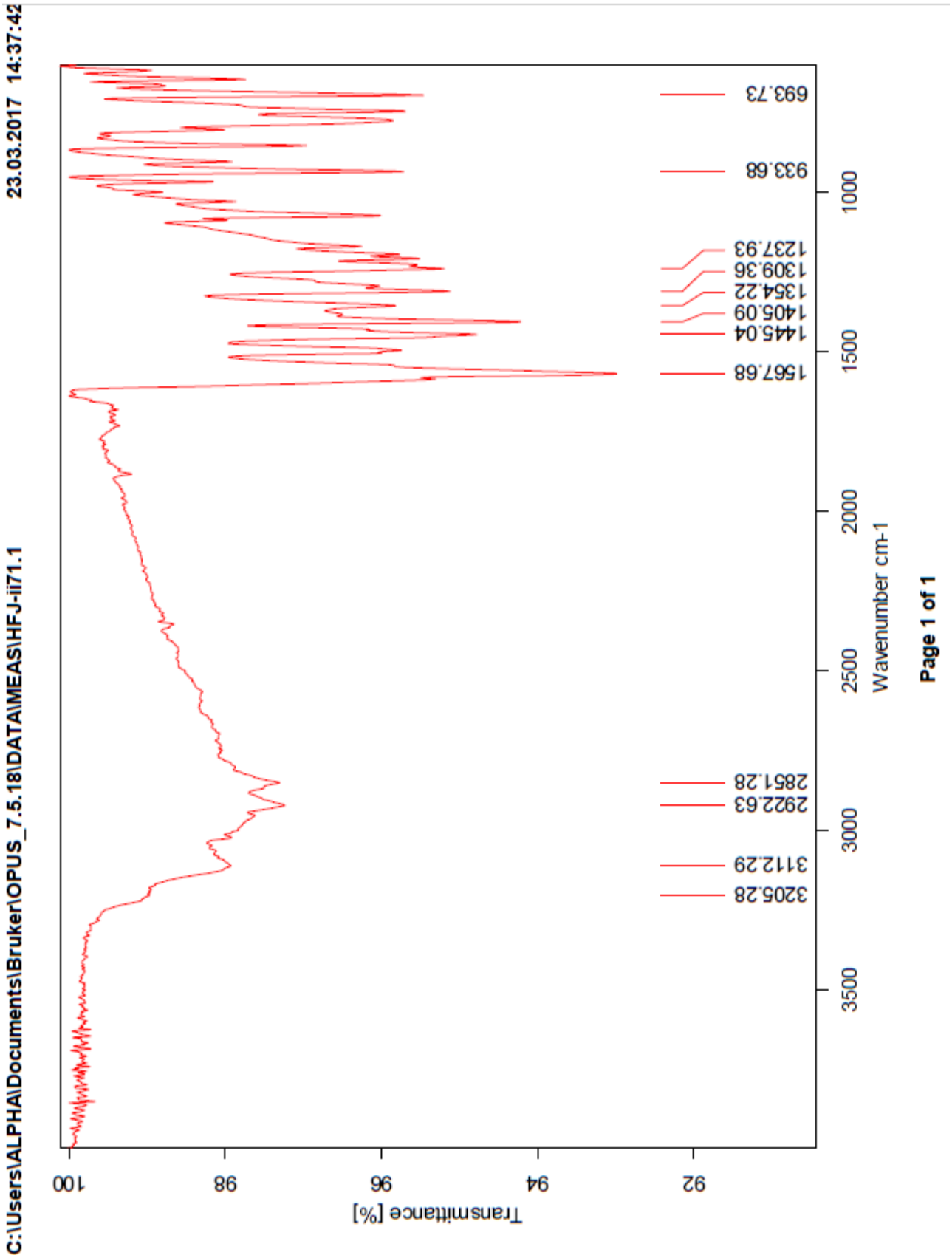


**Figure P.6**: IR spectrum of compound **7e.**

**Elemental Composition Report** Page 1

**Single Mass Analysis**
Tolerance = 2.0 PPM / DBE: min = -1.5, max = 50.0
Element prediction: Off
Number of isotope peaks used for i-FIT = 3

Monoisotopic Mass, Even Electron Ions
411 formula(e) evaluated with 1 results within limits (all results (up to 1000) for each mass)
Elements Used:
C: 1-500 H: 1-1000 N: 1-10 O: 1-25
2017-156 202 (3.947) AM2 (Ar,35000.0,0.00,0.00); Cm (197:202)
1: TOF MS ASAP+

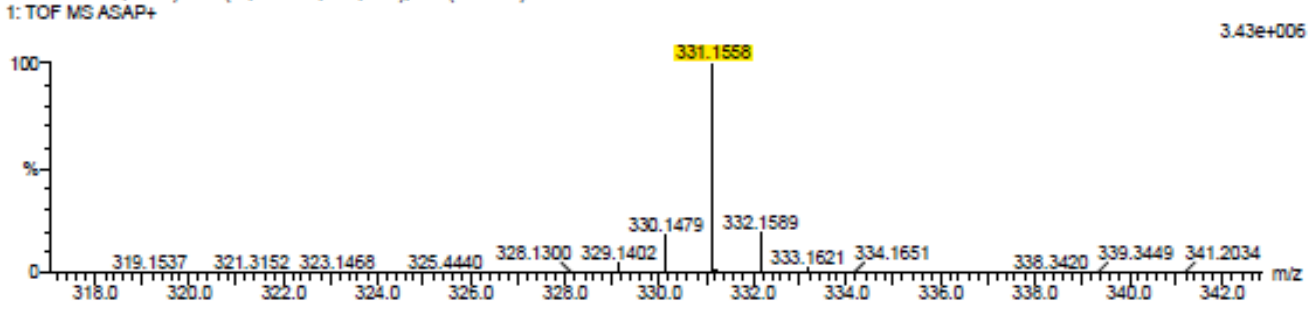


| | | | | | | | | |
|---|---|---|---|---|---|---|---|---|
| Minimum: | | | | -1.5 | | | | |
| Maximum: | | 2.0 | 2.0 | 50.0 | | | | |
| Mass | Calc. Mass | mDa | PPM | DBE | i-FIT | Norm | Conf(%) | Formula |
| 331.1558 | 331.1559 | -0.1 | -0.3 | 13.5 | 1325.6 | n/a | n/a | C20 H19 N4 O ion observed [M+H] |

**Figure P.7** MS spectrum of compound **7e.**

# Q Spectroscopic data for compound 7f

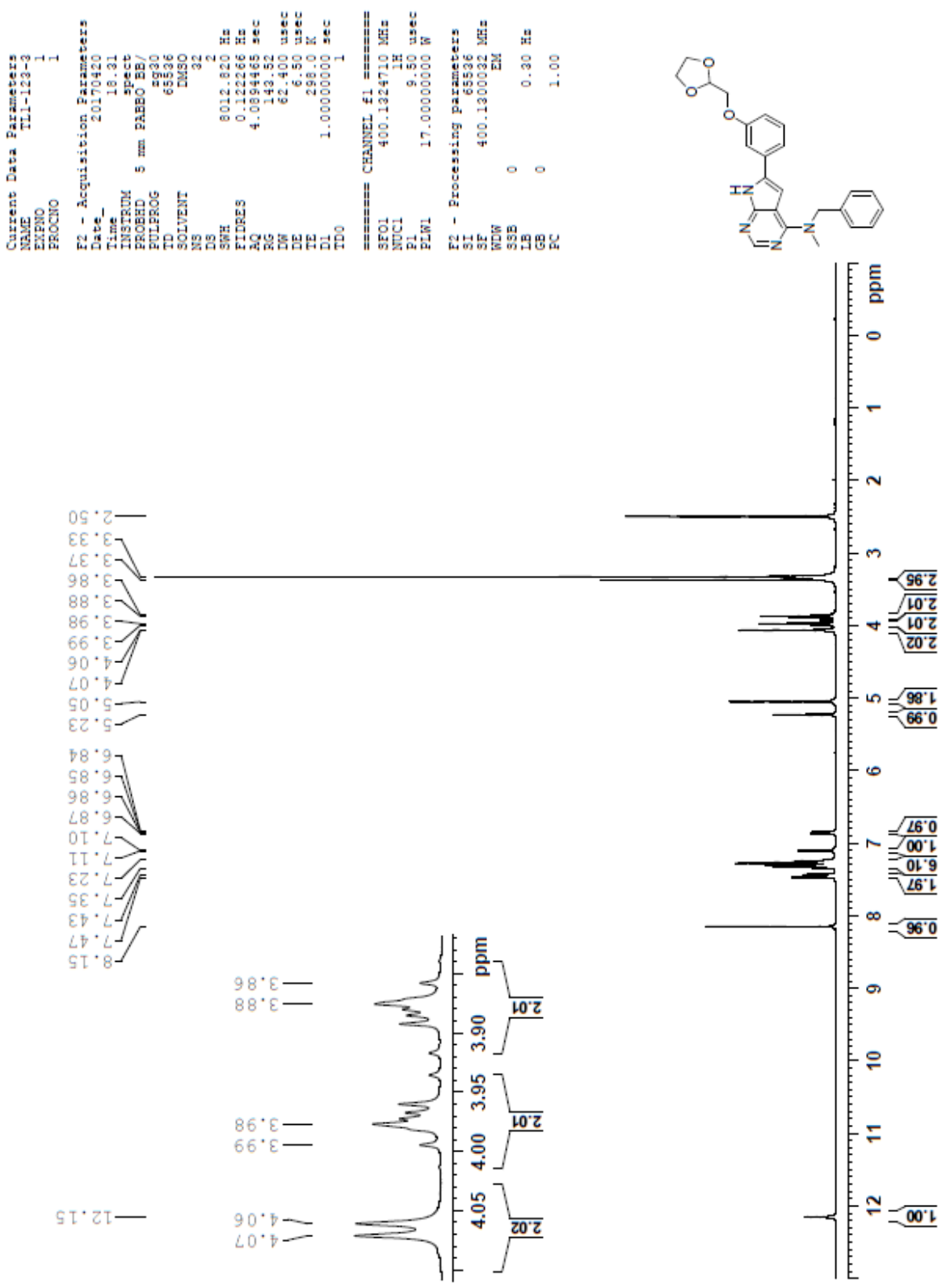


**Figure Q.1**: $^{1}$H NMR spectrum of compound **7f.**

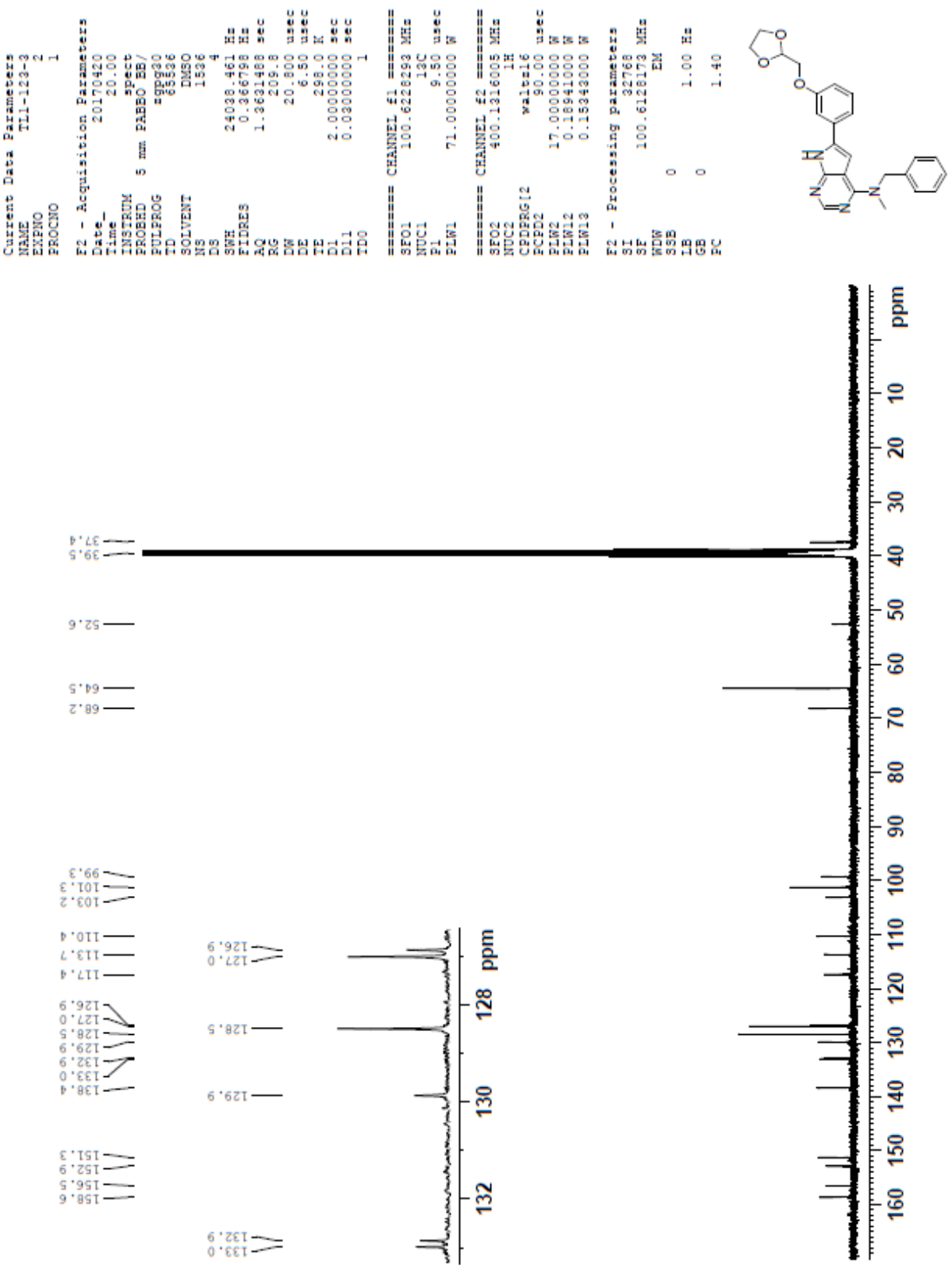


**Figure Q.2**: $^{13}$C NMR spectrum of compound **7f.**

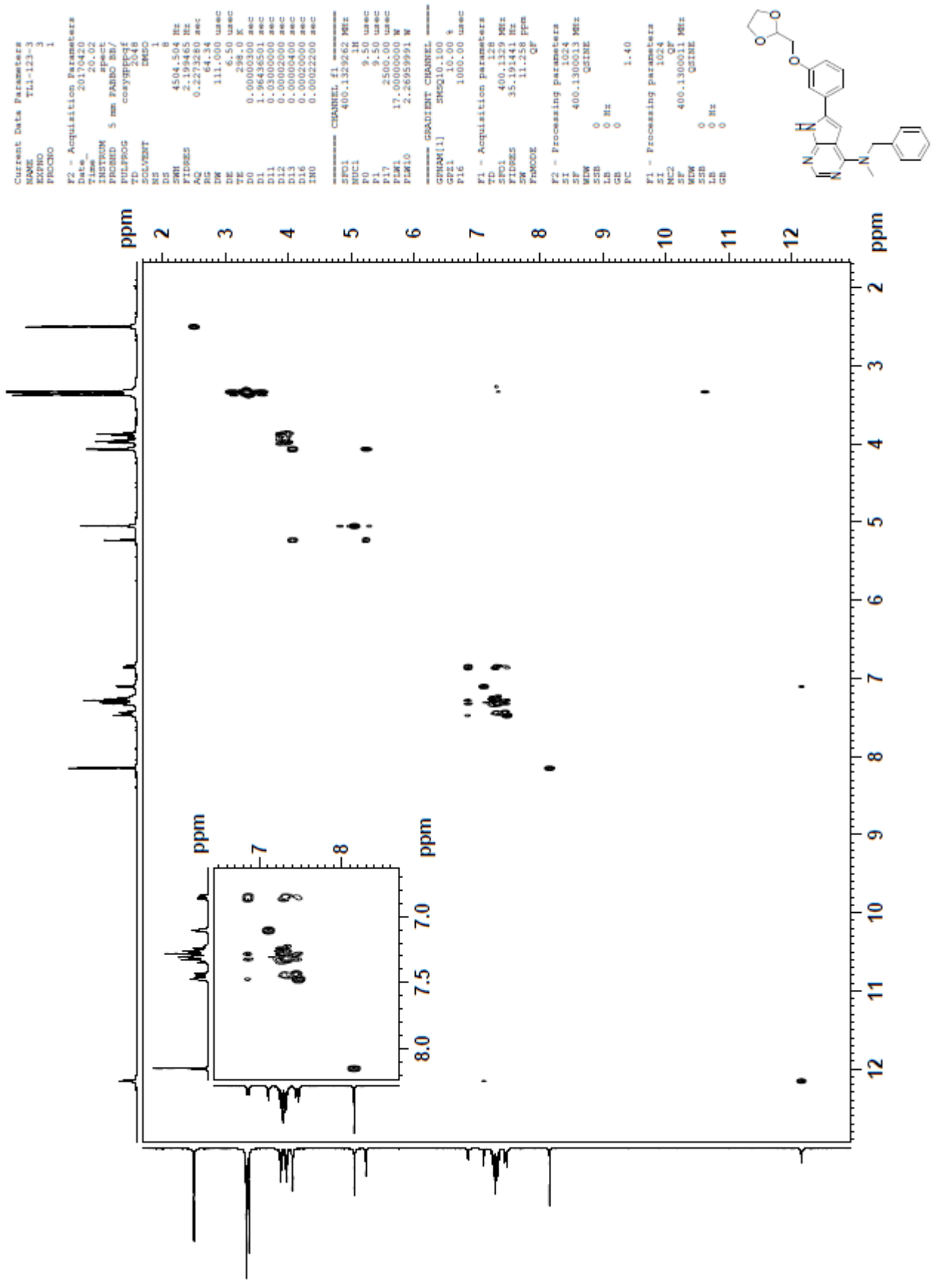

**Figure Q.3**: COSY spectrum of compound **7f.**

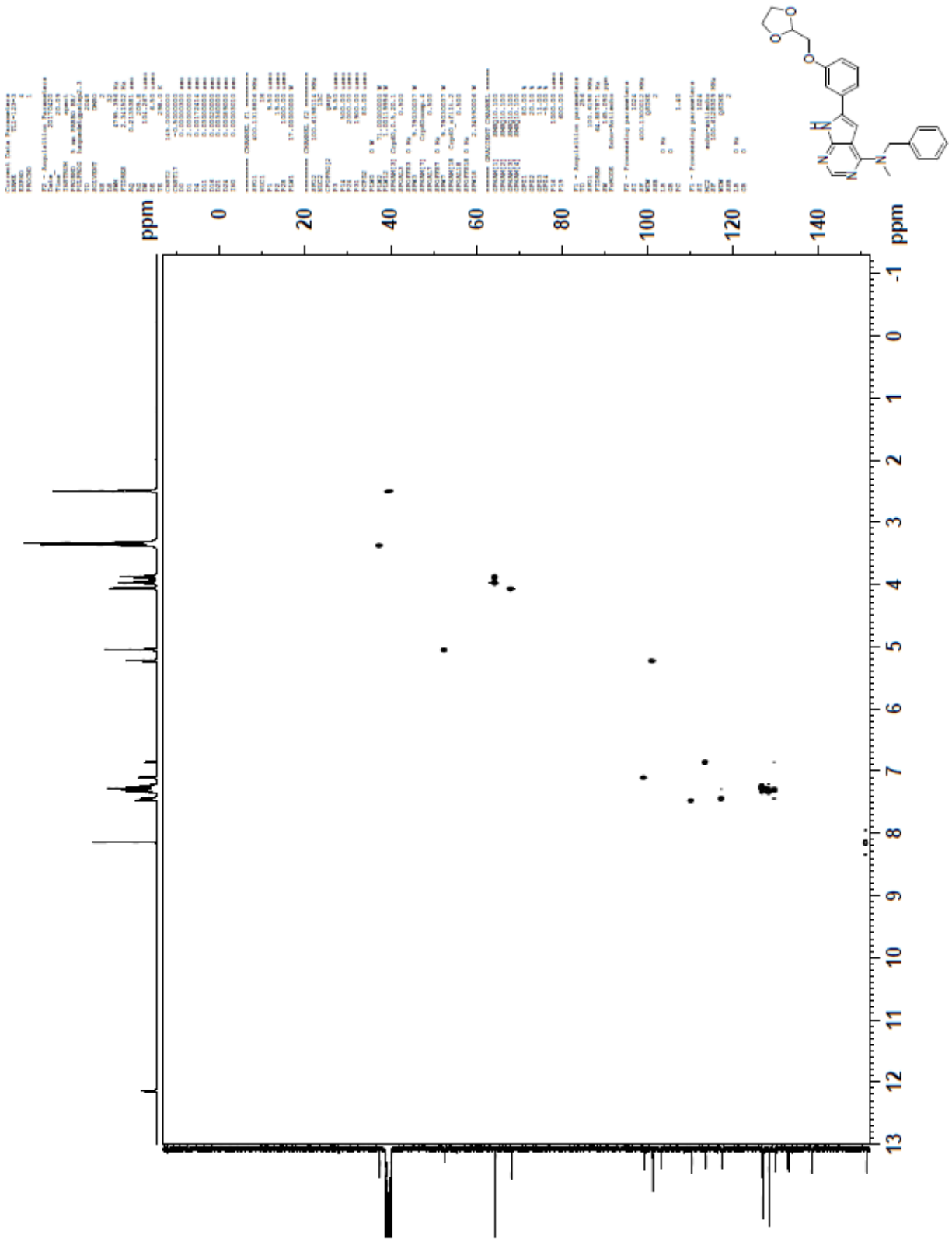


**Figure Q.4**: HSQC spectrum of compound **7f.**

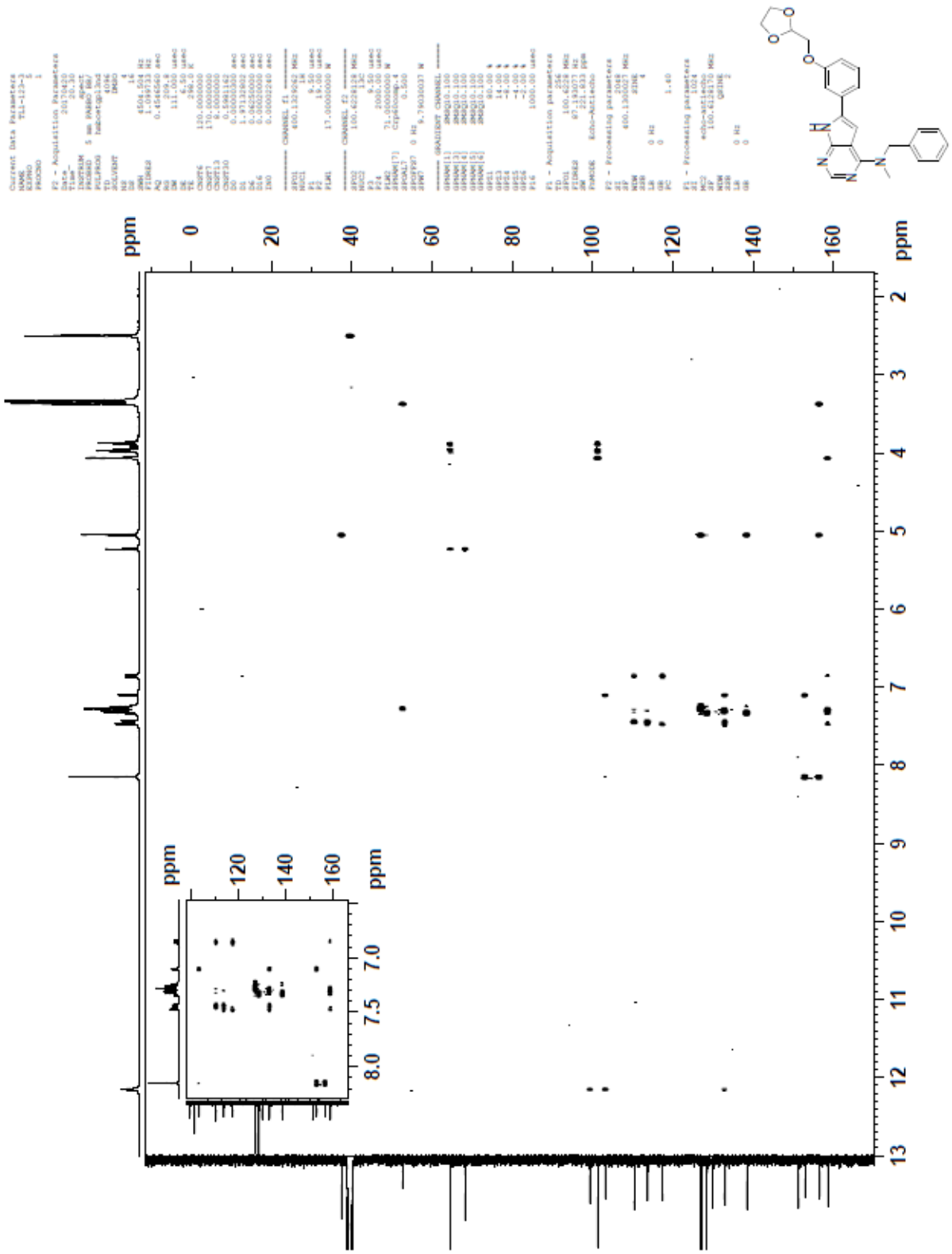

**Figure Q.5**: HMBC spectrum of compound **7f**.

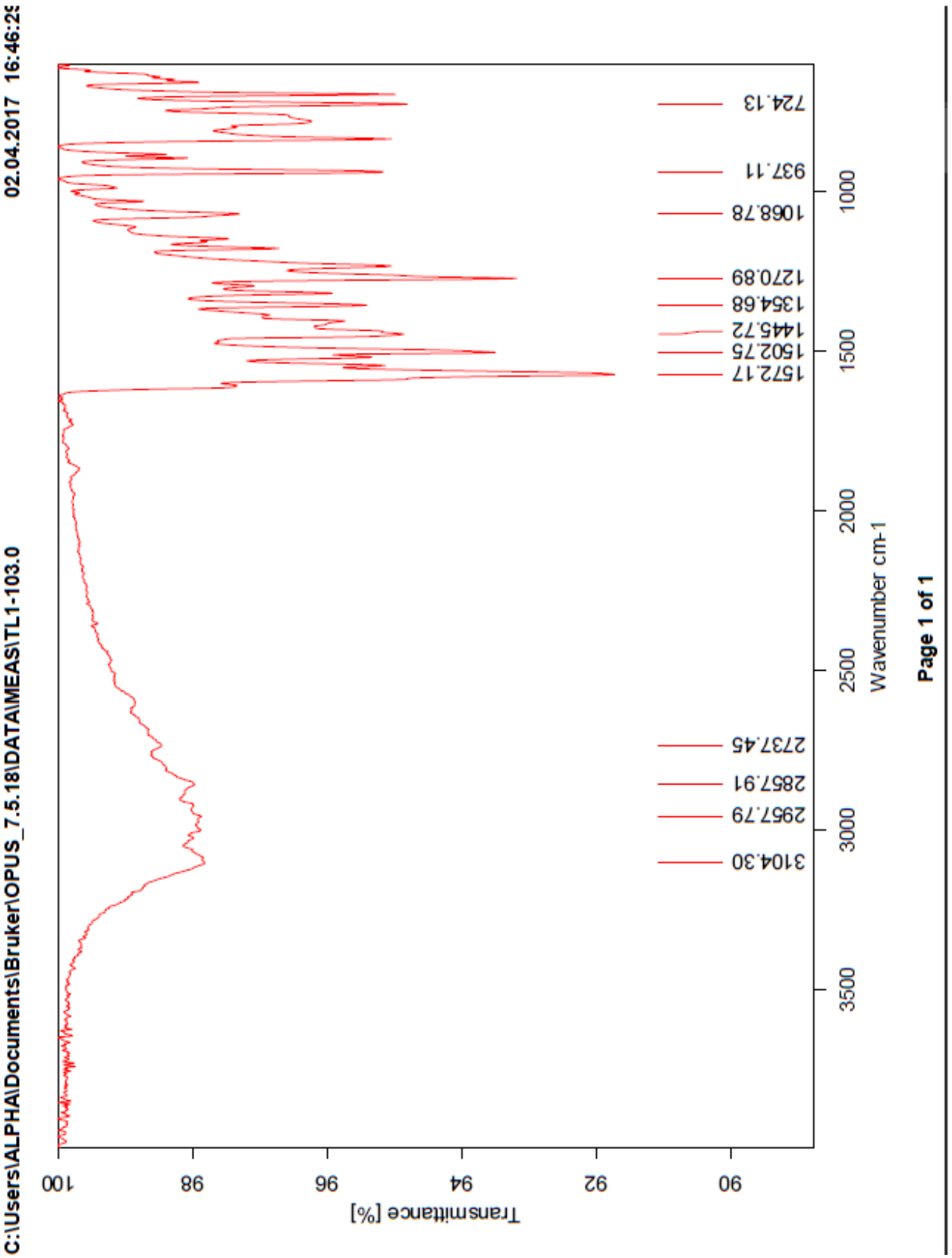


**Figure Q.6** IR spectrum of compound **7f.**

**Elemental Composition Report** Page 1

**Single Mass Analysis**
Tolerance = 5.0 PPM / DBE: min = -1.5, max = 50.0
Element prediction: Off
Number of isotope peaks used for i-FIT = 3

Monoisotopic Mass, Even Electron Ions
809 formula(e) evaluated with 3 results within limits (all results (up to 1000) for each mass)
Elements Used:
C: 1-500 H: 1-1000 N: 0-10 O: 0-25
2017-177 182 (3.549) AM2 (Ar,35000.0,0.00,0.00); Cm (175:184)
1: TOF MS ASAP+

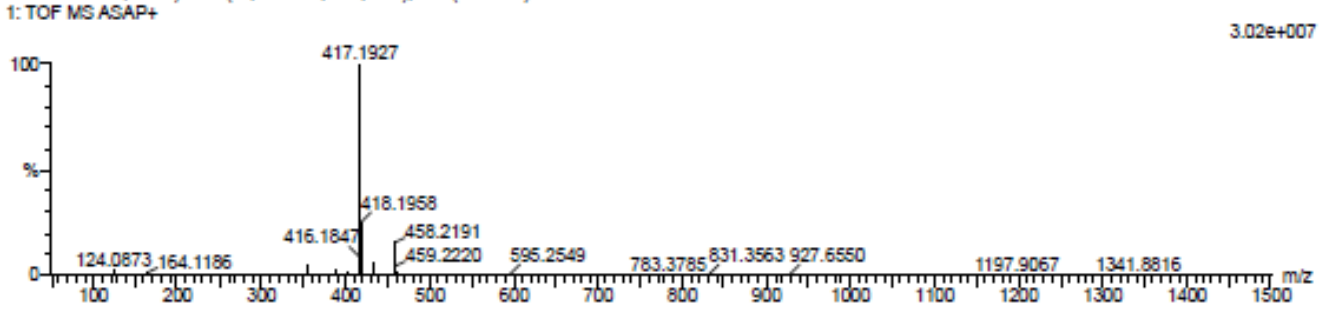


| | | | | | | | | |
|---|---|---|---|---|---|---|---|---|
| Minimum: | | | | -1.5 | | | | |
| Maximum: | | 2.0 | 5.0 | 50.0 | | | | |
| Mass | Calc. Mass | mDa | PPM | DBE | i-FIT | Norm | Conf(%) | Formula |
| 417.1927 | 417.1927 | 0.0 | 0.0 | 14.5 | 1545.6 | 0.264 | 76.79 | C24 H25 N4 O3 ion observed [M+H] |
| | 417.1913 | 1.4 | 3.4 | 9.5 | 1546.8 | 1.466 | 23.09 | C23 H29 O7 |
| | 417.1945 | -1.8 | -4.3 | 1.5 | 1552.0 | 6.686 | 0.12 | C12 H29 N6 O10 |

**Figure Q.7**: MS spectrum of compound **7f.**

# R Spectroscopic data for compound 7g

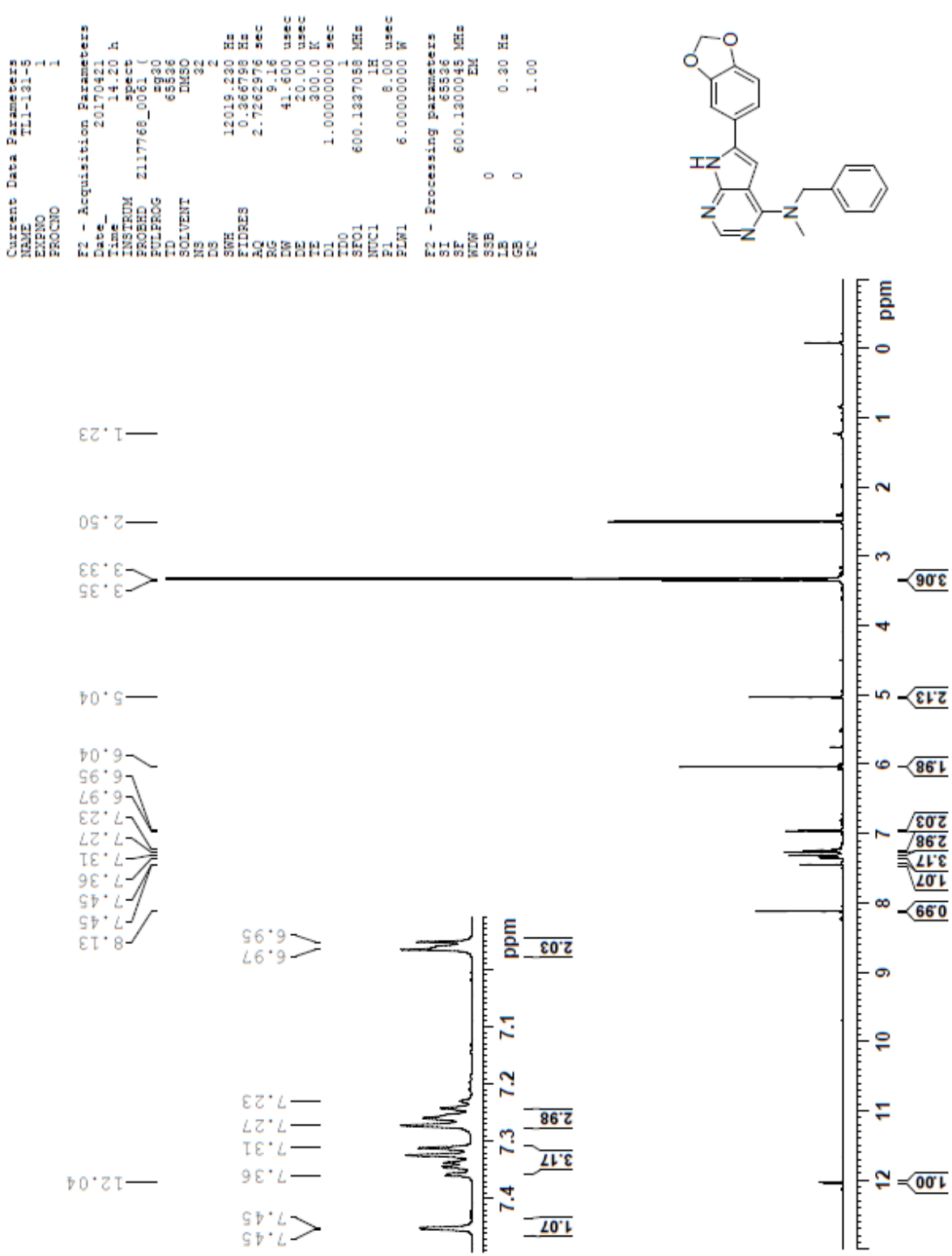


**Figure R.1**: $^{1}$H NMR spectrum of compound **7g.**

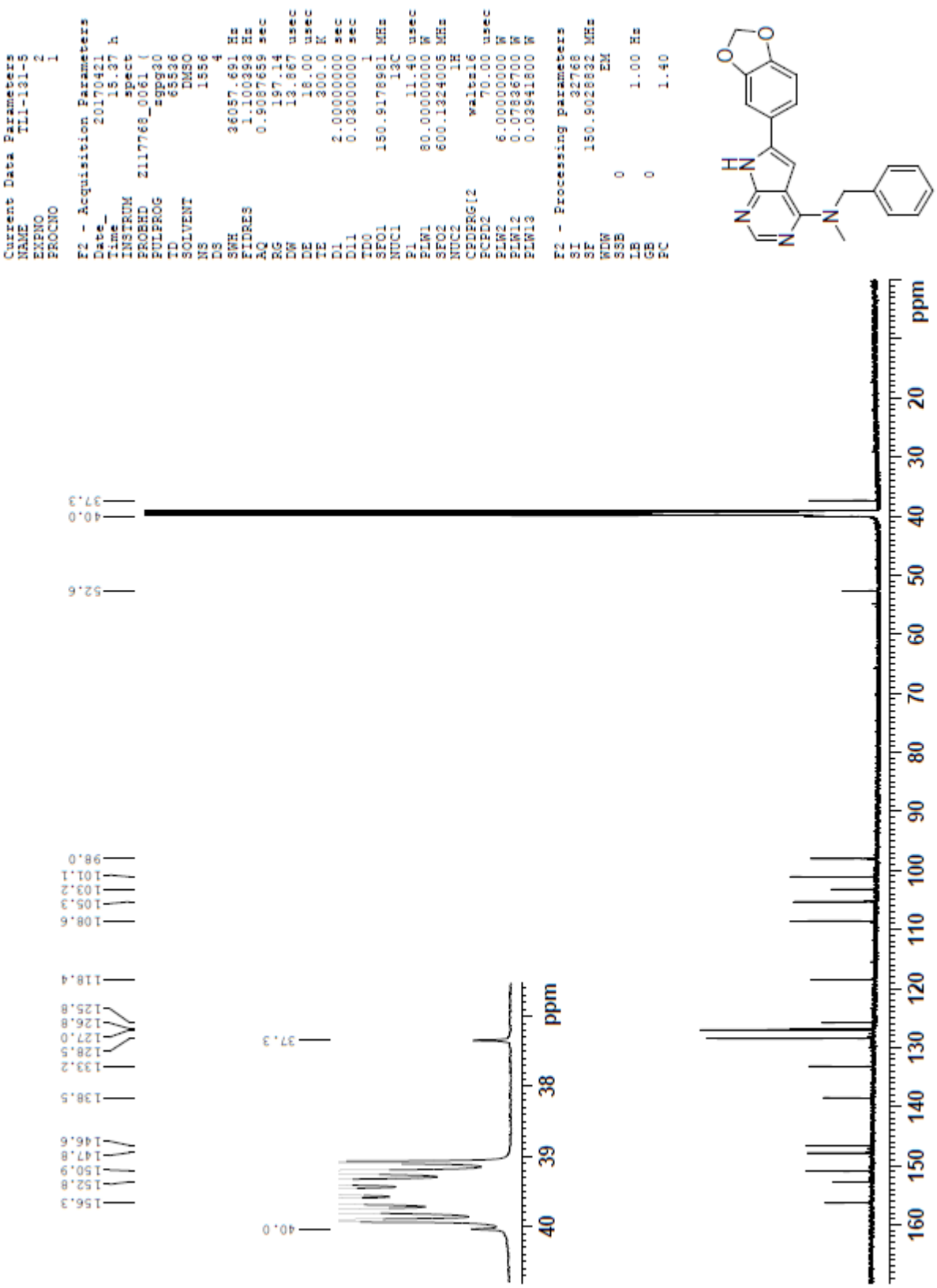


**Figure R.2**: $^{13}C$ NMR spectrum of compound **7g.**

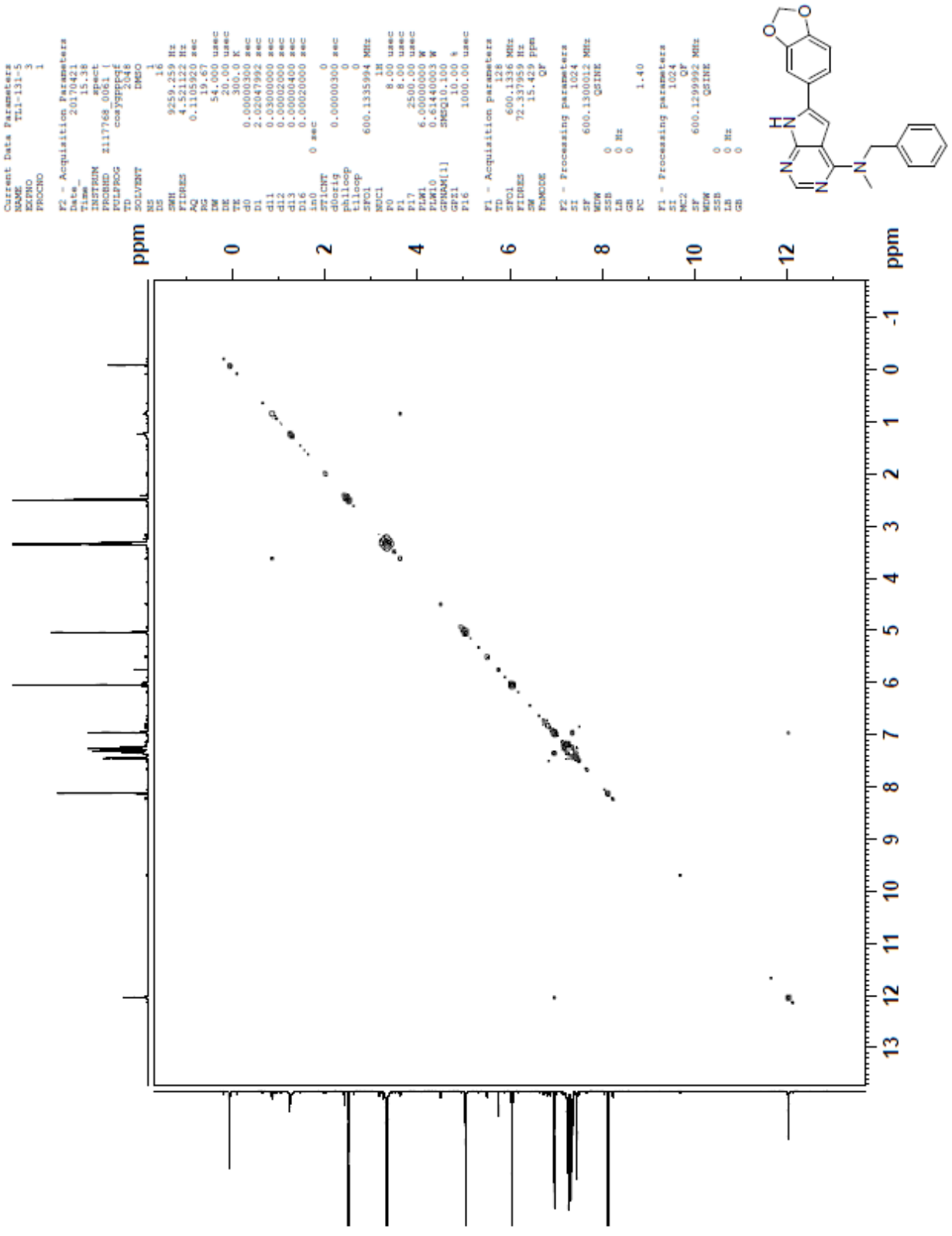


**Figure R.3**: COSY spectrum of compound **7g.**

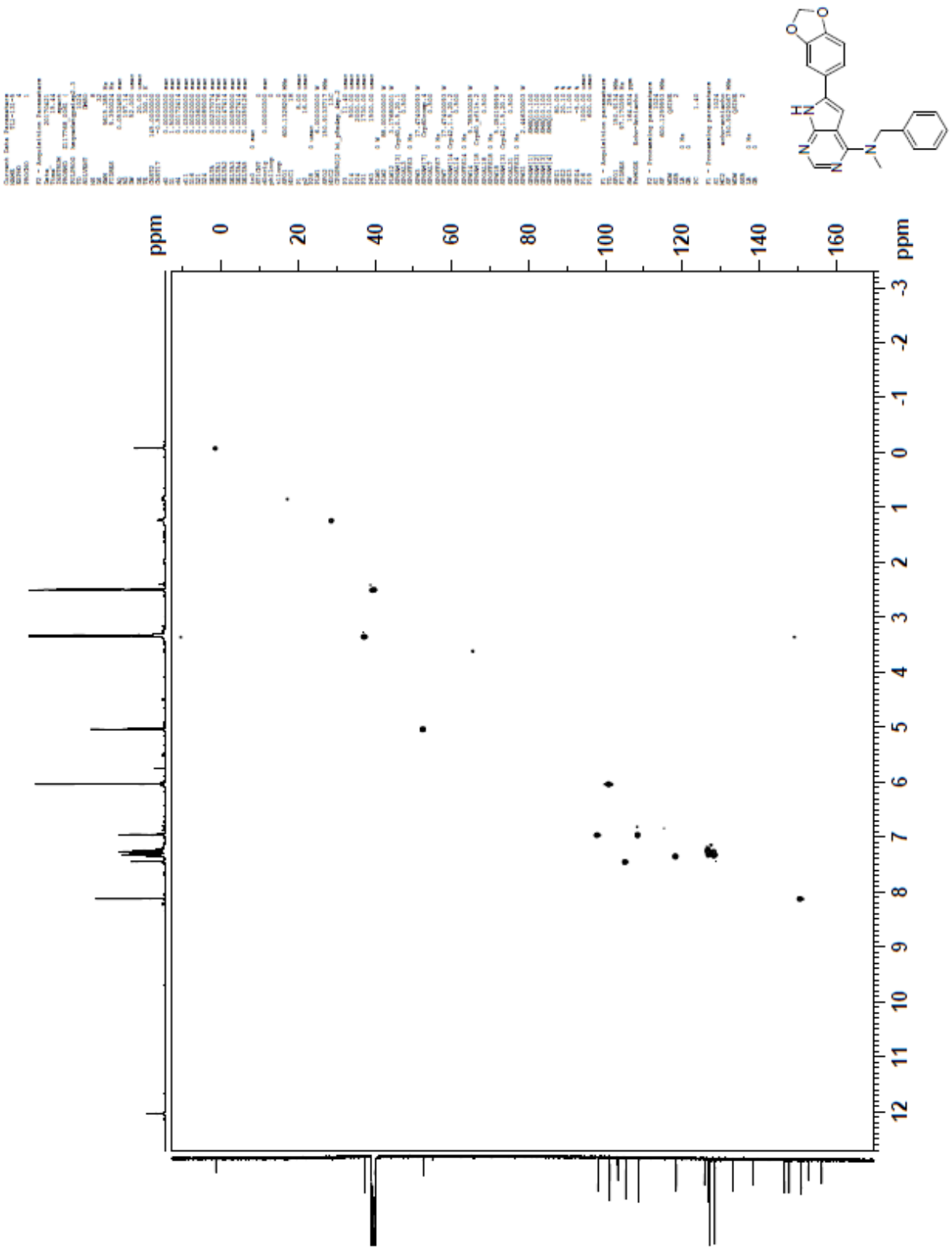


**Figure R.4**: HSQC spectrum of compound **7g.**

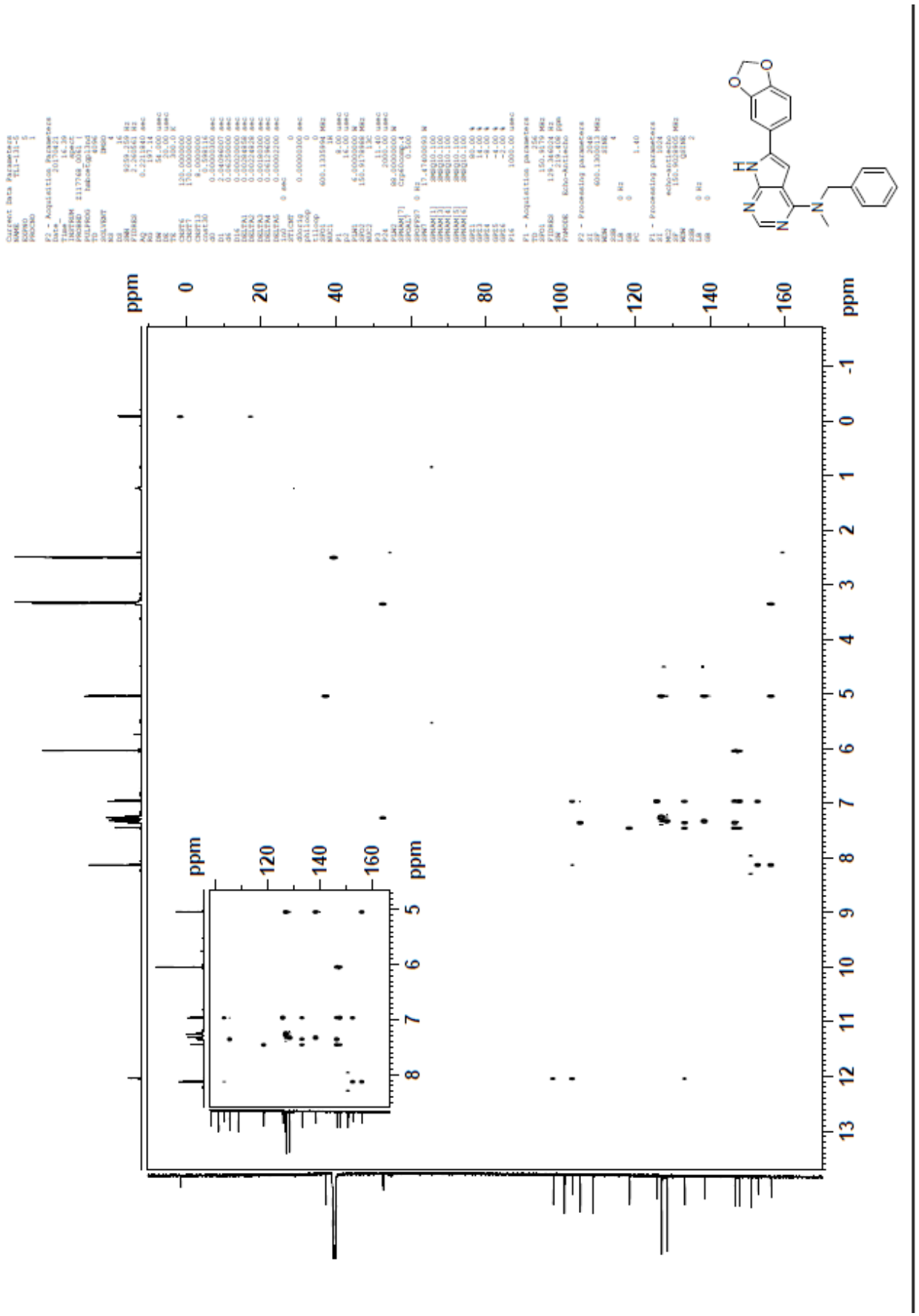

**Figure R.5**: HMBC spectrum of compound **7g**.

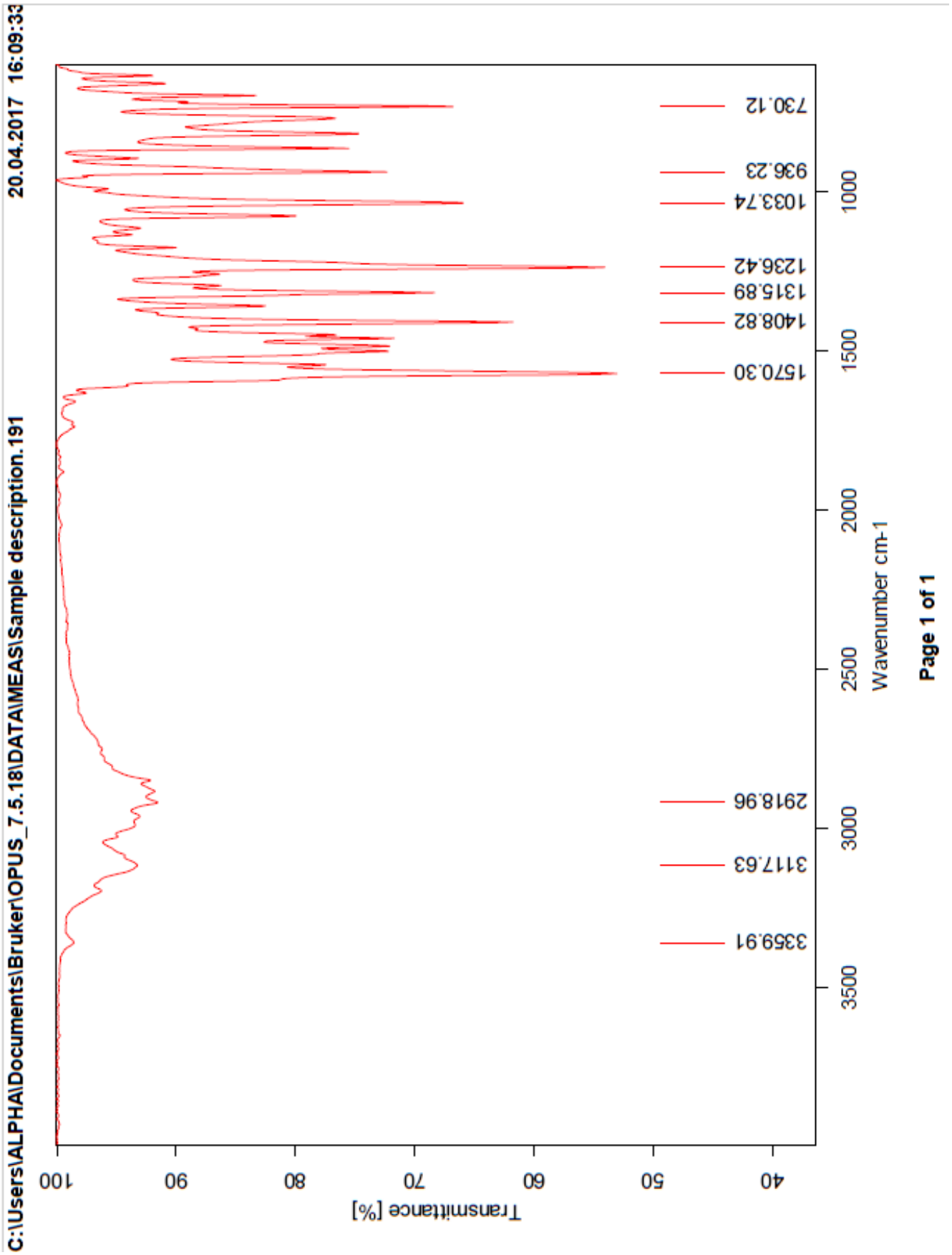


**Figure R.6**: IR spectrum of compound **7g.**

## Elemental Composition Report



### Single Mass Analysis

Tolerance = 2.0 PPM / DBE: min = -1.5, max = 50.0
Element prediction: Off
Number of isotope peaks used for i-FIT = 3

Monoisotopic Mass, Even Electron Ions
861 formula(e) evaluated with 2 results within limits (all results (up to 1000) for each mass)
Elements Used:
C: 3-100 H: 0-1000 N: 0-20 O: 0-25

NT-MSLAB-Operator-SVG
2017-219 235 (4.584) AM2 (Ar,35000.0,0.00,0.00); Cm (227:254)

1: TOF MS ASAP+
4.01e+006

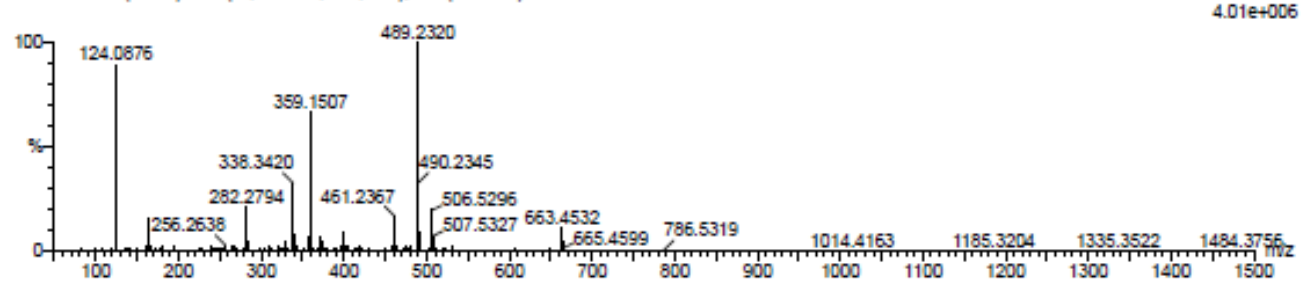


| | | | | | | | | |
|---|---|---|---|---|---|---|---|---|
| Minimum: | | | | -1.5 | | | | |
| Maximum: | | 5.0 | 2.0 | 50.0 | | | | |
| Mass | Calc. Mass | mDa | PPM | DBE | i-FIT | Norm | Conf(%) | Formula |
| 359.1507 | 359.1508 | -0.1 | -0.3 | 14.5 | 1367.2 | 0.000 | 100.00 | C21 H19 N4 O2 |
| | 359.1513 | -0.6 | -1.7 | 7.5 | 1381.1 | 13.900 | 0.00 | C6 H15 N16 O3 |

Ion observed [M+H]

**Figure R.7**: MS spectrum of compound **7g.**

# S Spectroscopic data for compound 7h

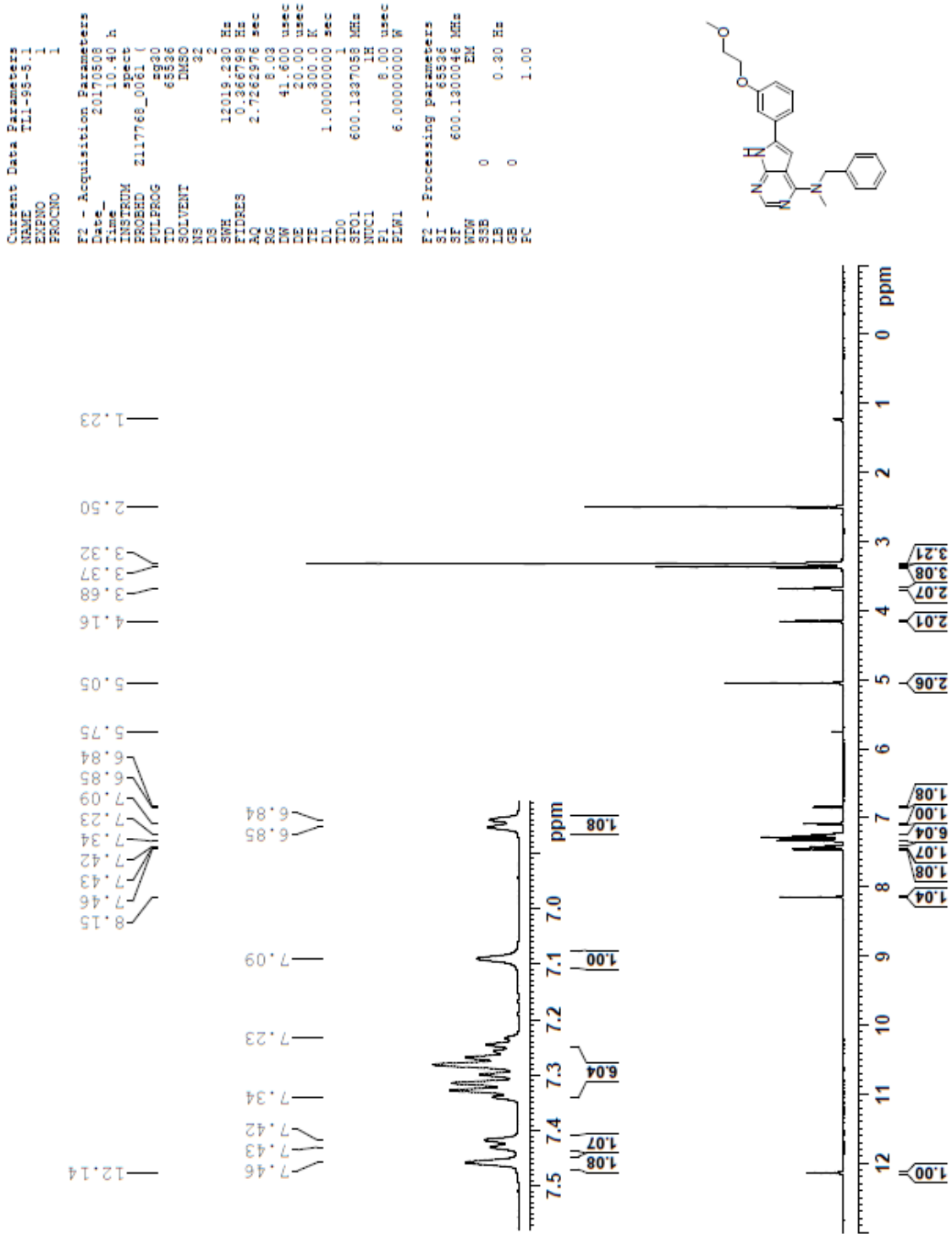

**Figure S.1**: $^{1}$H NMR spectrum of compound **7h.**

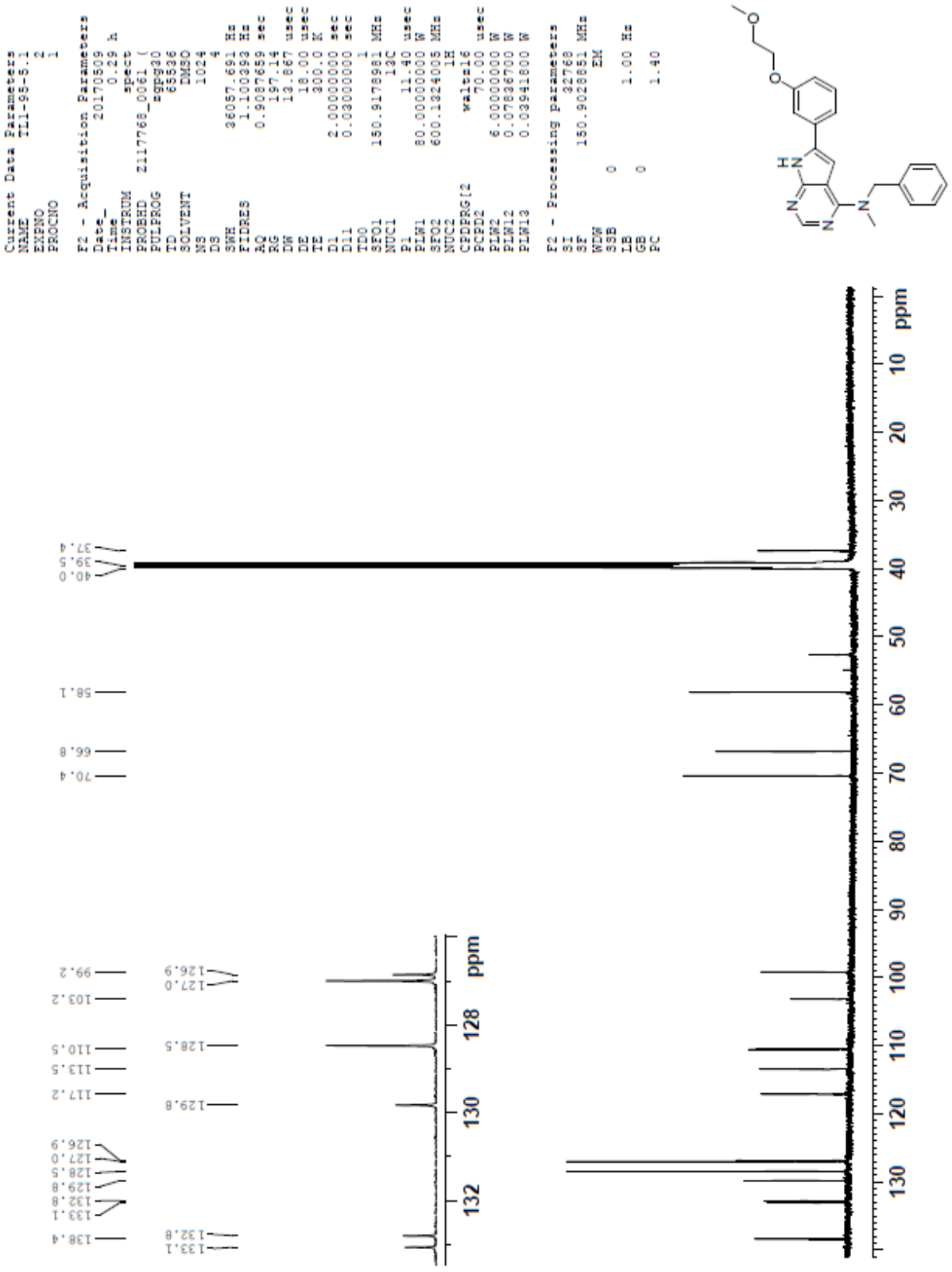


**Figure S.2**: $^{13}C$ NMR spectrum of compound **7h.**

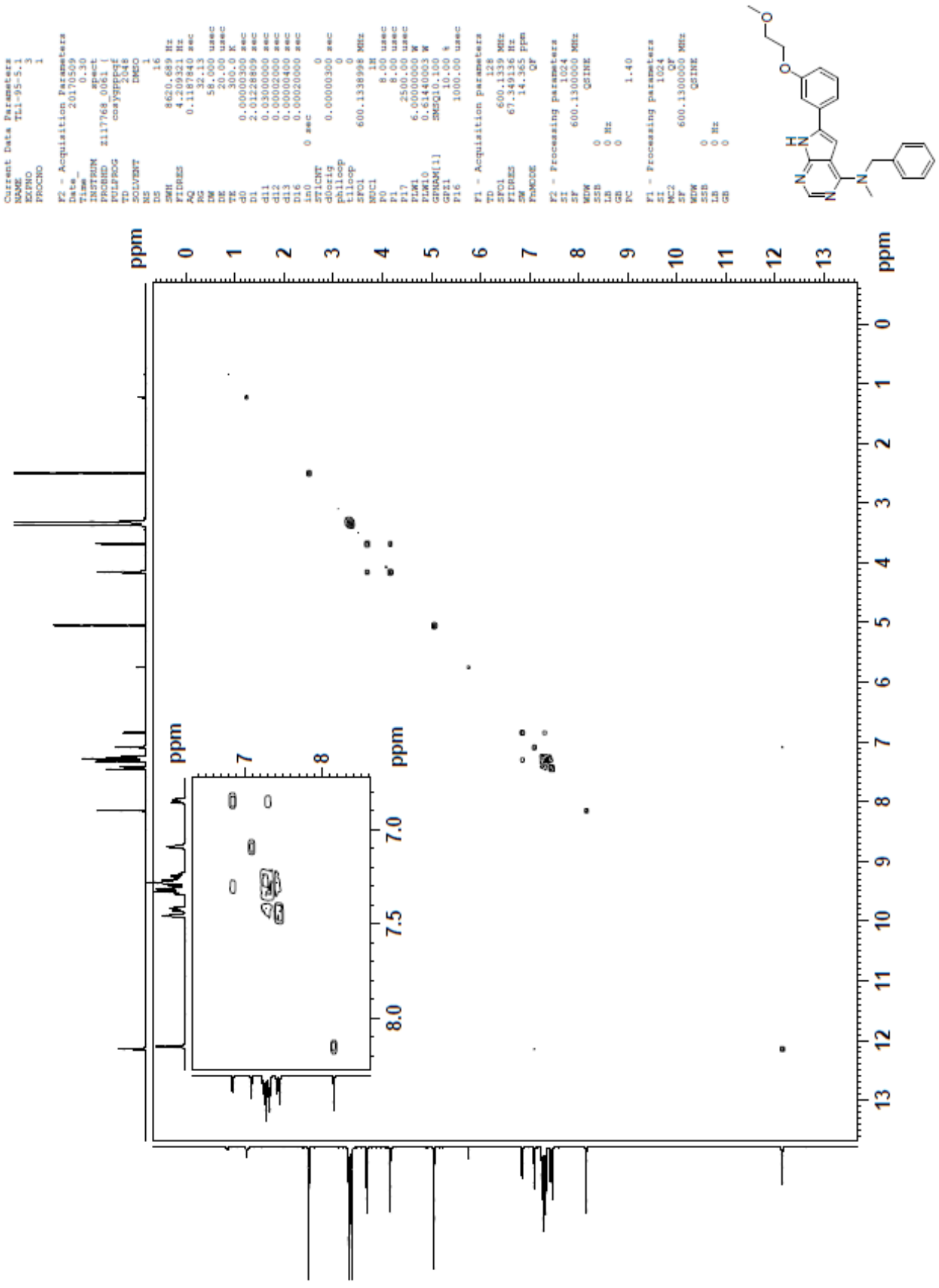

**Figure S.3**: COSY spectrum of compound **7h.**

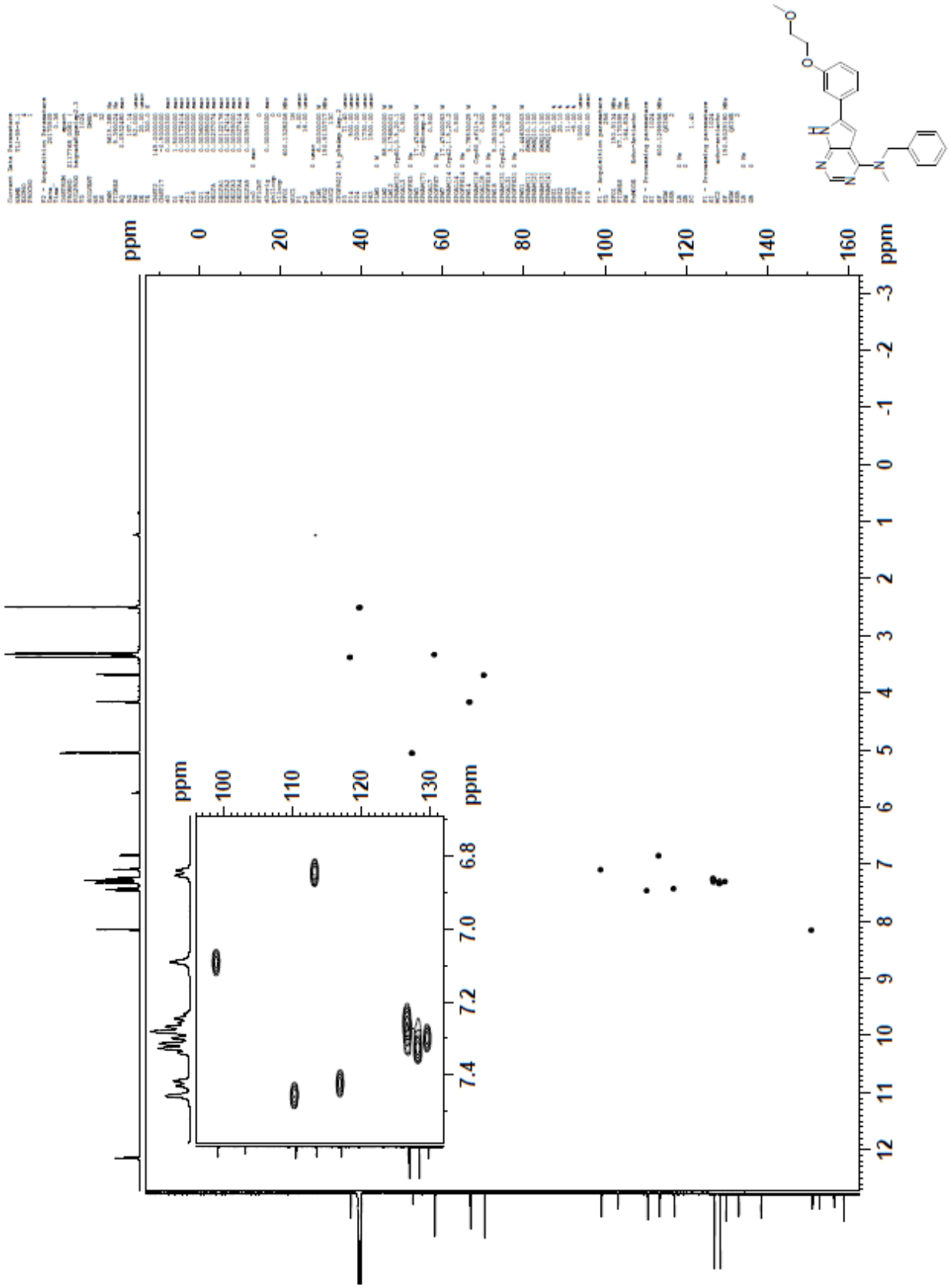

**Figure S.4**: HSQC spectrum of compound **7h.**

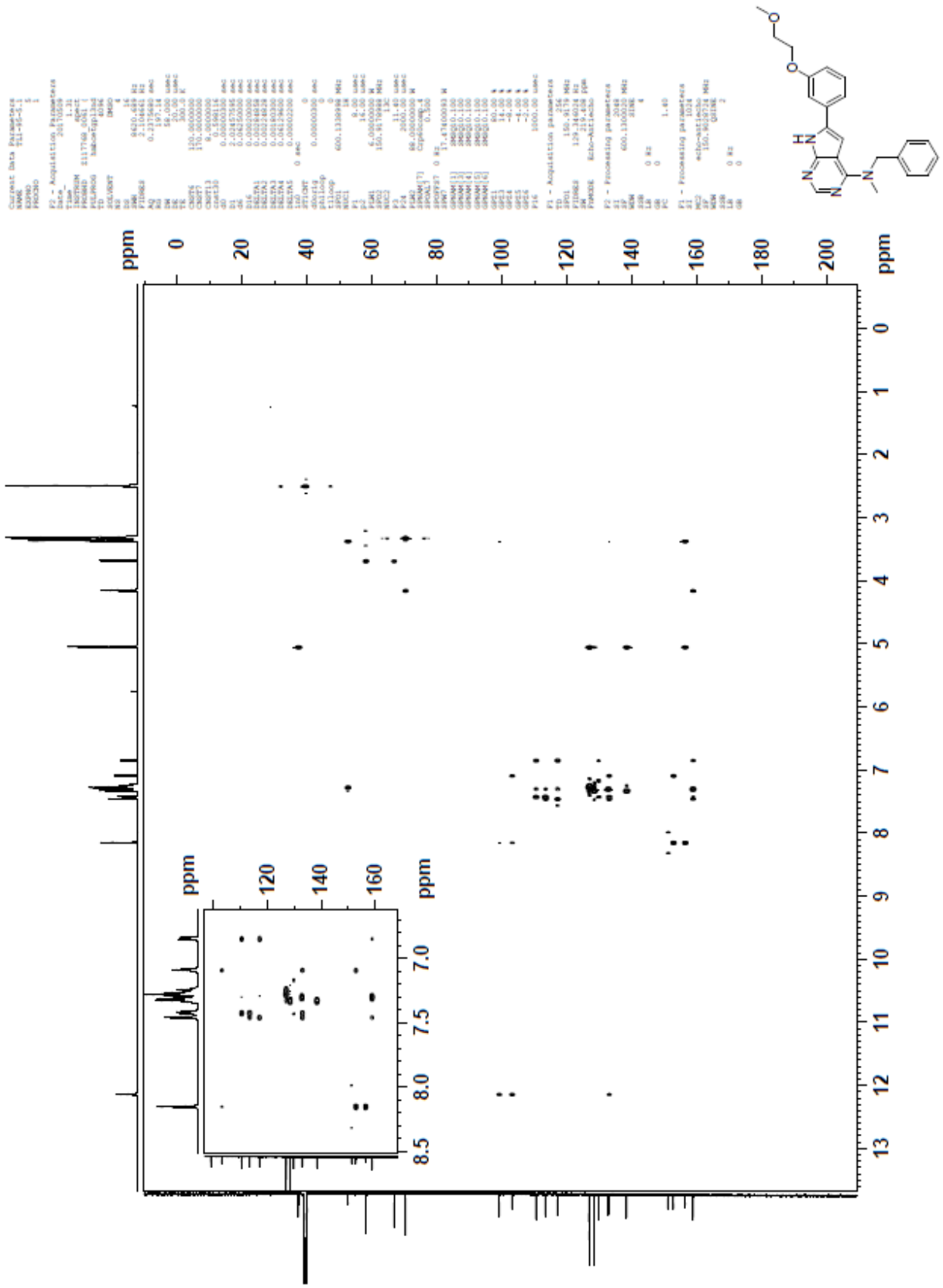

**Figure S.5**: HMBC spectrum of compound **7h**.

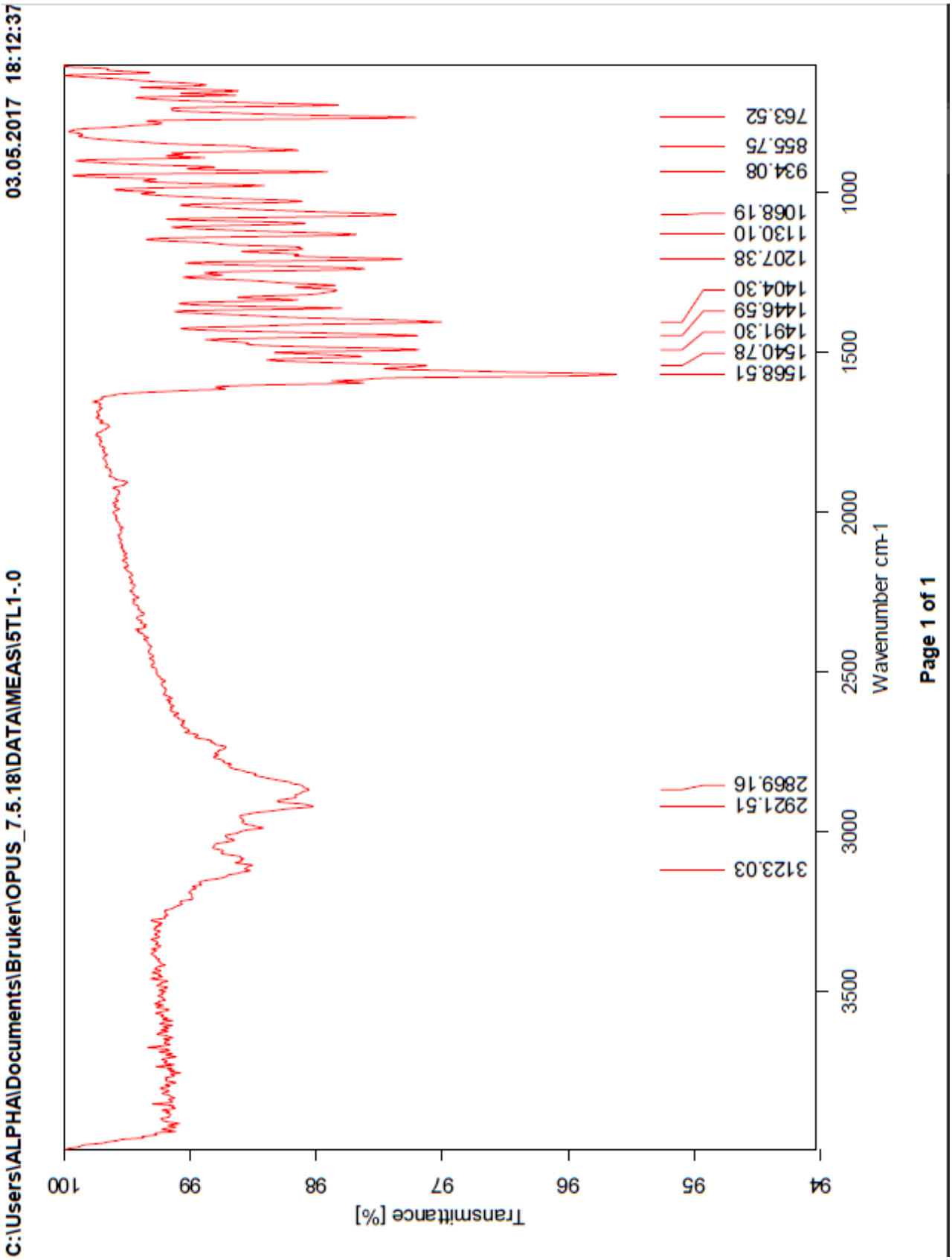


**Figure S.6**: IR spectrum of compound **7h.**

**Elemental Composition Report** Page 1

**Single Mass Analysis**
Tolerance = 2.0 PPM / DBE: min = -1.5, max = 50.0
Element prediction: Off
Number of isotope peaks used for i-FIT = 3

Monoisotopic Mass, Even Electron Ions
702 formula(e) evaluated with 2 results within limits (all results (up to 1000) for each mass)
Elements Used:
C: 1-500 H: 1-1000 N: 0-10 O: 0-25
2017-251 187 (3.654) AM2 (Ar,35000.0,0.00,0.00); Cm (186:200)
1: TOF MS ASAP+

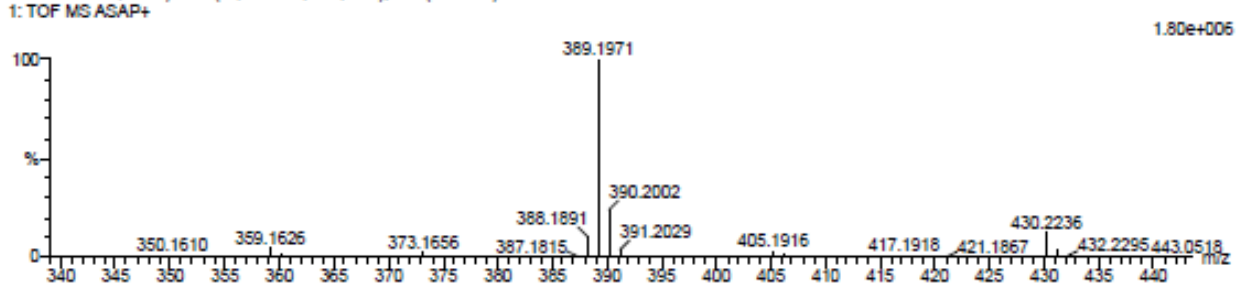


| | | | | | | | | |
|---|---|---|---|---|---|---|---|---|
| Minimum: | | | | -1.5 | | | | |
| Maximum: | | 2.0 | 2.0 | 50.0 | | | | |
| Mass | Calc. Mass | mDa | PPM | DBE | i-FIT | Norm | Conf(%) | Formula |
| 389.1971 | 389.1978 | -0.7 | -1.8 | 13.5 | 1279.3 | 1.909 | 14.82 | C23 H25 N4 O2 ion observed [M+H] |
| | 389.1964 | 0.7 | 1.8 | 8.5 | 1277.5 | 0.160 | 85.18 | C22 H29 O6 |

**Figure S.7**: MS spectrum of compound **7h.**

# U Biological testing

**Table 18**: Summary of the percent inhibition (at 500 nM) and $IC_{50}$-values, with deviations for the tested pyrrolopyrimidines against CSF-1R.Dasatanib included in the table as reference compounds.

| Compound | Percent inhibition CSF-1R | $IC_{50}$ CSF-1R [nM] |
|---|---|---|
| Dasatanib | 101 | 0.4 ± 0.0 |
| **7a** | 103 | 1,30 ±0.3 |
| **7b** | 96 | 2 ± 0.1 |
| **7d** | 96 | 5,2 ± 0.1 |
| **7e** | 87 | 2,8 ± 0.5 |
| **7f** | 97 | 3,70 ± 0.3 |
| **7h** | 90 | 2,3 ± 0.3 |